Electronic Supplementary Material (ESI) for Dalton Transactions.

Supporting Information

Reduction of Nitrite to Nitric Oxide and Generation of Reactive Chalcogen Species by Mononuclear Fe(II) and Zn(II) Complexes of Thiolate and Selenolate

Sayan Atta, Amit Mandal, Rahul Saha, and Amit Majumdar*

School of Chemical Sciences, Indian Association for the Cultivation of Science, 2A & 2B Raja S. C. Mullick Road, Kolkata 700032, India.

*Corresponding author email: icam@iacs.res.in

Experimental Procedures.

Experimental Procedure for the Generation, identification, and quantification of NO.

Reaction of [(Py2ald)Zn(ONO)] (3^{Zn}) with 2 equiv of ^{t}BuSH. To a solution of 18.1 mg (0.04 mmol) of $\mathbf{3^{Zn}}$ in 0.5 mL of CH_2Cl_2 was added a solution of 7.2 mg (0.08 mmol) of ^{t}BuSH in 0.5 mL of CH_2Cl_2 and the solution was allowed to stir overnight. The reaction mixture was then filtered through Celite. The filtrate was evaporated to dryness and the yellow solid residue thus obtained was washed twice with 2 mL of Et_2O. The solid product was then dried under vacuum, dissolved in a mixture of MeCN and MeOH and the resulting solution was filtered through Celite. Et_2O was allowed to diffuse into the filtrate at 0°C overnight to obtain the product as yellow, needle-shaped, crystals (12.5 mg, 68%). The identity of the product as the starting material ($\mathbf{3^{Zn}}$) was confirmed by unit cell determination of the single crystals and ^{1}H NMR spectroscopy. **NO trapping.** The experiment was carried out in a vial-inside-vial setup, to quantitatively trap nitric oxide (NO) by reaction with the (TPP)Co^{II} complex. A smaller vial containing $\mathbf{3^{Zn}}$ (9.2 mg, 0.02 mmol) dissolved in CH_2Cl_2 (~0.2 mL) was placed inside a larger vial containing (TPP)Co^{II} (13.4 mg, 0.02 mmol) in CH_2Cl_2 (~2 mL). The outer vial was sealed with a rubber septum. A solution of ^{t}BuSH (3.6 mg, 0.04 mmol) in CH_2Cl_2 (~0.2 mL) was injected into the inner vial and allowed it to stand at room temperature for overnight with occasional shaking. The solution of the outer vial was evaporated to dryness, and the solid thus obtained was analyzed using FTIR and ^{1}H NMR spectroscopy. The yield of NO was found to be 11%, based on the relative integrals of the ^{1}H NMR resonances of (TPP)Co(NO) and unreacted (TPP)Co^{II}.

Reaction of [(Py2ald)Zn(ONO)] (3^{Zn}) with 2 equiv of $PhCH_2SH$. To a solution of 18.1 mg (0.04 mmol) of **($\mathbf{3^{Zn}}$)** in 0.5 mL of CH_2Cl_2 was added a solution of 9.9 mg (0.08 mmol) of $PhCH_2SH$ in 0.5 mL of CH_2Cl_2 and the solution was allowed to stir overnight. Following this, 6.6 mg (0.06 mmol) of sodium tetrafluoroborate ($NaBF_4$) was added into the reaction mixture and was further stirred for an additional 2 hours. The reaction mixture was then filtered through

Celite. Et_2O was subsequently added to the filtrate until the complete precipitation of the metal complex took place. The solution was then again filtered through Celite. The filtrate was kept for GC-MS experiment. The solid residue was washed twice with 2 mL of Et_2O and dried under vacuum. The solid was then dissolved in a mixture of CH_2Cl_2 and MeOH and filtered through Celite. Et_2O was allowed to diffuse into the filtrate at 0°C overnight to obtain the product as yellow, needle-shaped, crystals (8.4 mg, 42%). The identity of the product, $[(Py2ald)M]_2(BF_4)_2$ (**5**$(BF_4)_2$), was confirmed by a unit cell determination of the single crystals, mass spectrometry and ^{1}H NMR spectroscopy. **NO trapping:** The experiment was carried out in a vial-inside-vial setup as described in the preceding experiment for the reaction of $\mathbf{3^{Zn}}$ with 2 equiv of ^{t}BuSH but by using $\mathbf{3^{Zn}}$ (9.2 mg, 0.02 mmol) and $PhCH_2SH$ (5.0 mg, 0.04 mmol). Yield of NO = 41%.

Reaction of [(Py2ald)Zn(ONO)] ($\mathbf{3^{Zn}}$) with 1 equiv of PhSH. A procedure similar to that described for $\mathbf{3^{Zn}}$ with 2 equiv of $PhCH_2SH$ was followed but by using $\mathbf{3^{Zn}}$ (18.1 mg, 0.04 mmol) and PhSH (4.4 mg, 0.04 mmol) to obtain $[(Py2ald)Zn]_2(BF_4)_2$ (**5**$(BF_4)_2$) as the product (11.6 mg, 58%). The identity of the product was confirmed by a unit cell determination of the single crystals, mass spectrometry and ^{1}H NMR spectroscopy. **NO trapping:** The experiment was carried out in a vial-inside-vial setup as described in the preceding experiment for the reaction of $\mathbf{3^{Zn}}$ with 2 equiv of ^{t}BuSH but by using $\mathbf{3^{Zn}}$ (9.2 mg, 0.02 mmol) and PhSH (2.2 mg, 0.02 mmol). Yield of NO = 71%.

[(Py2ald)Zn(ONO)] ($\mathbf{3^{Zn}}$) with 2 equiv of PhSH. A procedure similar to that described for $\mathbf{3^{Zn}}$ with 2 equiv of $PhCH_2SH$ was followed but by using using $\mathbf{3^{Zn}}$ (18.1 mg, 0.04 mmol) and PhSH (8.8 mg, 0.08 mmol) to obtain [(Py2ald)Zn(SPh)] ($\mathbf{1a^{Zn}}$) as the product (15 mg, 72%). The identity of the product was confirmed by a unit cell determination of the single crystals, and ^{1}H NMR spectroscopy. **NO trapping:** The experiment was carried out in a vial-inside-vial setup as described in the preceding experiment for the reaction of $\mathbf{3^{Zn}}$ with 2 equiv of ^{t}BuSH but by using $\mathbf{3^{Zn}}$ (9.2 mg, 0.02 mmol) and PhSH (4.4 mg, 0.04 mmol). Yield of NO = 74%.

[(Py2ald)Zn(ONO)] (3^{Zn}) with 2 equiv of PhSeH. A procedure similar to that described for $\mathbf{3}^{Zn}$ with 2 equiv of $PhCH_2SH$ was followed but by using using $\mathbf{3}^{Zn}$ (18.1 mg, 0.04 mmol) and PhSeH (12.6 mg, 0.08 mmol) to obtain [(Py2ald)Zn(SePh)] ($\mathbf{2}^{Zn}$) as the product (16.1 mg, 71%). The identity of the product was confirmed by a unit cell determination of the single crystals, and ^{1}H NMR spectroscopy. **NO trapping:** The experiment was carried out in a vial-inside-vial setup as described in the preceding experiment for the reaction of $\mathbf{3}^{Zn}$ with 2 equiv of ^{t}BuSH but by using $\mathbf{3}^{Zn}$ (9.2 mg, 0.02 mmol) and PhSeH (6.3 mg, 0.04 mmol). Yield of NO = 81%.

Trapping of NO generated in the reaction of $[(Py2ald)Fe]_2(BF_4)_2$ ($5^{Fe}(BF_4)_2$) with 4 equiv of $(Bu_4N)(NO_2)$. The experiment was carried out in a vial-inside-vial setup, to quantitatively trap nitric oxide (NO) by reaction with the $(TPP)Co^{II}$ complex. A smaller vial containing $\mathbf{5}^{Fe}(BF_4)_2$ (20 mg, 0.02 mmol) dissolved in CH_2Cl_2 (~0.3 mL) was placed inside a larger vial containing $(TPP)Co^{II}$ (26.8 mg, 0.04 mmol) in CH_2Cl_2 (~4 mL). The outer vial was sealed with a rubber septum. A solution of $(Bu_4N)(NO_2)$ (23 mg, 0.08 mmol) in CH_2Cl_2 (~0.3 mL) was injected into The solution of the outer vial was evaporated to dryness, and the solid thus obtained was analyzed using FTIR and ^{1}H NMR spectroscopy. The yield of NO was found to be 1.80 equiv, based on the relative integrals of the ^{1}H NMR resonances of (TPP)Co(NO) and unreacted $(TPP)Co^{II}$.

Trapping of NO generated in the reaction of [(Py2ald)Fe(SPh)] ($\mathbf{1a}^{Fe}$) with 3 equiv of $(Bu_4N)(NO_2)$. The experiment was carried out in a vial-inside-vial setup as described in the preceding experiment for the reaction of $\mathbf{5}(BF_4)_2$ with 4 equiv of $(Bu_4N)(NO_2)$ was followed but by using $\mathbf{1a}^{Fe}$ (10.3 mg, 0.02 mmol) and $(Bu_4N)(NO_2)$ (17.3 mg, 0.06 mmol). Yield of NO = 1.56 equiv.

Trapping of NO generated in the reaction of [(Py2ald)Fe(SePh)] ($\mathbf{2}^{Fe}$) with 3 equiv of $(Bu_4N)(NO_2)$. The experiment was carried out in a vial-inside-vial setup as described in the preceding experiment for the reaction of $\mathbf{5}(BF_4)_2$ with 4 equiv of $(Bu_4N)(NO_2)$ was followed

but by using **2^{Fe}** (11.2 mg, 0.02 mmol) and (Bu_4N)(NO_2) (17.3 mg, 0.06 mmol). Yield of NO = 1.65 equiv.

Reaction of [{(Py2ald)(ONO)Fe}$_2$-μ_2-O] (8^{Fe}) with 4 equiv of PhSH. To a solution of 36.5 mg (0.04 mmol) of **8^{Fe}** in 0.5 mL of DCM was added a solution of 17.6 mg (0.16 mmol) of PhSH in 0.5 mL of CH_2Cl_2 and the solution was allowed to stir overnight. The reaction mixture was then filtered through Celite. Et_2O was subsequently added to the filtrate until the complete precipitation of the metal complex took place. The solution was then again filtered through Celite. The filtrate was kept for GC-MS experiment. The solid residue was washed twice with 2 mL of Et_2O and dried under vacuum. The solid product was dissolved in 1 mL MeOH followed by the addition of $NaBPh_4$ (20.5 mg, 0.06 mmol). The solution was stirred for 30 min during which the precipitation of a brown solid was observed. The brown solid was separated from the reaction mixture, washed twice with MeOH followed by Et_2O and dried under vacuum. The solid was then dissolved in DMF and filtered through Celite. Et_2O was allowed to diffuse into the filtrate at 0°C overnight to obtain the product as brown, needle-shaped, crystals of **[{(Py2ald)Fe}$_2$](BPh$_4$)$_2$** (**5^{Fe}**(BPh_4)$_2$) (31.8 mg, 55%). The product was identified by unit cell determination of the single crystals and mass spectrometry. **NO trapping:** The experiment was carried out in a vial-inside-vial setup (mentioned earlier), to quantitatively trap nitric oxide (NO) with the (TPP)Co^{II} complex. A smaller vial containing **8^{Fe}** (18.25 mg, 0.02 mmol) dissolved in CH_2Cl_2 (~0.2 mL) was placed inside a larger vial containing (TPP)Co^{II} (26.8 mg, 0.04 mmol) in CH_2Cl_2 (~4 mL). The outer vial was sealed with a rubber septum. A solution of PhSH (8.8 mg, 0.08 mmol) in CH_2Cl_2 (~0.2 mL) was injected into the inner vial and allowed it to stand at RT for overnight with occasional shaking. The solution of the outer vial was evaporated to dryness, and the solid thus obtained was analyzed using FTIR and ^{1}H NMR spectroscopy. Yield of NO = 1.42 equiv.

Reaction of [{(Py2ald)(ONO)Fe}$_2$-μ_2-O] (8^{Fe}) with 6 equiv of PhSH. The procedure described above for the reaction of **8^{Fe}** with 4 equiv of PhSH was followed but by using **8^{Fe}**

(36.5 mg, 0.04 mmol) and PhSH (26.4 mg, 0.24 mmol) while addition of $NaBPh_4$ was not required. The product, **[(Py2ald)Fe(SPh)]** (**1a**^{Fe}) was obtained as orange, needle-shaped, crystals (23.7 mg, 58%) and was identified by unit cell determination of the single crystals. **NO trapping:** The procedure described above for the reaction of **8**^{Fe} with 4 equiv of PhSH was followed but by using **8**^{Fe} (18.25 mg, 0.02 mmol) and PhSH (13.2 mg, 0.12 mmol). Yield of NO = 1.70 equiv.

Reaction of [{(Py2ald)(ONO)Fe}$_2$-μ_2-O] (**8**^{Fe}) **with 4 equiv of PhSeH.** The procedure described above for the reaction of **8**^{Fe} with 4 equiv of PhSH was followed but by using **8**^{Fe} (36.5 mg, 0.04 mmol), PhSeH (25.1 mg, 0.16 mmol) and $NaBPh_4$ (20.5 mg, 0.06 mmol). The product, **[{(Py2ald)Fe}$_2$](BPh$_4$)$_2$** (**5**^{Fe}(BPh_4)$_2$) was obtained as brown, needle-shaped, crystals (32.8 mg, 57%) and was identified by unit cell determination of the single crystals and mass spectrometry. **NO trapping:** The procedure described above for the reaction of **8**^{Fe} with 4 equiv of PhSH was followed but by using **8**^{Fe} (18.25 mg, 0.02 mmol) and PhSeH (12.6 mg, 0.08 mmol). Yield of NO = 1.66 equiv.

Reaction of [{(Py2ald)(ONO)Fe}$_2$-μ_2-O] (**8**^{Fe}) **with 6 equiv of PhSeH.** The procedure described above for the reaction of **8**^{Fe} with 4 equiv of PhSH was followed but by using **8**^{Fe} (36.5 mg, 0.04 mmol) and PhSeH (37.7 mg, 0.24 mmol) while addition of $NaBPh_4$ was not required. The product, **[(Py2ald)Fe(SePh)]** (**2**^{Fe}) was obtained as orange, needle-shaped, crystals (28.1 mg, 63%) and was identified by unit cell determination of the single crystals. **NO trapping:** The procedure described above for the reaction of **8**^{Fe} with 4 equiv of PhSH was followed but by using **8**^{Fe} (18.25 mg, 0.02 mmol) and PhSeH ((18.8 mg, 0.12 mmol). Yield of NO = 1.76 equiv.

Experimental Procedure for Transfer Reactions.

Reaction of [(Py2ald)Zn(SPh)] (1a^{Zn}) with MeI. To a solution of 20.8 mg (0.04 mmol) of **1a**^{Zn} in 0.5 mL of DMF was added a solution of 5.7 mg (0.04 mmol) of Iodomethane (MeI) in 0.5 mL of DMF and the solution was allowed to stir overnight. Following this, 6.6 mg (0.06

mmol) of sodium tetrafluoroborate ($NaBF_4$) was added into the reaction mixture and further stirred for an additional 2 hours. The reaction mixture was then filtered through Celite. Et_2O was subsequently added to the filtrate until the complete precipitation of the metal complex occurred. The solution was then again filtered through Celite. The resulting solid residue was washed twice with 2 mL of Et_2O and the remaining solution was kept for GC-MS experiment. The solid product was then dried under vacuum, dissolved in a mixture of 0.5 mL MeOH and 0.5 mL EtOH and the resulting solution was filtered through Celite. Et_2O was allowed to diffuse into the filtrate at 0°C overnight to obtain the product as yellow, needle-shaped, crystals of $[(Py2ald)Zn]_2(BF_4)_2$ ($\mathbf{5^{Zn}}(BF_4)_2$) in 62% yield (12.4 mg). The compound, $\mathbf{5^{Zn}}(BF_4)_2$, was identified by ^{1}H NMR spectroscopy and mass spectrometry.

A similar procedure was followed for the following transfer reactions using the specified amount of the reactants. The compound, $\mathbf{5^{Zn}}(BF_4)_2$, was identified by ^{1}H NMR spectroscopy and mass spectrometry in each case.

Reaction of [(Py2ald)Zn(SPh)] ($\mathbf{1a^{Zn}}$) with $PhCH_2Br$. 20.8 mg (0.04 mmol) of $\mathbf{1a^{Zn}}$ and 6.8 mg (0.04 mmol) of $PhCH_2Br$ in DMF. Yield of $\mathbf{5^{Zn}}(BF_4)_2$ = 59% (11.8 mg).

Reaction of [(Py2ald)Zn(SPh)] ($\mathbf{1a^{Zn}}$) with MeC(O)Cl. 20.8 mg (0.04 mmol) of $\mathbf{1a^{Zn}}$ and 3.1 mg (0.04 mmol) of MeC(O)Cl in DMF. Yield of $\mathbf{5^{Zn}}(BF_4)_2$ = 58% (11.6 mg).

Reaction of [(Py2ald)Zn(SPh)] ($\mathbf{1a^{Zn}}$) with PhC(O)Cl. 20.8 mg (0.04 mmol) of $\mathbf{1a^{Zn}}$ and 5.6 mg (0.04 mmol) of PhC(O)Cl in MeCN. Yield of $\mathbf{5^{Zn}}(BF_4)_2$ = 67% (13.4 mg).

Reaction of [(Py2ald)Zn(SPh)] ($\mathbf{1a^{Zn}}$) with CH_2Br_2. 20.8 mg (0.04 mmol) of $\mathbf{1a^{Zn}}$ and 3.5 mg (0.03 mmol) of CH_2Br_2 in DMF. Yield of $\mathbf{5^{Zn}}(BF_4)_2$ = 71% (14.2 mg).

Reaction of [(Py2ald)Zn(SePh)] ($\mathbf{2^{Zn}}$) with MeI. 22.7 mg (0.04 mmol) of $\mathbf{2^{Zn}}$ and 5.7 mg (0.04 mmol) of MeI in DMF. Yield of $\mathbf{5^{Zn}}(BF_4)_2$ = 38% (7.6 mg).

Reaction of [(Py2ald)Zn(SePh)] ($\mathbf{2^{Zn}}$) with $PhCH_2Br$. 22.7 mg (0.04 mmol) of $\mathbf{2^{Zn}}$ and 6.8 mg (0.04 mmol) of $PhCH_2Br$ in DMF. Yield of $\mathbf{5^{Zn}}(BF_4)_2$ = 55% (11 mg).

Reaction of [(Py2ald)Zn(SePh)] (2^{Zn}) with MeC(O)Cl. 22.7 mg (0.04 mmol) of $\mathbf{2^{Zn}}$ and 3.1 mg (0.04 mmol) of MeC(O)Cl in DMF. Yield of $\mathbf{5^{Zn}}(BF_4)_2$ = 40% (8 mg).

Reaction of [(Py2ald)Zn(SePh)] (2^{Zn}) with PhC(O)Cl. 22.7 mg (0.04 mmol) of $\mathbf{2^{Zn}}$ and 5.6 mg (0.04 mmol) of PhC(O)Cl in MeCN. Yield of $\mathbf{5^{Zn}}(BF_4)_2$ = 52% (10.4 mg).

Reaction of [(Py2ald)Zn(SePh)] (2^{Zn}) with CH_2Br_2. 22.7 mg (0.04 mmol) of $\mathbf{2^{Zn}}$ and 3.5 mg (0.03 mmol) of CH_2Br_2 in DMF. Yield of $\mathbf{5^{Zn}}(BF_4)_2$ = 68% (13.6 mg).

Reaction of [(Py2ald)Fe(SPh)] ($1a^{Fe}$) with MeI. To a solution of 20.5 mg (0.04 mmol) of $\mathbf{1a^{Fe}}$ in 0.5 mL of DMF was added a solution of 5.7 mg (0.04 mmol) of Iodomethane (MeI) and the solution was allowed to stir overnight. The reaction mixture was then filtered through Celite. Et_2O was subsequently added to the filtrate until the complete precipitation of the metal complex occurred. The solution was then again filtered through Celite. The resulting solid residue was washed twice with 2 mL of Et_2O and the remaining solution was kept for GC-MS experiment. The solid product was then dried under vacuum and dissolved in 1 mL MeOH. Following this, 20.5 mg (0.06 mmol) of sodium tetraphenylborate ($NaBPh_4$) was added into the solution and further stirred for an additional 30 min. During this period, immediate precipitation of a brown solid was observed. Then the brown solid is separated from the reaction mixture and washed twice with MeOH and Et_2O and dried under vacuum. The solid was then redissolved in DMF and filtered through Celite. Et_2O was allowed to diffuse into the filtrate at 0°C overnight to obtain the product as brown, needle-shaped, crystals of $[(Py2ald)Fe]_2(BPh_4)_2$ ($\mathbf{5^{Fe}}(BPh_4)_2$) in 63% yield (18.2 mg). The compound was identified by unit cell determination of the single crystals and mass spectrometry.

A similar procedure was followed for the following transfer reactions using the specified amount of the reactants. The compound, $\mathbf{5^{Fe}}(BPh_4)_2$, was identified by unit cell determination of the single crystals and mass spectrometry in each case.

Reaction of [(Py2ald)Fe(SPh)] ($1a^{Fe}$) with $PhCH_2Br$. 20.5 mg (0.04 mmol) of $\mathbf{1a^{Fe}}$ and 6.8 mg (0.04 mmol) of $PhCH_2Br$ in DMF. Yield of ($\mathbf{5^{Fe}}(BPh_4)_2$) = 78% (22.5 mg).

Reaction of [(Py2ald)Fe(SPh)] ($\mathbf{1a^{Fe}}$) with MeC(O)Cl. 20.5 mg (0.04 mmol) of $\mathbf{1a^{Fe}}$ and 3.1 mg (0.04 mmol) of MeC(O)Cl in DMF. Yield of ($\mathbf{5^{Fe}}(BPh_4)_2$) = 76% (22 mg).

Reaction of [(Py2ald)Fe(SPh)] ($\mathbf{1a^{Fe}}$) with PhC(O)Cl. 20.5 mg (0.04 mmol) of $\mathbf{1a^{Fe}}$ and 5.6 mg (0.04 mmol) of PhC(O)Cl in MeCN. Yield of ($\mathbf{5^{Fe}}(BPh_4)_2$) = 59% (17 mg).

Reaction of [(Py2ald)Fe(SPh)] ($\mathbf{1a^{Fe}}$) with $\mathbf{CH_2Br_2}$. 20.5 mg (0.04 mmol) of $\mathbf{1a^{Fe}}$ and 3.5 mg (0.03 mmol) of CH_2Br_2 in DMF. Yield ($\mathbf{5^{Fe}}(BPh_4)_2$) = 87% (25.1 mg).

Reaction of [(Py2ald)Fe(SePh)] ($\mathbf{2^{Fe}}$) with MeI. 22.3 mg (0.04 mmol) of $\mathbf{2^{Fe}}$ and 5.7 mg (0.04 mmol) of MeI in DMF. Yield ($\mathbf{5^{Fe}}(BPh_4)_2$) = 34% (9.8 mg).

Reaction of [(Py2ald)Fe(SePh)] ($\mathbf{2^{Fe}}$) with $\mathbf{PhCH_2Br}$. 22.3 mg (0.04 mmol) of $\mathbf{2^{Fe}}$ and 6.8 mg (0.04 mmol) of $PhCH_2Br$ in DMF. Yield ($\mathbf{5^{Fe}}(BPh_4)_2$) = 58% (16.7 mg).

Reaction of [(Py2ald)Fe(SePh)] ($\mathbf{2^{Fe}}$) with MeC(O)Cl. 22.3 mg (0.04 mmol) of $\mathbf{2^{Fe}}$ and 3.1 mg (0.04 mmol) of MeC(O)Cl in DMF. Yield ($\mathbf{5^{Fe}}(BPh_4)_2$) = 43% (12.4 mg).

Reaction of [(Py2ald)Fe(SePh)] ($\mathbf{2^{Fe}}$) with PhC(O)Cl. 22.3 mg (0.04 mmol) of $\mathbf{2^{Fe}}$ and 5.6 mg (0.04 mmol) of PhC(O)Cl in MeCN. Yield ($\mathbf{5^{Fe}}(BPh_4)_2$) = 55% (15.9 mg).

Reaction of [(Py2ald)Fe(SePh)] ($\mathbf{2^{Fe}}$) with $\mathbf{CH_2Br_2}$. 22.3 mg (0.04 mmol) of $\mathbf{2^{Fe}}$ and 3.5 mg (0.03 mmol) of CH_2Br_2 in DMF. Yield ($\mathbf{5^{Fe}}(BPh_4)_2$) = 83% (24 mg).

Experimental Procedure for the Transfer of Reactive Sulfur/Selenium Species.

Reaction of [(Py2ald)Zn(SPh)] ($\mathbf{1a^{Zn}}$) with $\mathbf{S_8}$ and MeI. To a solution of 20.8 mg (0.04 mmol) of $\mathbf{1a^{Zn}}$ in 1 mL of DMF was added 5.1 mg (0.02 mmol) of S_8 and the solution was allowed to stir for 4h. After that 5.7 mg (0.04 mmol) of Iodomethane (MeI) was added to the reaction mixture and the solution was allowed to stir overnight. Following this, 6.6 mg (0.06 mmol) of sodium tetrafluoroborate ($NaBF_4$) was added into the reaction mixture and further stirred for an additional 2 hours. The reaction mixture was then filtered through Celite. Et_2O was subsequently added to the filtrate until the complete precipitation of the metal complex occurred. The solution was then again filtered through Celite. The resulting solid residue was washed twice with 2 mL of Et_2O and the remaining solution was kept for GC-MS experiment.

The solid product was then dried under vacuum, dissolved in a mixture of 0.5 mL MeOH and 0.5 mL EtOH and the resulting solution was filtered through Celite. Et_2O was allowed to diffuse into the filtrate at 0°C overnight to obtain the product as yellow, needle-shaped, crystals of $[(Py2ald)Zn]_2(BF_4)_2$ ($\mathbf{5^{Zn}}(BF_4)_2$) in 53% yield (10.6 mg). The compound, $\mathbf{5^{Zn}}(BF_4)_2$, was identified by ^1H NMR spectroscopy and mass spectrometry.

A similar procedure was followed for the following reactions using the specified amount of the reactants. The compound, $\mathbf{5^{Zn}}(BF_4)_2$, was identified by ^1H NMR spectroscopy and mass spectrometry in each case.

Reaction of [(Py2ald)Zn(SPh)] ($\mathbf{1a^{Zn}}$) with S_8 and $PhCH_2Br$. 20.8 mg (0.04 mmol) of $\mathbf{1a^{Zn}}$, 5.1 mg (0.02 mmol) of S_8 and 6.8 mg (0.04 mmol) of $PhCH_2Br$ in DMF. Yield of $\mathbf{5^{Zn}}(BF_4)_2$ = 51% (10.2 mg).

Reaction of [(Py2ald)Zn(SC_6H_4-2,6-Me_2)] ($\mathbf{1b^{Zn}}$) with S_8 and MeI. 21.92 mg (0.04 mmol) of $\mathbf{1b^{Zn}}$, 5.1 mg (0.02 mmol) of S_8 and 5.7 mg (0.04 mmol) of MeI in DMF. Yield of $\mathbf{5^{Zn}}(BF_4)_2$ = 55% (11 mg).

Reaction of [(Py2ald)Zn(SC_6H_4-2,6-Me_2)] ($\mathbf{1b^{Zn}}$) with S_8 and $PhCH_2Br$. 21.92 mg (0.04 mmol) of $\mathbf{1b^{Zn}}$, 5.1 mg (0.02 mmol) of S_8 and 6.8 mg (0.04 mmol) of $PhCH_2Br$ in DMF. Yield of $\mathbf{5^{Zn}}(BF_4)_2$ = 47% (9.4 mg).

Reaction of [(Py2ald)Zn(SePh)] ($\mathbf{2^{Zn}}$) with S_8 and MeI. 22.7 mg (0.04 mmol) of $\mathbf{2^{Zn}}$, 5.1 mg (0.02 mmol) of S_8 and 5.7 mg (0.04 mmol) of MeI in DMF. Yield of $\mathbf{5^{Zn}}(BF_4)_2$ = 48% (9.6 mg).

Reaction of [(Py2ald)Zn(SePh)] ($\mathbf{2^{Zn}}$) with S_8 and EtBr. 22.7 mg (0.04 mmol) of $\mathbf{2^{Zn}}$, 5.1 mg (0.02 mmol) of S_8 and 4.35 mg (0.04 mmol) of EtBr in DMF. Yield of $\mathbf{5^{Zn}}(BF_4)_2$ = 53% (10.6 mg).

Reaction of [(Py2ald)Fe(SPh)] ($\mathbf{1a^{Fe}}$) with S_8 and MeI. To a solution of 20.5 mg (0.04 mmol) of $\mathbf{1a^{Fe}}$ in 1 mL of DMF was added 5.1 mg (0.02 mmol) of S_8 and the solution was allowed to stir for 4h. After that 5.7 mg (0.04 mmol) of Iodomethane (MeI) was added to the reaction

mixture and the solution was allowed to stir overnight. The reaction mixture was then filtered through Celite. Et_2O was subsequently added to the filtrate until the complete precipitation of the metal complex occurred. The solution was then again filtered through Celite. The resulting solid residue was washed twice with 2 mL of Et_2O and the remaining solution was kept for GC-MS experiment. The solid product was then dried under vacuum and dissolved in 1 mL MeOH. Following this, 20.5 mg (0.06 mmol) of sodium tetraphenylborate ($NaBPh_4$) was added into the solution and further stirred for an additional 30 min. During this period, immediate precipitation of a brown solid was observed. Then the brown solid is separated from the reaction mixture and washed twice with MeOH and Et_2O and dried under vacuum. The solid was then redissolved in DMF and filtered through Celite. Et_2O was allowed to diffuse into the filtrate at 0°C overnight to obtain the product as brown, needle-shaped, crystals of $[(Py2ald)Fe]_2(BPh_4)_2$ ($\mathbf{5^{Fe}}(BPh_4)_2$) in 61% yield (17.6 mg).

A similar procedure was followed for the following reactions using the specified amount of the reactants. The compound, $\mathbf{5^{Fe}}(BPh_4)_2$, was identified by unit cell determination of the single crystals and mass spectrometry in each case.

Reaction of [(Py2ald)Fe(SPh)] ($\mathbf{1a^{Fe}}$) with S_8 and $PhCH_2Br$. 20.5 mg (0.04 mmol) of $\mathbf{1a^{Fe}}$, 5.1 mg (0.02 mmol) of S_8 and 6.8 mg (0.04 mmol) of $PhCH_2Br$ in DMF. Yield of $\mathbf{5^{Fe}}(BPh_4)_2$ = 62% (17.9 mg).

Reaction of [(Py2ald)Fe(SC_6H_4-2,6-Me_2)] ($\mathbf{1b^{Fe}}$) with S_8 and MeI. 21.58 mg (0.04 mmol) of $\mathbf{1b^{Fe}}$, 5.1 mg (0.02 mmol) of S_8 and 5.7 mg (0.04 mmol) of MeI in DMF. Yield of $\mathbf{5^{Fe}}(BPh_4)_2$ = 59% (17 mg).

Reaction of [(Py2ald)Fe(SC_6H_4-2,6-Me_2)] ($\mathbf{1b^{Fe}}$) with S_8 and $PhCH_2Br$. 21.58 mg (0.04 mmol) of $\mathbf{1b^{Fe}}$, 5.1 mg (0.02 mmol) of S_8 and 6.8 mg (0.04 mmol) of $PhCH_2Br$ in DMF. Yield of $\mathbf{5^{Fe}}(BPh_4)_2$ = 61% (17.6 mg).

Reaction of [(Py2ald)Fe(SePh)] (2^{Fe}) with S_8 and MeI. 22.3 mg (0.04 mmol) of $\mathbf{2^{Fe}}$, 5.1 mg (0.02 mmol) of S_8 and 5.7 mg (0.04 mmol) of MeI in DMF. Yield of $\mathbf{5^{Fe}}(BPh_4)_2$ = 56% (16.2 mg).

Reaction of [(Py2ald)Fe(SePh)] (2^{Fe}) with S_8 and EtBr. 22.3 mg (0.04 mmol) of $\mathbf{2^{Fe}}$, 5.1 mg (0.02 mmol) of S_8 and 4.35 mg (0.04 mmol) of EtBr in DMF. Yield of $\mathbf{5^{Fe}}(BPh_4)_2$ = 49% (14.2 mg).

Reaction of [{(Py2ald)Fe}$_2$](BF$_4$)$_2$ (5^{Fe}(BF$_4$)$_2$) with 2 equiv of (Cp$_2$Fe)(BF$_4$) and (Bu$_4$N)(NO$_2$). To a solution of $\mathbf{5^{Fe}}(BF_4)_2$ (20 mg, 0.02 mmol) in MeCN (~0.3 mL) was added a solution of $(Cp_2Fe)(BF_4)$ (10.9 mg, 0.04 mmol) in MeCN (~4 mL) and the solution was allowed to stir overnight. Then a solution of $(Bu_4N)(NO_2)$ (11.5 mg, 0.04 mmol) in MeCN (~0.3 mL) was added into the reaction mixture and allowed it to stir for 4 h. The reaction mixture was then evaporated to dryness and the brown solid residue thus obtained was washed twice with 2 mL of Et_2O. The solid product was then dried under vacuum, dissolved in a mixture of CH_2Cl_2 and EtOH and the resulting solution was filtered through Celite. Et_2O was allowed to diffuse into the filtrate at 0°C overnight to obtain the product as brown, needle-shaped, crystals (13 mg, 62%). The compound was identified to be [{(Py2ald)(ONO)Fe}$_2$-μ_2-O] ($\mathbf{8^{Fe}}$) by unit cell determination of the single crystals.

Reaction of [{(Py2ald)(ONO)Fe}$_2$-μ_2-O] (8^{Fe}) with 4 equiv of Cp$_2$Co. To a solution of 36.5 mg (0.04 mmol) of $\mathbf{8^{Fe}}$ in 0.5 mL of CH_2Cl_2 was added a solution of 30.3 mg (0.16 mmol) of Cp_2Co in 0.5 mL of CH_2Cl_2 and the solution was allowed to stir overnight. The reaction mixture was then evaporated to dryness and the brown-colored solid residue thus obtained was washed twice with 2 mL of Et_2O. The solid product was then dried under vacuum and dissolved in 1 mL MeOH. Following this, 20.5 mg (0.06 mmol) of sodium tetraphenylborate ($NaBPh_4$) was added into the solution and further stirred for an additional 30 min. During this period, immediate precipitation of a brown solid was observed. Then the brown solid was separated

from the reaction mixture and washed twice with MeOH and Et_2O and dried under vacuum. The solid was then dissolved in DMF and filtered through Celite. Et_2O was allowed to diffuse into the filtrate at 0°C overnight to obtain the product as brown, needle-shaped, crystals (44 mg, 76%). The compound was identified to be $[\{(Py2ald)Fe\}_2](BPh_4)_2$ ($\mathbf{5^{Fe}}(BPh_4)_2$) by unit cell determination of the single crystals.

Reaction of [(Py2ald)Zn(SPh)] ($\mathbf{1a^{Zn}}$) with (Cp_2Fe)(BF_4). To a solution of 20.8 mg (0.04 mmol) of $\mathbf{1a^{Zn}}$ in 0.5 mL of CH_2Cl_2 was added a solution of 10.91 mg (0.04 mmol) of (Cp_2Fe)(BF_4) in 0.5 mL of CH_2Cl_2 and the reaction mixture was allowed to stir for 12 h. The reaction mixture was then filtered through Celite, the filtrate was evaporated to dryness and the solid residue thus obtained was washed twice with 2 mL of Et_2O. The solid product was then dried under vacuum, dissolved in a mixture of 0.5 mL MeOH and 0.5 mL EtOH and the resulting solution was filtered through Celite. Et_2O was allowed to diffuse into the filtrate at 0°C overnight to obtain the product, $[(Py2ald)Zn]_2(BF_4)_2$ ($\mathbf{5^{Zn}}(BF_4)_2$), as yellow, needle-shaped, crystals (13.2 mg, 66%). Identity of the compound was confirmed by unit cell determination of the single crystals, ^{1}H NMR spectroscopy and mass spectrometry.

Reaction of [(Py2ald)Fe(SPh)] ($\mathbf{1a^{Fe}}$) with (Cp_2Fe)(BF_4). To a solution of 20.5 mg (0.04 mmol) of $\mathbf{1a^{Fe}}$ in 0.5 mL of CH_2Cl_2 was added a solution of 10.91 mg (0.04 mmol) of (Cp_2Fe)(BF_4) in 0.5 mL of CH_2Cl_2 and the reaction mixture was allowed to stir for 12 h. The reaction mixture was then filtered through Celite, the filtrate was evaporated to dryness and the solid residue thus obtained was washed twice with 2 mL of Et_2O. The solid product was then dried under vacuum and dissolved in 1 mL MeOH. $NaBPh_4$ (20.5 mg, 0.06 mmol) was added into the solution and the solution was stirred for an additional 30 min. During this period, immediate precipitation of a brown solid was observed. Then the brown solid was separated from the reaction mixture, washed twice with MeOH and Et_2O and dried under vacuum. The solid was then dissolved in DMF and filtered through Celite. Et_2O was allowed to diffuse into

the filtrate at 0°C overnight to obtain the product, [{(Py2ald)Fe}$_2$](BPh$_4$)$_2$ (**5**^{Fe}(BPh$_4$)$_2$), as brown, needle-shaped, crystals (20.5 mg, 71%). Identity of the compound was confirmed by unit cell determination of the single crystals and mass spectrometry.

Reaction of [(Py2ald)Fe(2,6-Me$_2$-C$_6$H$_3$S)] (1b^{Fe}) with (Cp$_2$Fe)(BF$_4$). A procedure similar to that described above for the reaction of **1a**^{Fe} with (Cp$_2$Fe)(BF$_4$) was followed but by using **1b**^{Fe} (21.58 mg , 0.04 mmol), (Cp$_2$Fe)(BF$_4$) (10.91 mg, 0.04 mmol) and NaBPh$_4$ (20.5 mg, 0.06 mmol). Identity of the product, [{(Py2ald)Fe}$_2$](BPh$_4$)$_2$ (**5**^{Fe}(BPh$_4$)$_2$), (16.6 mg, 68%) was confirmed by unit cell determination of the single crystals and mass spectrometry.

Reaction of [(Py2ald)Fe(SePh)] (2^{Fe}) with (Cp$_2$Fe)(BF$_4$). A procedure similar to that described above for the reaction of **1a**^{Fe} with (Cp$_2$Fe)(BF$_4$) was followed but by using **2**^{Fe} (22.3 mg, 0.04 mmol), (Cp$_2$Fe)(BF$_4$) (10.91 mg, 0.04 mmol) and NaBPh$_4$ (20.5 mg, 0.06 mmol). Identity of the product, [{(Py2ald)Fe}$_2$](BPh$_4$)$_2$ (**5**^{Fe}(BPh$_4$)$_2$), (21.6 mg, 75%) was confirmed by unit cell determination of the single crystals and mass spectrometry.

Table S1. Unit cell parameters for $\mathbf{5}^{\mathbf{Zn}}(BF_4)_2$ obtained from different reactions.

Reactions (in the presence of $NaBF_4$)	**Unit cell parameters**						
	a (Å)	b (Å)	c (Å)	α (°)	β (°)	γ (°)	V $(Å)^3$
$\mathbf{1a}^{\mathbf{Zn}}$ + MeI	9.63	10.14	10.45	103.14°	90.22°	91.44°	993
$\mathbf{1a}^{\mathbf{Zn}}$ + $PhCH_2Br$	9.87	10.10	10.51	105.21°	90.94°	91.21°	1011
$\mathbf{1a}^{\mathbf{Zn}}$ + MeC(O)Cl	9.84	10.15	10.56	105.00°	90.92°	91.31°	1018
$\mathbf{1a}^{\mathbf{Zn}}$ + PhC(O)Cl	9.87	10.12	10.50	105.66°	90.62°	91.45°	1010
$\mathbf{1a}^{\mathbf{Zn}}$ + CH_2Br_2	9.87	10.10	10.51	105.21°	90.94°	91.21°	1011
$\mathbf{2}^{\mathbf{Zn}}$ + MeI	9.86	10.31	10.43	104.23°	90.58°	91.50°	1027
$\mathbf{2}^{\mathbf{Zn}}$ + $PhCH_2Br$	9.85	10.29	10.50	104.24°	90.64°	91.75°	1031
$\mathbf{2}^{\mathbf{Zn}}$ + MeC(O)Cl	9.86	10.15	10.46	104.95°	90.99°	91.58°	1010
$\mathbf{2}^{\mathbf{Zn}}$ + PhC(O)Cl	9.86	10.22	10.38	105.35°	90.77°	91.79°	1008
$\mathbf{2}^{\mathbf{Zn}}$ + CH_2Br_2	9.90	10.29	10.45	104.75°	90.87°	91.77°	1029
$\mathbf{1a}^{\mathbf{Zn}}$ + S_8 + MeI	10.06	10.13	10.48	104.23°	91.61°	92.49°	1027
$\mathbf{1a}^{\mathbf{Zn}}$ + S_8 + $PhCH_2Br$	9.94	10.09	10.44	105.01°	90.58°	91.54°	1011
$\mathbf{1b}^{\mathbf{Zn}}$ + S_8 + MeI	9.89	10.17	10.50	105.31°	90.57°	91.62°	1018
$\mathbf{1b}^{\mathbf{Zn}}$ + S_8 + $PhCH_2Br$	9.93	10.09	10.44	104.93°	90.66°	91.61°	1011
$\mathbf{2}^{\mathbf{Zn}}$ + S_8 + MeI	9.88	10.09	10.49	105.62°	90.55°	91.79°	1006
$\mathbf{2}^{\mathbf{Zn}}$ + S_8 + EtBr	9.91	10.14	10.50	105.78°	91.07°	91.78°	1015
$\mathbf{1a}^{\mathbf{Zn}}$ + $(Cp_2Fe)(BF_4)$	9.81	10.34	10.37	105.41°	91.30°	90.46°	1014
$\mathbf{3}^{\mathbf{Zn}}$ + 2 equiv $PhCH_2SH$	9.93	10.19	10.49	104.85°	90.71°	91.29°	1026
$\mathbf{3}^{\mathbf{Zn}}$ + 1 equiv PhSH	9.91	10.11	10.50	105.27°	90.80°	91.96°	1013
Authentic sample of $\mathbf{5}^{\mathbf{Zn}}(BF_4)_2$	9.8506	10.1305	10.4984	105.549°	90.387°	91.566°	1008.8

Table S2. Unit cell parameters for **1a^{Zn}** obtained from different reactions.

Reactions	Unit cell parameters						
	a (Å)	b (Å)	c (Å)	α (°)	β (°)	γ (°)	V (Å)^3
3^{Zn} + 2 equiv PhSH	10.59	12.13	19.06	90°	90°	90°	2447
3^{Zn} + 1 equiv NaSPh	10.44	12.05	18.60	90°	90°	90°	2339
Authentic sample of **1a^{Zn}**	19.047	12.115	10.586	90°	90°	90°	2442.7

Table S3. Unit cell parameters for **2^{Zn}** obtained from different reactions.

Reactions	Unit cell parameters						
	a (Å)	b (Å)	c (Å)	α (°)	β (°)	γ (°)	V (Å)^3
3^{Zn} + 2 equiv PhSeH	10.38	12.10	19.18	90°	90°	90°	2410
Authentic sample of **2^{Zn}**	19.1361	12.0931	10.4127	90°	90°	90°	2409.65

Table S4. Unit cell parameters for **3^{Zn}** obtained from different reactions.

Reactions	Unit cell parameters						
	a (Å)	b (Å)	c (Å)	α (°)	β (°)	γ (°)	V (Å)^3
3^{Zn} + 2 equiv ^{t}BuSH	11.91	15.52	21.30	90°	90°	90°	3936
Authentic sample of **3^{Zn}**	15.507	11.929	21.331	90°	90°	90°	3945.9

Table S5. Unit cell parameters for $\mathbf{5}^{Fe}(BPh_4)_2$ obtained from different reactions.

Reaction (in the presence of $NaBPh_4$)	**Unit cell parameters**						
	a (Å)	b (Å)	c (Å)	α (°)	β (°)	γ (°)	V $(Å)^3$
$\mathbf{1a}^{Fe}$ + MeI	11.29	12.60	14.94	103.51°	110.11°	104.92°	1803
$\mathbf{1a}^{Fe}$ + $PhCH_2Br$	11.27	12.60	14.92	103.29°	110.22°	105.02°	1796
$\mathbf{1a}^{Fe}$ + MeC(O)Cl	11.26	12.59	14.89	103.27°	110.27°	105.08°	1789
$\mathbf{1a}^{Fe}$ + PhC(O)Cl	11.26	12.60	14.91	103.26°	110.25°	105.05°	1794
$\mathbf{1a}^{Fe}$ + CH_2Br_2	11.27	12.61	14.92	103.17°	110.12°	105.07°	1798
$\mathbf{2}^{Fe}$ + MeI	11.26	12.59	14.90	103.26°	110.27°	105.08°	1789
$\mathbf{2}^{Fe}$ + $PhCH_2Br$	11.30	12.63	14.96	103.40°	110.12°	104.97°	1812
$\mathbf{2}^{Fe}$ + MeC(O)Cl	11.26	12.61	14.90	103.23°	110.24°	105.10°	1794
$\mathbf{2}^{Fe}$ + PhC(O)Cl	11.26	12.59	14.89	103.33°	110.18°	105.04°	1792
$\mathbf{2}^{Fe}$ + CH_2Br_2	11.28	12.63	14.91	103.25°	110.21°	105.12°	1800
$\mathbf{1a}^{Fe}$ + S_8 + MeI	11.30	12.65	14.94	103.37°	110.06°	104.99°	1831
$\mathbf{1a}^{Fe}$ + S_8 + $PhCH_2Br$	11.29	12.62	14.94	103.34°	110.13°	105.00°	1807
$\mathbf{1b}^{Fe}$ + S_8 + MeI	11.28	12.62	14.90	103.17°	110.25°	105.19°	1798
$\mathbf{1b}^{Fe}$ + S_8 + $PhCH_2Br$	11.31	12.65	14.95	103.39°	110.06°	104.99°	1817
$\mathbf{2}^{Fe}$+ S_8 + MeI	11.26	12.60	14.90	103.26°	110.27°	105.06°	1791
$\mathbf{2}^{Fe}$+ S_8 + EtBr	11.28	12.61	14.93	103.26°	110.24°	105.03°	1801
$\mathbf{1a}^{Fe}$ + $(Cp_2Fe)(BF_4)$	11.27	12.62	14.90	103.06°	110.31°	105.20°	1797
$\mathbf{1b}^{Fe}$ + $(Cp_2Fe)(BF_4)$	11.28	12.63	14.89	103.05°	110.28°	105.22°	1798
$\mathbf{2}^{Fe}$ + $(Cp_2Fe)(BF_4)$	11.30	12.66	14.94	103.30°	110.13°	105.04°	1815
$\mathbf{8}^{Fe}$ + 4 equiv PhSH	11.30	12.64	14.95	103.45°	110.10°	105.02°	1812
$\mathbf{8}^{Fe}$ + 4 equiv PhSeH	11.27	12.62	14.90	103.06°	110.31°	105.20°	1797
$\mathbf{8}^{Fe}$ + 4 equiv Cp_2Co	11.27	12.61	14.92	103.15°	110.27°	105.10°	1800
Authentic sample of $\mathbf{5}^{Fe}(BPh_4)_2$	11.1974	12.5730	14.8997	103.670°	110.022°	104.957°	1778.1

Table S6. Unit cell parameters for $\mathbf{8^{Fe}}$ obtained from different reactions.

Reactions	**Unit cell parameters**						
	a (Å)	b (Å)	c (Å)	α (°)	β (°)	γ (°)	V $(Å)^3$
$\mathbf{1a^{Fe}}$ + 3 equiv $(Bu_4N)(NO_2)$	10.63	15.39	14.45	90°	98.79°	90°	2336
$\mathbf{2^{Fe}}$ + 3 equiv $(Bu_4N)(NO_2)$	10.60	15.74	14.65	90°	99.78°	90°	2409
$\mathbf{5^{Fe}}(BPh_4)_2$ + 2 equiv $(Cp_2Fe)(BF_4)$ + 2 equiv $(Bu_4N)(NO_2)$	10.81	15.56	14.51	90°	100.42°	90°	2400
Authentic sample of $\mathbf{8^{Fe}}$	10.613	15.673	14.617	90°	100.532°	90°	2390.5

Table S7. Unit cell parameters for $\mathbf{1a^{Fe}}$ obtained from different reactions.

Reactions	**Unit cell parameters**						
	a (Å)	b (Å)	c (Å)	α (°)	β (°)	γ (°)	V $(Å)^3$
$\mathbf{8^{Fe}}$ + 6 equiv PhSH	10.44	12.04	19.04	90°	90°	90°	2393
Authentic sample of $\mathbf{1a^{Fe}}$	19.0369	12.0159	10.4305	90°	90°	90°	2385.9

Table S8. Unit cell parameters for $\mathbf{2^{Fe}}$ obtained from different reactions.

Reactions	**Unit cell parameters**						
	a (Å)	b (Å)	c (Å)	α (°)	β (°)	γ (°)	V $(Å)^3$
$\mathbf{8^{Fe}}$ + 6 equiv PhSeH	10.47	12.06	19.07	90°	90°	90°	2410
Authentic sample of $\mathbf{2^{Fe}}$	19.172	12.076	10.439	90°	90°	90°	2416.7

Table S9. Yields (GC) of products obtained by the transfer of reactive sulfur / selenium species (generated insitu by selected Zn(II) and Fe(II) compounds and elemental sulfur/selenium).

reactants	reactive sulfur / selenium species and by-products (yield)	
	MeI	$PhCH_2Br$ / EtBr (for $\mathbf{2^{Zn/Fe}}$)
$\mathbf{1a^{Zn}}$ + S_8	Me-S-S-Ph (46%) Me-S-S-S-Me (3%) Me-S-Ph (8%) PhS-SPh (18%)	$PhCH_2$-S-S-Ph (58%) $PhCH_2$-S-S-S-CH_2Ph (3%) $PhCH_2$-S-S-CH_2Ph (8%) $PhCH_2$-S-Ph (5%), PhS-SPh (18%)
$\mathbf{1b^{Zn}}$ + S_8	Me-S-S-2,6-Me_2-C_6H_4 (46%) (2,6-Me_2-C_6H_4-S)$_2$ (15%)	$PhCH_2$-S-S-2,6-Me_2-C_6H_4 (38%) (2,6-Me_2-C_6H_4-S)$_2$ (5%)
$\mathbf{1a^{Fe}}$ + S_8	Me-S-S-Ph (58%) PhS-SPh (18%)	$PhCH_2$-S-S-Ph (61%) $PhCH_2$-S-Ph (5%) PhS-SPh (16%)
$\mathbf{1b^{Fe}}$ + S_8	Me-S-S-2,6-Me_2-C_6H_4 (62%) (2,6-Me_2-C_6H_4-S)$_2$ (15%)	$PhCH_2$-S-S-2,6-Me_2-C_6H_4 (71%) (2,6-Me_2-C_6H_4-S)$_2$ (11%)
$\mathbf{2^{Zn}}$ + S_8	Me-S-Se-Ph (11%) Ph-Se-Se-Ph (24%) Me-S-S-S-S-Me (13%)	Et-S-Se-Ph (13%) Et-S-S-S-Et (11%) Et-Se-Ph (4%) Ph-Se-Se-Ph (33%)
$\mathbf{2^{Fe}}$ + S_8	Me-S-Se-Ph (14%) Ph-Se-Se-Ph (30%)	Et-S-Se-Ph (15%) Et-S-S-S-Et (13%) Ph-Se-Se-Ph (34%)

Table S10. X-ray crystallographic data for compounds $\mathbf{1a^{Zn}}$, $\mathbf{1b^{Zn}}$, $\mathbf{2^{Zn}}$, $\mathbf{3^{Zn}}$, $\mathbf{4^{Zn}}$, $\mathbf{5^{Zn}}(BF_4)_2$, $\mathbf{6^{Zn}}$ and $\mathbf{7^{Zn}}$.[a]

Compounds	$\mathbf{1a^{Zn}}$	$\mathbf{1b^{Zn}}$	$\mathbf{2^{Zn}}$	$\mathbf{3^{Zn}}$	$\mathbf{4^{Zn}}$	$\mathbf{5^{Zn}}(BF_4)_2$	$\mathbf{6^{Zn}}$	$\mathbf{7^{Zn}}$
CCDC deposition number	2191754	2236890	2208800	2286781	2265576	2226860	2265573	2281940
temp (K)	273	147	145	150	149	146	297	148
formula	$C_{27}H_{25}N_3O_2SZn$	$C_{29}H_{29}N_3O_2SZn$	$C_{27}H_{25}N_3O_2SeZn$	$C_{21}H_{20}N_4O_4Zn$	$C_{21}H_{21}Br_2N_3O_2Zn$	$C_{42}H_{40}B_2F_8N_6O_4Zn_2$	$C_{21}H_{20}BrN_3O_2Zn$	$C_{25}H_{21}N_5O_2S_2Zn$
formula weight	520.93	548.98	567.83	457.78	572.60	997.16	491.68	552.96
Crystal system	orthorhombic	monoclinic	orthorhombic	orthorhombic	triclinic	triclinic	orthorhombic	monoclinic
space group	$Pca2_1$	$P2_1/n$	$Pca2_1$	Pbca	$P\bar{1}$	$P\bar{1}$	Pbca	$P2_1/n$
a, Å	19.047(6)	11.2316(14)	19.1361(8)	15.507(4)	7.734(2)	9.8506(14)	15.2257(12)	9.4688(5)
b, Å	12.115(4)	14.8312(18)	12.0931(5)	11.929(3)	8.957(3)	10.1305(15)	12.0543(9)	13.1273(8)
c, Å	10.586(4)	15.672(2)	10.4127(4)	21.331(5)	16.769(5)	10.4984(13)	21.5492(17)	20.2985(11)
α, deg	90	90	90	90	96.920(10)	105.549(12)	90	90
β, deg	90	103.532(13)	90	90	92.869(10)	90.387(11)	90	97.877(2)
γ, deg	90	90	90	90	92.869(10)	91.566(12)	90	90
V, $Å^3$	2442.7(14)	2538.1(6)	2409.65(17)	3945.9(17)	1062.3(5)	1008.8(2)	3955.0(5)	2499.3(2)
Z	4	4	4	8	2	1	8	4
ρ_{calcd}, gm/cm^3	1.417	1.437	1.565	1.541	1.790	1.641	1.651	1.470
μ, mm^{-1}	1.120	1.082	2.560	1.282	4.940	1.279	3.284	1.182
θ range, deg	1.992-25.889	1.916-25.681	2.715-25.722	2.318-25.026	2.600-25.718	2.866-25.026	2.353-25.703	2.267-25.703
completeness to θ, %	1.000	0.998	0.998	0.998	0.988	0.982	0.992	0.998
reflections collected	38165	23582	26224	28645	10448	8880	41854	26743
independent reflections	4728	4813	4240	3477	4001	3498	3740	4744
R(int)	0.0690	0.1444	0.0579	0.1141	0.0428	0.0865	0.0514	0.0648
Restraints [b]	1	0	1	5	0	0	0	0
parameters	309	328	309	270	257	290	255	264
Max., min. transmission	0.7453, 0.5752	1.00000, 0.25991	0.7453, 0.5300	0.7452, 0.6011	0.7453, 0.4585	1.00000, 0.61984	0.7453, 0.5103	0.7453, 0.6076
R1[c](wR2)[d] [I>2sigma(I)]	0.0309 (0.0567)	0.0777 (0.1676)	0.0289 (0.0550)	0.0451 (0.1051)	0.0399 (0.1045)	0.0757 (0.1615)	0.0262 (0.0611)	0.0805 (0.2142)
R1[c](wR2)[c]	0.0551 (0.0640)	0.1338 (0.2056)	0.0371 (0.0584)	0.0735 (0.1249)	0.0461 (0.1084)	0.1155 (0.1864)	0.0366 (0.0656)	0.1220 (0.2486)
GOF(F2)[e]	1.009	1.024	1.048	1.037	1.020	1.019	1.026	1.026
[f]max, min peaks,e.$Å^{-3}$	0.295, -0.229	0.992, -0.650	0.334, -0.264	0.439, -0.433	2.162, -0.638	0.887, -1.094	0.469, -0.380	1.667, -2.072

[a]Mo Kα radiation (λ = 0.71073 Å). [b]$\mathbf{3^{Zn}}$, disordered nitrite. [c]$R1 = \Sigma||Fo|-|Fc||/\Sigma|Fo|$. [d]$wR2 = \{\Sigma[w(Fo2-Fc2)2]/\Sigma[w(Fo2)2]\}^{1/2}$. [e]$GOF = \{\Sigma[w(Fo2-Fc2)_2]/(n-p)\}^{1/2}$, where n is the number of data and p is the number of refined parameters.[f]electron density near:$\mathbf{1a^{Zn}}$, phenyl ring of benzenethiolate; $\mathbf{1b^{Zn}}$,sulfur atom; $\mathbf{2^{Zn}}$, selenium atom;$\mathbf{3^{Zn}}$, one pyridyl ring of the ligand;$\mathbf{4^{Zn}}$, methyl group of the ligand;$\mathbf{5^{Zn}}(BF_4)_2$, zinc atom;$\mathbf{6^{Zn}}$, bromine atom; $\mathbf{7^{Zn}}$, phenyl ring of the ligand.

Table S11. X-ray crystallographic data for compounds $\mathbf{1a}^{Fe}$, $\mathbf{1b}^{Fe}$, $\mathbf{2}^{Fe}$, $\mathbf{5}^{Fe}(BPh_4)_2$ and $\mathbf{8}^{Fe}$.[a]

Compounds	$\mathbf{1a}^{Fe}$	$\mathbf{1b}^{Fe}$	$\mathbf{2}^{Fe}$	$\mathbf{5}^{Fe}(BPh_4)_2$	$\mathbf{8}^{Fe}$
CCDC deposition number	2227144	2227145	2233141	2233689	2288735
temp (K)	155	160	148	145	125
formula	$C_{27}H_{25}FeN_3O_2S$	$C_{29}H_{29}FeN_3O_2S$	$C_{27}H_{25}FeN_3O_2Se$	$C_{90}H_{76}B_2Fe_2N_6O_4$	$C_{42}H_{40}Fe_2N_8O_9$
formula weight	511.41	539.46	558.31	1438.88	912.52
Crystal system	orthorhombic	monoclinic	orthorhombic	triclinic	monoclinic
space group	$Pca2_1$	$P2_1/n$	$Pca2_1$	$P\bar{1}$	$P2_1/c$
a, Å	19.0369(15)	11.3033(5)	19.172(5)	11.1974(12)	10.613(4)
b, Å	12.0159(9)	14.9444(6)	12.076(3)	12.5730(12)	15.673(6)
c, Å	10.4305(8)	15.7897(7)	10.439(3)	14.8997(12)	14.617(6)
α, deg	90	90	90	103.670(3)	90
β, deg	90	103.715(4)	90	110.022(3)	100.532(12)
γ, deg	90	90	90	104.957(3)	90
V, $Å^3$	2385.9(3)	2591.2(2)	2416.7(11)	1778.1(3)	2390.5(16)
Z	4	4	4	1	2
ρ_{calcd}, gm/cm^3	1.424	1.383	1.534	1.344	1.268
μ, mm^{-1}	0.750	0.694	2.160	0.468	0.664
θ range, deg	2.730-25.675	1.902-25.681	2.713-25.776	2.767-25.070	2.549-25.841
completeness to θ, %	0.997	0.991	0.998	0.990	0.988
reflections collected	22153	24063	23000	16800	22154
independent reflections	4519	4868	4643	6248	4562
R(int)	0.0462	0.0440	0.0552	0.0618	0.0631
Restraints [b]	1	0	1	1	4
parameters	309	328	309	468	273
Max., min. transmission	1.00000, 0.69378	1.00000, 0.75874	0.7453, 0.6194	0.7452, 0.6730	0.7453, 0.5331
R1[c](wR2)[d] [I>2sigma(I)]	0.0305 (0.0637)	0.0296 (0.0743)	0.0305 (0.0644)	0.0659 (0.1421)	0.0545 (0.1467)
R1[c](wR2)[c]	0.0347 (0.0663)	0.0327 (0.0764)	0.0398 (0.0683)	0.1019 (0.1637)	0.0727 (0.1604)
GOF(F2)[e]	1.036	1.027	1.036	1.035	1.092
[f]max, min peaks,e.$Å^{-3}$	0.181, -0.270	0.363, -0.279	0.232, -0.373	1.401, -0.561	0.391 -0.617

[a]Mo Kα radiation (λ = 0.71073 Å). [b]$\mathbf{8}^{Fe}$, disordered nitrite and aldehyde group. [c]$R1 = \Sigma||Fo|-|Fc||/\Sigma|Fo|$. [d]$wR2 = \{\Sigma[w(Fo2-Fc2)2]/\Sigma[w(Fo2)2]\}^{1/2}$. [e]$GOF = \{\Sigma[w(Fo2-Fc2)_2]/(n-p)\}^{1/2}$, where n is the number of data and p is the number of refined parameters.[f]electron density near:$\mathbf{1a}^{Fe}$, iron atom; $\mathbf{1b}^{Fe}$, phenyl ring of the ligand; $\mathbf{2}^{Fe}$, selenium; $\mathbf{5}^{Fe}(BPh_4)_2$, phenyl ring of the ligand; $\mathbf{8}^{Fe}$, disordered nitrite.

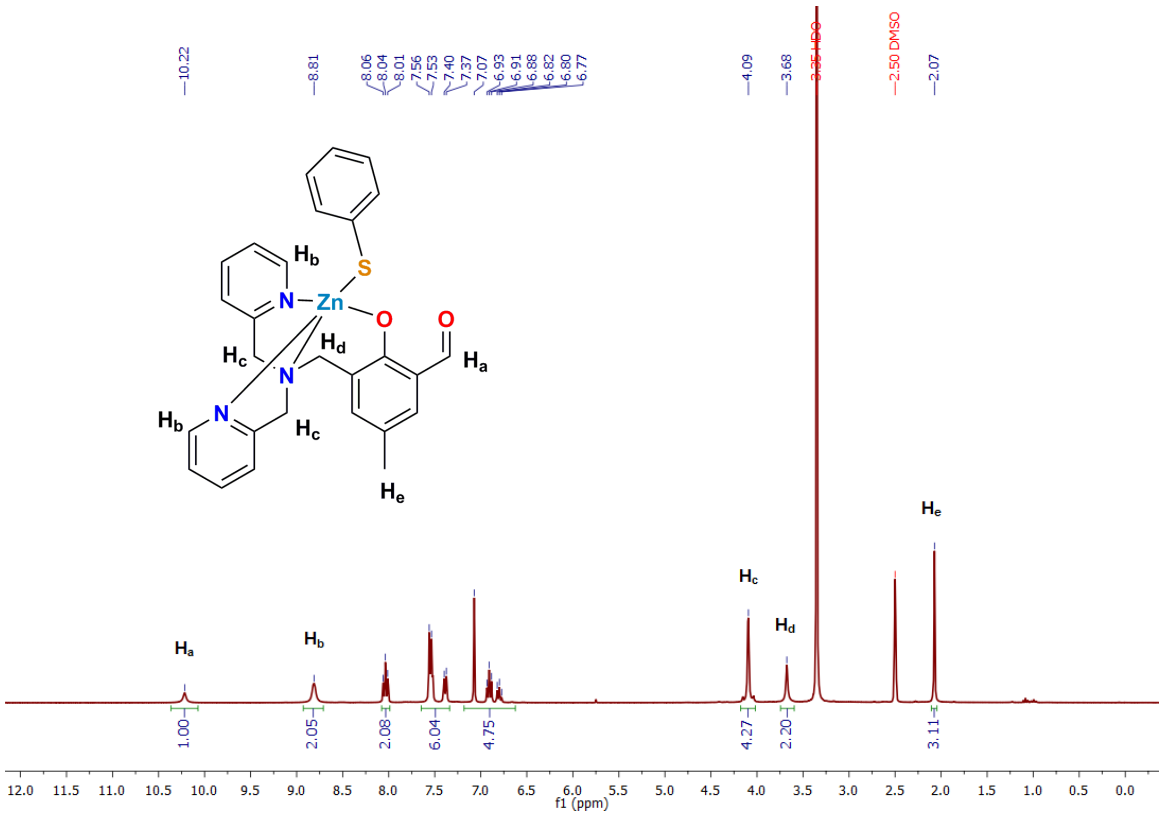

Figure S1. ^{1}H NMR (300 MHz, DMSO-d^{6}) spectrum of [(Py2ald)Zn(SPh)] (**1a^{Zn}**).

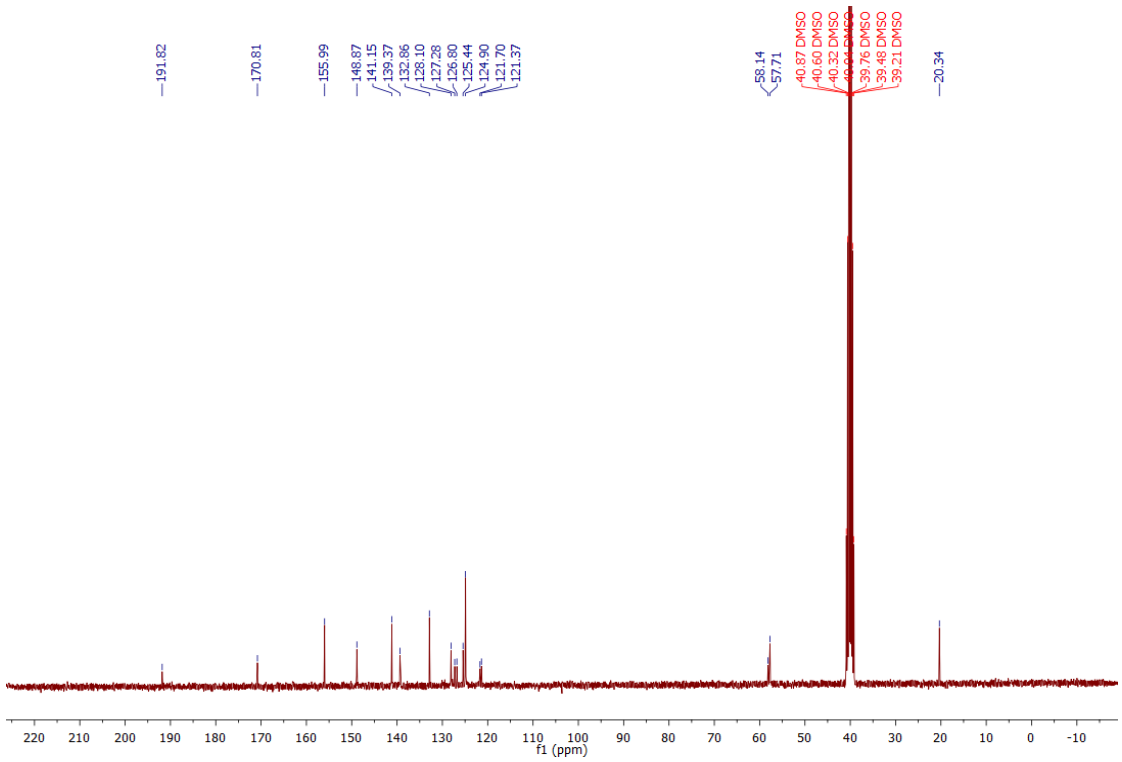

Figure S2. ^{13}C NMR (75 MHz, DMSO-d^{6}) spectrum of [(Py2ald)Zn(SPh)] (**1a^{Zn}**).

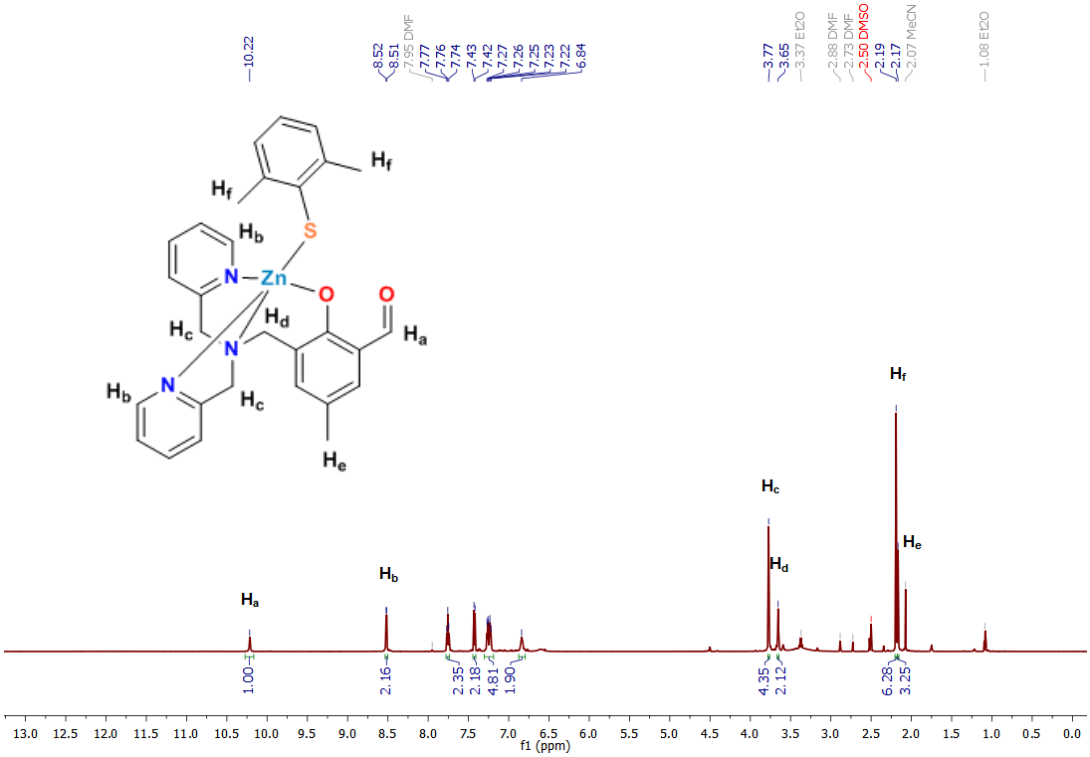

Figure S3. ^{1}H NMR (600 MHz, DMSO-d^{6}) spectrum of [(Py2ald)Zn(SC$_6$H$_4$-2,6-Me$_2$)] (**1b^{Zn}**).

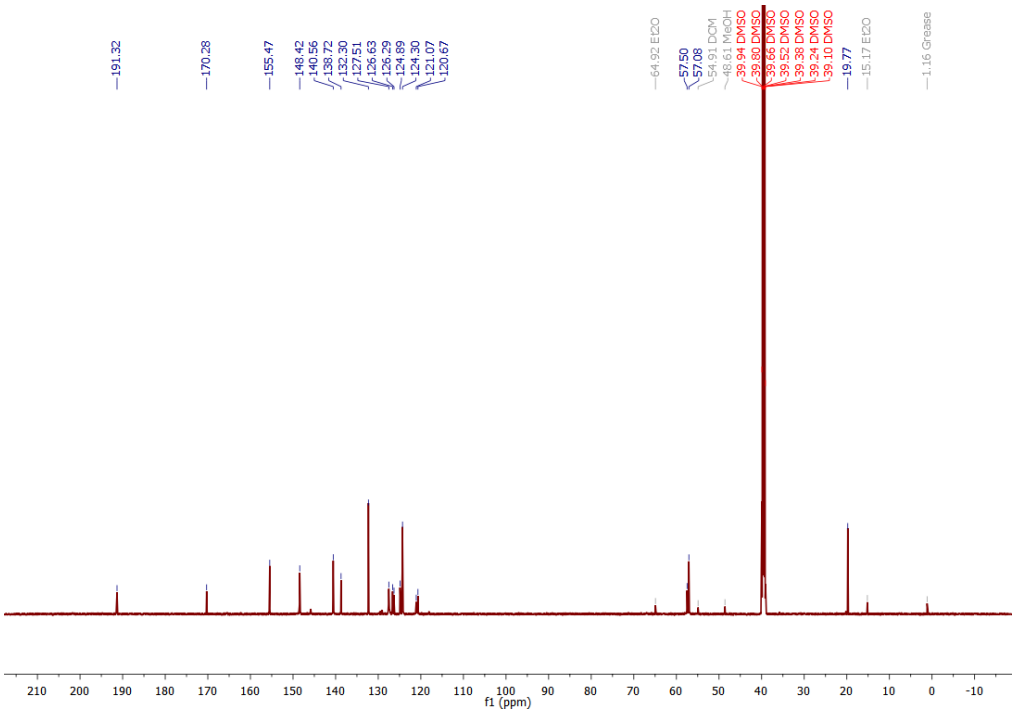

Figure S4. ^{13}C NMR (150 MHz, DMSO-d^{6}) spectrum of [(Py2ald)Zn(SC$_6$H$_4$-2,6-Me$_2$)] (**1b^{Zn}**).

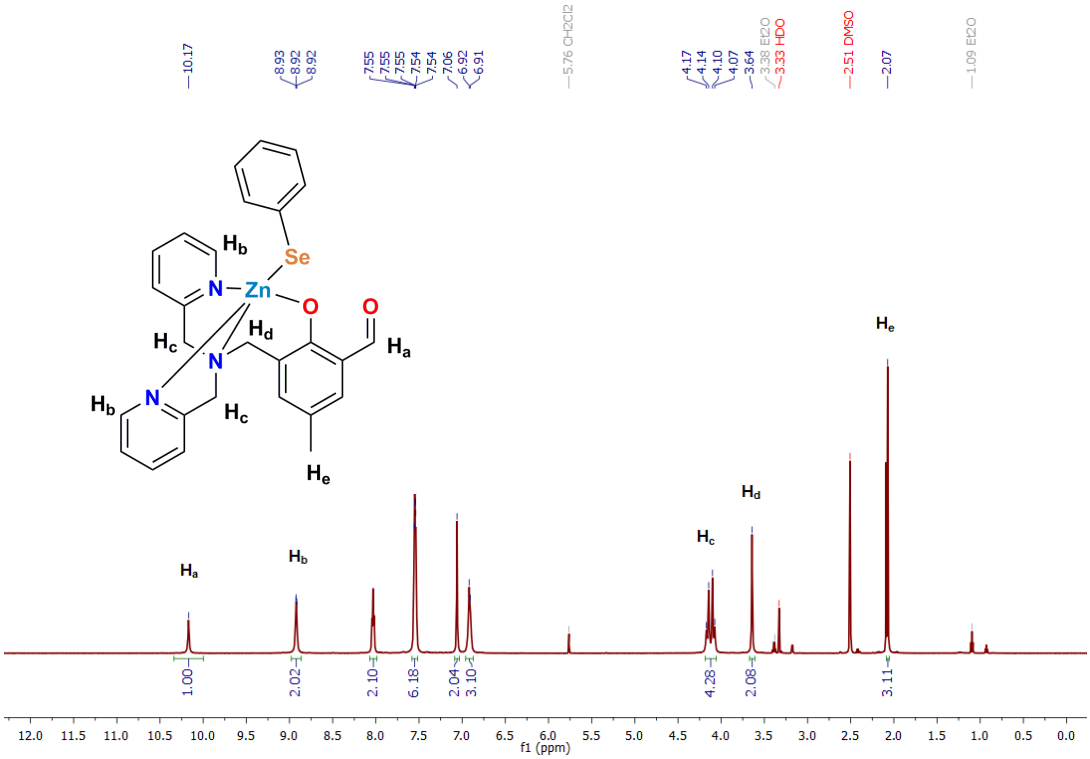

Figure S5. ^{1}H NMR (600 MHz, DMSO-d^{6}) spectrum of [(Py2ald)Zn(SePh)] (**2^{Zn}**).

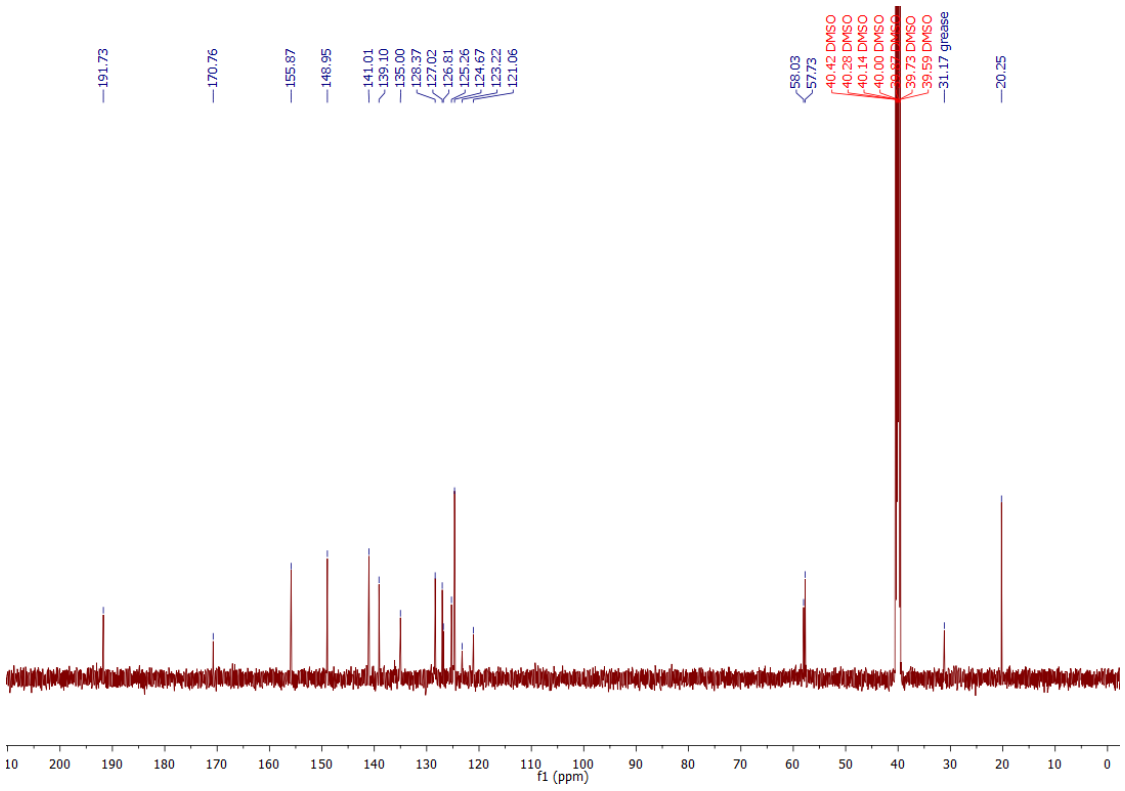

Figure S6. ^{13}C NMR (151 MHz, DMSO-d^{6}) spectrum of [(Py2ald)Zn(SePh)] (**2^{Zn}**).

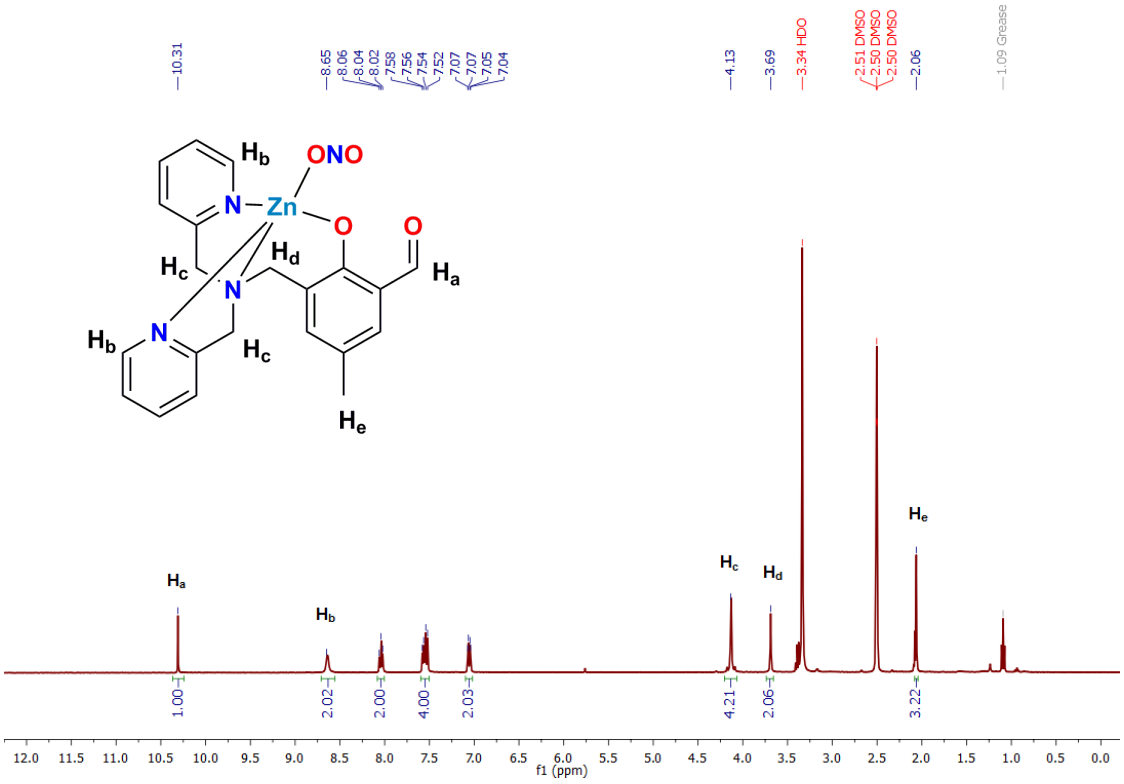

FigureS7. ^{1}H NMR (400 MHz, DMSO-d^{6}) spectrum of [(Py2ald)Zn(ONO)] (**3^{Zn}**).

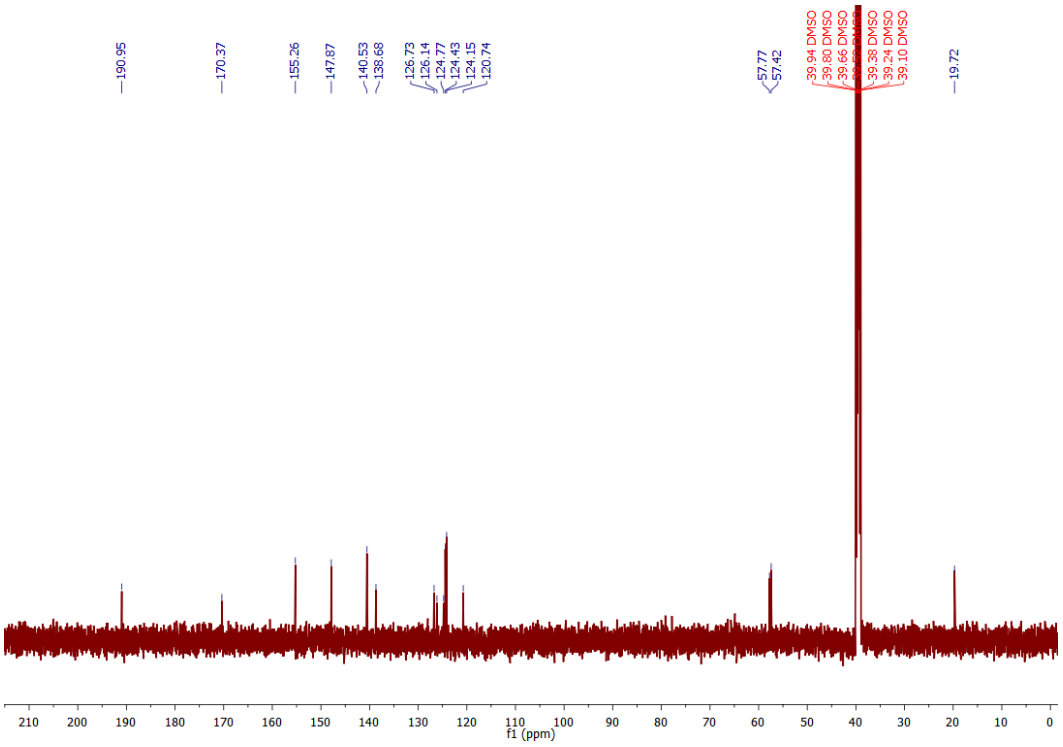

Figure S8. ^{13}C NMR (150 MHz, DMSO-d^{6}) spectrum of [(Py2ald)Zn(ONO)] (**3^{Zn}**).

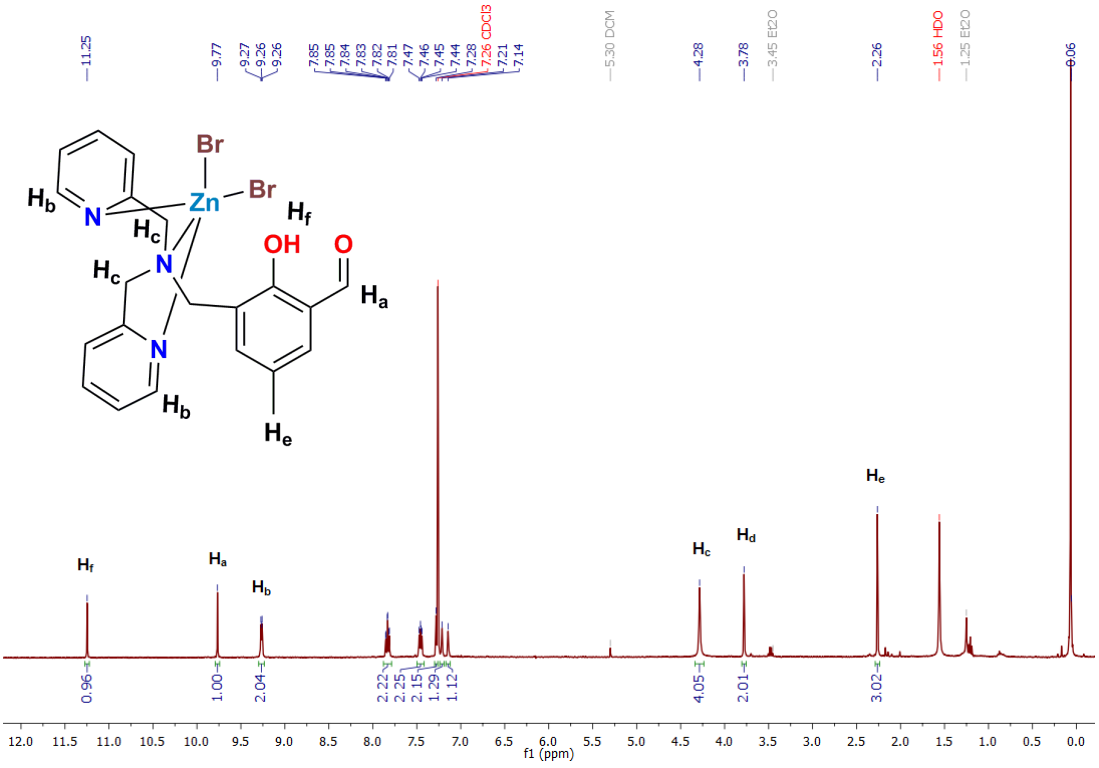

Figure S9. ^{1}H NMR (400 MHz, $CDCl_3$) spectrum of [(Py2ald)Zn(Br)$_2$] (**4^{Zn}**).

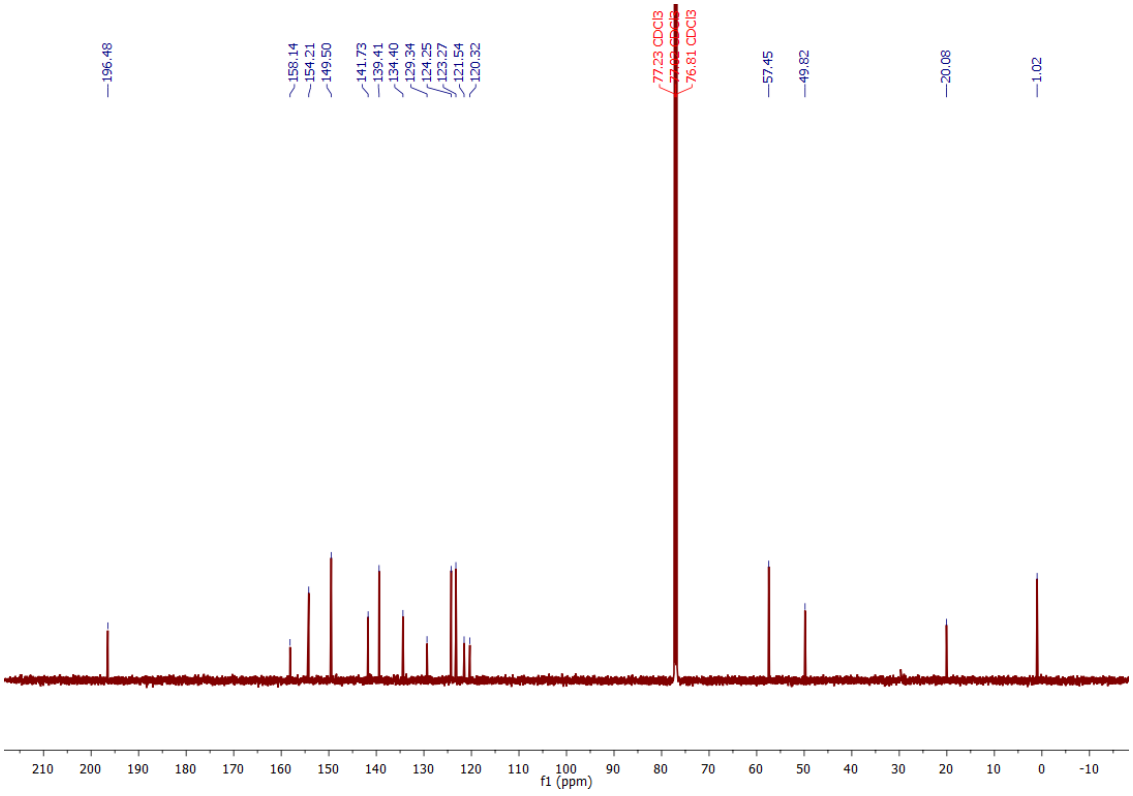

Figure S10. ^{13}C NMR (150 MHz, $CDCl_3$) spectrum of [(Py2ald)Zn(Br)$_2$] (**4^{Zn}**).

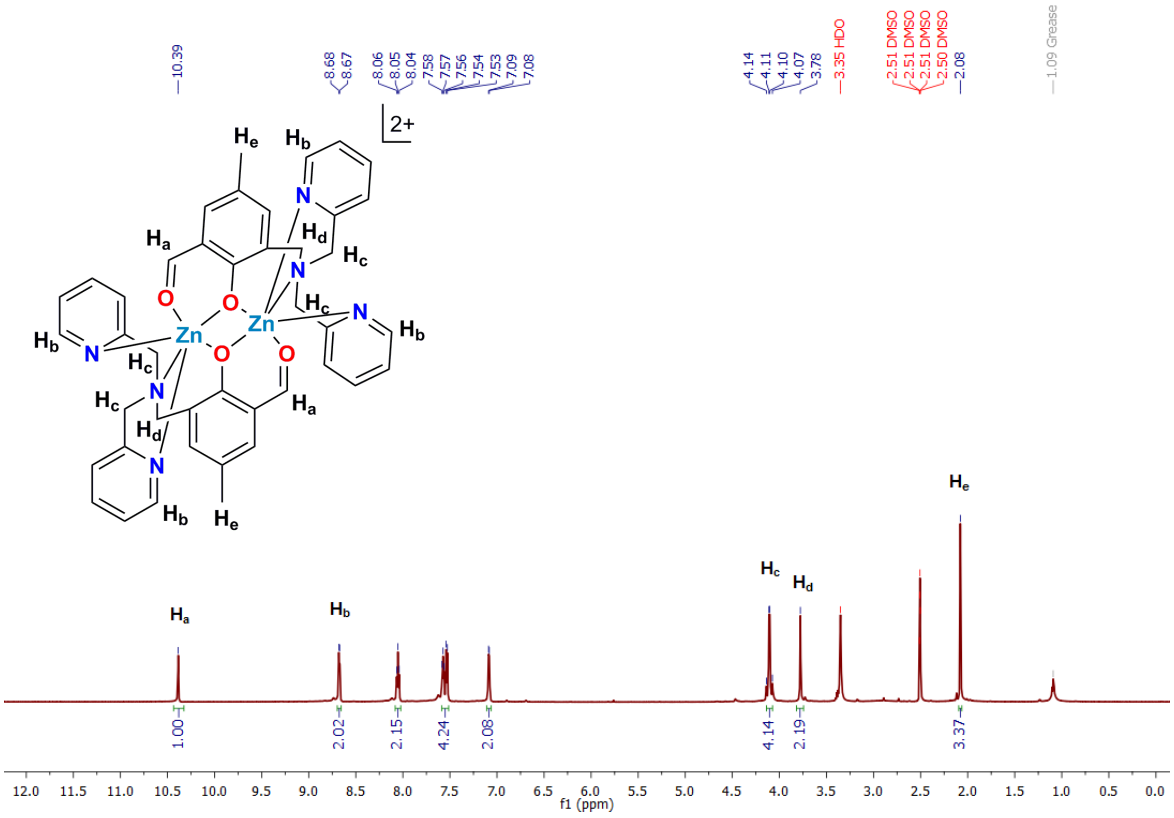

Figure S11. ^{1}H NMR (600 MHz, DMSO-d^{6}) spectrum of [(Py2ald)Zn]$_2$(BF$_4$)$_2$(**5**$^{\mathbf{Zn}}$(BF$_4$)$_2$).

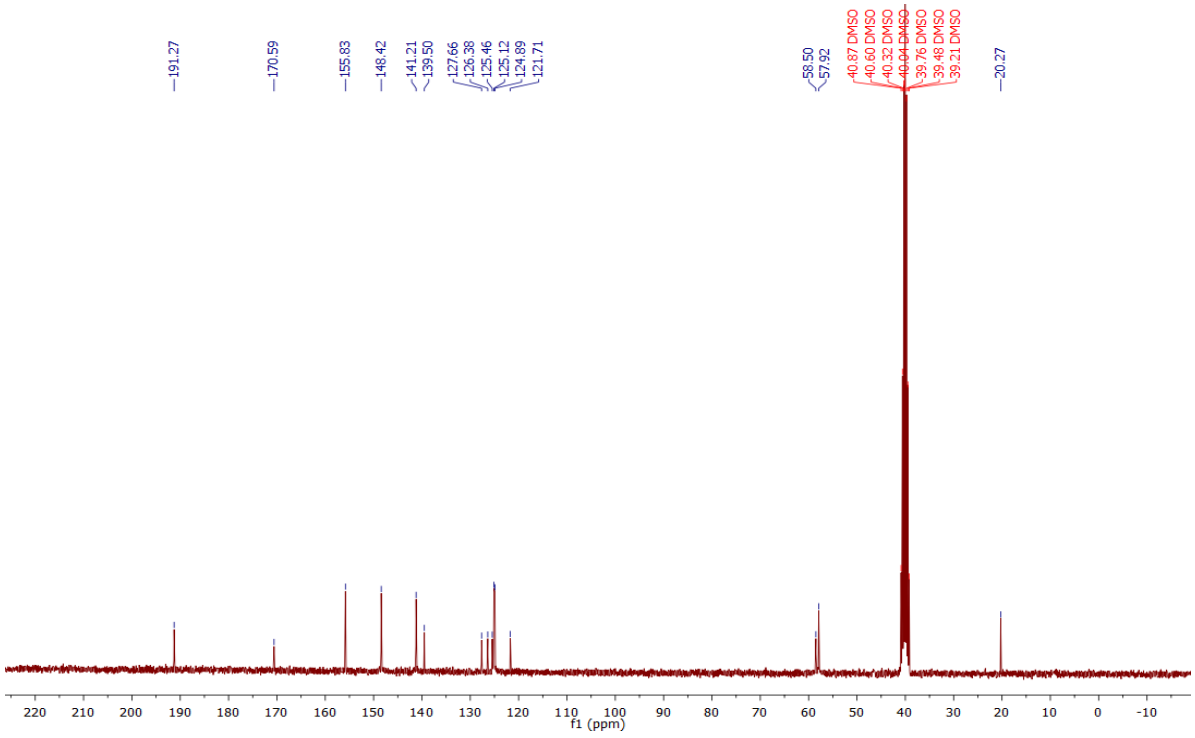

Figure S12. ^{13}C NMR (75 MHz, DMSO-d^{6}) spectrum of [(Py2ald)Zn]$_2$(BF$_4$)$_2$(**5**$^{\mathbf{Zn}}$(BF$_4$)$_2$).

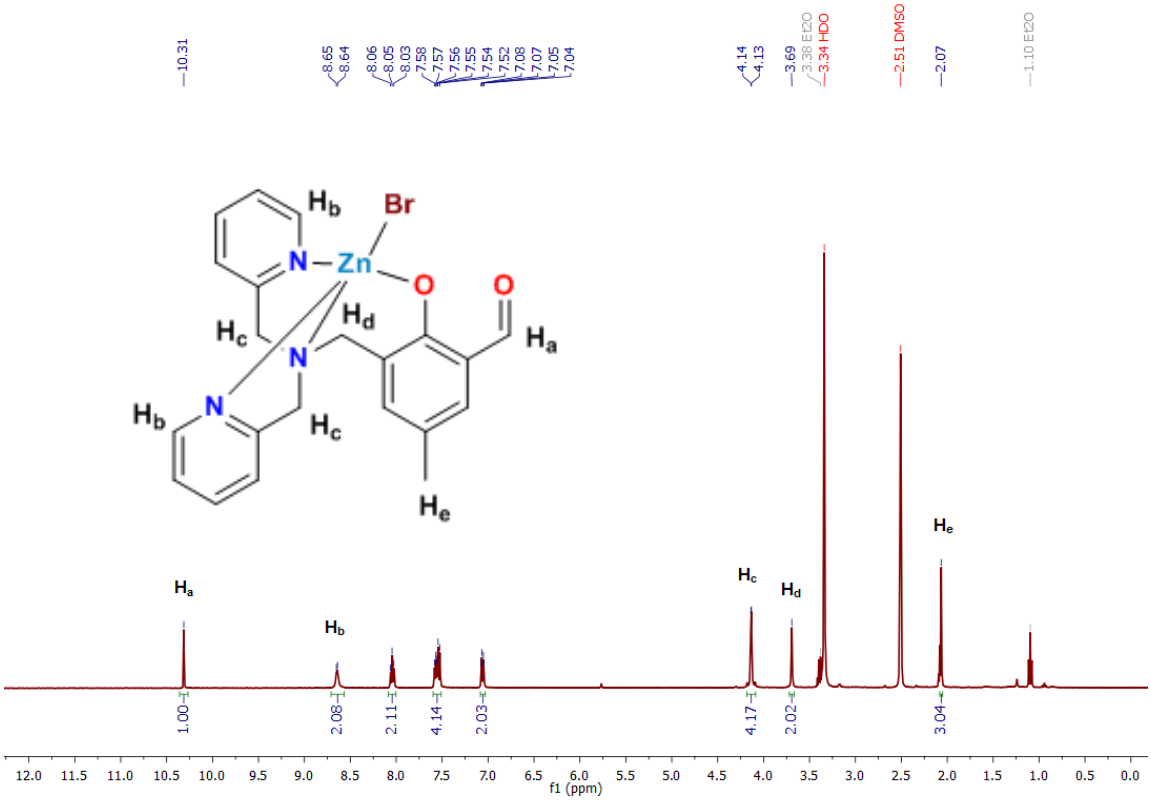

Figure S13. ^{1}H NMR (400 MHz, DMSO-d^{6}) spectrum of [(Py2ald)Zn(Br)] (**6^{Zn}**).

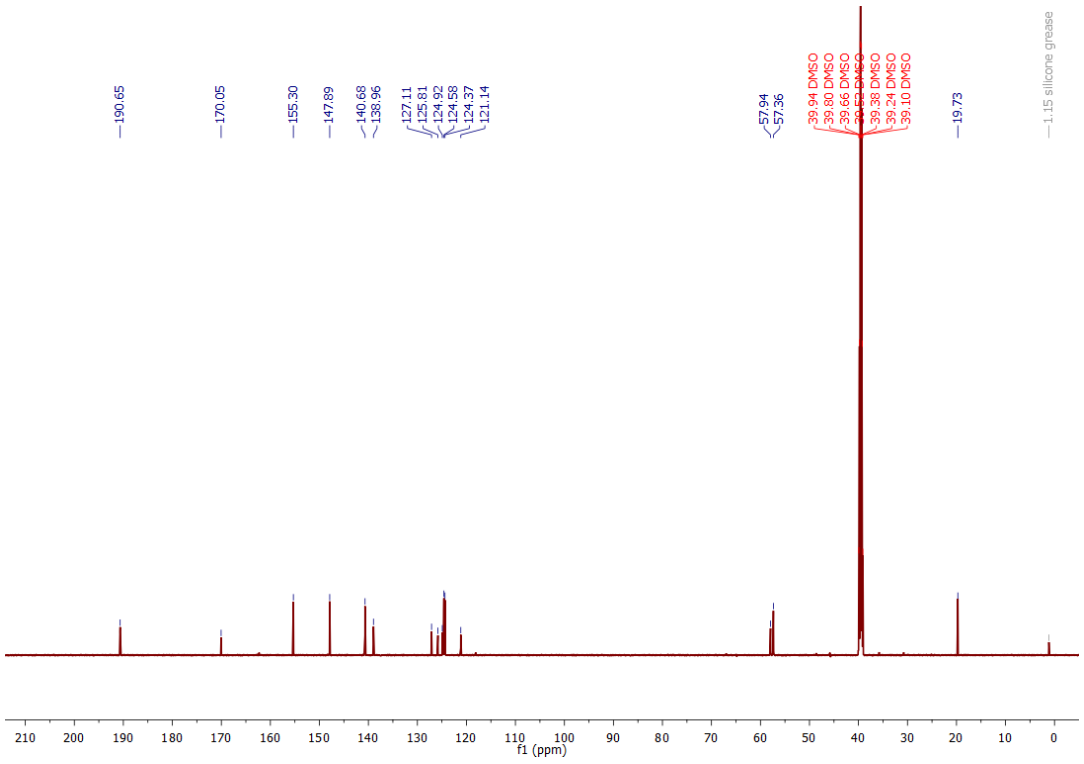

Figure S14. ^{13}C NMR (150 MHz, DMSO-d^{6}) spectrum of [(Py2ald)Zn(Br)] (**6^{Zn}**).

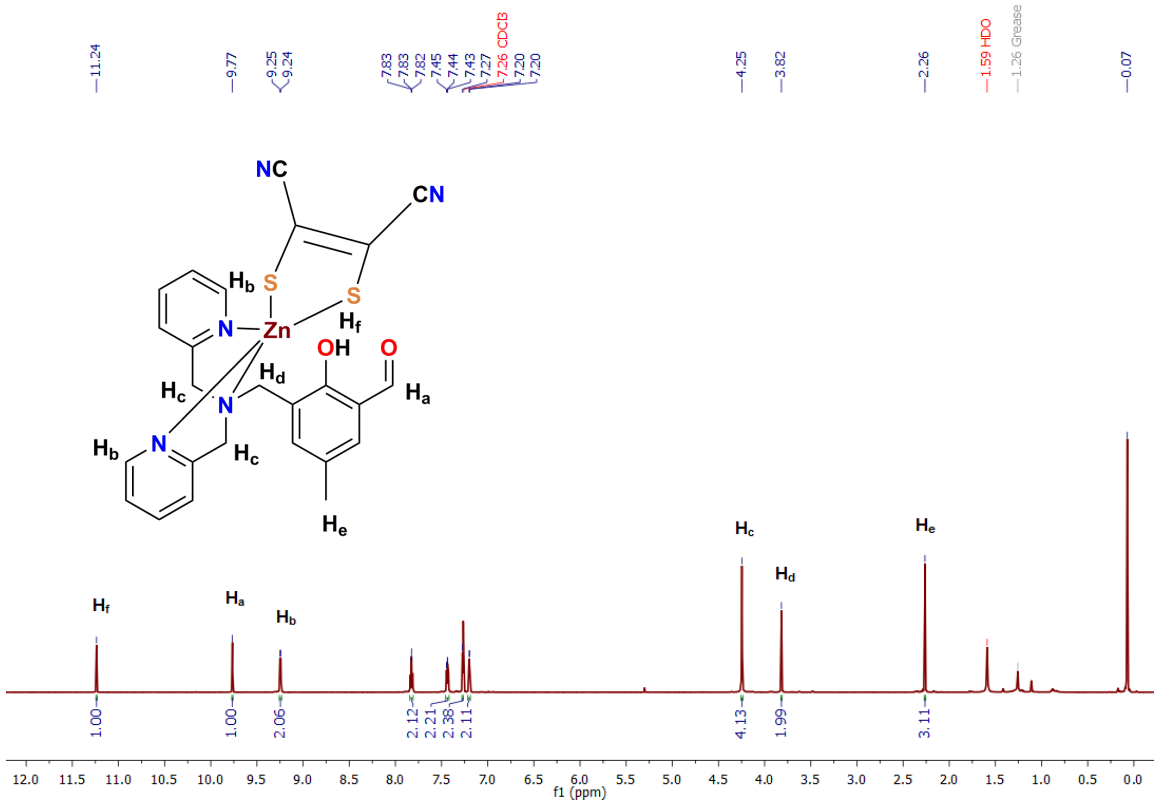

Figure S15. ^{1}H NMR (600 MHz, $CDCl_3$) spectrum of [(Py2ald)Zn(mnt)] (**7^{Zn}**).

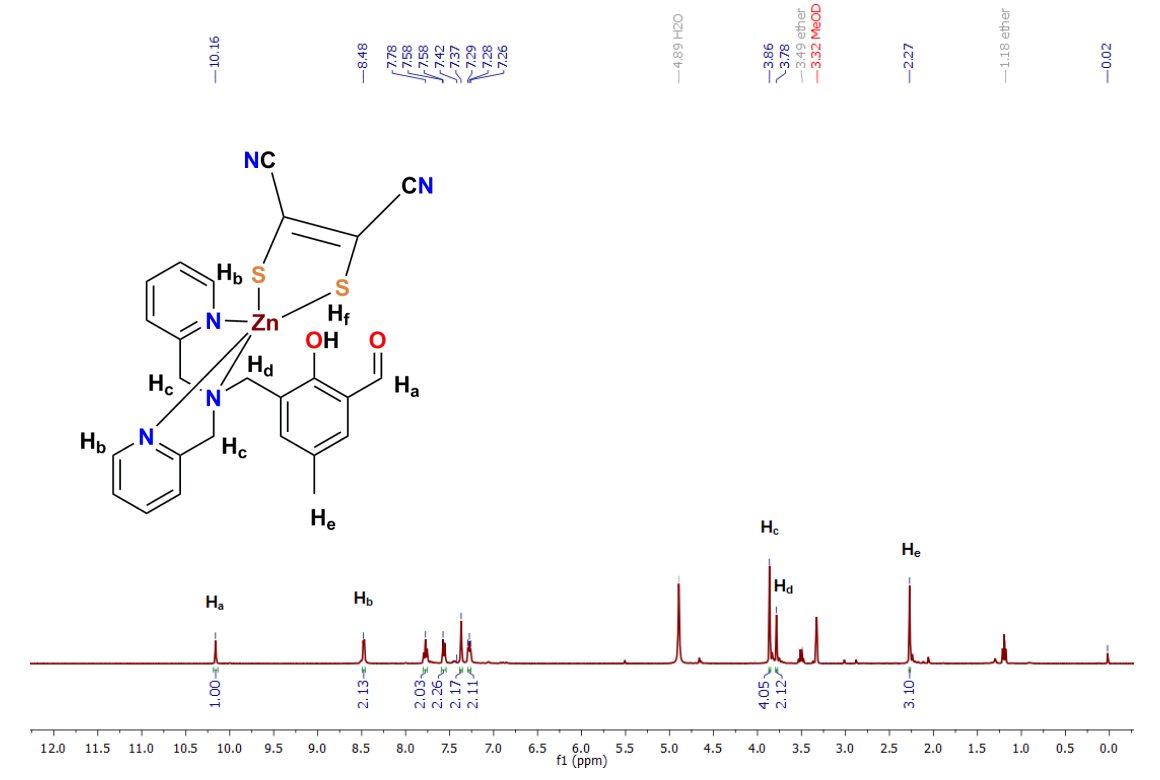

Figure S16. ^{1}H NMR (400 MHz, CD_3OD) spectrum of [(Py2ald)Zn(mnt)] (**7^{Zn}**).

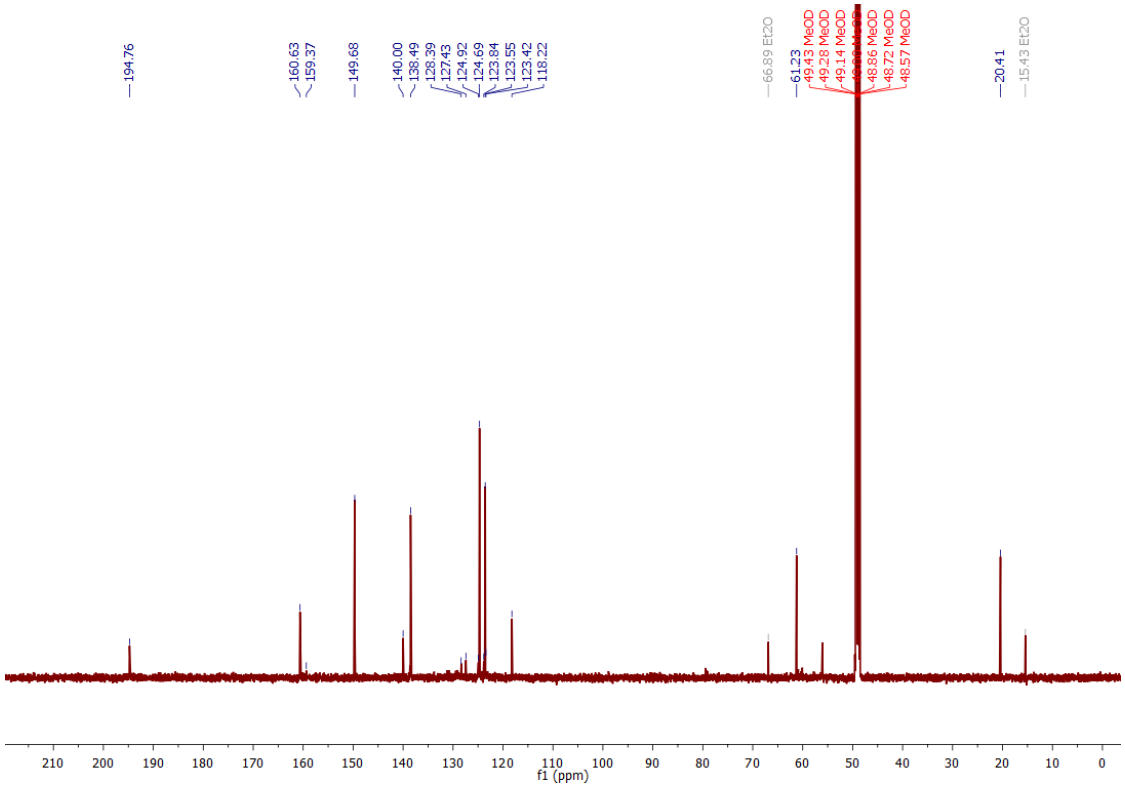

Figure S17. ^{13}C NMR (150 MHz, $CDCl_3$) spectrum of[(Py2ald)Zn(mnt)] (**7^{Zn}**).

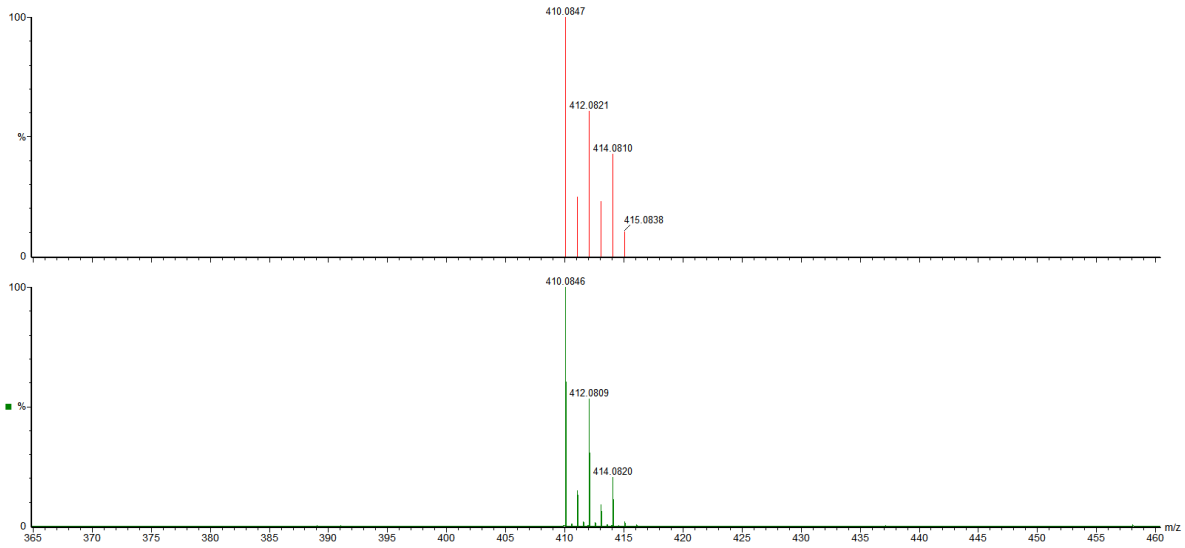

Figure S18. Mass spectrometric data (in MeCN) for $[(Py2ald)Zn]_2(BF_4)_2$ (**5^{Zn}**$(BF_4)_2$) shows the presence of $[(Py2ald)Zn]^+$ (m/z: 410.0847, simulated data, orange line; 410.0846, observed data, green line).

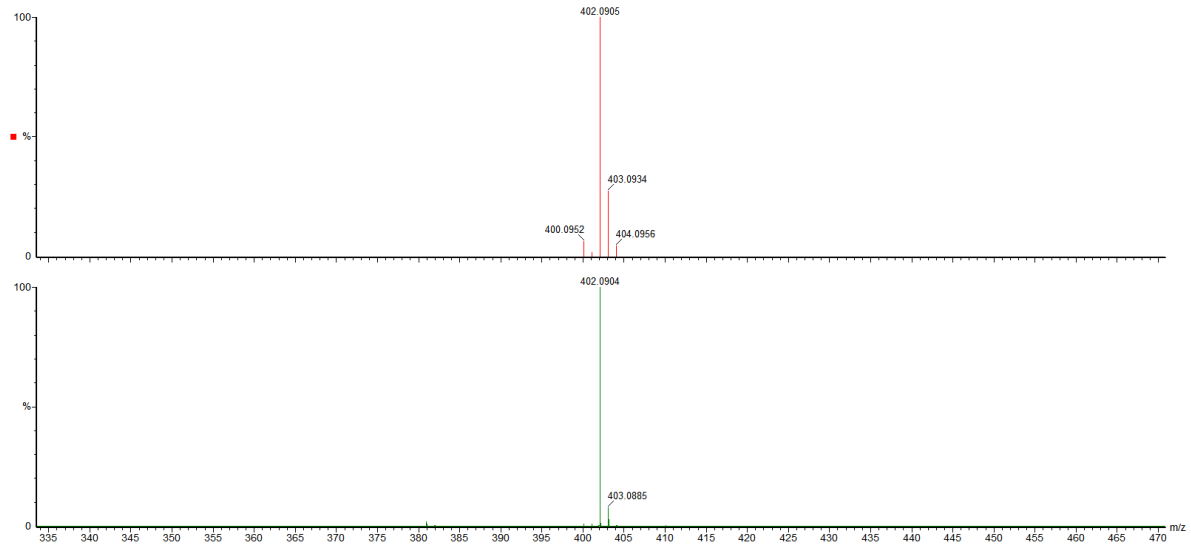

Figure S19. Mass spectrometric data (in MeCN) for $[(Py2ald)Fe]_2(BF_4)_2$ ($\mathbf{5^{Fe}}(BF_4)_2$) shows the presence of $[(Py2ald)Fe]^+$ (m/z: 402.0905, simulated data, orange line; 402.0904, observed data, green line).

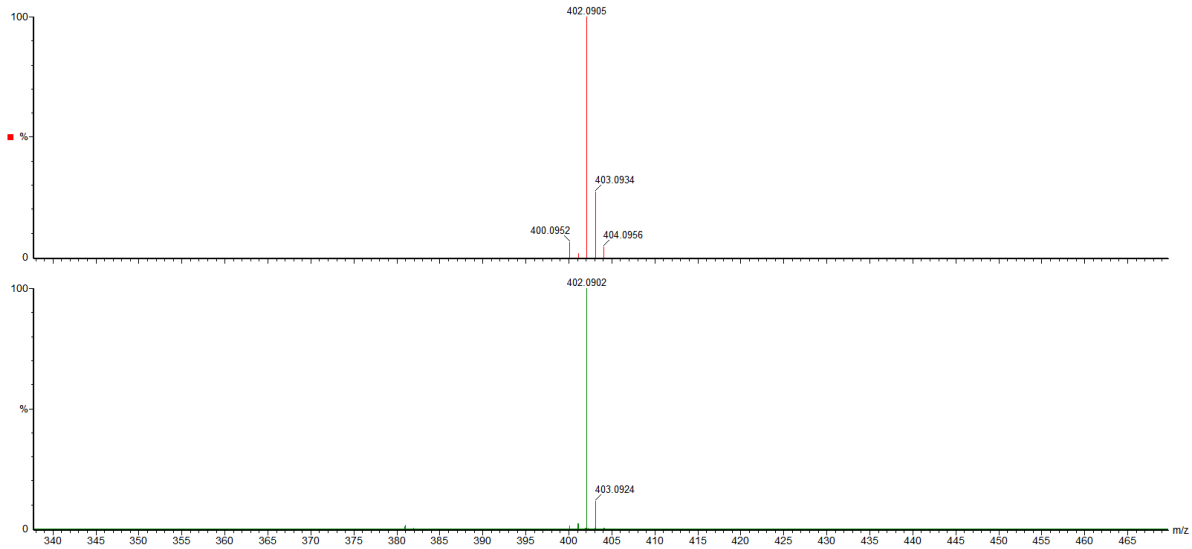

Figure S20. Mass spectrometric data (in MeCN) for $[(Py2ald)Fe]_2(BPh_4)_2$ ($\mathbf{5^{Fe}}(BPh_4)_2$) shows the presence of $[(Py2ald)Fe]^+$ (m/z: 402.0905, simulated data, orange line; 402.0902, observed data, green line).

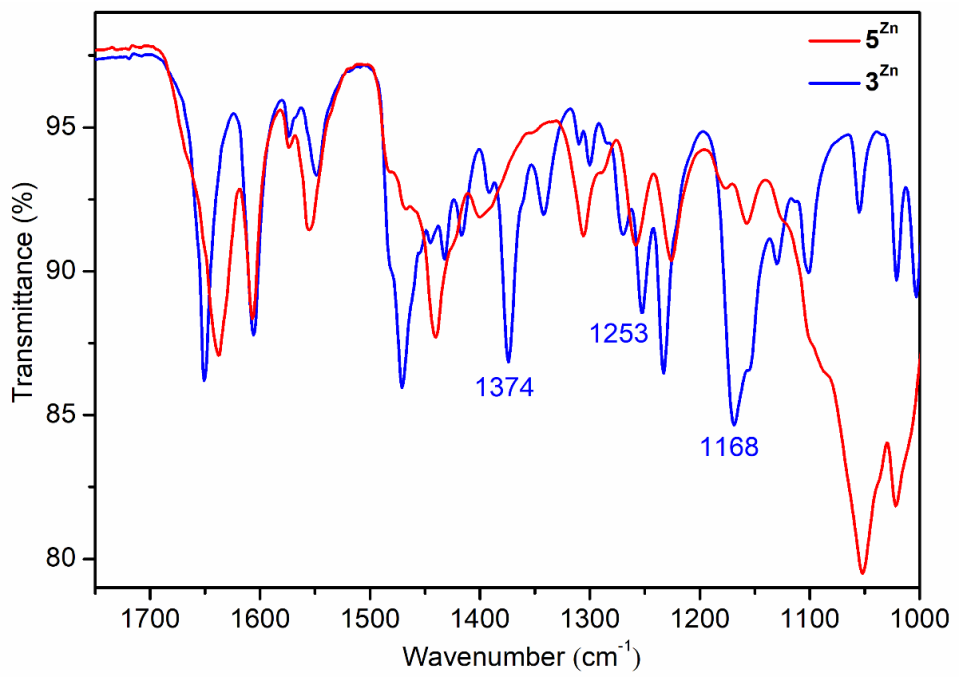

Figure S21. IR spectra (ATR) of [(Py2ald)Zn(ONO)] (**3^{Zn}**) along with that of [(Py2ald)Zn]$_2$(BF$_4$)$_2$ (**5^{Zn}**(BF$_4$)$_2$) used as a control.

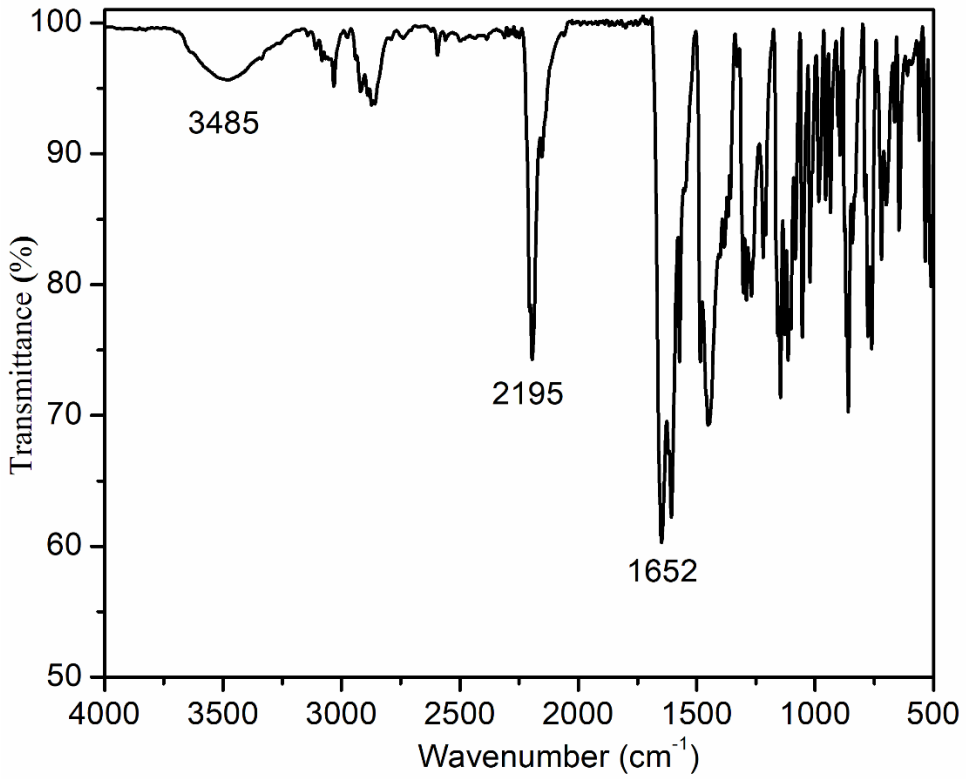

Figure S22. IR spectra (KBr pellet) of [(Py2ald)Zn(mnt)] (**7^{Zn}**) shows $\nu_{O\text{-}H\ (H\text{-}bonded)}$ = 3485 cm^{-1}, ν_{CN} = 2195 cm^{-1} and ν_{CHO} = 1652 cm^{-1}.

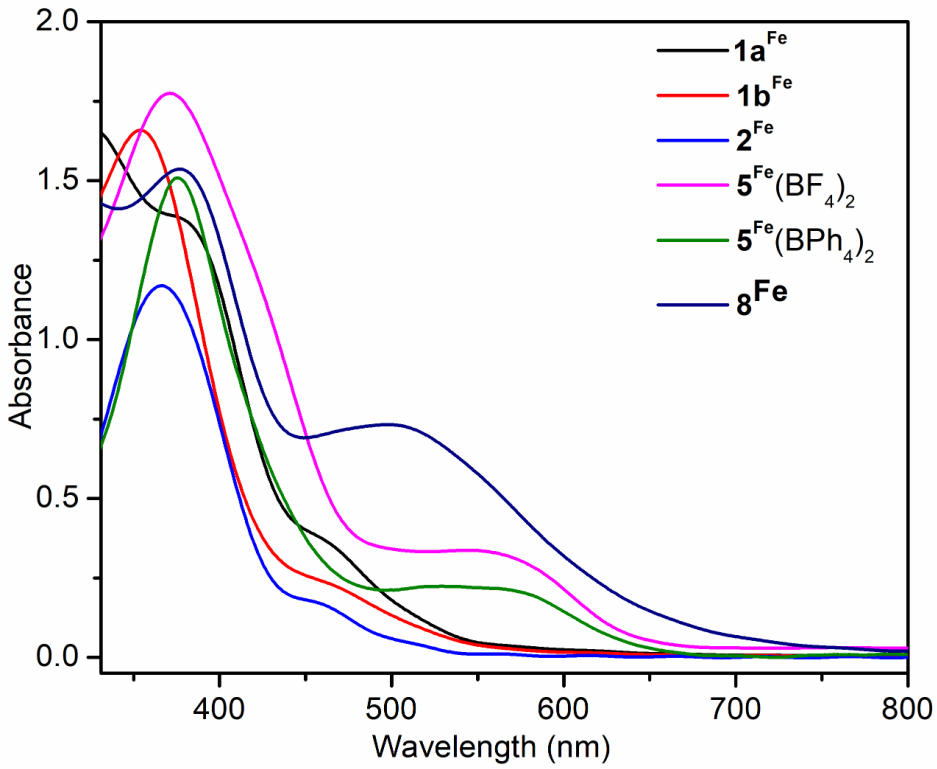

Figure S23. Electronic absorption spectroscopic signatures for the iron compounds in CH_2Cl_2 (0.25 mM).

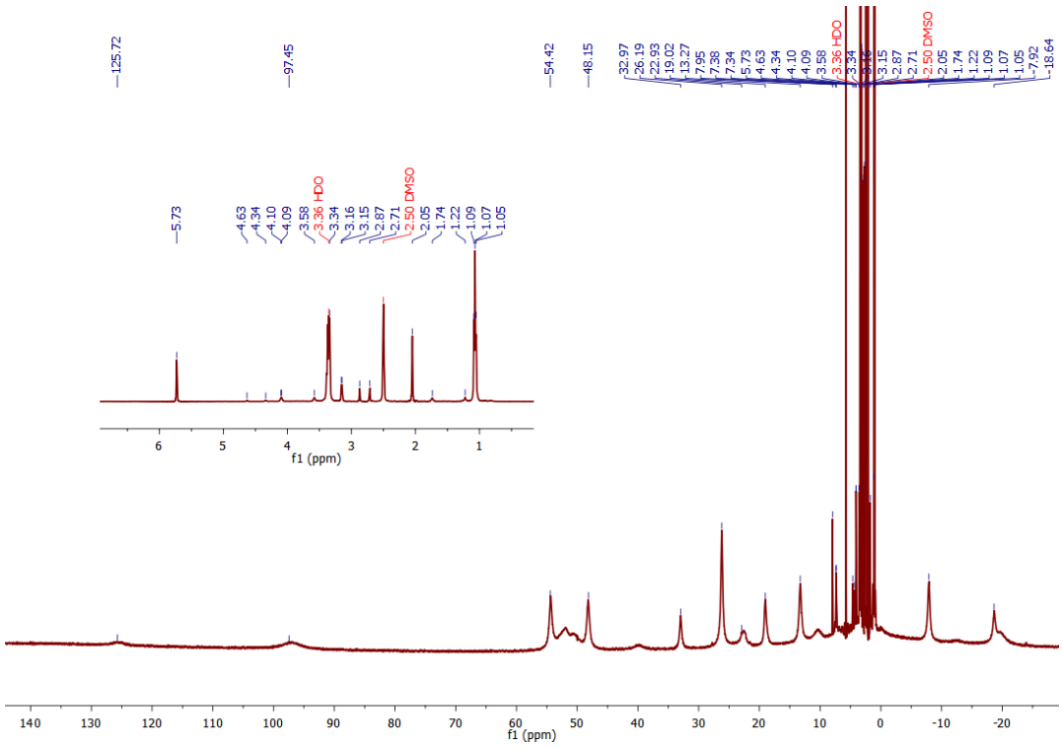

Figure S24. ^{1}H NMR (400 MHz, DMSO-d^6) spectrum of [(Py2ald)Fe(SPh)] (**1a^{Fe}**).

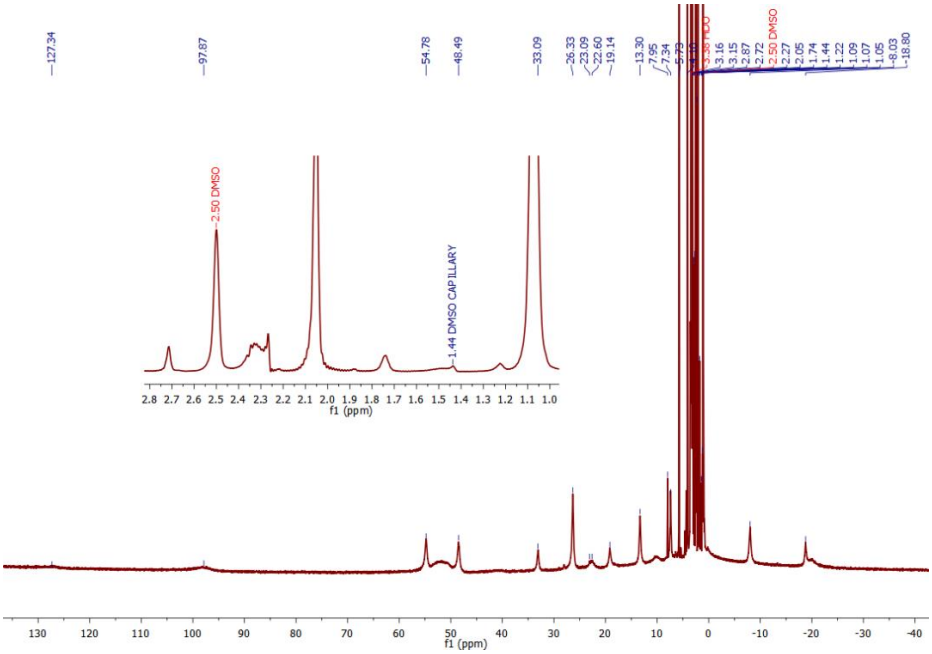

Figure S25. ^{1}H NMR (400 MHz, DMSO-d^{6}) spectrum of [(Py2ald)Fe(SPh)] (**1a^{Fe}**), recorded in a coaxial NMR tube, with DMSO-d^{6} inside. Inset shows a shift in the peak of DMSO-d^{6}. Solution magnetic moment (μ_{eff}) = 4.63 BM (calculated spin only magnetic moment = 4.90 BM).

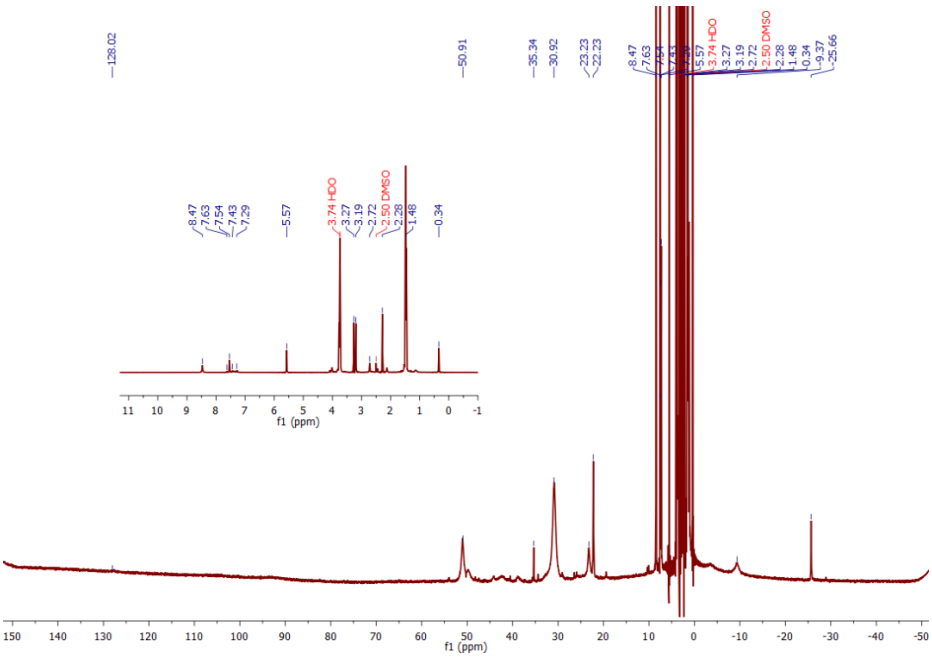

Figure S26. ^{1}H NMR (400 MHz, DMSO-d^{6}) spectrum of [(Py2ald)Fe(SC$_6$H$_4$-2,6-Me$_2$)] (**1b^{Fe}**).

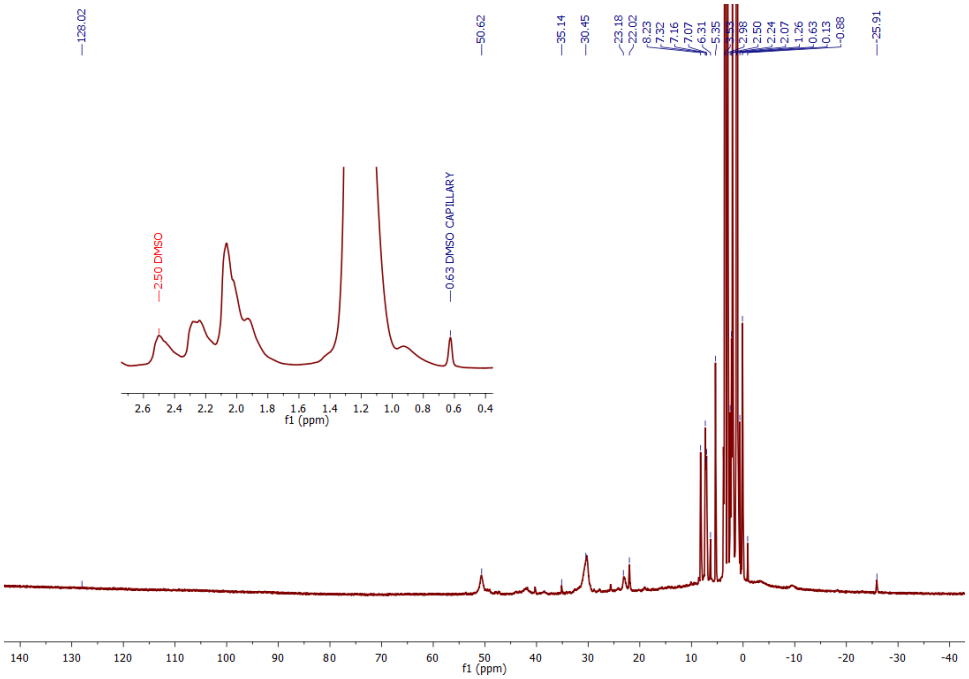

Figure S27. ^{1}H NMR (400 MHz, DMSO-d^{6}) spectrum of[(Py2ald)Fe(SC_6H_4-2,6-Me_2)] (**1b^{Fe}**).recorded in a coaxial NMR tube, with DMSO-d^{6} inside. Inset shows a shift in the peak of DMSO-d^{6}. Solution magnetic moment (μ_{eff}) = 4.71 BM (calculated spin only magnetic moment = 4.90 BM).

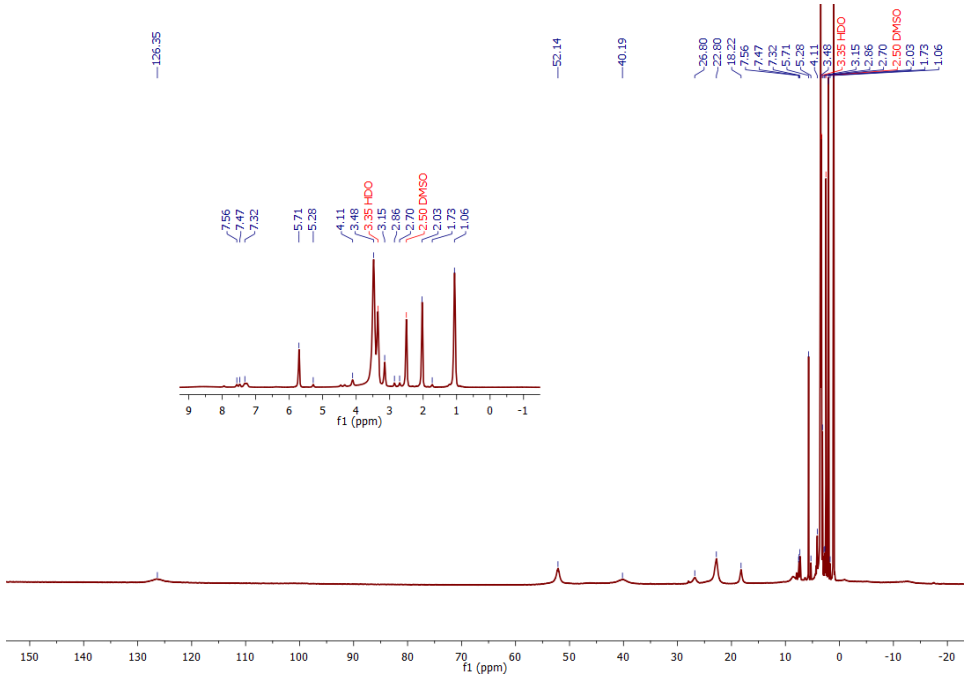

Figure S28. ^{1}H NMR (400 MHz, DMSO-d^{6}) spectrum of [(Py2ald)Fe(SePh)] (**2^{Fe}**).

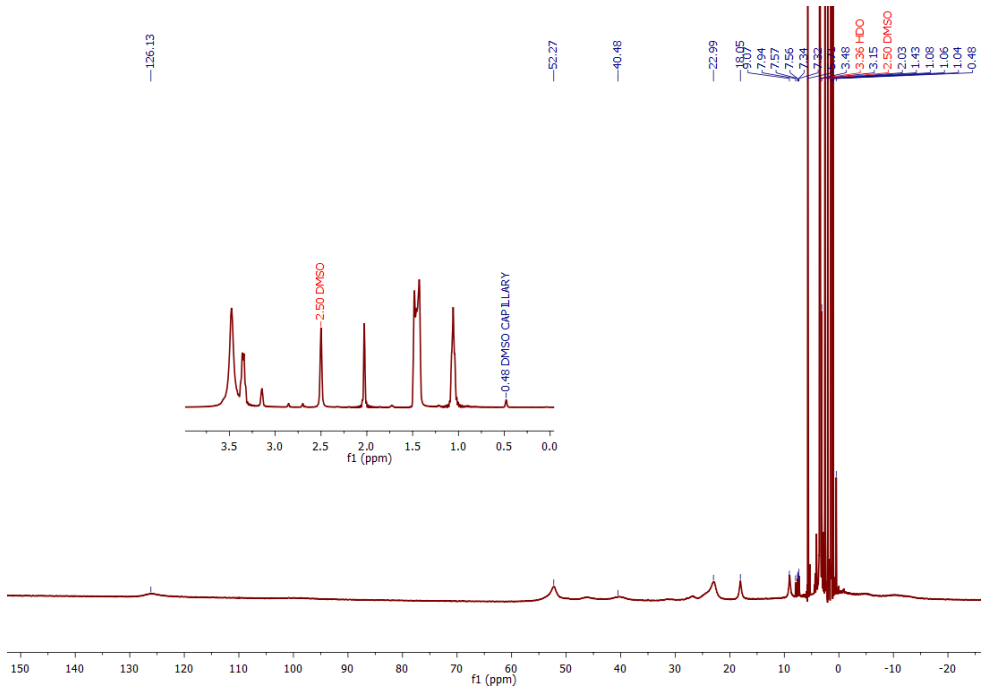

Figure S29. ^{1}H NMR (400 MHz, DMSO-d^{6}) spectrum of[(Py2ald)Fe(SePh)] (**2^{Fe}**) recorded in a coaxial NMR tube, with DMSO-d^{6} inside. Inset shows a shift in the peak of DMSO-d^{6}. Solution magnetic moment (μ_{eff}) = 4.79 BM (calculated spin only magnetic moment = 4.90 BM).

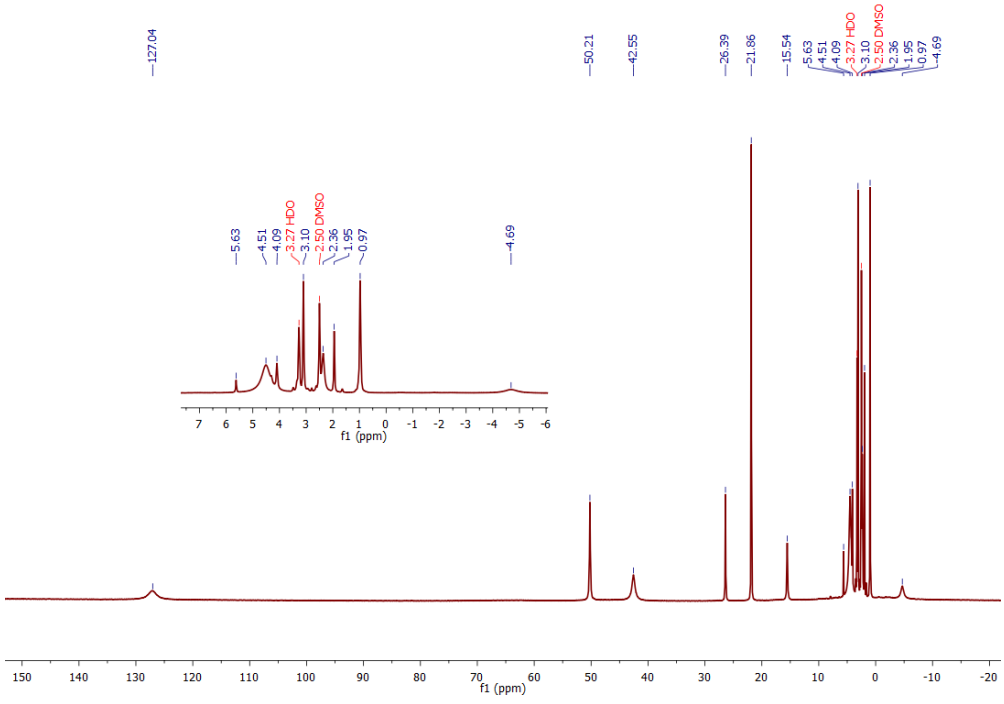

Figure S30. ^{1}H NMR (400 MHz, DMSO-d^{6}) spectrum of [(Py2ald)Fe]$_2$(BF$_4$)$_2$(**5^{Fe}**(BF$_4$)$_2$).

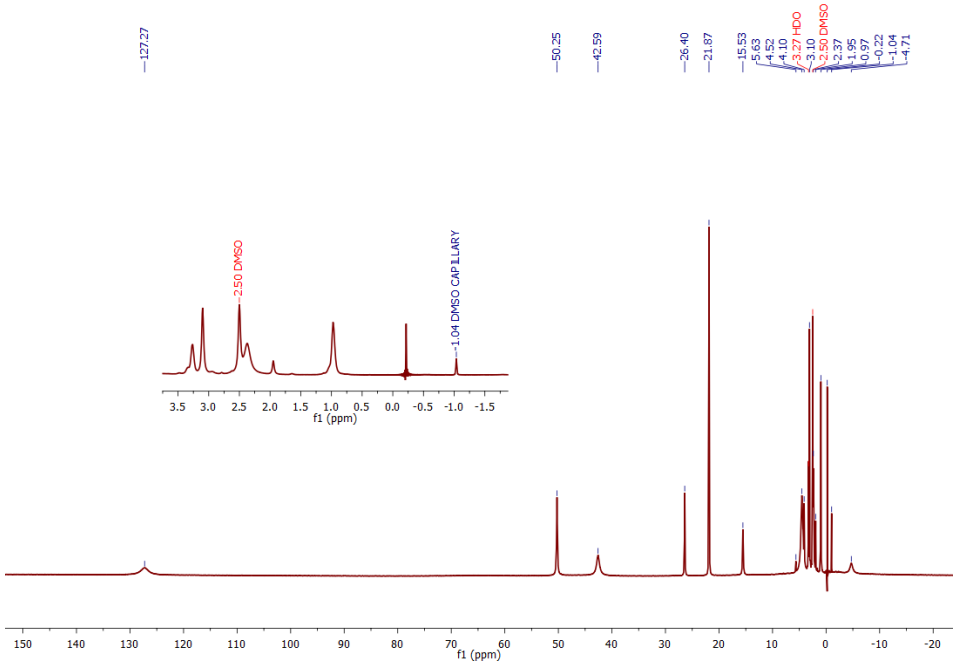

Figure S31. ^{1}H NMR (400 MHz, DMSO-d^{6}) spectrum of [(Py2ald)Fe]$_2$(BF$_4$)$_2$(**5**$^{\mathbf{Fe}}$(BF$_4$)$_2$)recorded in a coaxial NMR tube, with inside DMSO-d^{6}, inset shows a shift in the peak of DMSO-d^{6}.Solution magnetic moment (μ_{eff}) = 8.52 BM (calculated spin only magnetic moment = 8.94 BM).

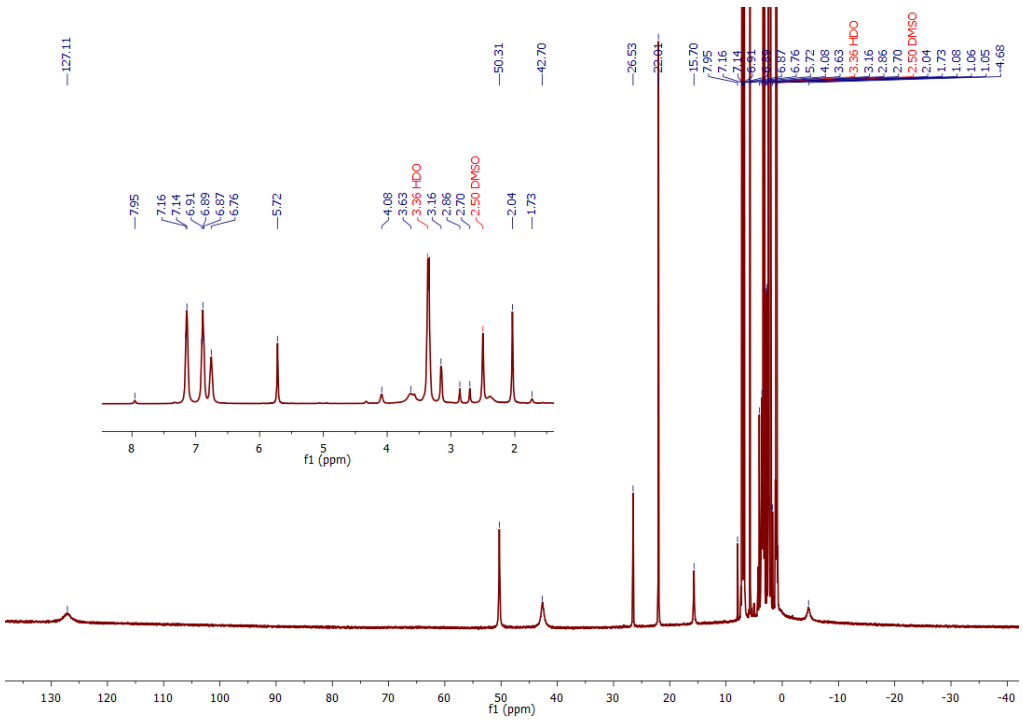

Figure S32. ^{1}H NMR (400 MHz, DMSO-d^{6}) spectrum of [(Py2ald)Fe]$_2$(BPh$_4$)$_2$(**5**$^{\mathbf{Fe}}$(BPh$_4$)$_2$).

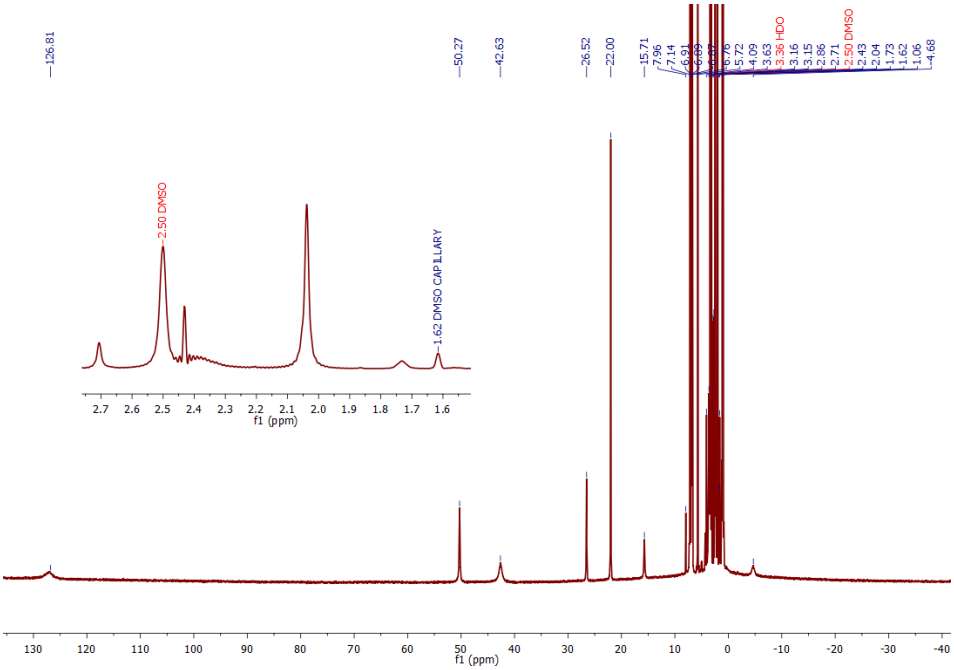

Figure S33. ^{1}H NMR (400 MHz, DMSO-d^{6}) spectrum of [(Py2ald)Fe]$_2$(BPh$_4$)$_2$(**5**$^{\mathbf{Fe}}$(BPh$_4$)$_2$), recorded in a coaxial NMR tube, with DMSO-d^{6} inside, inset shows a shift in the peak of DMSO-d^{6}. Solution magnetic moment (μ_{eff}) = 8.62 BM (calculated spin only magnetic moment = 8.94 BM).

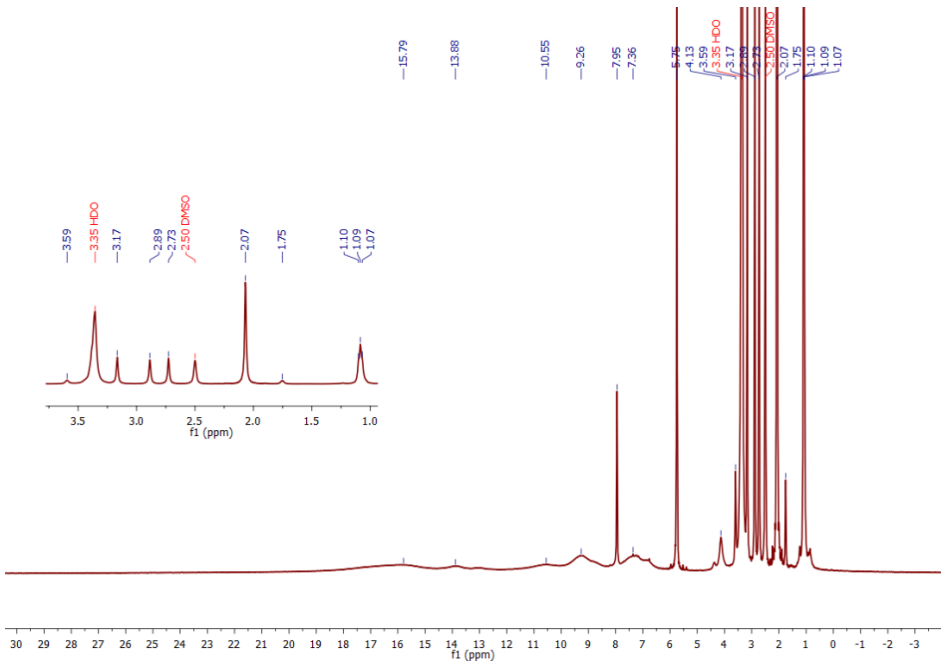

Figure S34. ^{1}H NMR (400 MHz, DMSO-d^{6}) spectrum of [{(Py2ald)(ONO)Fe}$_2$-μ_2-O](**8**$^{\mathbf{Fe}}$).

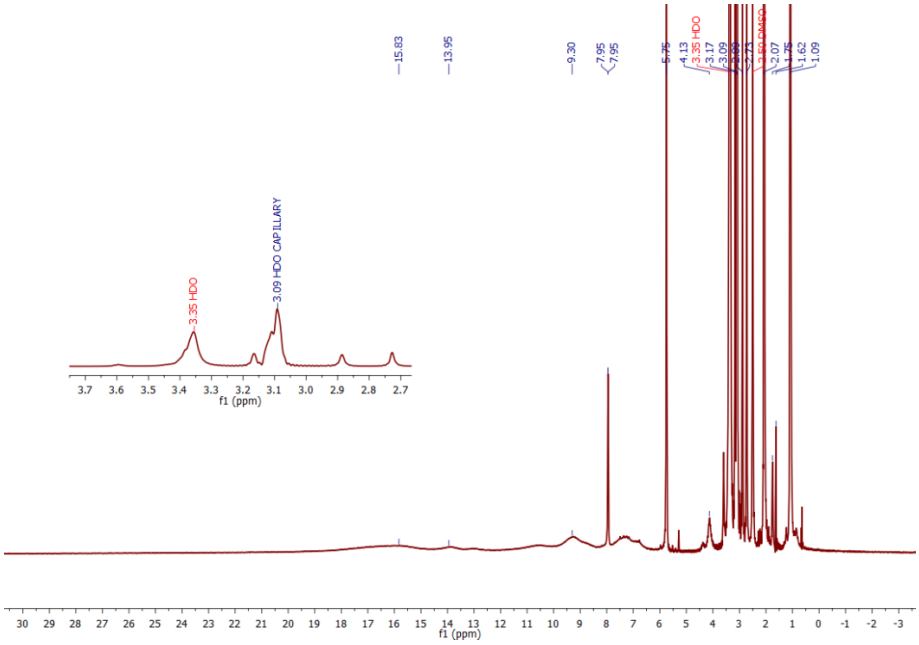

Figure S35. ^{1}H NMR (400 MHz, DMSO-d^{6}) spectrum of [{(Py2ald)(ONO)Fe}$_2$-μ_2-O](**8^{Fe}**),recorded in a coaxial NMR tube, with DMSO-d^{6} inside, inset shows a shift in the peak of water.Solution magnetic moment (μ_{eff}) = 2.43 BM (calculated spin only magnetic moment considering 10 unpaired electrons = 10.95 BM and calculated spin only magnetic moment for only two unpaired electron is 2.83).

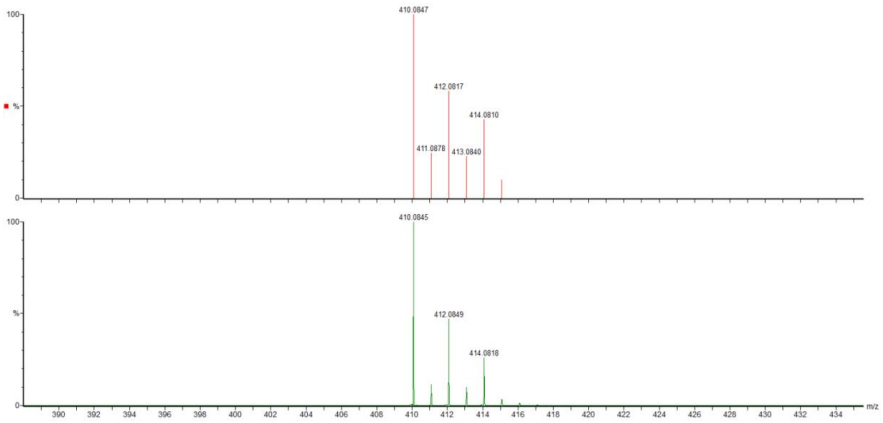

Figure S36. Mass spectrometric data (in MeCN) for [(Py2ald)Zn]$_2$(BF$_4$)$_2$ (**5^{Zn}**(BF$_4$)$_2$) obtained from the reaction of [(Py2ald)Zn(SPh)] (**1a^{Zn}**) with 1 equiv of (Cp$_2$Fe)(BF$_4$), shows the presence of [(Py2ald)Zn]$^{+}$ (m/z: 410.0847, simulated data, orange line; 410.0845, observed data, green line).

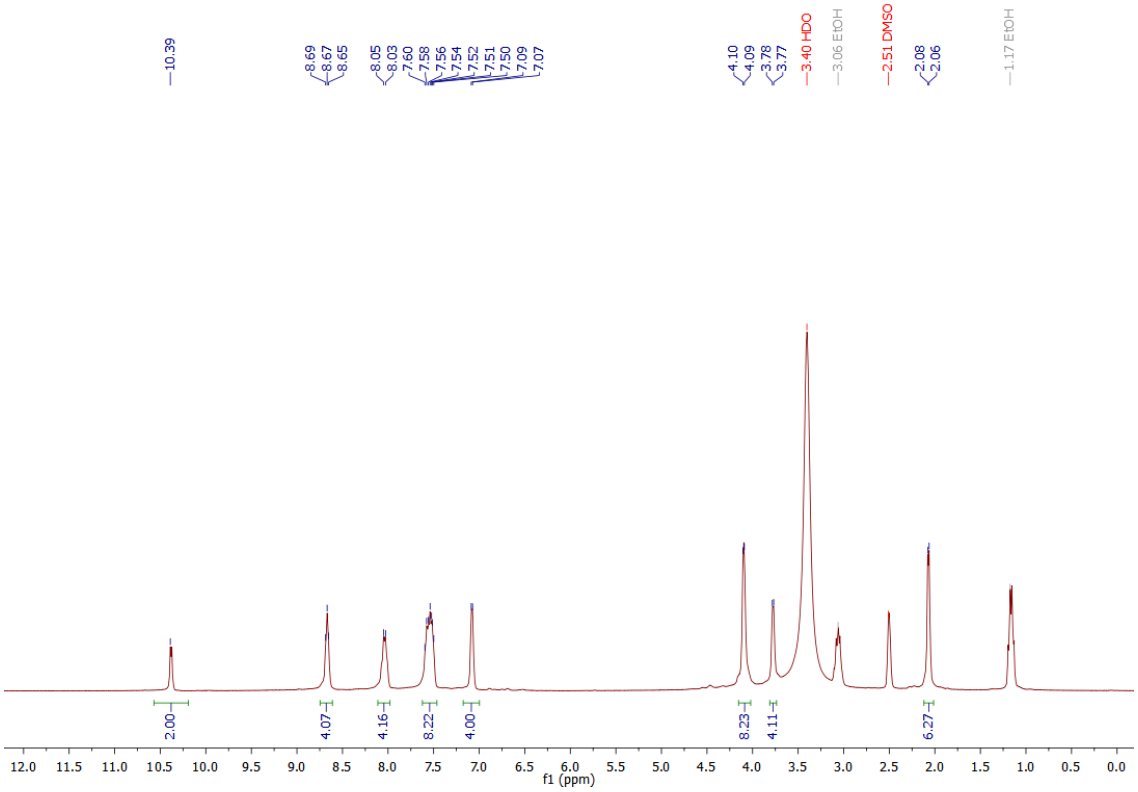

Figure S37. ^{1}H NMR (300 MHz, DMSO-d^{6}) spectrum of [(Py2ald)Zn]$_2$(BF$_4$)$_2$ (**5**$^{\mathbf{Zn}}$(BF$_4$)$_2$) obtained from the reaction [(Py2ald)Zn(SPh)] (**1a**$^{\mathbf{Zn}}$) with 1 equiv of (Cp$_2$Fe)(BF$_4$).

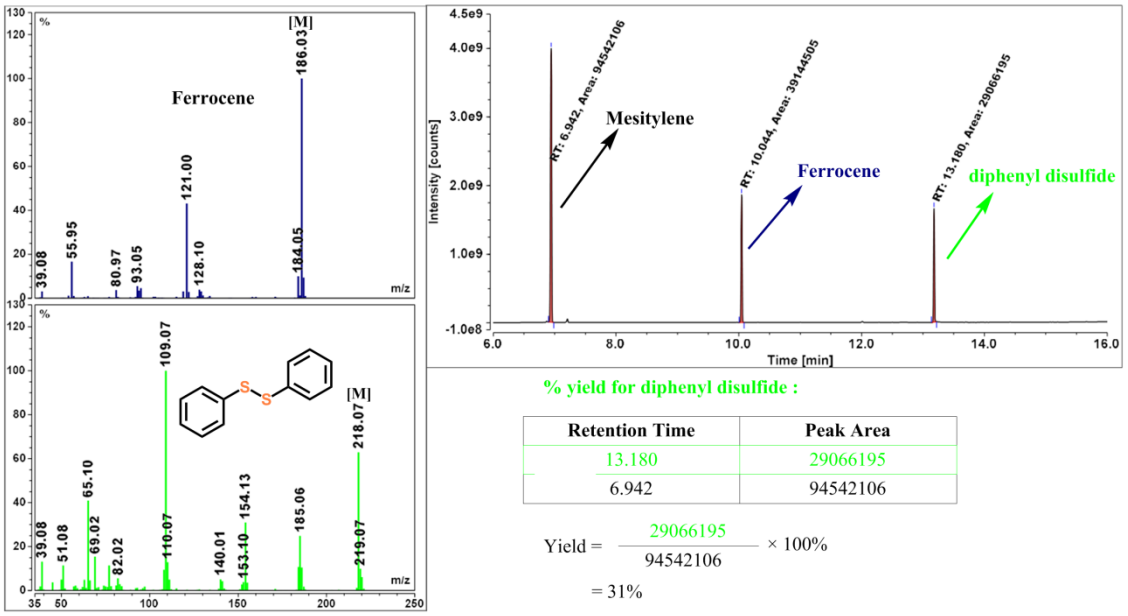

Figure S38. GC-MS data for the identification and yield (31%) calculation of diphenyl disulfide produced in the reaction of [(Py2ald)Zn(SPh)] (**1a**$^{\mathbf{Zn}}$) with 1 equiv of (Cp$_2$Fe)(BF$_4$).

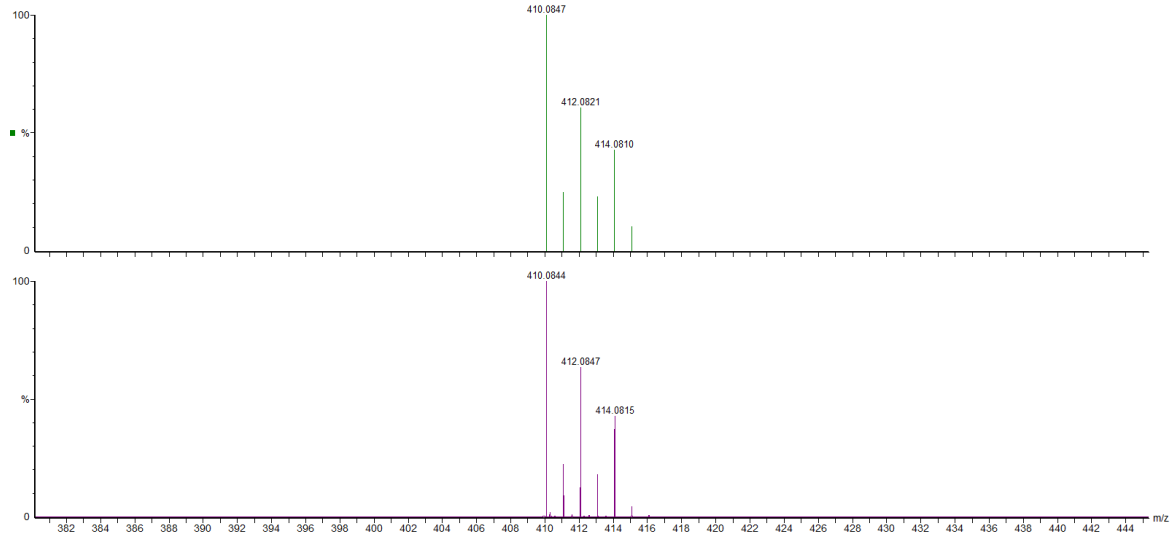

Figure S39. Mass spectrometric data (in MeCN) for $[(Py2ald)Zn]_2(BF_4)_2$ ($\mathbf{5^{Zn}}(BF_4)_2$) obtained from the reaction of [(Py2ald)Zn(ONO)] ($\mathbf{3^{Zn}}$) with 1 equiv of PhSH shows the presence of $[(Py2ald)Zn]^+$ (m/z: 410.0847, simulated data, green line; 410.0844, observed data, purple line).

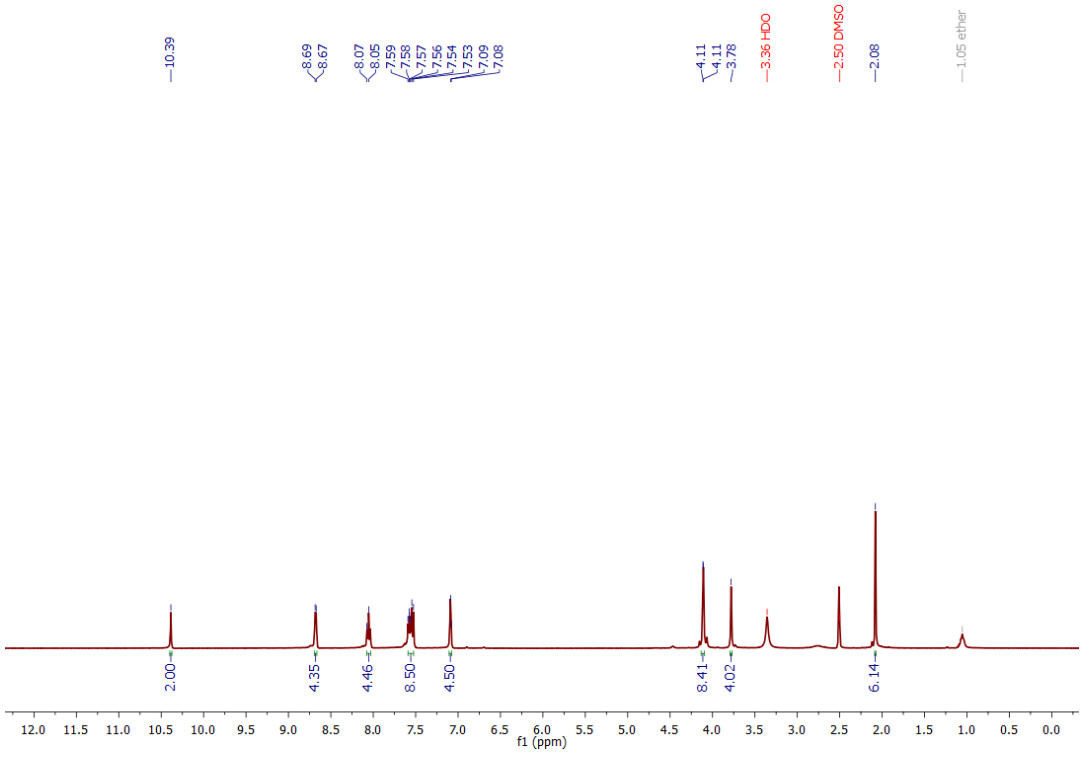

Figure S40. ^{1}H NMR (400 MHz, DMSO-d^6) spectrum of $[(Py2ald)Zn]_2(BF_4)_2$ ($\mathbf{5^{Zn}}(BF_4)_2$) obtained from the reaction of [(Py2ald)Zn(ONO)] ($\mathbf{3^{Zn}}$) with 1 equiv of PhSH.

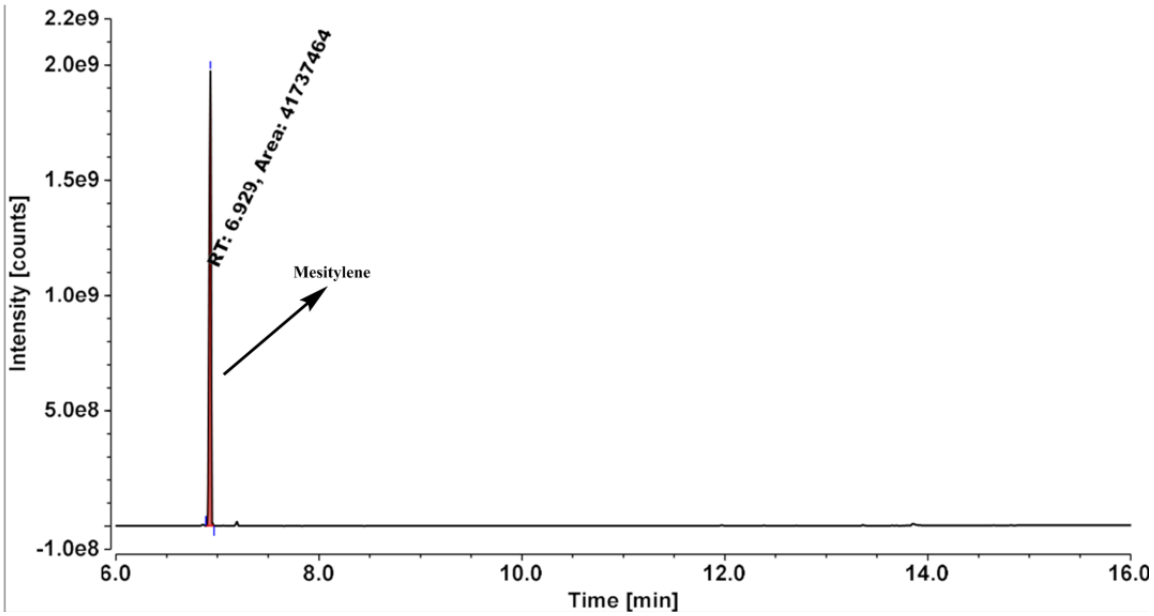

Figure S41. GC-MS data shows that no diphenyldisulfide was generated in the reaction of [(Py2ald)Zn(ONO)] (**3**$^{\mathbf{Zn}}$) with 1 equiv of NaSPh.

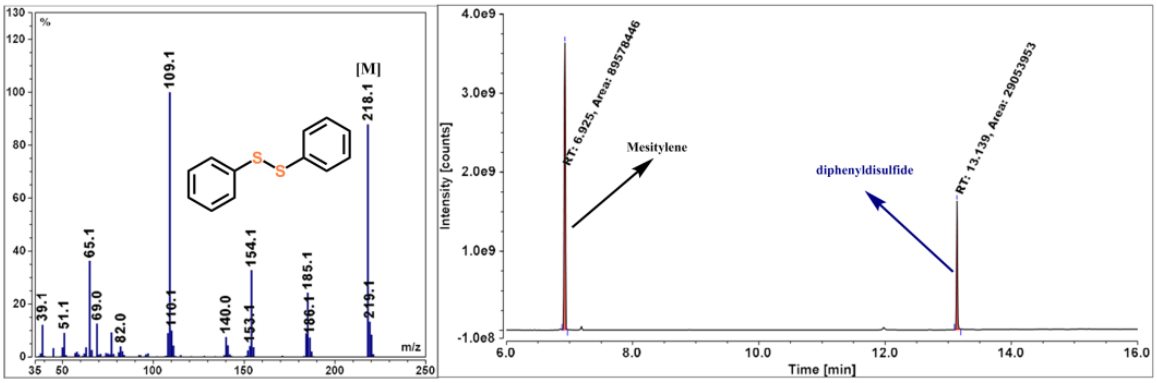

% yield for diphenyldisulfide :

Retention Time	Peak Area
13.139	29053953
6.925	89578446

$$\text{Yield} = \frac{29053953}{89578446} \times 100\%$$

$$= 32\%$$

Figure S42. GC-MS data for the identification and yield (32%) calculation of diphenyldisulfide produced in the reaction of [(Py2ald)Zn(ONO)] (**3**$^{\mathbf{Zn}}$) with 1 equiv of PhSH.

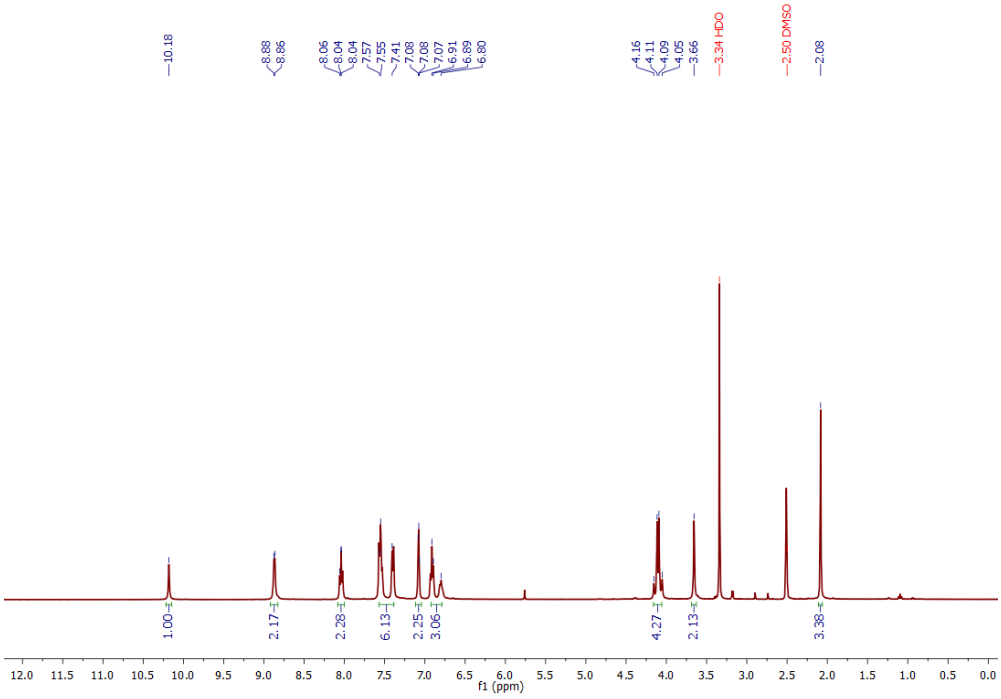

Figure S43. ^{1}H NMR (400 MHz, DMSO-d^{6}) spectrum of [(Py2ald)Zn(SPh)] (**1a^{Zn}**) obtained from the reaction of [(Py2ald)Zn(ONO)] (**3^{Zn}**) with 2 equiv of PhSH.

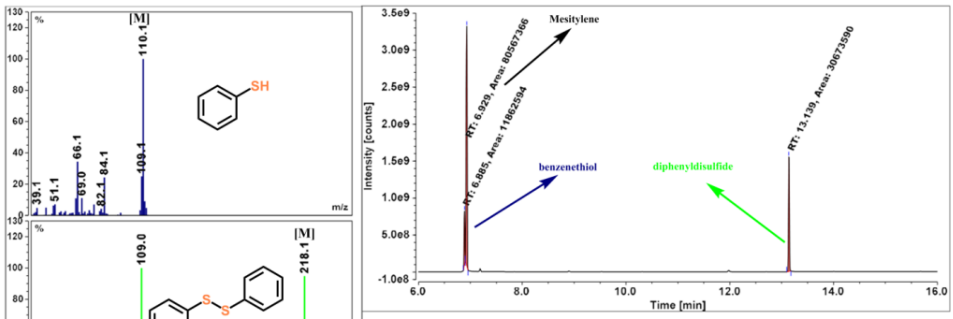

% yield for benzenethiol :

Retention Time	Peak Area
6.885	11862594
6.929	80567366

$$\text{Yield} = \frac{11862594}{80567366} \times 100\%$$

$$= 15\%$$

% yield for diphenyldisulfide :

Retention Time	Peak Area
13.139	30673590
6.925	80567366

$$\text{Yield} = \frac{30673590}{80567366} \times 100\%$$

$$= 38\%$$

Figure S44. GC-MS data for the identification and yield (38%) calculation of diphenyldisulfide produced in the reaction of [(Py2ald)Zn(ONO)] (**3^{Zn}**) with 2 equiv of PhSH.

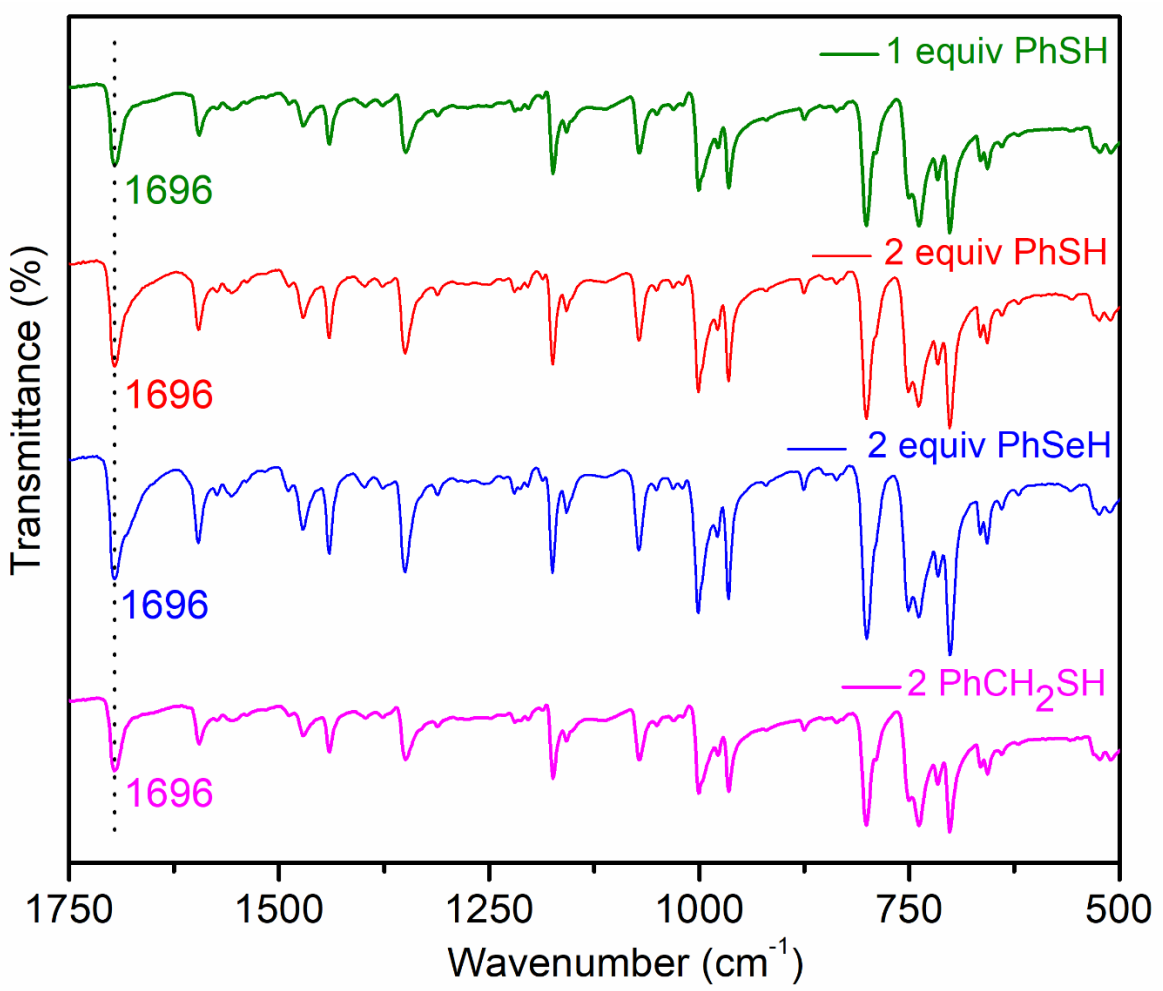

Figure S45. IR spectra of [(TPP)Co(NO)] (ν_{NO} = 1696 cm^{-1}) generated by the trapping of NO gas (generated by the reaction of [(Py2ald)Zn(ONO)] (**3**^{Zn}) with PhSH, $PhCH_2SH$ and PhSeH) by $(TPP)Co^{II}$.

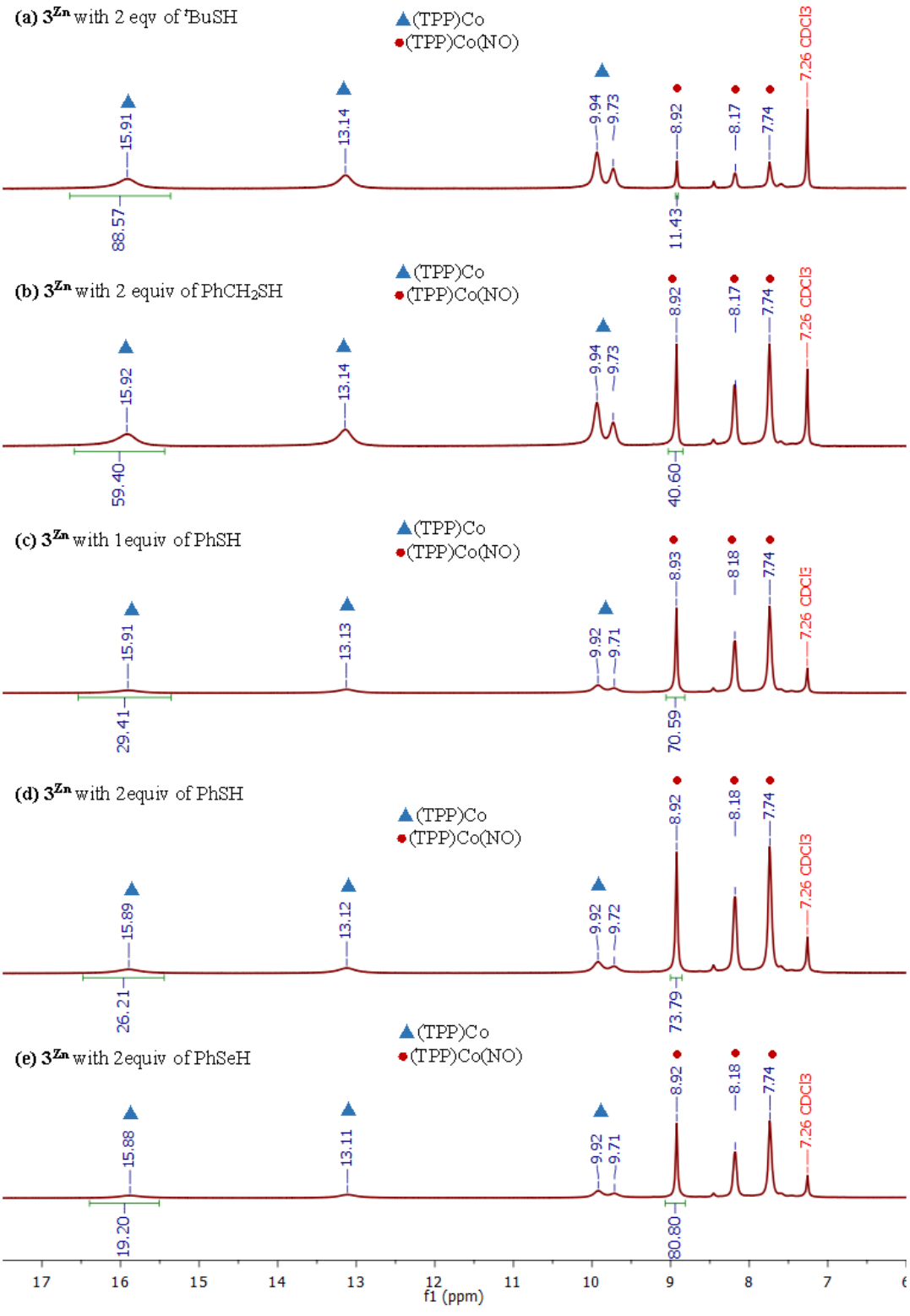

Figure S46. ^{1}H NMR (400 MHz, $CDCl_3$) spectra of (TPP)Co^{II} after trapping the NO gas generated by the reaction of [(Py2ald)Zn(ONO)] (**3^{Zn}**) with (a) ^{t}BuSH (2 equiv), (b) $PhCH_2SH$ (2 equiv), (c) PhSH (1 equiv), (d) PhSH (2equiv) and (e) PhSeH (2 equiv).

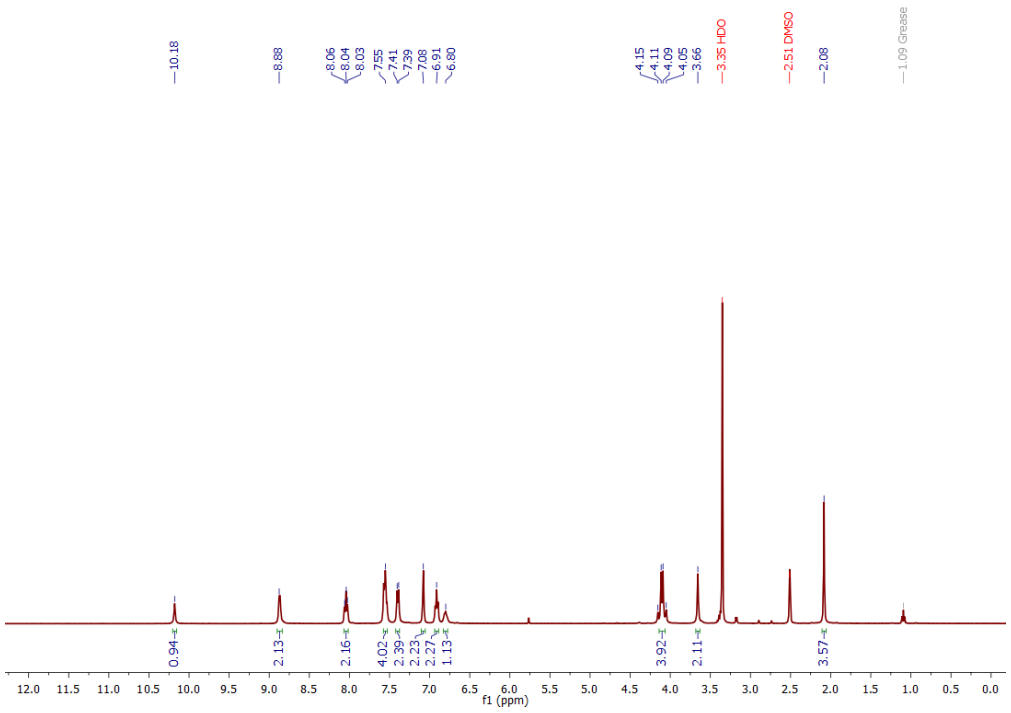

Figure S47. ^{1}H NMR (400 MHz, DMSO-d^{6}) spectrum of [(Py2ald)Zn(SePh)] (**2^{Zn}**) obtained from the reaction of [(Py2ald)Zn(ONO)] (**3^{Zn}**) with 2 equiv of PhSeH.

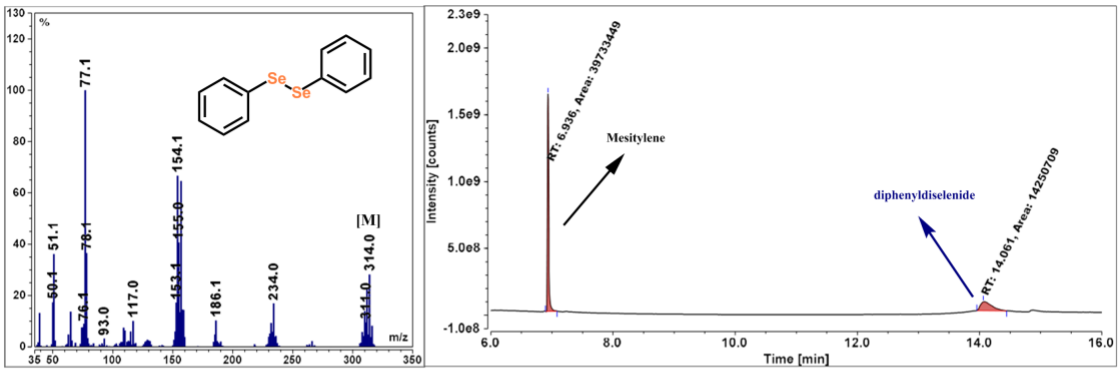

% yield for diphenyldiselenide:

Retention Time	Peak Area
14.061	14250709
6.936	39733449

$$\text{Yield} = \frac{14250709}{39733449} \times 100\%$$

$$= 35\%$$

Figure S48. Gas chromatographic data for the identification and yield calculation (35%) of diphenyldiselenide produced in the reaction of [(Py2ald)Zn(ONO)] (**3^{Zn}**) with 2 equiv of PhSeH.

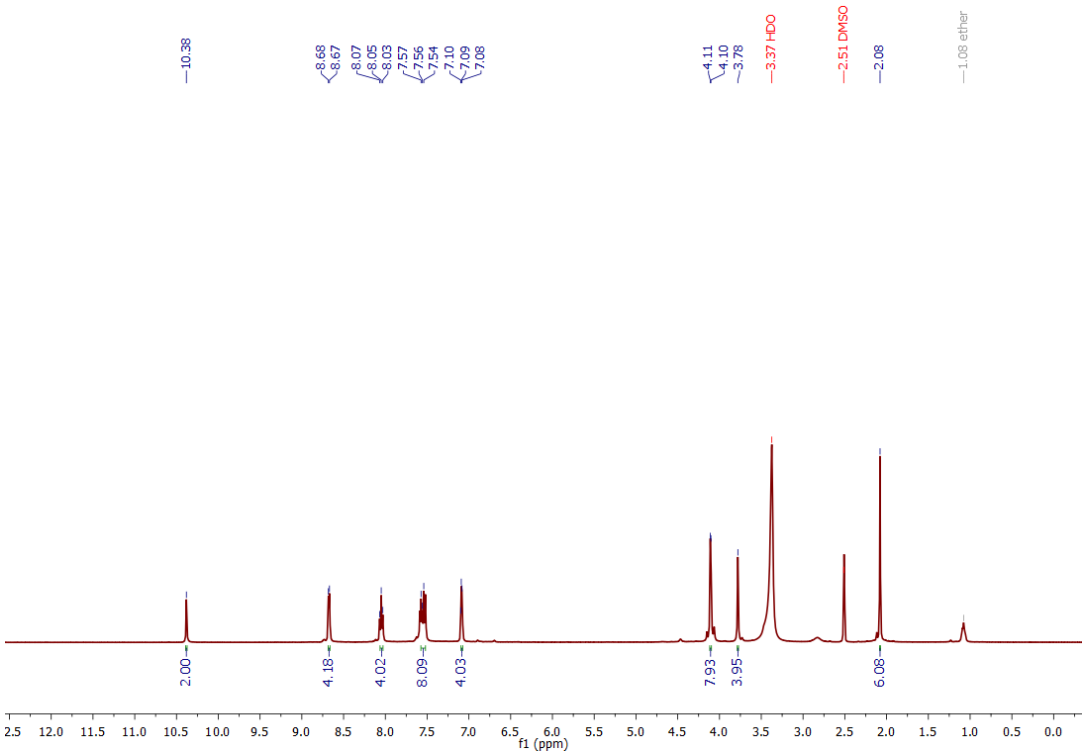

Figure S49. ^{1}H NMR (400 MHz, DMSO-d^{6}) spectrum of [(Py2ald)Zn]$_2$((BF$_4$)$_2$ (**5**^{Zn}(BF$_4$)$_2$) obtained from the reaction of [(Py2ald)Zn(ONO)] (**3**^{Zn}) and 2 equiv of PhCH$_2$SH.

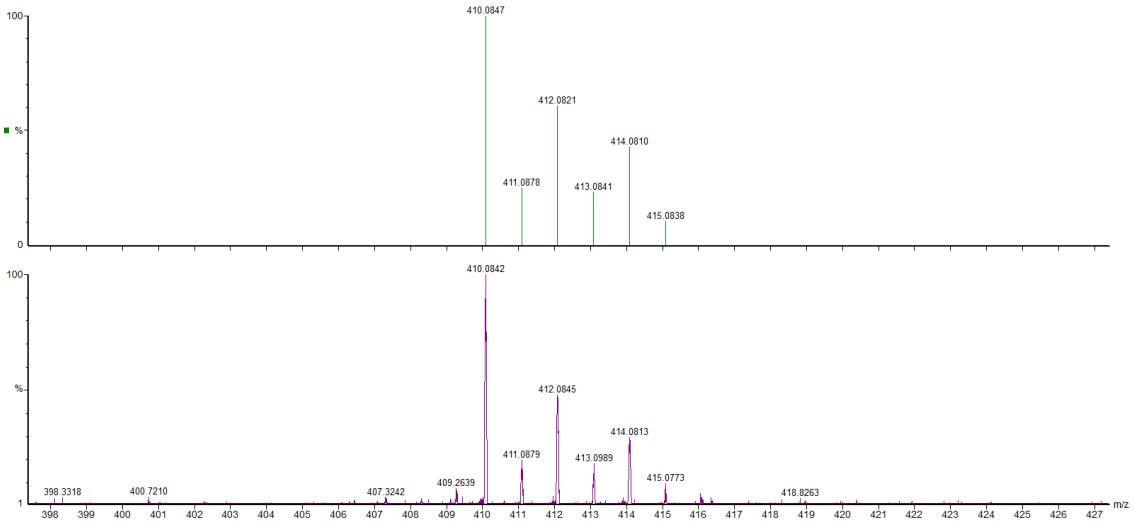

Figure S50. Mass spectrometric data (in MeCN) for [(Py2ald)Zn]$_2$((BF$_4$)$_2$ (**5**^{Zn}(BF$_4$)$_2$) obtained from the reaction of [(Py2ald)Zn(ONO)] (**3**^{Zn}) and 2 equiv of PhCH$_2$SH shows the presence of [(Py2ald)Zn]$^{+}$ (m/z: 410.0847, simulated data, green line; 410.0842, observed data, purple line).

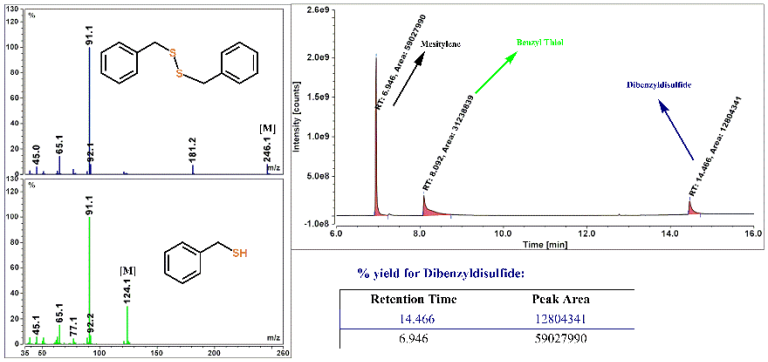

% yield for Dibenzyldisulfide:

Retention Time	Peak Area
14.466	12804341
6.946	59027990

$$\text{Yield} = \frac{12804341}{59027990} \times 100\% = 22\%$$

% yield for Benzyl Thiol:

Retention Time	Peak Area
8.092	31238839
6.946	59027990

$$\text{Yield} = \frac{31238839}{59027990} \times 100\% = 53\%$$

Figure S51. Gas chromatographic data for the identification and yield calculation of dibenzyldisulfide produced in the reaction of [(Py2ald)Zn(ONO)] (**3**$^{\mathbf{Zn}}$) with 2 equiv of $PhCH_2SH$. Yields: 32% ($PhCH_2S$-SCH_2Ph), 53% (unreacted $PhCH_2SH$).

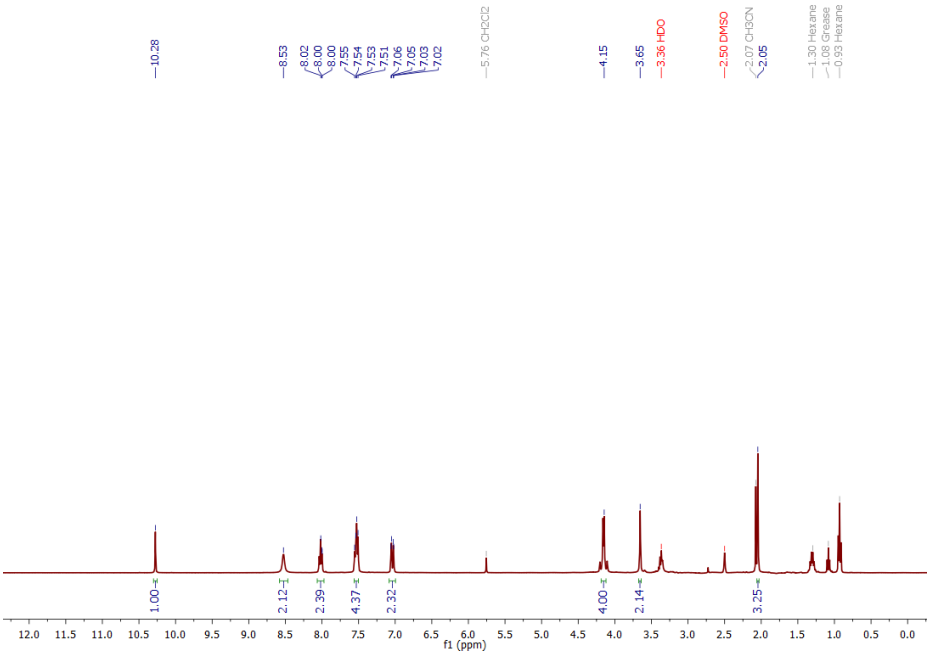

Figure S52. ^{1}H NMR (400 MHz, DMSO-d^6) spectrum of the unreacted [(Py2ald)Zn(ONO)] (**3**$^{\mathbf{Zn}}$) obtained from the reaction of **3**$^{\mathrm{Zn}}$ with 2 equiv of ^{t}BuSH. Note that the yield of NO in this reaction was only 9% .

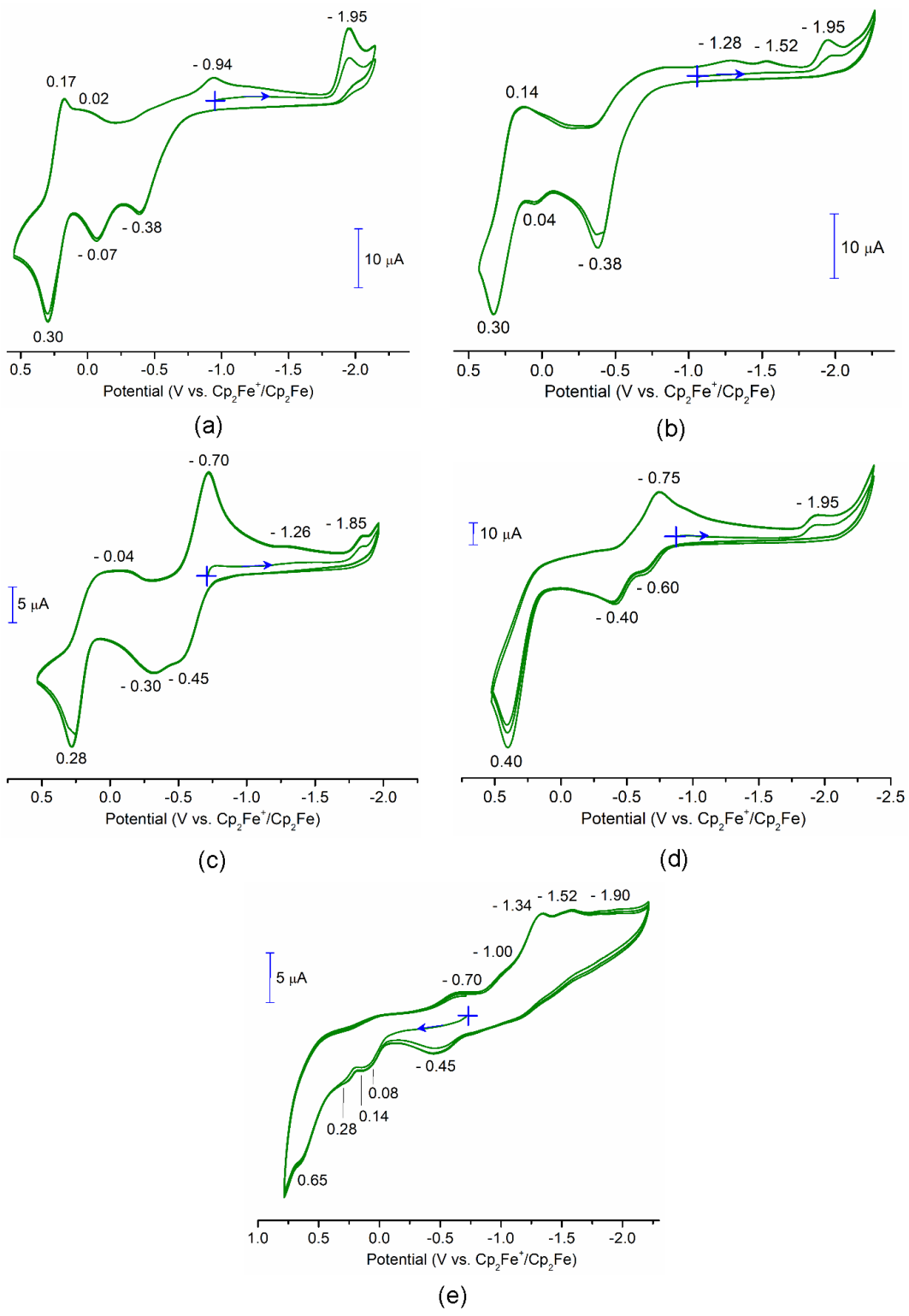

Figure S53. Cyclic voltammograms of **1a**^{Fe} (a) **1b**^{Fe} (b), **2**^{Fe} (c), **5**^{Fe} (d), and **8**^{Fe} (e) in CH_2Cl_2 (multiple scans, scan rate = 100 mV/scan). See Figure S54 for the cyclic voltammograms of Zn(II) complexes which helped to identify the redox events related with the Py2ald^{1-} ligand.

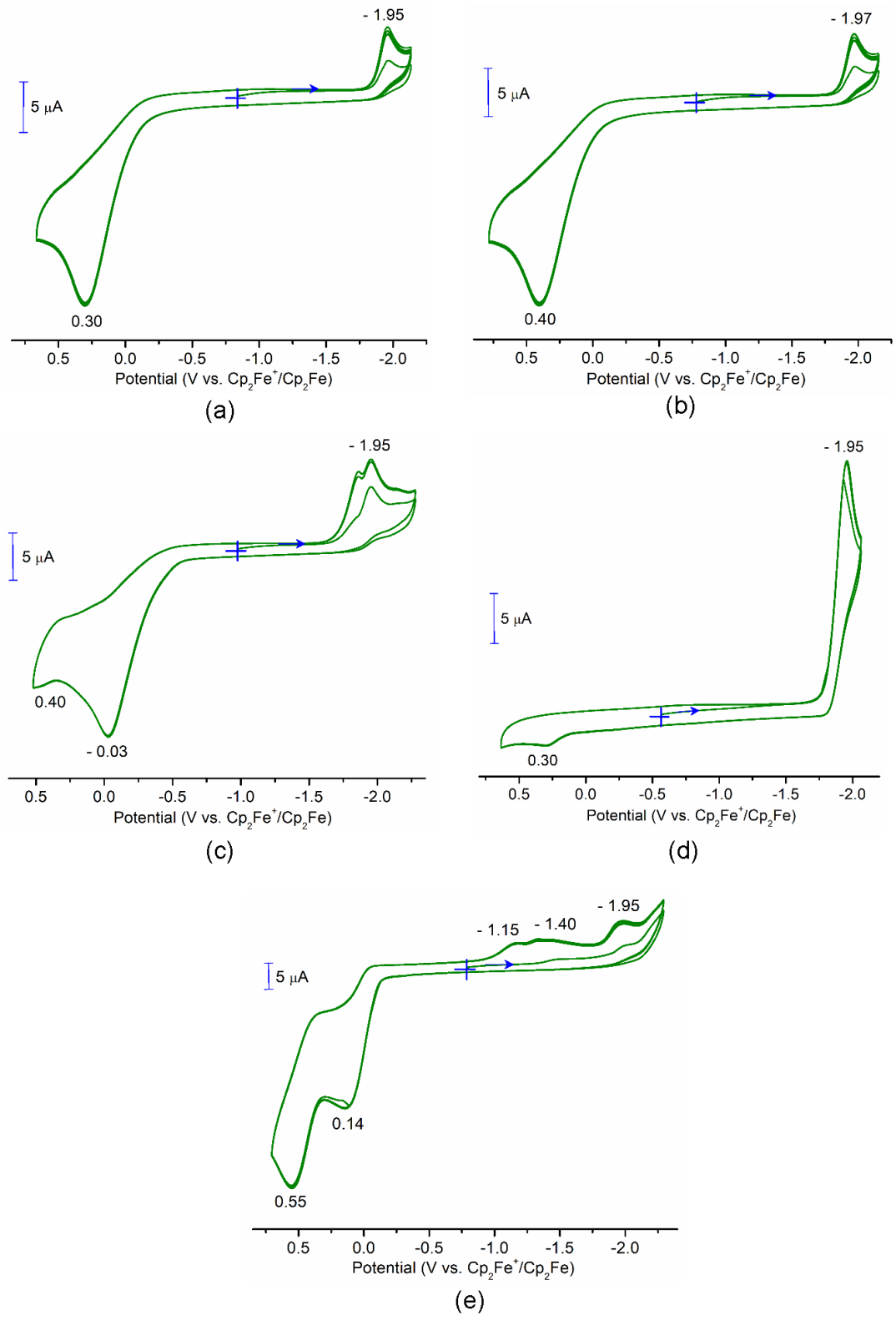

Figure S54. Cyclic voltammograms of **1a**^{Zn} (a) **1b**^{Zn} (b), **2**^{Zn} (c), **5**^{Zn} (d), and **3**^{Zn} (e) in CH_2Cl_2 (multiple scans, scan rate = 100 mV/scan).

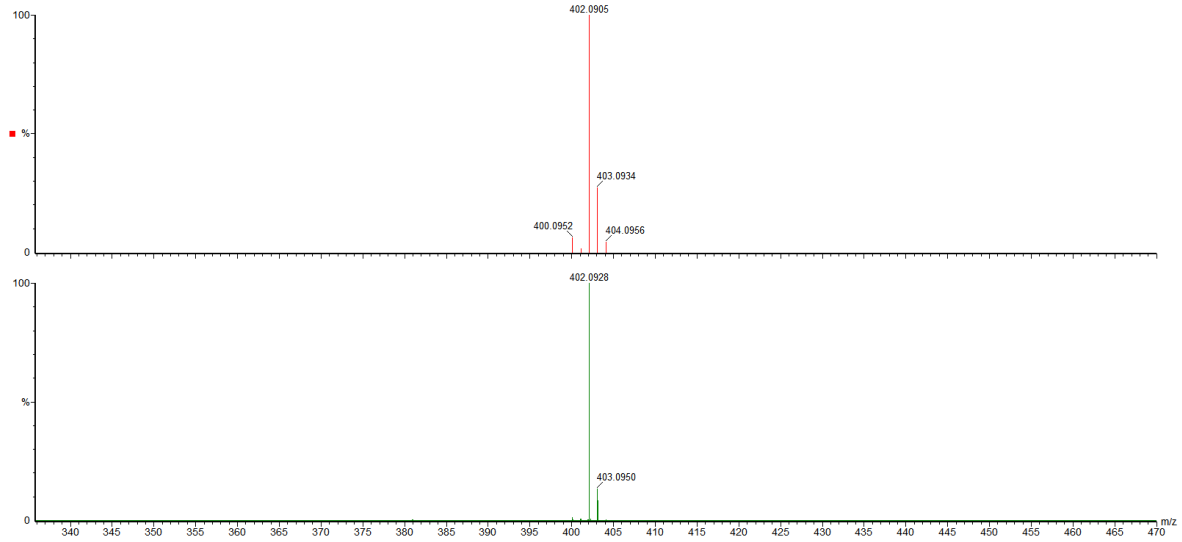

Figure S55. Mass spectrometric data (in MeCN) for $[(Py2ald)Fe]_2(BPh_4)_2$ ($\mathbf{5^{Fe}}(BPh_4)_2$) obtained from the reaction between [(Py2ald)Fe(SPh)] ($\mathbf{1a^{Fe}}$) with 1 equiv of $(Cp_2Fe)(BF_4)$ in the presence of $NaBPh_4$, shows the presence of $[(Py2ald)Fe]^+$ (m/z: 402.0905, simulated data, orange line; 402.0928, observed data, green line).

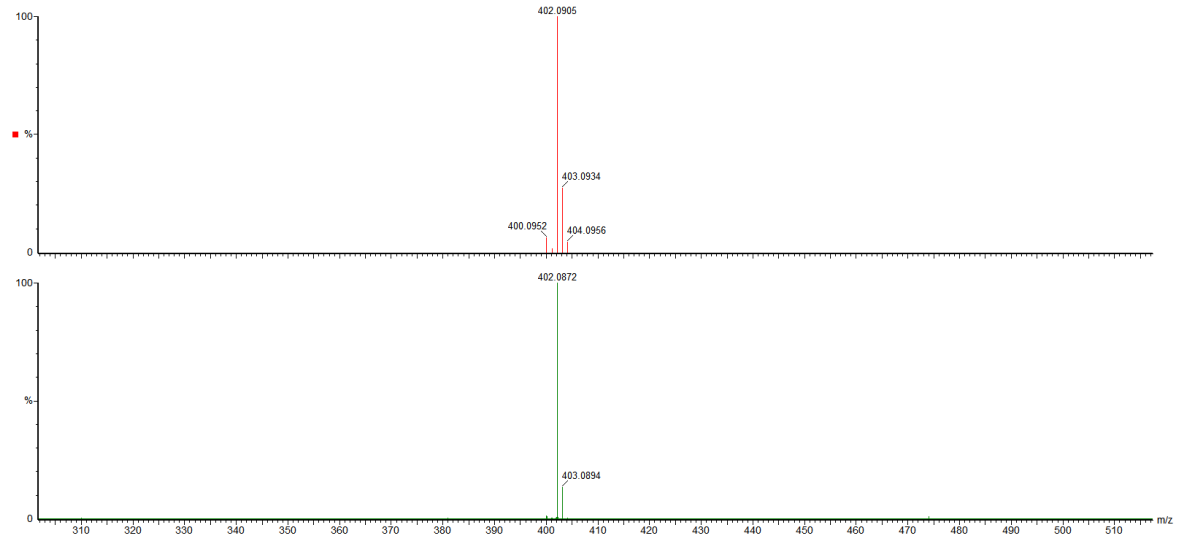

Figure S56. Mass spectrometric data (in MeCN) for $[(Py2ald)Fe]_2(BPh_4)_2$ ($\mathbf{5^{Fe}}(BPh_4)_2$) obtained from the reaction between [(Py2ald)Fe(SePh)] ($\mathbf{2^{Fe}}$) with 1 equiv of $(Cp_2Fe)(BF_4)$) in the presence of $NaBPh_4$, shows the presence of $[(Py2ald)Fe]^+$ (m/z: 402.0905, simulated data, orange line; 402.0872, observed data, green line).

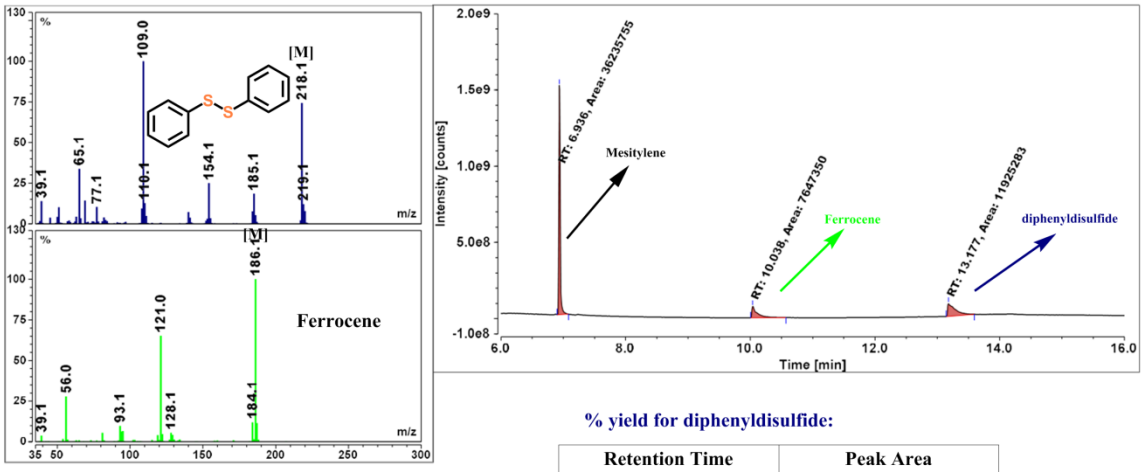

% yield for diphenyldisulfide:

Retention Time	Peak Area
13.177	11925283
6.936	36235755

$$\text{Yield} = \frac{11925283}{36235755} \times 100\%$$

$$= 33\%$$

Figure S57. GC-MS data for the identification and yield (33%) calculation of diphenyl disulfide produced in the reaction of [(Py2ald)Fe(SPh)] (**1a**^{Fe}) with 1 equiv of $(Cp_2Fe)(BF_4)$ in the presence of $NaBPh_4$.

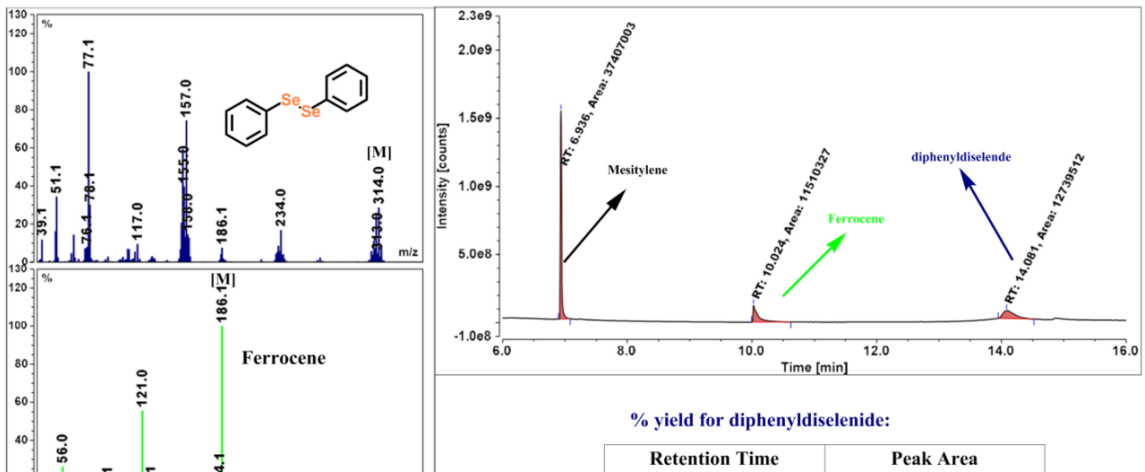

% yield for diphenyldiselenide:

Retention Time	Peak Area
14.081	12739512
6.936	37407003

$$\text{Yield} = \frac{12739512}{37407003} \times 100\%$$

$$= 34\%$$

Figure S58. GC-MS data for the identification and yield (34%) calculation of diphenyl diselenide produced in the reaction of [(Py2ald)Fe(SePh)] (**2**^{Fe}) with 1 equiv of $(Cp_2Fe)(BF_4)$ in the presence of $NaBPh_4$.

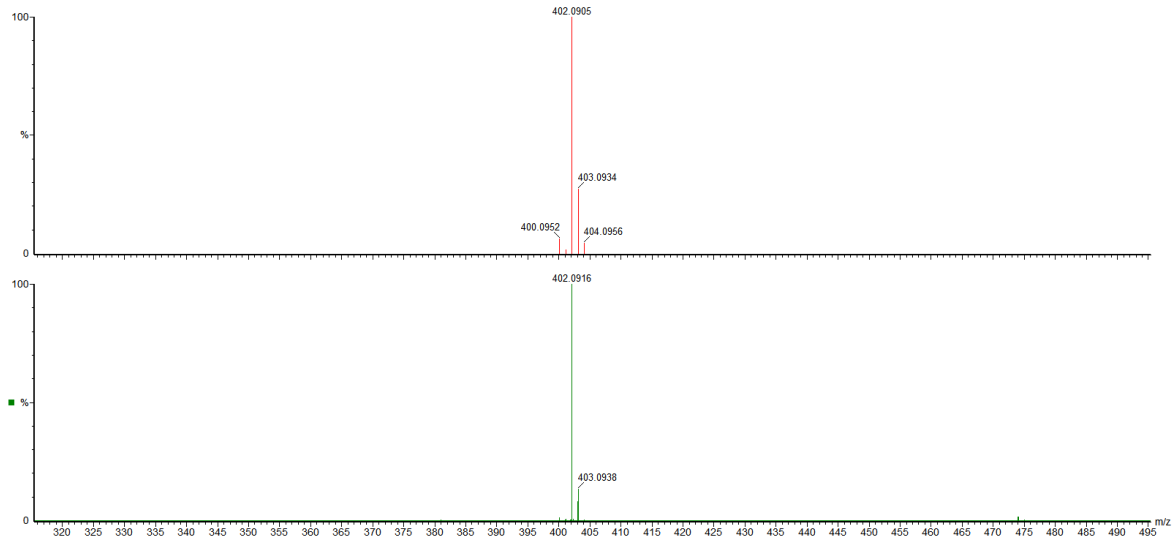

Figure S59. Mass spectrometric data (in MeCN) for $[(Py2ald)Fe]_2(BPh_4)_2$ ($\mathbf{5^{Fe}}(BPh_4)_2$) obtained from the reaction of $[(Py2ald)Fe(S\text{-}C_6H_4\text{-}2,6\text{-}Me_2)]$ ($\mathbf{1b^{Fe}}$) with 1 equiv of $(Cp_2Fe)(BF_4)$ in the presence of $NaBPh_4$, shows the presence of $[(Py2ald)Fe]^+$ (m/z: 402.0905, simulated data, orange line; 402.0916, observed data, green line).

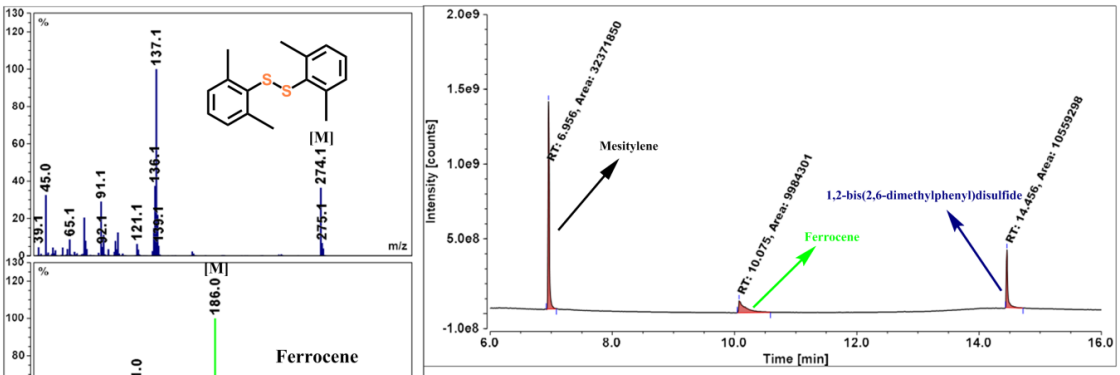

% yield for 1,2-bis(2,6-dimethylphenyl)disulfide:

Retention Time	Peak Area
14.456	10559298
6.956	32371850

$$\text{Yield} = \frac{11204662}{32371850} \times 100\% = 33\%$$

Figure S60. GC-MS data for the identification and yield (33%) calculation of 1, 2-bis(2,6-dimethylphenyl)disulfide produced in the reaction of $[(Py2ald)Fe(S\text{-}C_6H_4\text{-}2,6\text{-}Me_2)]$ ($\mathbf{1b^{Fe}}$) with 1 equiv of $(Cp_2Fe)(BF_4)$ in the presence of $NaBPh_4$.

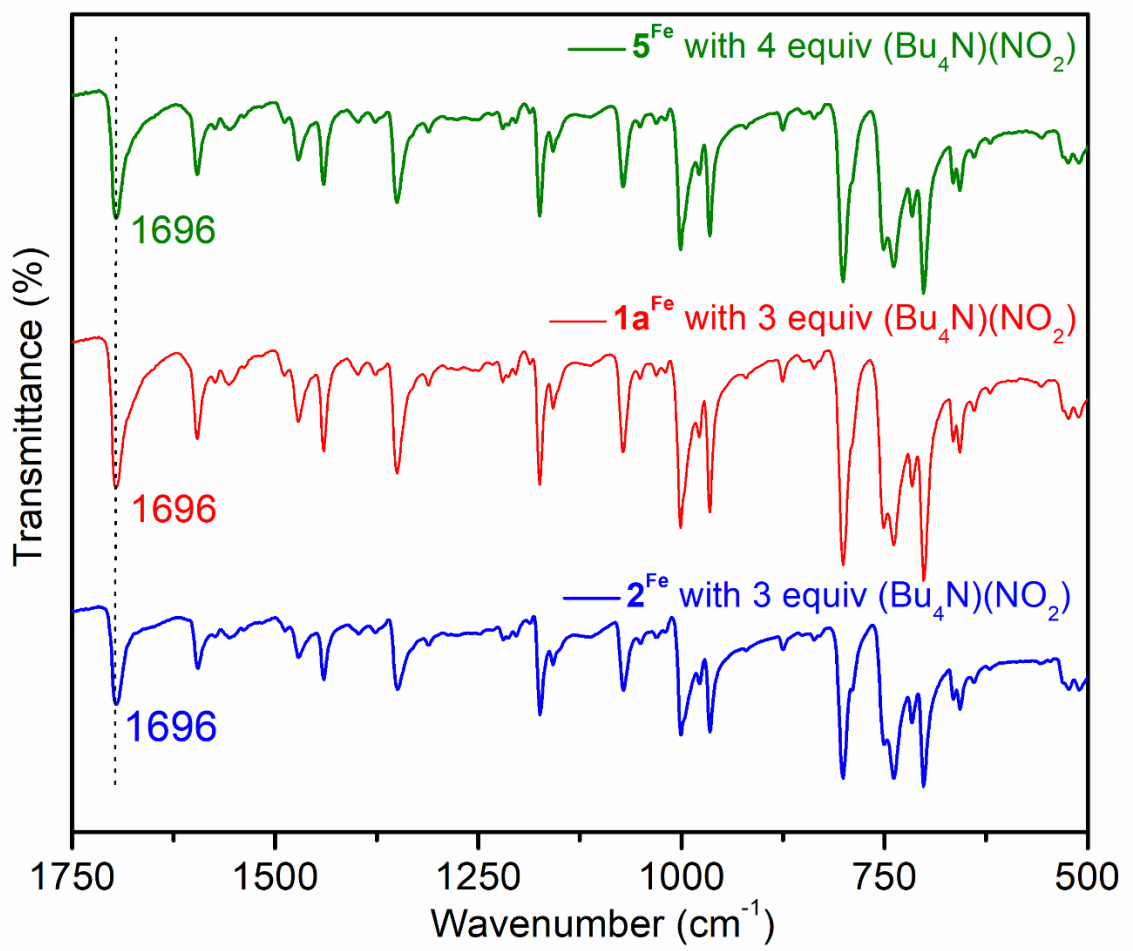

Figure S61. IR spectra of [(TPP)Co(NO)] (ν_{NO} = 1696 cm^{-1}) obtained by the trapping of NO gas which was generated by the reaction of $[(Py2ald)Fe]_2(BF_4)_2$ ($\mathbf{5}^{Fe}(BF_4)_2$) and [(Py2ald)Fe(EPh)] (E = S, $\mathbf{1a}^{Fe}$, E = Se, $\mathbf{2}^{Fe}$) with 4 and 3 equiv of $(Bu_4N)(NO_2)$, respectively.

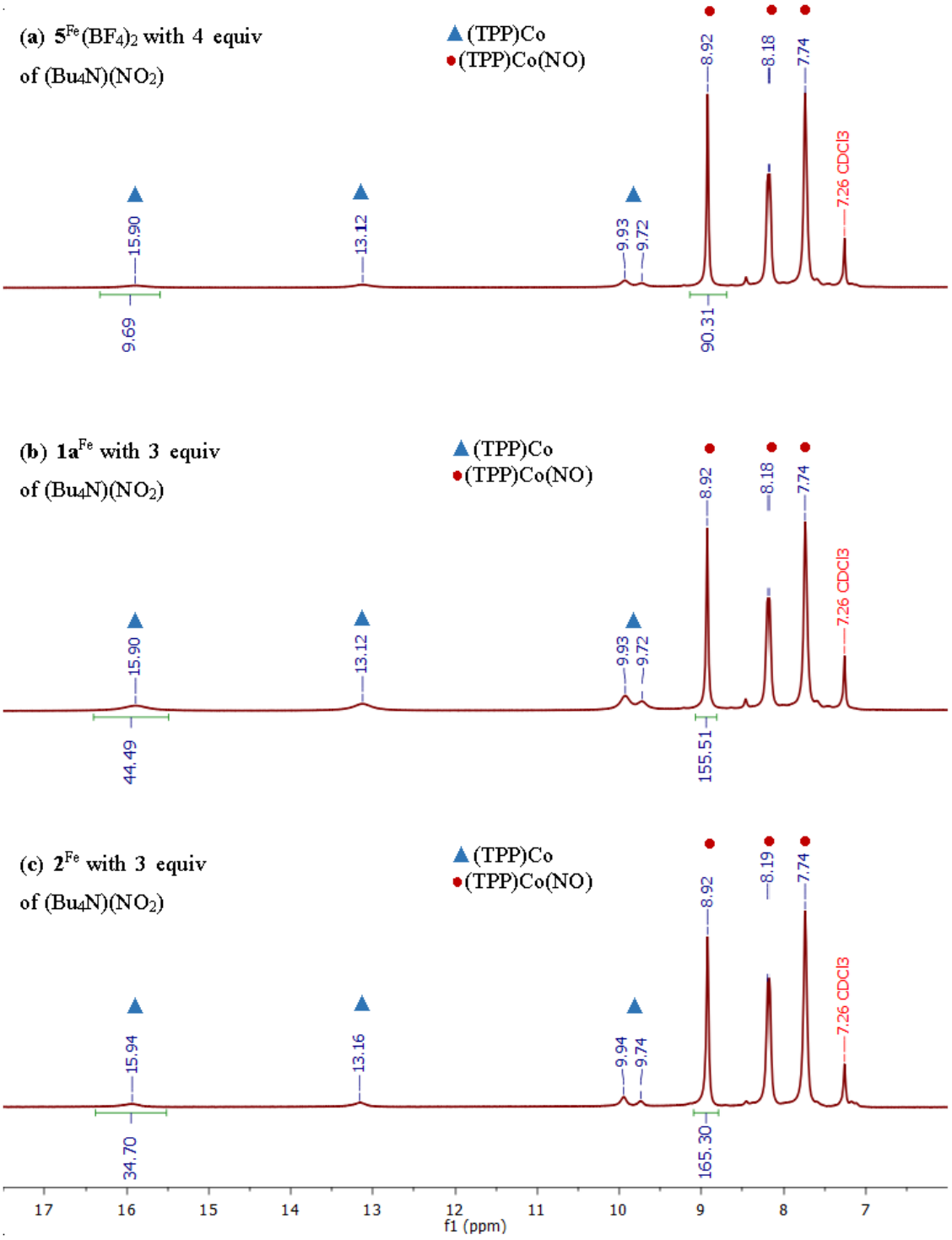

Figure S62. ^{1}H NMR (400 MHz, $CDCl_3$) spectra of $(TPP)Co^{II}$ after trapping the NO gas which was generated by the reaction of $[(Py2ald)Fe]_2(BF_4)_2$ (**5**$^{Fe}(BF_4)_2$) and [(Py2ald)Fe(EPh)] (E = S, **1a**^{Fe}, E = Se, **2**^{Fe}) with 4 and 3 equiv of $(Bu_4N)(NO_2)$, respectively.

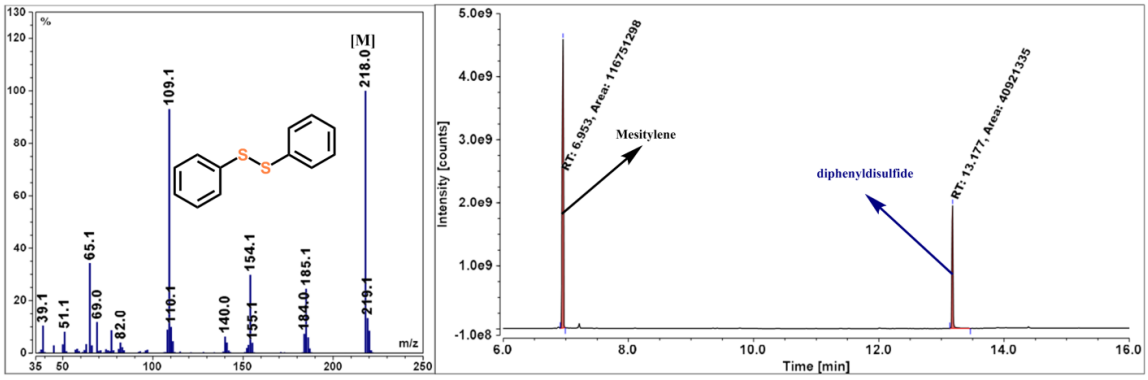

% yield for diphenyldisulfide :

Retention Time	Peak Area
13.177	40921335
6.953	116751298

$$\text{Yield} = \frac{40921335}{116751298} \times 100\%$$

$$= 35\%$$

Figure S63. GC-MS data for the identification and yield (35%) calculation of diphenyldisulfide produced in the reaction of [(Py2ald)Fe(SPh)] (**1a**^{Fe}) with 3 equiv of (Bu_4N)(NO_2).

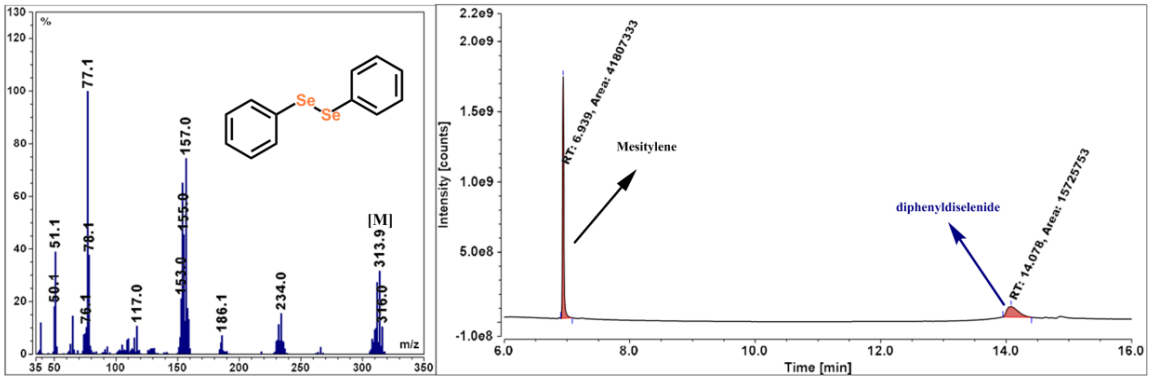

% yield for diphenyldiselenide:

Retention Time	Peak Area
14.078	15725753
6.939	41807333

$$\text{Yield} = \frac{15725753}{41807333} \times 100\%$$

$$= 38\%$$

Figure S64. Gas chromatographic data for the identification and yield calculation of diphenyldiselenide (38%) produced in the reaction of [(Py2ald)Fe(SePh)] (**2**^{Fe}) with 3 equiv of (Bu_4N)(NO_2).

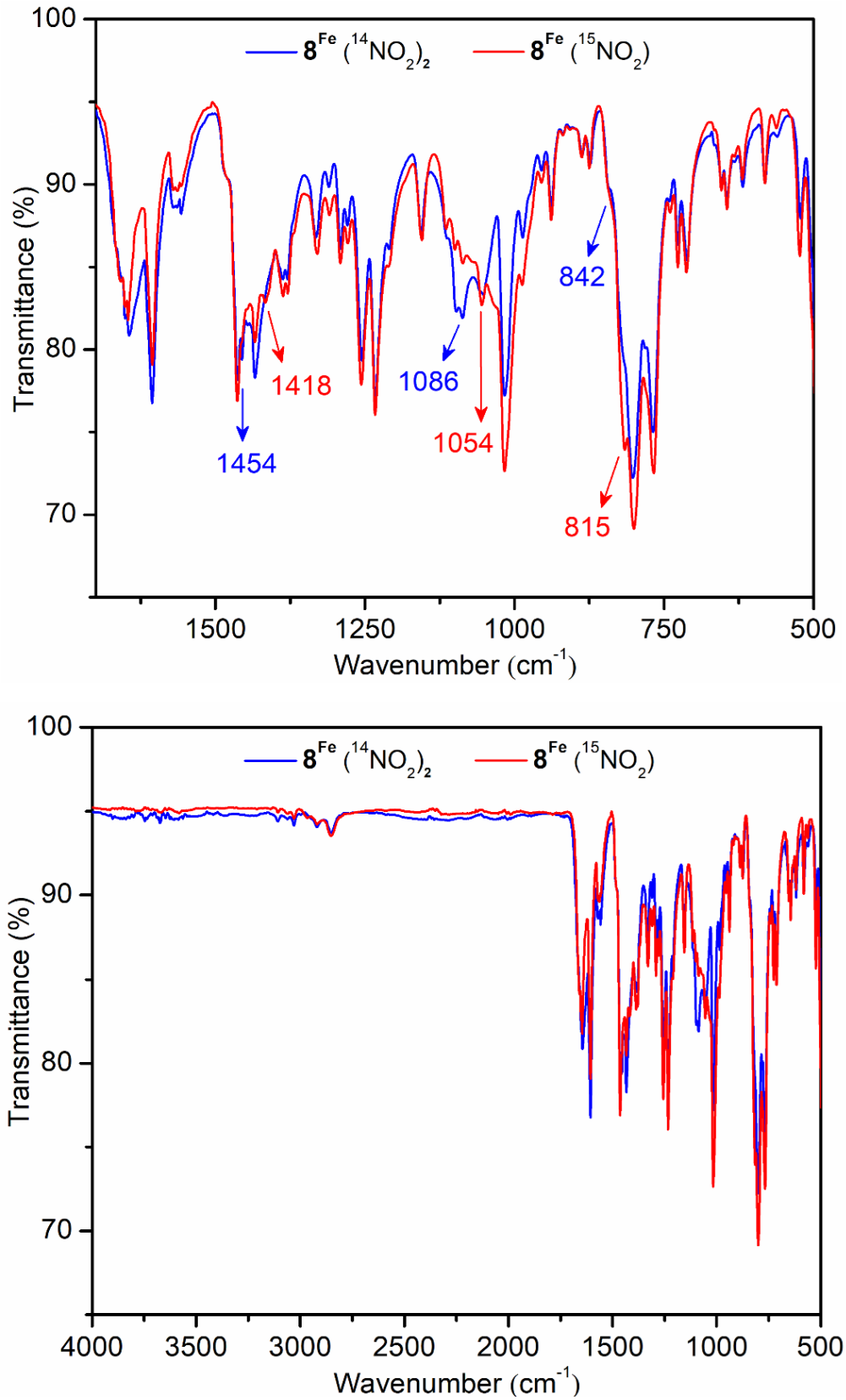

Figure S65. IR spectra (ATR) of [{(Py2ald)(ONO)Fe}$_2$-μ_2-O] (**8^{Fe}**) and the corresponding ^{15}N labelled compound, **8^{Fe}**($^{15}NO_2$).

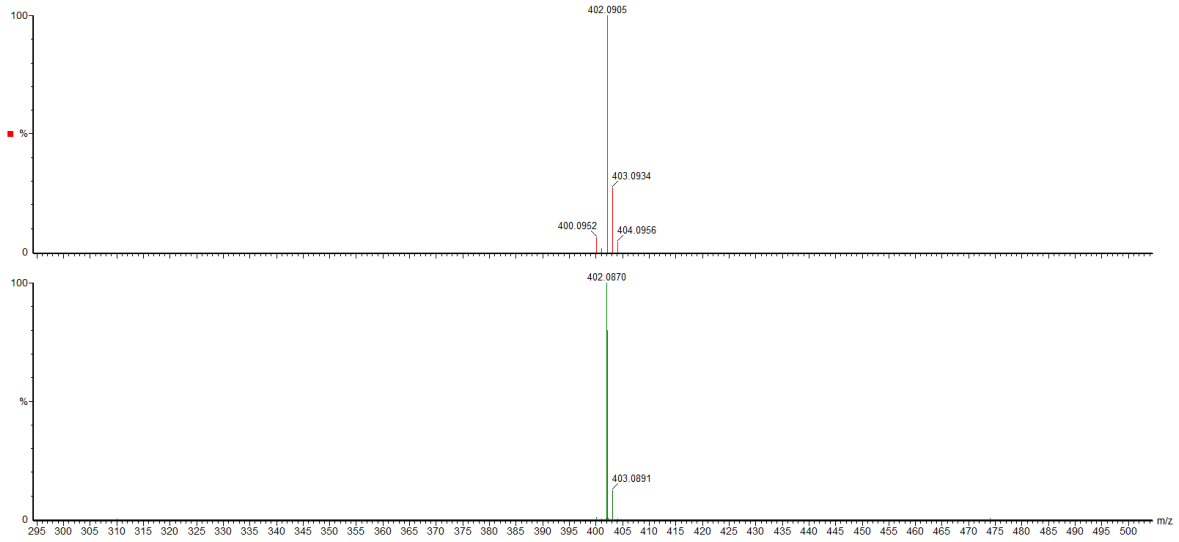

Figure S66 Mass spectrometric data (in MeCN) for $[(Py2ald)Fe]_2(BF_4)_2$ ($\mathbf{5^{Fe}}(BF_4)_2$) obtained from the reaction between $[\{(Py2ald)(ONO)Fe\}_2\text{-}\mu_2\text{-}O]$ ($\mathbf{8^{Fe}}$) and 4 equiv of Cp_2Co shows the presence of $[(Py2ald)Fe]^+$ (m/z: 402.0905, simulated data, orange line; 402.0870, observed data, green line).

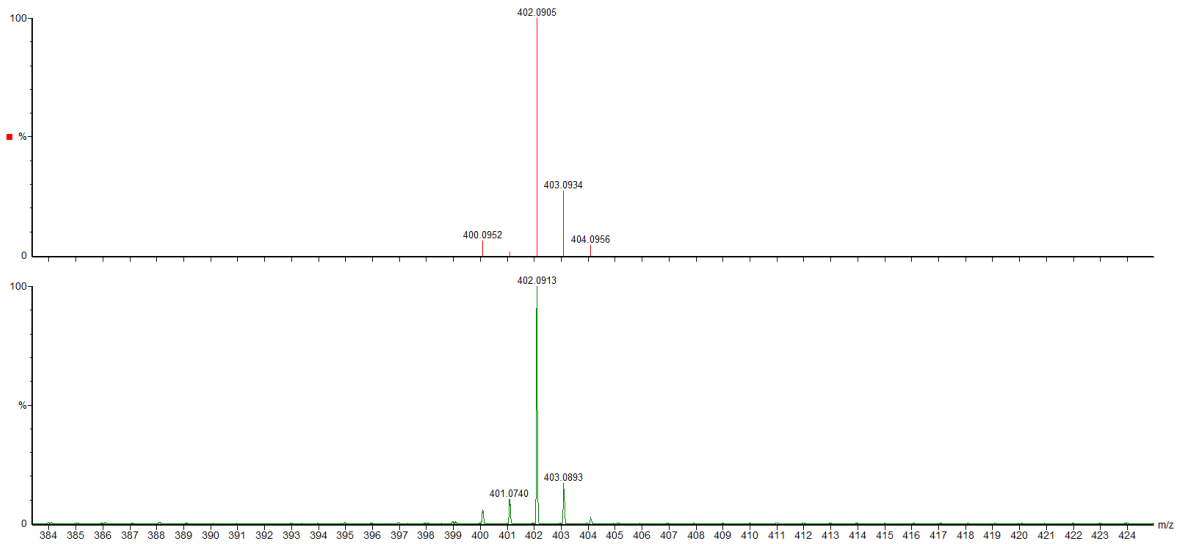

Figure S67. Mass spectrometric data (in MeCN) for $[(Py2ald)Fe]_2(BF_4)_2$ ($\mathbf{5^{Fe}}(BPh_4)_2$) obtained from the reaction between $[\{(Py2ald)(ONO)Fe\}_2\text{-}\mu_2\text{-}O]$ ($\mathbf{8^{Fe}}$) with 4 equiv of PhSH (in the presence of 2 equiv of $NaBPh_4$) shows the presence of $[(Py2ald)Fe]^+$ (m/z: 402.0905, simulated data, orange line; 402.0913, observed data, green line).

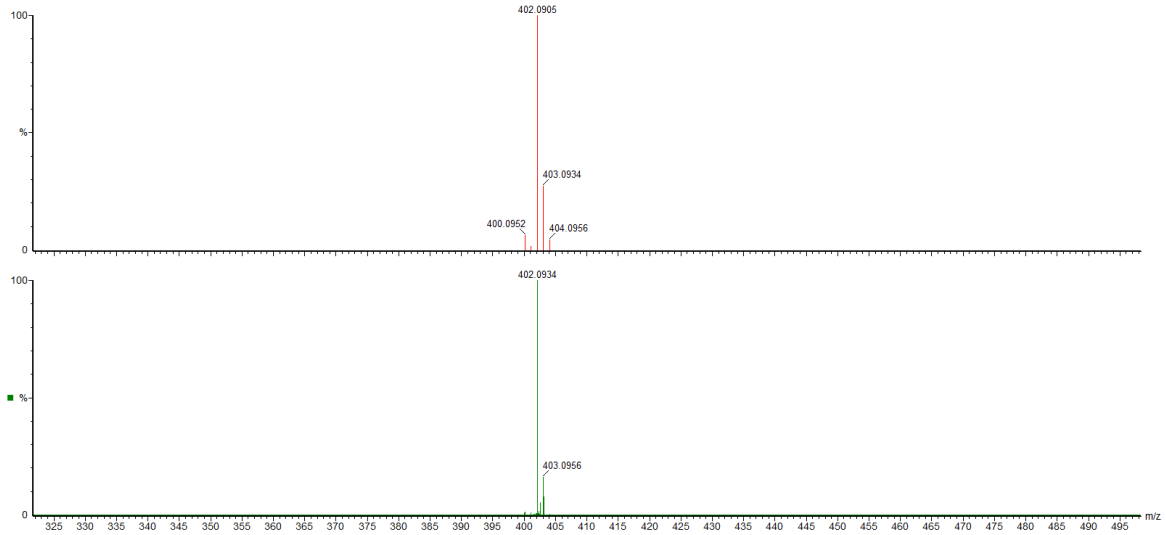

Figure S68. Mass spectrometric data (in MeCN) for $[(Py2ald)Fe]_2(BF_4)_2$ ($\mathbf{5}^{Fe}(BPh_4)_2$) obtained from the reaction between $[\{(Py2ald)(ONO)Fe\}_2\text{-}\mu_2\text{-}O]$ ($\mathbf{8}^{Fe}$) with 4 equiv of PhSeH (in the presence of 2 equiv of $NaBPh_4$) shows the presence of $[(Py2ald)Fe]^+$ (m/z:402.0905, simulated data, orange line; 402.0934, observed data, green line).

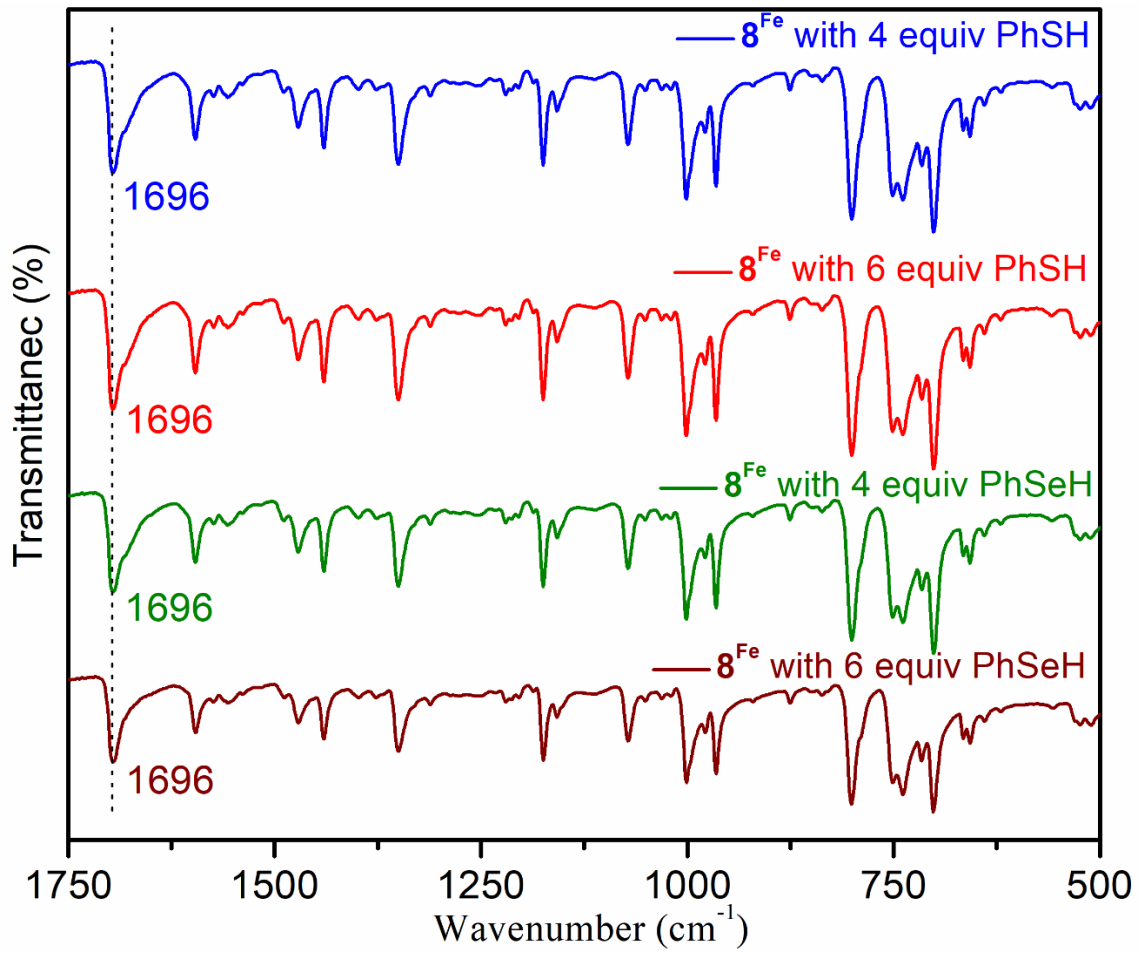

Figure S69. IR spectra of [(TPP)Co(NO)] (ν_{NO} = 1696 cm^{-1}) obtained by the trapping of NO gas which was generated by the reaction of [{(Py2ald)(ONO)Fe}$_2$-μ_2-O] (**8^{Fe}**) with 4 and 6 equiv of PhEH (E = S, Se).

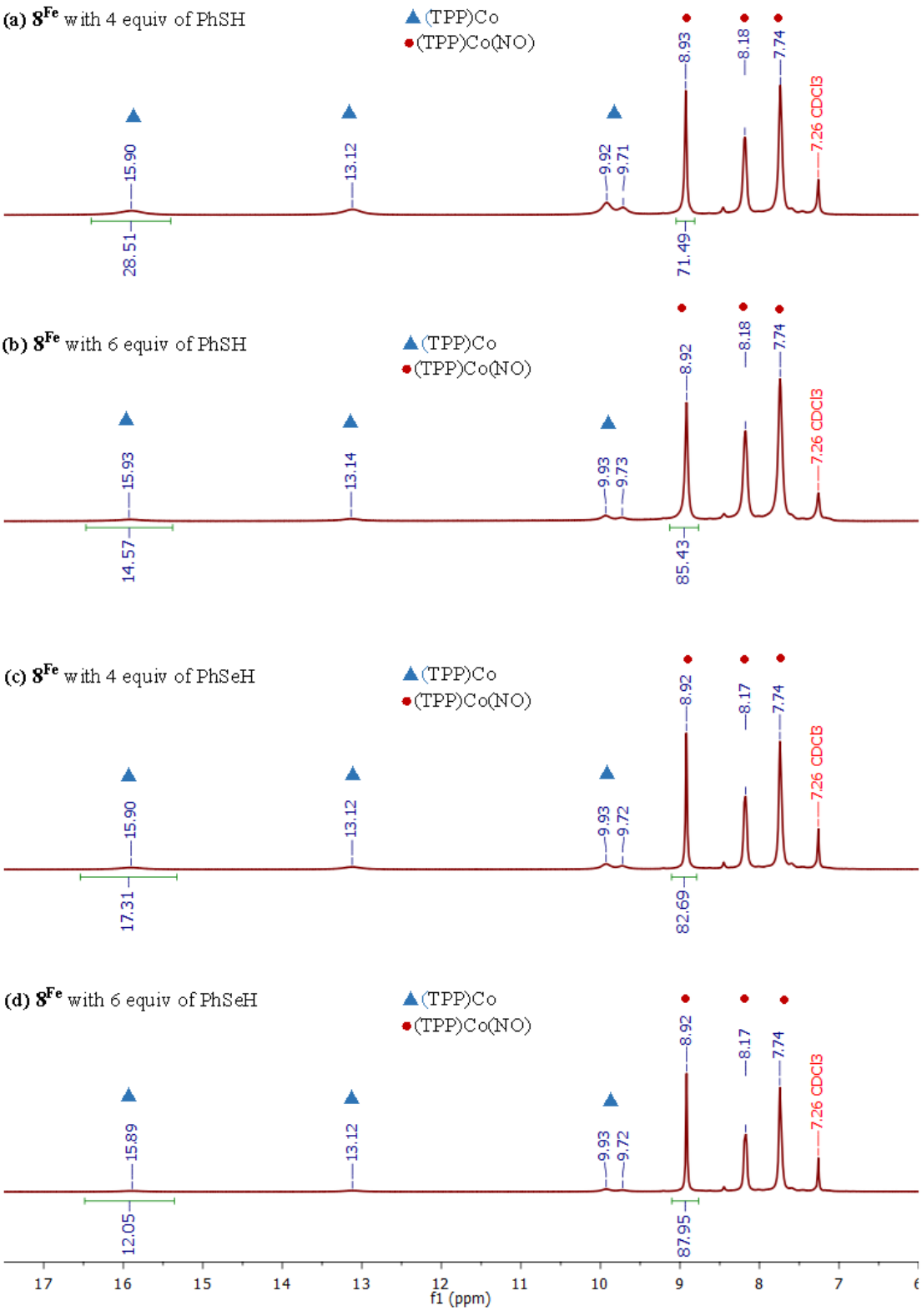

Figure S70. ^{1}H NMR (400 MHz, CDCl3) spectra of (TPP)Co^{II} after trapping the NO gas generated by the reaction of [{(Py2ald)(ONO)Fe}$_2$-μ_2-O] (**8^{Fe}**) with 4 and 6 equiv of PhEH (E = S, Se).

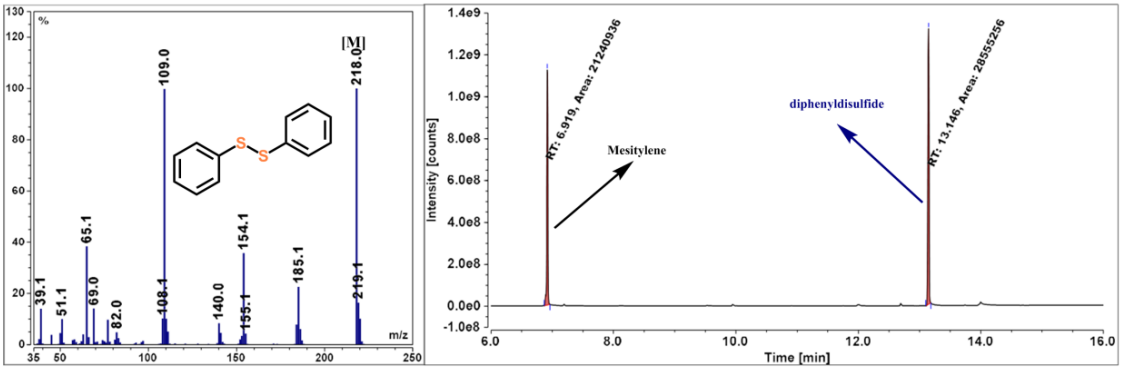

% yield for diphenyldisulfide :

Retention Time	Peak Area
13.146	28555256
6.919	21240936

$$\text{Yield} = \frac{28555256}{21240936} \times 100\%$$

$$= 134\%$$

Figure S71. GC-MS data for the identification and yield calculation (1.34 equiv) of diphenyldisulfide produced in the reaction of [{(Py2ald)(ONO)Fe}$_2$-μ_2-O] (**8**^{Fe}) with 4 equiv PhSH.

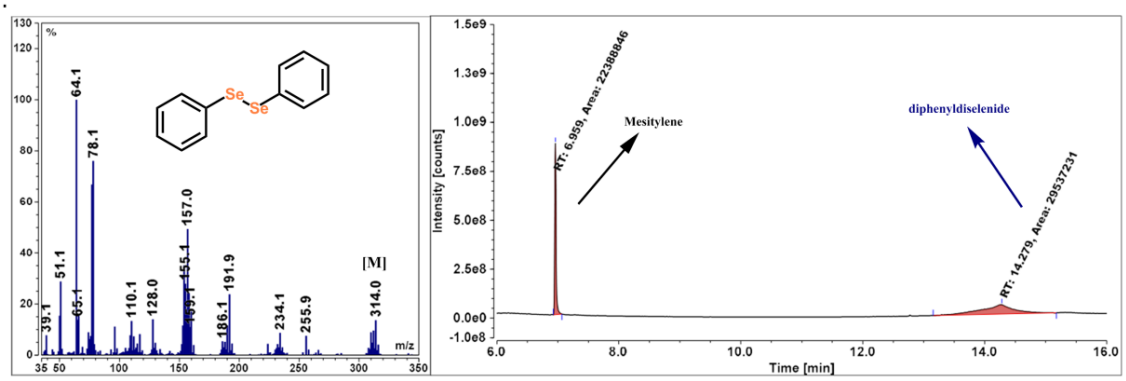

% yield for diphenyldiselenide:

Retention Time	Peak Area
14.279	29537231
6.959	22388846

$$\text{Yield} = \frac{29537231}{22388846} \times 100\%$$

$$= 132\%$$

Figure S72. GC-MS data for the identification and yield calculation (1.32 equiv) of diphenyldiselenide produced in the reaction of [{(Py2ald)(ONO)Fe}$_2$-μ_2-O] (**8**^{Fe}) with 4 equiv PhSeH.

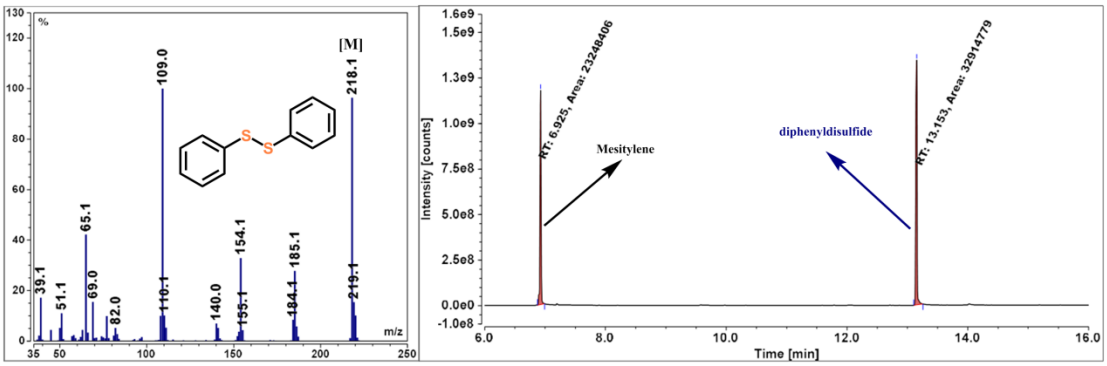

% yield for diphenyldisulfide :

Retention Time	Peak Area
13.153	32914779
6.925	23248406

$$\text{Yield} = \frac{32914779}{23248406} \times 100\%$$

$$= 141\%$$

Figure S73. GC-MS data for the identification and yield (1.41 equiv) calculation of diphenyldisulfide produced in the reaction of [{(Py2ald)(ONO)Fe}$_2$-μ_2-O] (**8**$^{\mathbf{Fe}}$) with 6 equiv of PhSH.

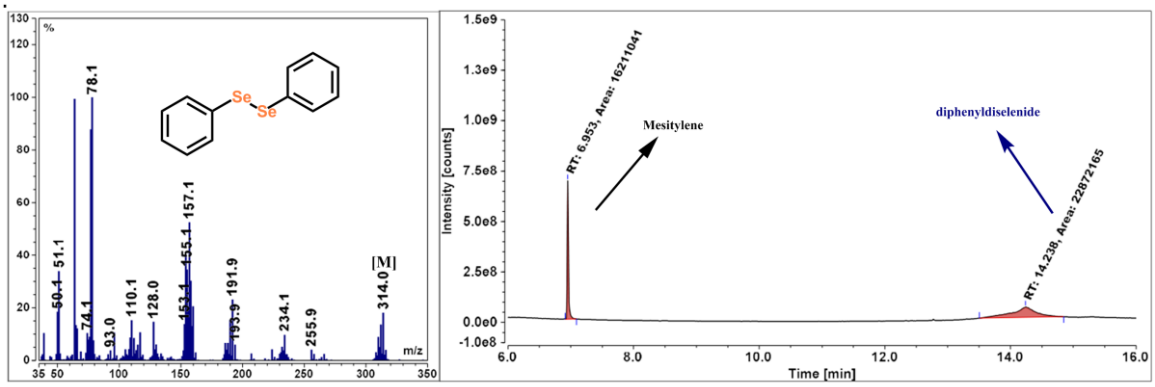

% yield for diphenyldiselenide:

Retention Time	Peak Area
14.238	22872165
6.953	16211041

$$\text{Yield} = \frac{22872165}{16211041} \times 100\%$$

$$= 141\%$$

Figure S74. GC-MS data for the identification and yield calculation (1.41 equiv) of diphenyldiselenide produced in the reaction of [{(Py2ald)(ONO)Fe}$_2$-μ_2-O] (**8**$^{\mathbf{Fe}}$) with 6 equiv of PhSeH.

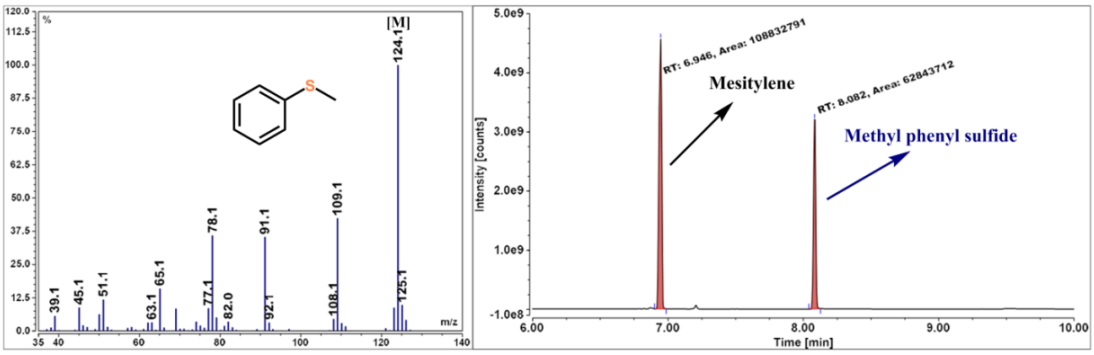

% yield for Methyl phenyl sulfide :

Retention Time	Peak Area
8.082	62843712
6.946	108832791

$$\text{Yield} = \frac{62843712}{108832791} \times 100\%$$

$$= 58\%$$

Figure S75. GC-MS data for the identification and yield (58%) calculation of methylphenyl sulfide produced in the reaction of [(Py2ald)Zn(SPh)] (**1a^{Zn}**) with MeI in 1:1 ratio.

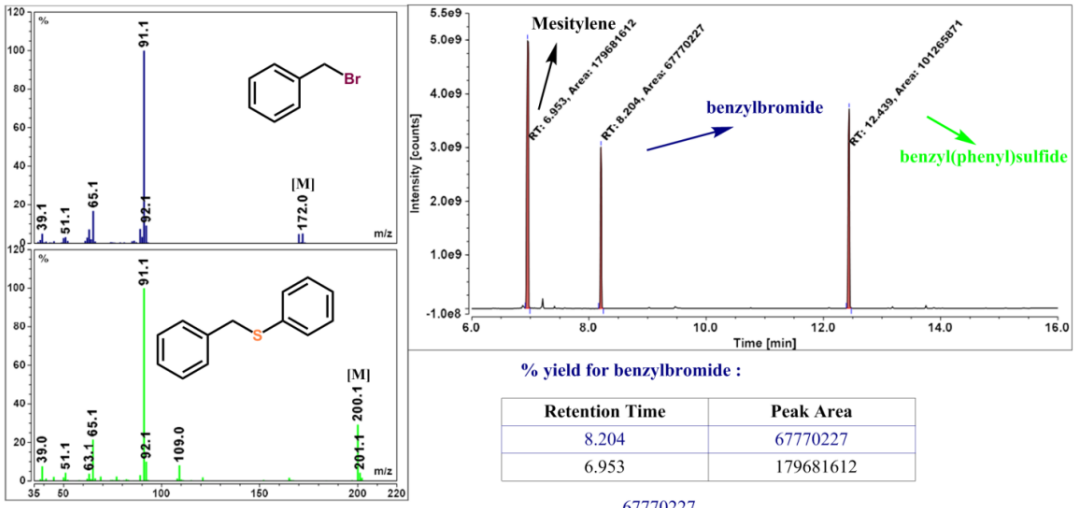

% yield for benzylbromide :

Retention Time	Peak Area
8.204	67770227
6.953	179681612

$$\text{Yield} = \frac{67770227}{179681612} \times 100\%$$

$$= 38\%$$

% yield for benzyl(phenyl)sulfide **:**

Retention Time	Peak Area
12.439	101265871
6.953	179681612

$$\text{Yield} = \frac{101265871}{179681612} \times 100\%$$

$$= 56\%$$

Figure S76. GC-MS data for the identification and yield (56%) calculation of benzyl(phenyl)sulfide produced in the reaction of [(Py2ald)Zn(SPh)] (**1a^{Zn}**) with $PhCH_2Br$ in 1:1 ratio.

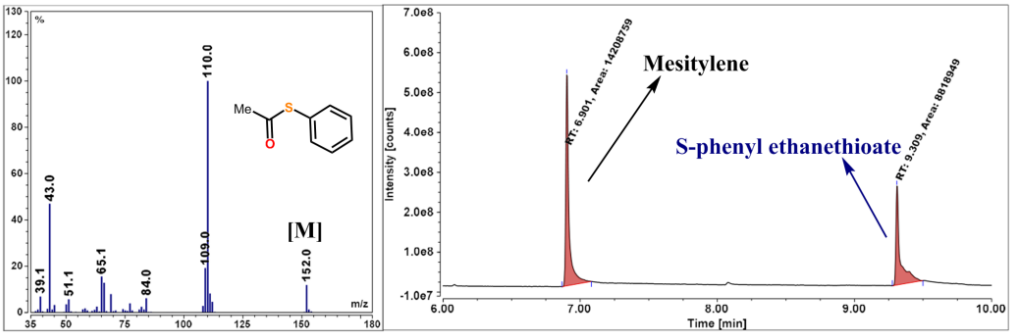

% yield for S-phenyl ethanethioate:

Retention Time	Peak Area
9.309	8818949
6.901	14208759

$$\text{Yield} = \frac{8818949}{14208759} \times 100\%$$

$$= 62\%$$

Figure S77. GC-MS data for the identification and yield (62%) calculation of S-phenyl ethanethioate produced in the reaction of [(Py2ald)Zn(SPh)] (**1a**$^{\mathbf{Zn}}$) with MeCOCl in 1:1 ratio.

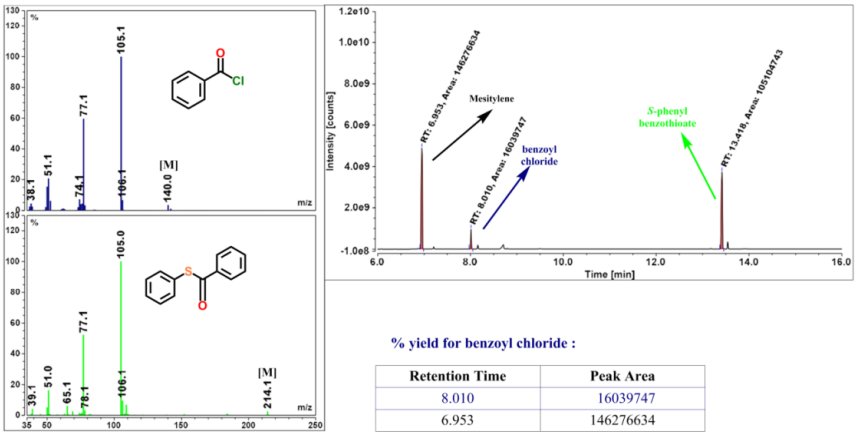

% yield for benzoyl chloride :

Retention Time	Peak Area
8.010	16039747
6.953	146276634

$$\text{Yield} = \frac{16039747}{146276634} \times 100\%$$

$$= 11\%$$

% yield for *S*-phenyl benzothioate :

Retention Time	Peak Area
13.148	105104743
6.946	146276634

$$\text{Yield} = \frac{105104743}{146276634} \times 100\%$$

$$= 72\%$$

Figure S78. GC-MS data for the identification and yield (72%) calculation of S-phenyl benzothioate produced in the reaction of [(Py2ald)Zn(SPh)] (**1a**$^{\mathbf{Zn}}$) with PhCOCl in 1:1 ratio.

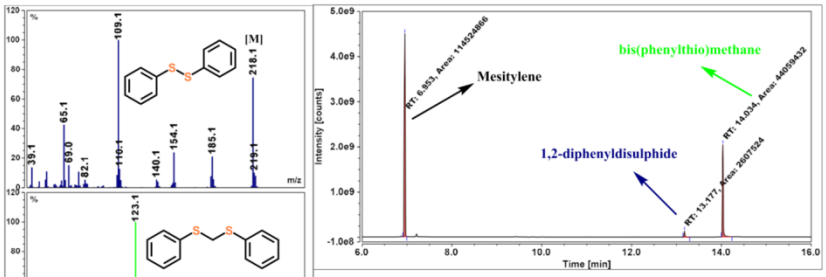

% yield for 1,2-diphenyldisulphide :

Retention Time	Peak Area
13.177	2607524
6.953	114524866

$$\text{Yield} = \frac{2607524}{114524866} \times 100\%$$

$$= 2\%$$

% yield for bis(phenylthio)methane :

Retention Time	Peak Area
14.034	44059432
6.953	114524866

$$\text{Yield} = \frac{44059432}{114524866} \times 100\%$$

$$= 38\%$$

Figure S79. Gas chromatographic data for the identification and yield (38%) calculation of bis(phenylthio)methane produced in the reaction of [(Py2ald)Zn(SPh)] (**1a**$^{\mathbf{Zn}}$) with CH_2Br_2 in 1:1 ratio.

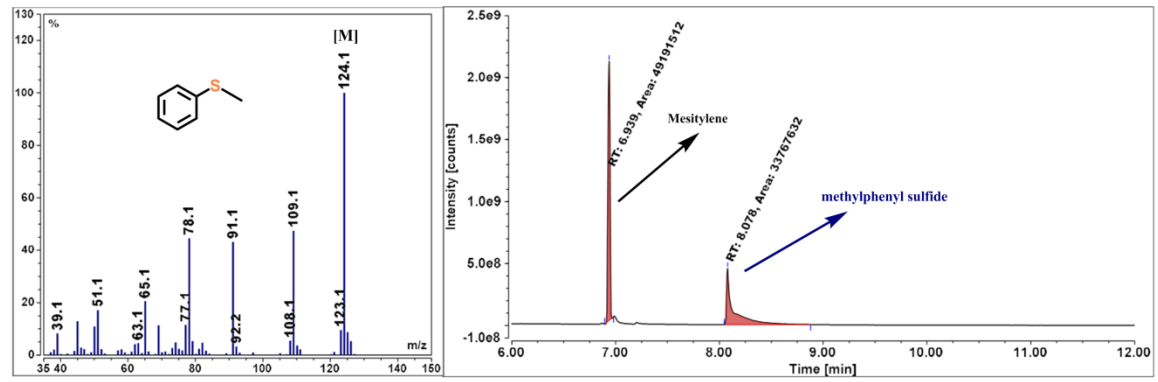

% yield for methylphenyl sulfide :

Retention Time	Peak Area
8.078	33767632
6.939	49191512

$$\text{Yield} = \frac{33767632}{49191512} \times 100\%$$

$$= 69\%$$

Figure S80. Gas chromatographic data for the identification and yield (69%) calculation of methylphenyl sulfide produced in the reaction of [(Py2ald)Fe(SPh)] (**1a**$^{\mathbf{Fe}}$) with MeI in 1:1 ratio.

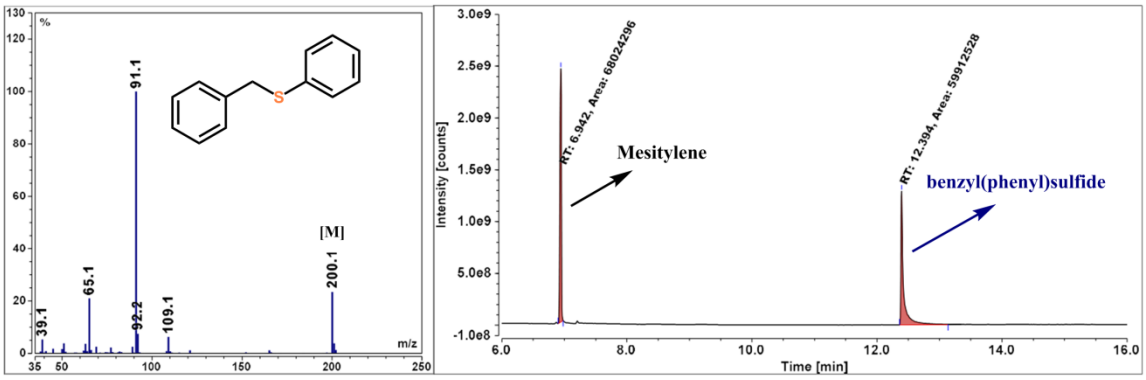

% yield for benzyl(phenyl)sulfide :

Retention Time	Peak Area
12.394	59912528
6.942	68024296

$$\text{Yield} = \frac{59912528}{68024296} \times 100\%$$

$$= 88\%$$

Figure S81. GC-MS data for the identification and yield (88%) calculation of benzyl(phenyl)sulfide produced in the reaction of [(Py2ald)Fe(SPh)] (**1a**^{Fe}) with $PhCH_2Br$ in 1:1 ratio.

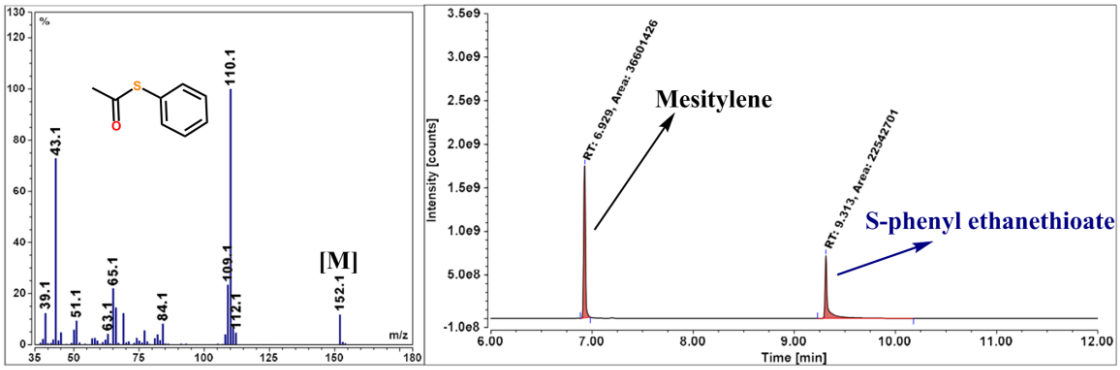

% yield for S-phenyl ethanethioate:

Retention Time	Peak Area
9.313	22542701
6.929	36601426

$$\text{Yield} = \frac{22542701}{36601426} \times 100\%$$

$$= 62\%$$

Figure S82. GC-MS data for the identification and yield (62%) calculation of S-phenyl ethanethioate produced in the reaction of [(Py2ald)Fe(SPh)] (**1a**^{Fe}) with MeCOCl in 1:1 ratio.

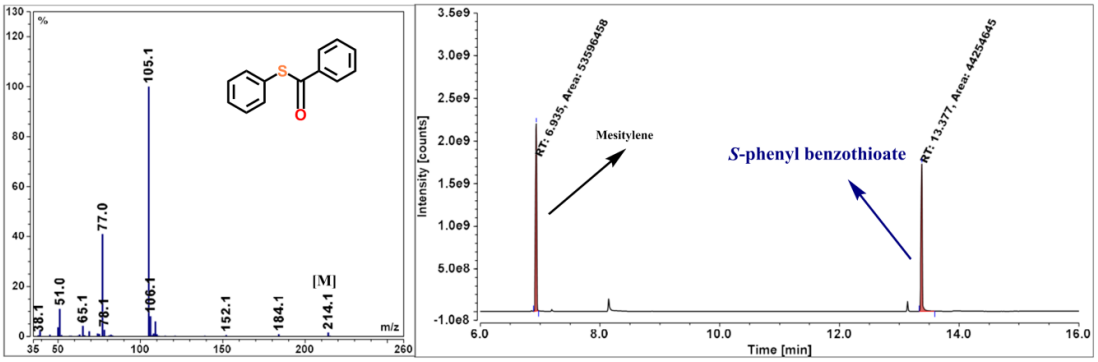

% yield for *S*-phenyl benzothioate:

Retention Time	Peak Area
13.377	44254645
6.935	53596458

$$\text{Yield} = \frac{44254645}{53596458} \times 100\%$$

$$= 83\%$$

Figure S83. GC-MS data for the identification and yield (83%) calculation of S-phenyl benzothioate produced in the reaction of [(Py2ald)Fe(SPh)] (**1a**^{Fe}) with PhCOCl in 1:1 ratio.

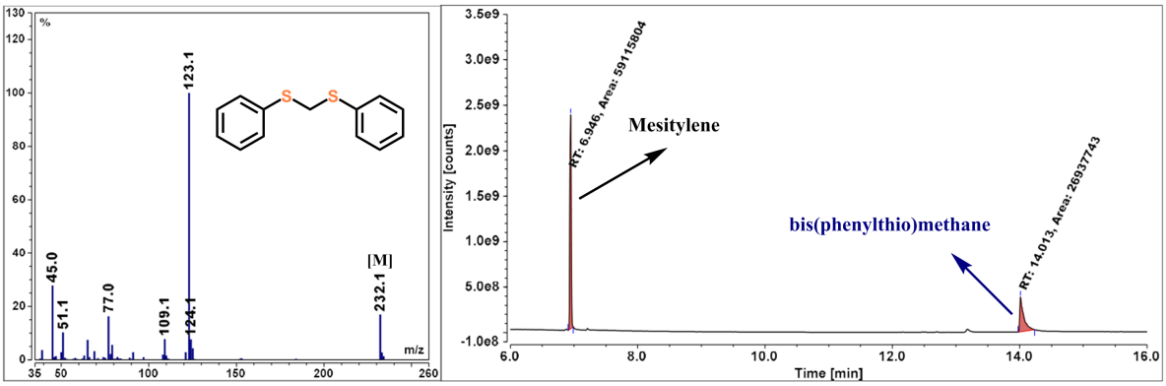

% yield for bis(phenylthio)methane :

Retention Time	Peak Area
14.013	26937743
6.946	59115804

$$\text{Yield} = \frac{26937743}{59115804} \times 100\%$$

$$= 46\%$$

Figure S84. GC-MS data for the identification and yield (46%) calculation of bis(phenylthio)methane produced in the reaction of [(Py2ald)Fe(SPh)] (**1a**^{Fe}) with CH_2Br_2 in 1:1 ratio.

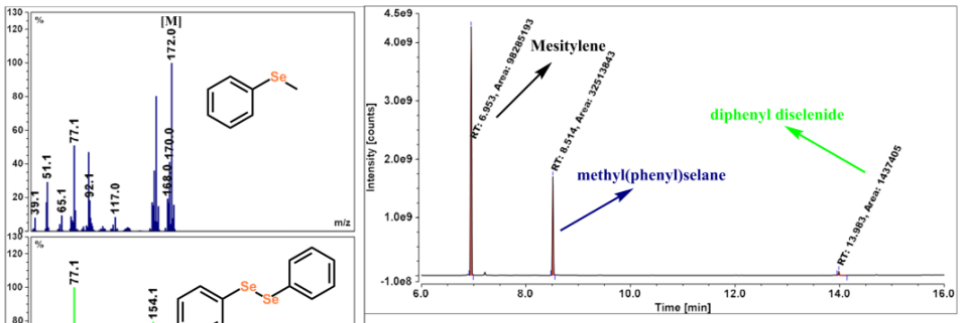

% yield for methyl(phenyl)selane :

Retention Time	Peak Area
8.514	32513843
6.953	98285193

$$\text{Yield} = \frac{32513843}{98285193} \times 100\%$$

$$= 33\%$$

% yield for diphenyl diselenide :

Retention Time	Peak Area
13.983	1437405
6.953	98285193

$$\text{Yield} = \frac{1437405}{98285193} \times 100\%$$

$$= 1\%$$

Figure S85. GC-MS data for the identification and yield (33%) calculation of methyl(phenyl)selane produced in the reaction of [(Py2ald)Zn(SePh)] (**2^{Zn}**) with MeI in 1:1 ratio.

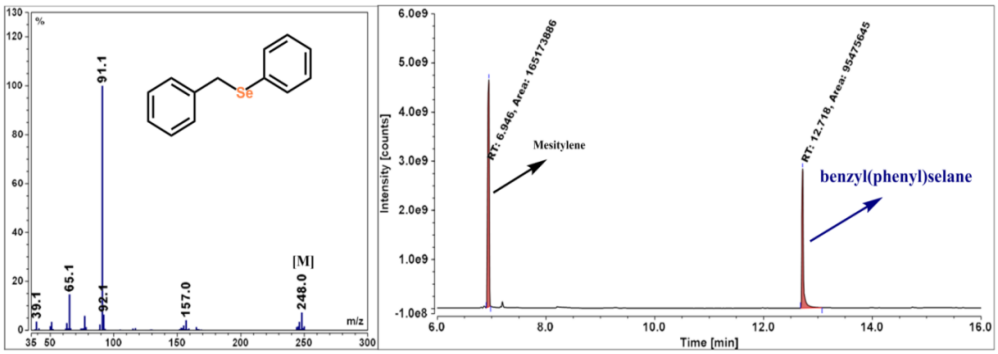

% yield for benzyl(phenyl)selane :

Retention Time	Peak Area
8.208	95475645
6.946	165173886

$$\text{Yield} = \frac{95475645}{165173886} \times 100\%$$

$$= 57\%$$

Figure S86. GC-MS data for the identification and yield (57%) calculation of benzyl(phenyl)selane produced in the reaction of [(Py2ald)Zn(SePh)] (**2^{Zn}**) with $PhCH_2Br$ in 1:1 ratio.

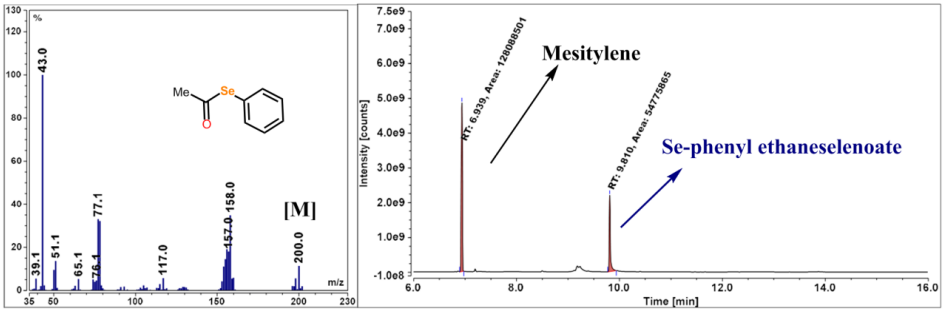

% yield for Se-phenyl ethaneselenoate:

Retention Time	Peak Area
9.309	54775865
6.901	128088501

$$\text{Yield} = \frac{54775865}{128088501} \times 100\%$$

$$= 45\%$$

Figure S87. GC-MS data for the identification and yield (45%) calculation of Se-phenyl ethaneselenoate produced in the reaction of [(Py2ald)Zn(SePh)] (**2**$^{\mathbf{Zn}}$) with MeCOCl in 1:1 ratio.

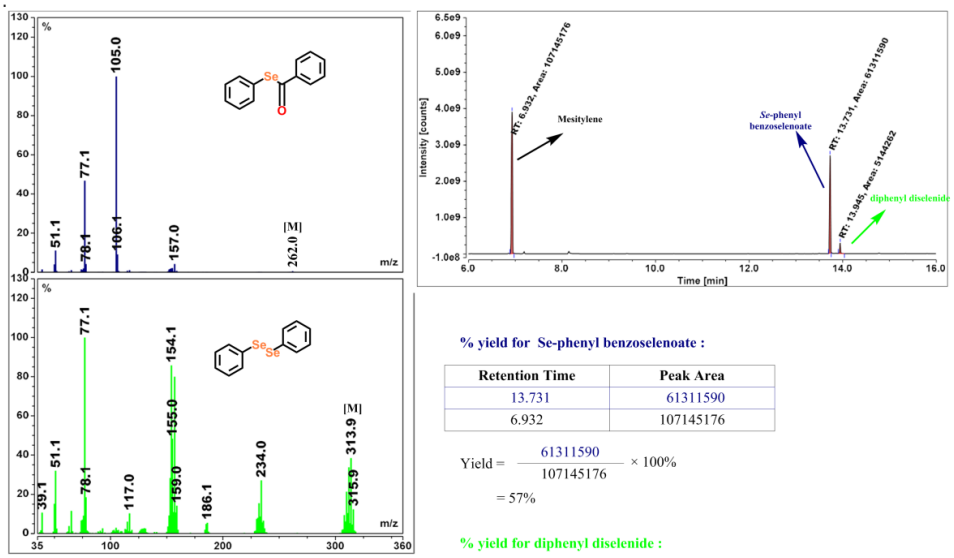

% yield for Se-phenyl benzoselenoate :

Retention Time	Peak Area
13.731	61311590
6.932	107145176

$$\text{Yield} = \frac{61311590}{107145176} \times 100\%$$

$$= 57\%$$

% yield for diphenyl diselenide :

Retention Time	Peak Area
13.945	5144262
6.953	107145176

$$\text{Yield} = \frac{5144262}{107145176} \times 100\%$$

$$= 5\%$$

Figure S88. GC-MS data for the identification and yield (57%) calculation of Se-phenyl benzoselenoate produced in the reaction of [(Py2ald)Zn(SePh)] (**2**$^{\mathbf{Zn}}$) with PhCOCl in 1:1 ratio.

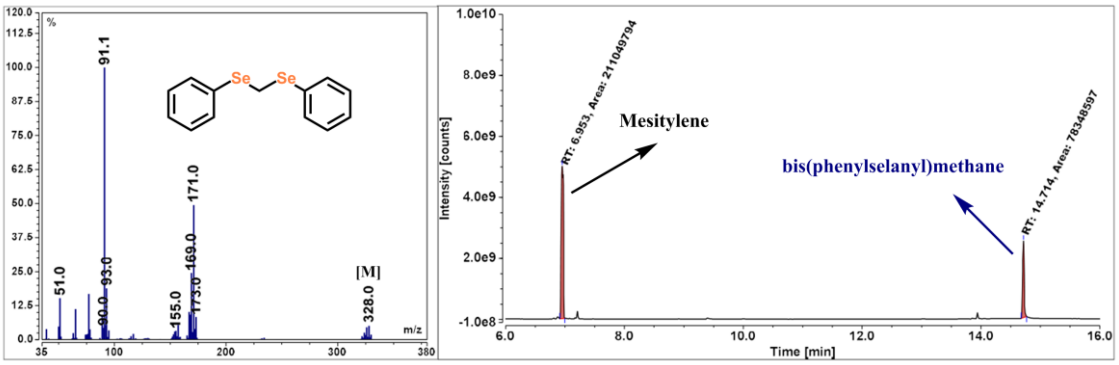

% yield for bis(phenylselanyl)methane :

Retention Time	Peak Area
13.177	78348597
6.953	211049794

$$\text{Yield} = \frac{78348597}{211049794} \times 100\%$$

$$= 37\%$$

Figure S89. GC-MS data for the identification and yield (37%) calculation of bis(phenylselanyl)methane produced in the reaction of [(Py2ald)Zn(SePh)] (**2**^{Zn}) with CH_2Br_2 in 1:1 ratio.

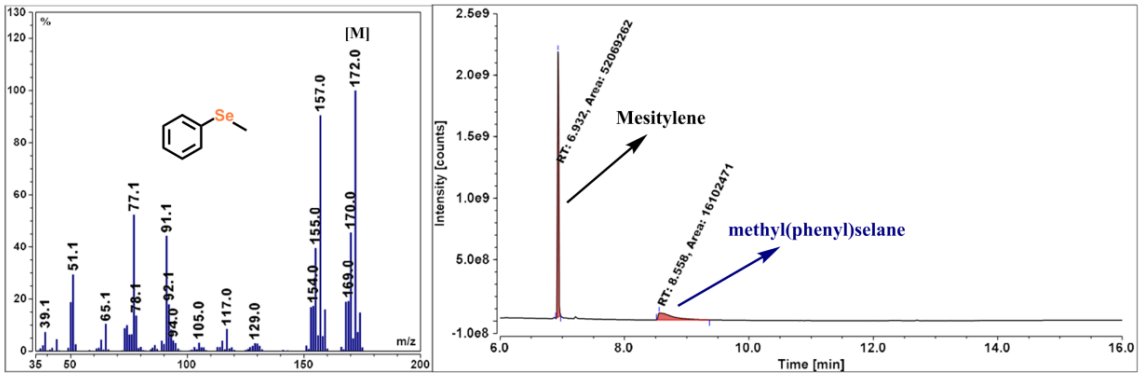

% yield for methyl(phenyl)sulfane :

Retention Time	Peak Area
8.558	16102471
6.932	52069262

$$\text{Yield} = \frac{16102471}{52069262} \times 100\%$$

$$= 31\%$$

Figure S90. GC-MS data for the identification and yield (31%) calculation of methyl(phenyl)selane produced in the reaction of [(Py2ald)Fe(SePh)] (**2**^{Fe}) with MeI in 1:1 ratio.

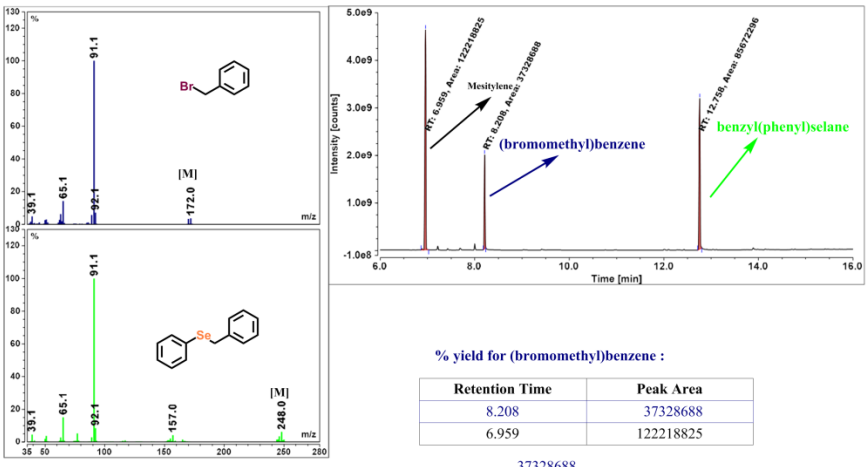

% yield for (bromomethyl)benzene :

Retention Time	Peak Area
8.208	37328688
6.959	122218825

$$\text{Yield} = \frac{37328688}{122218825} \times 100\%$$

$$= 29\%$$

% yield for benzyl(phenyl)selane :

Retention Time	Peak Area
12.758	85672296
6.946	122218825

$$\text{Yield} = \frac{85672296}{122218825} \times 100\%$$

$$= 70\%$$

Figure S91. GC-MS data for the identification and yield (70%) calculation of benzyl(phenyl)selane produced in the reaction of [(Py2ald)Fe(SePh)] (**2**^{Fe}) with $PhCH_2Br$ in 1:1 ratio.

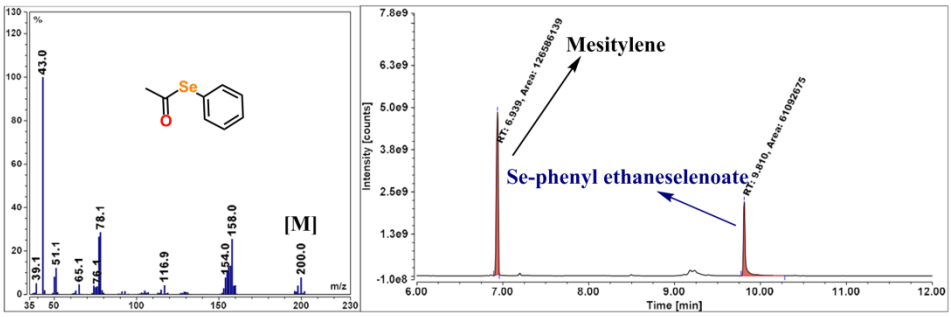

% yield for Se-phenyl ethaneselenoate:

Retention Time	Peak Area
9.810	61092675
6.939	126586139

$$\text{Yield} = \frac{61092675}{126586139} \times 100\%$$

$$= 48\%$$

Figure S92. GC-MS data for the identification and yield (48%) calculation of Se-phenyl ethaneselenoate produced in the reaction of [(Py2ald)Fe(SePh)] (**2**^{Fe}) with MeCOCl in 1:1 ratio.

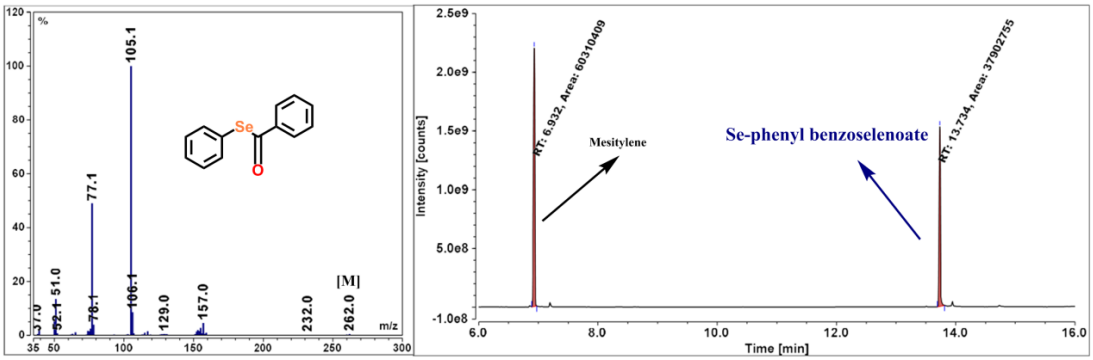

% yield for Se-phenyl benzoselenoate:

Retention Time	Peak Area
13.734	37902755
6.932	60310409

$$\text{Yield} = \frac{37902755}{60310409} \times 100\%$$

$$= 63\%$$

Figure S93. GC-MS data for the identification and yield (63%) calculation of Se-phenyl benzoselenoate produced in the reaction of [(Py2ald)Fe(SePh)] (**2**^{Fe}) with PhCOCl in 1:1 ratio.

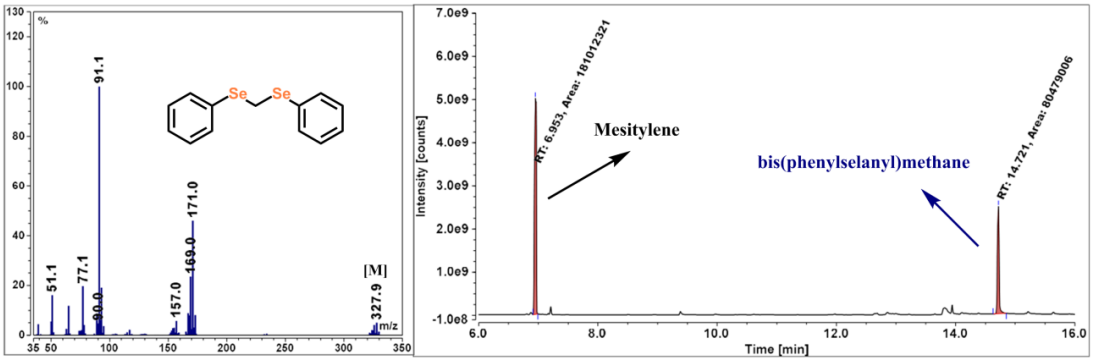

% yield for bis(phenylselanyl)methane :

Retention Time	Peak Area
14.721	80479006
6.953	181012321

$$\text{Yield} = \frac{80479006}{181012321} \times 100\%$$

$$= 44\%$$

Figure S94. GC-MS data for the identification and yield (44%) calculation of bis(phenylselanyl)methane produced in the reaction of [(Py2ald)Fe(SePh)] (**2**^{Fe}) with CH_2Br_2 in 1:1 ratio.

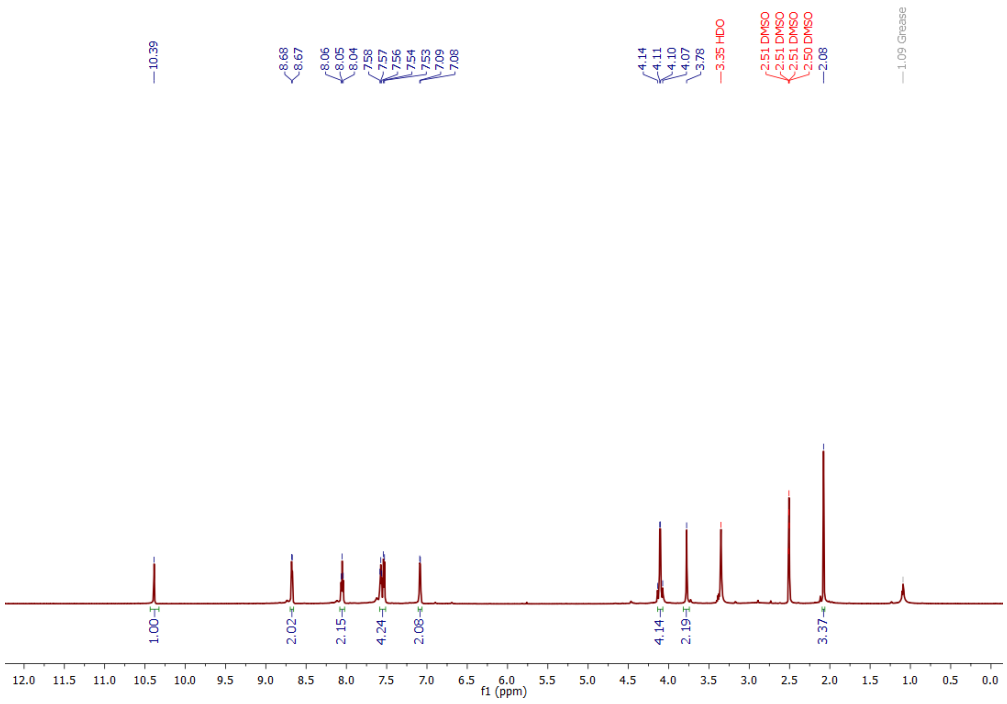

Figure 95. ^{1}H NMR (600 MHz, DMSO-d^{6}) spectrum of [(Py2ald)Zn]$_2$(BF$_4$)$_2$ (**5**$^{\mathbf{Zn}}$(BF$_4$)$_2$) obtained from the reaction of [(Py2ald)Zn(SPh)] (**1a**$^{\mathbf{Zn}}$) with MeI in DMF.

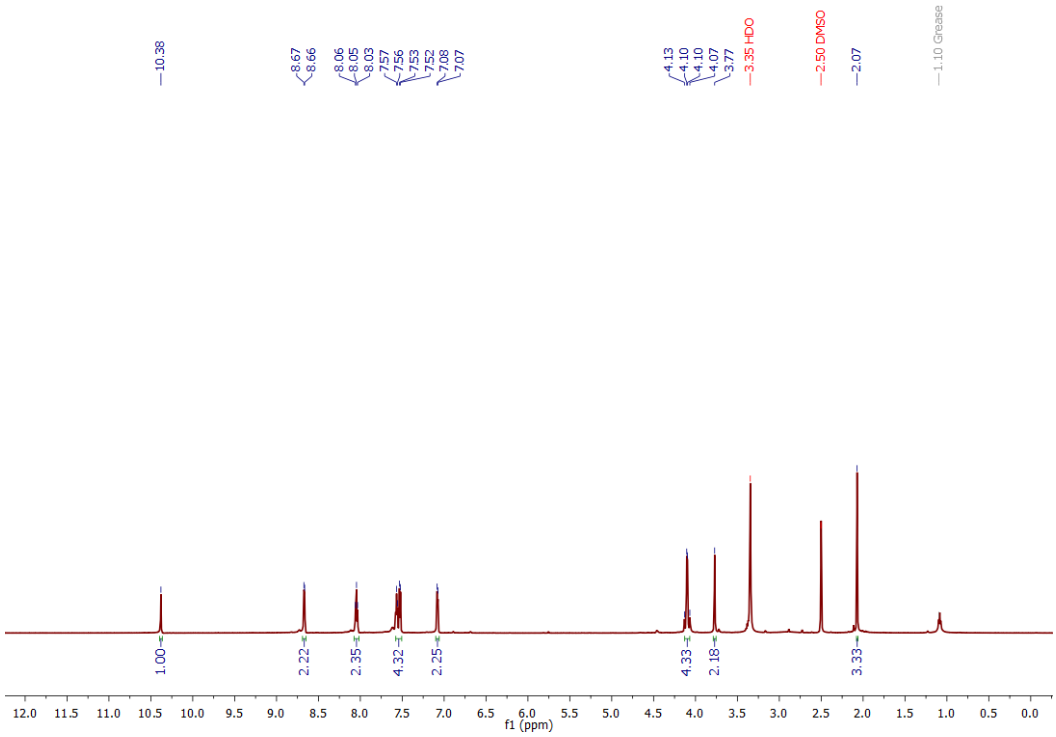

Figure S96. ^{1}H NMR (600 MHz, DMSO-d^{6}) spectrum of [(Py2ald)Zn]$_2$(BF$_4$)$_2$ (**5**$^{\mathbf{Zn}}$(BF$_4$)$_2$) obtained from the reaction of [(Py2ald)Zn(SPh)] (**1a**$^{\mathbf{Zn}}$) with PhCH$_2$Br in DMF.

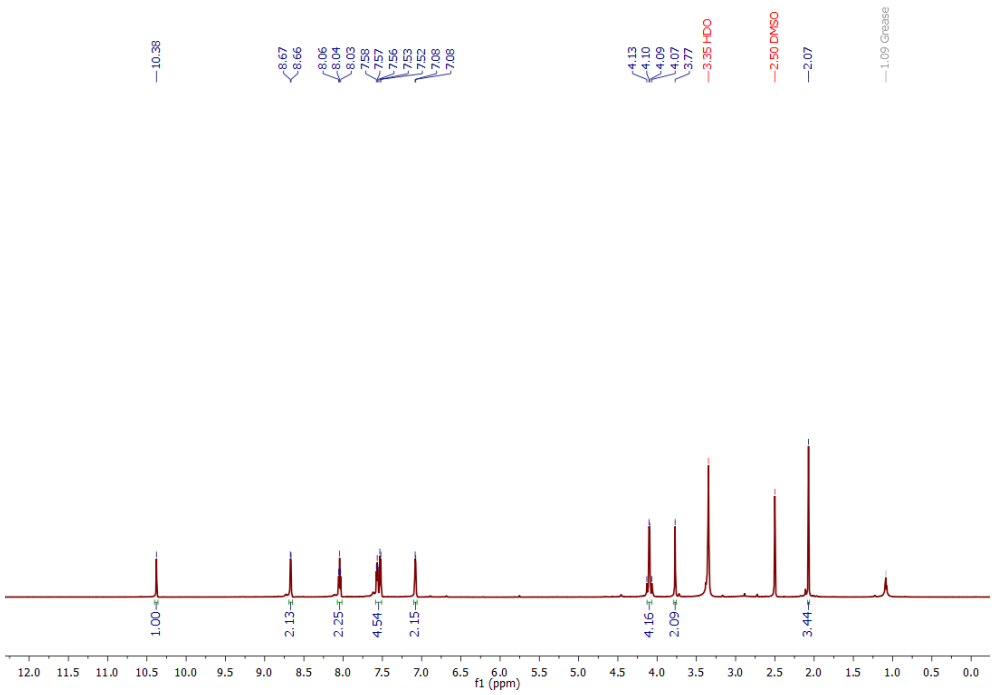

Figure S97. ^{1}H NMR (600 MHz, DMSO-d^{6}) spectrum of [(Py2ald)Zn]$_2$(BF$_4$)$_2$ (**5**$^{\mathbf{Zn}}$(BF$_4$)$_2$) obtained from the reaction of [(Py2ald)Zn(SPh)] (**1a**$^{\mathbf{Zn}}$) with MeC(O)Cl in DMF.

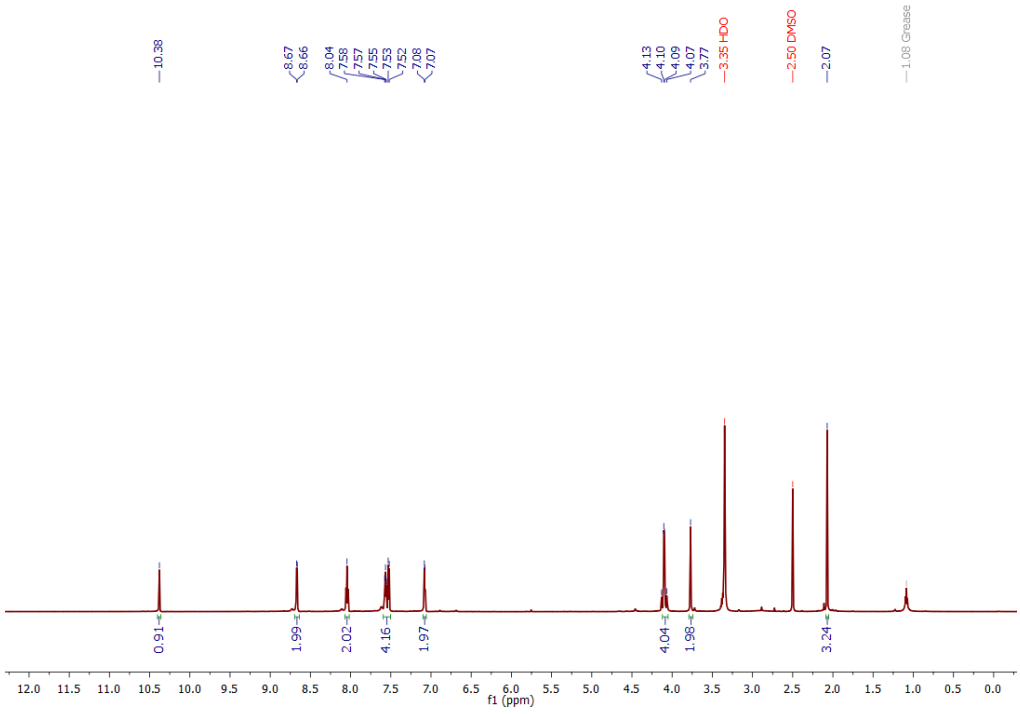

Figure S98. ^{1}H NMR (600 MHz, DMSO-d^{6}) spectrum of [(Py2ald)Zn]$_2$(BF$_4$)$_2$ (**5**$^{\mathbf{Zn}}$(BF$_4$)$_2$) obtained from the reaction of [(Py2ald)Zn(SPh)] (**1a**$^{\mathbf{Zn}}$) with PhC(O)Cl in MeCN.

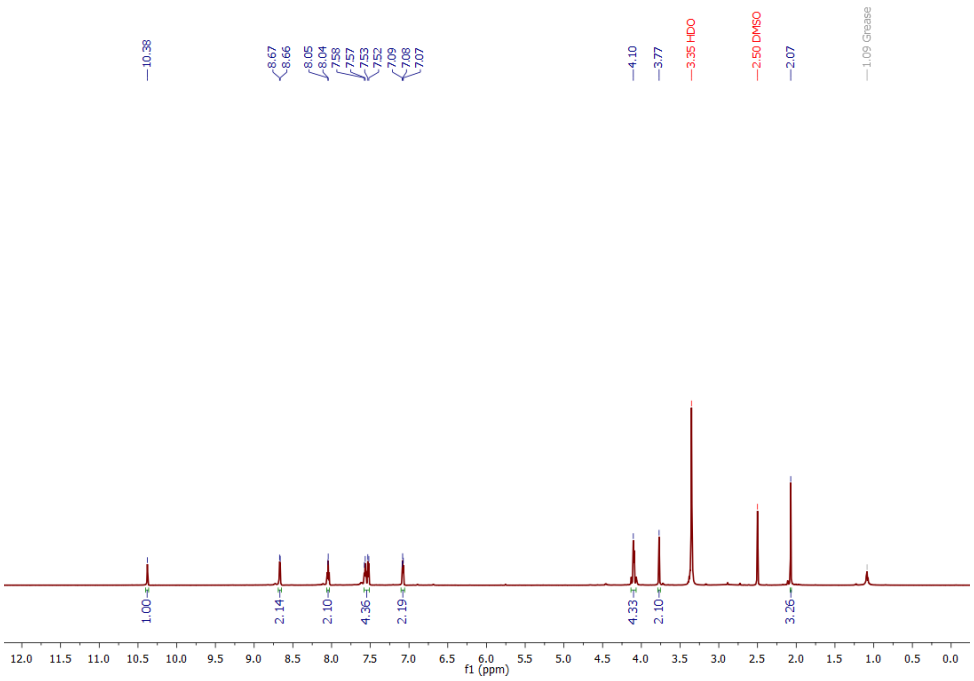

Figure S99. ^{1}H NMR (600 MHz, DMSO-d^{6}) spectrum of [(Py2ald)Zn]$_2$(BF$_4$)$_2$ (**5**$^{\mathbf{Zn}}$(BF$_4$)$_2$) obtained from the reaction of [(Py2ald)Zn(SPh)] (**1a**$^{\mathbf{Zn}}$) with CH_2Br_2 in DMF.

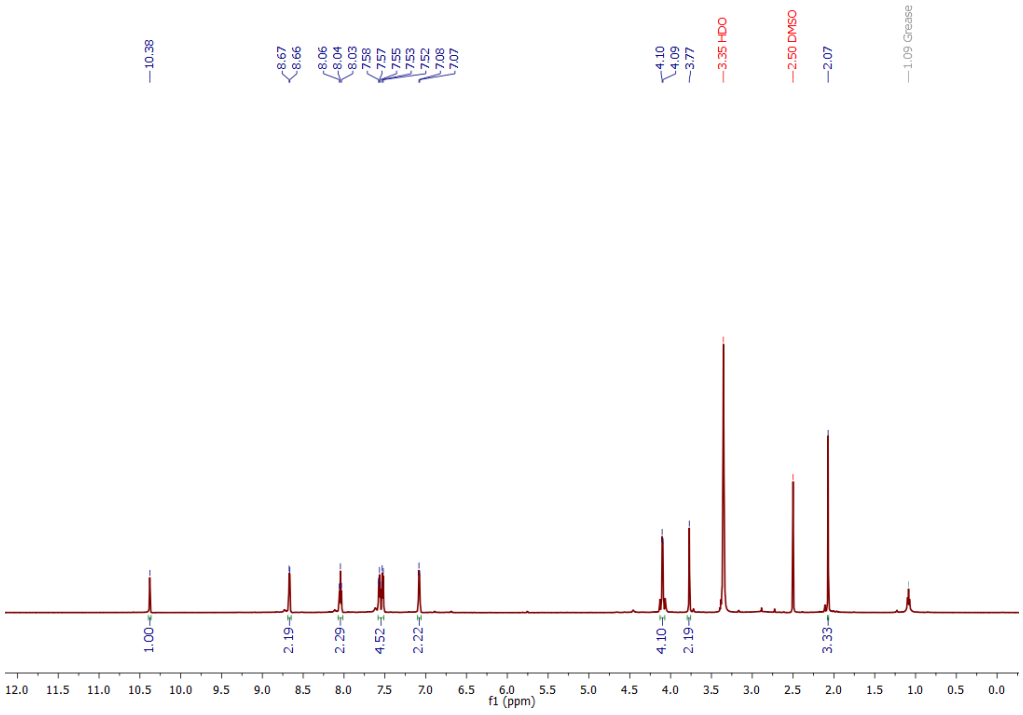

Figure S100. ^{1}H NMR (600 MHz, DMSO-d^{6}) spectrum of [(Py2ald)Zn]$_2$(BF$_4$)$_2$ (**5**$^{\mathbf{Zn}}$(BF$_4$)$_2$) obtained from the reaction of [(Py2ald)Zn(SePh)] (**2**$^{\mathbf{Zn}}$) with MeI in DMF solution.

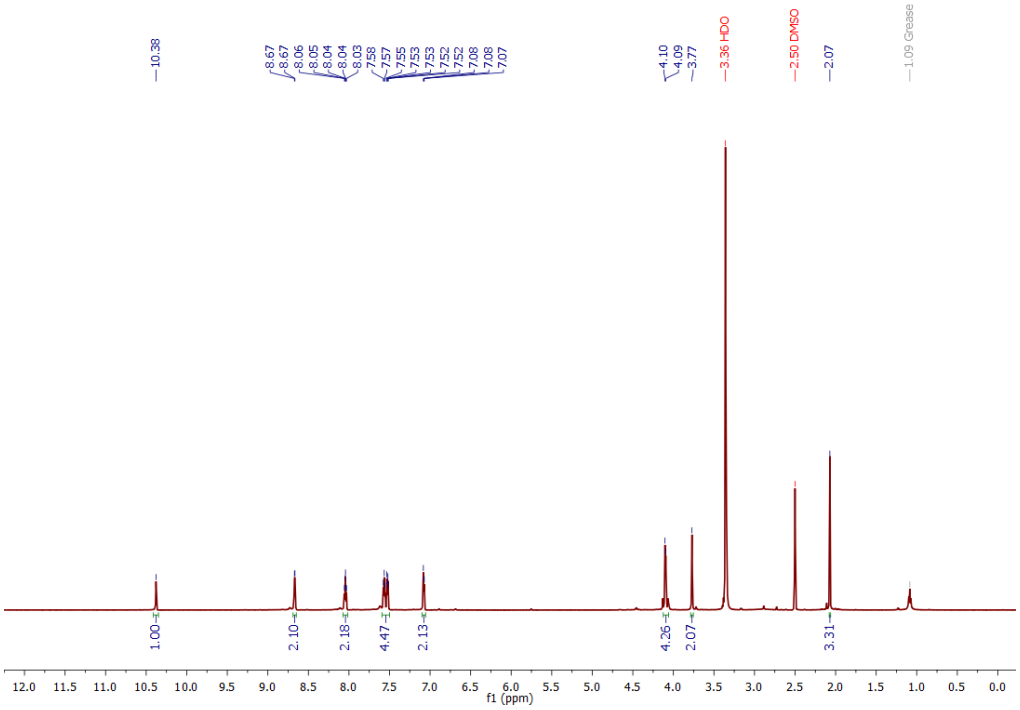

Figure S101. ^{1}H NMR (600 MHz, DMSO-d^{6}) spectrum of [(Py2ald)Zn]$_2$(BF$_4$)$_2$ (**5**$^{\mathbf{Zn}}$(BF$_4$)$_2$) obtained from the reaction of [(Py2ald)Zn(SePh)] (**2**$^{\mathbf{Zn}}$) with PhCH$_2$Br in DMF.

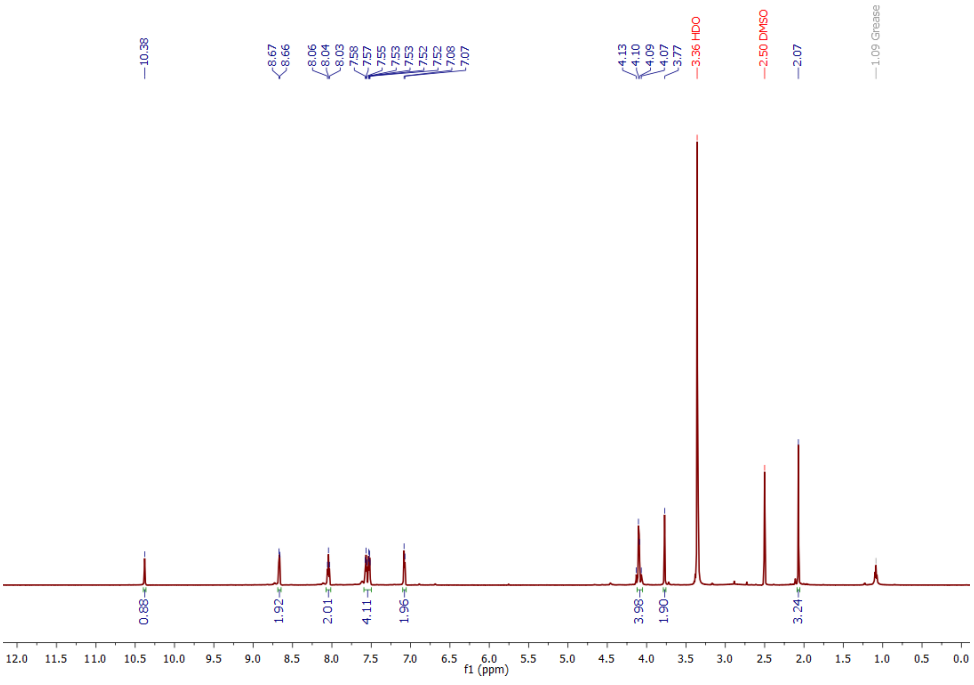

Figure S102. ^{1}H NMR (600 MHz, DMSO-d^{6}) spectrum of [(Py2ald)Zn]$_2$(BF$_4$)$_2$ (**5**$^{\mathbf{Zn}}$(BF$_4$)$_2$) obtained from the reaction of [(Py2ald)Zn(SePh)] (**2**$^{\mathbf{Zn}}$) with MeC(O)Cl in DMF solution.

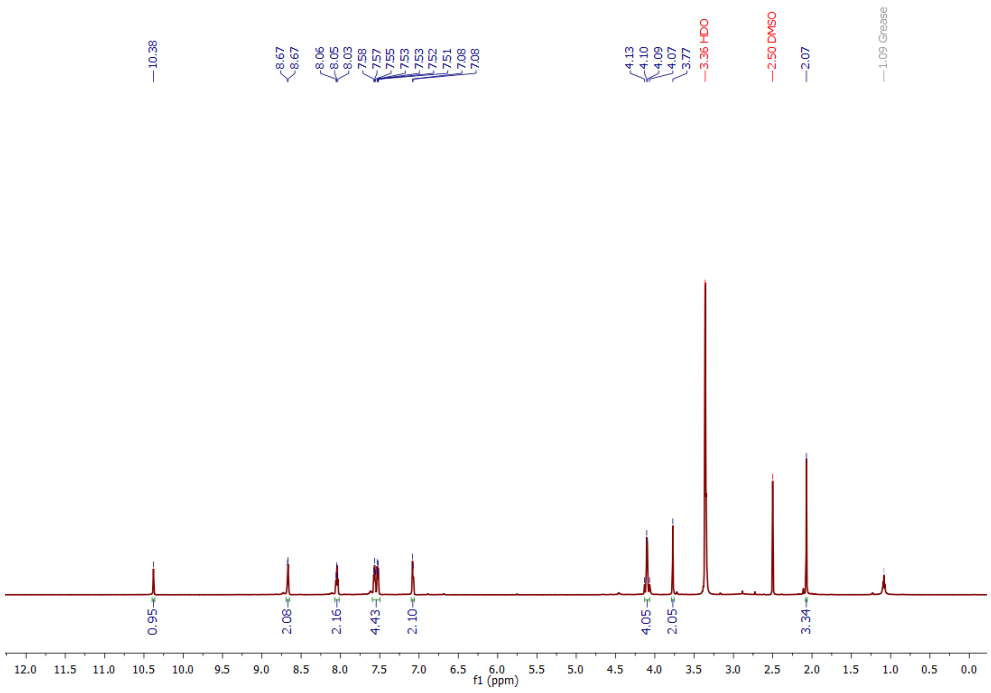

Figure S103. ^{1}H NMR (600 MHz, DMSO-d^{6}) spectrum of [(Py2ald)Zn]$_2$(BF$_4$)$_2$ (**5^{Zn}**(BF$_4$)$_2$) obtained from the reaction of [(Py2ald)Zn(SePh)] (**2^{Zn}**) with PhC(O)Cl in MeCN.

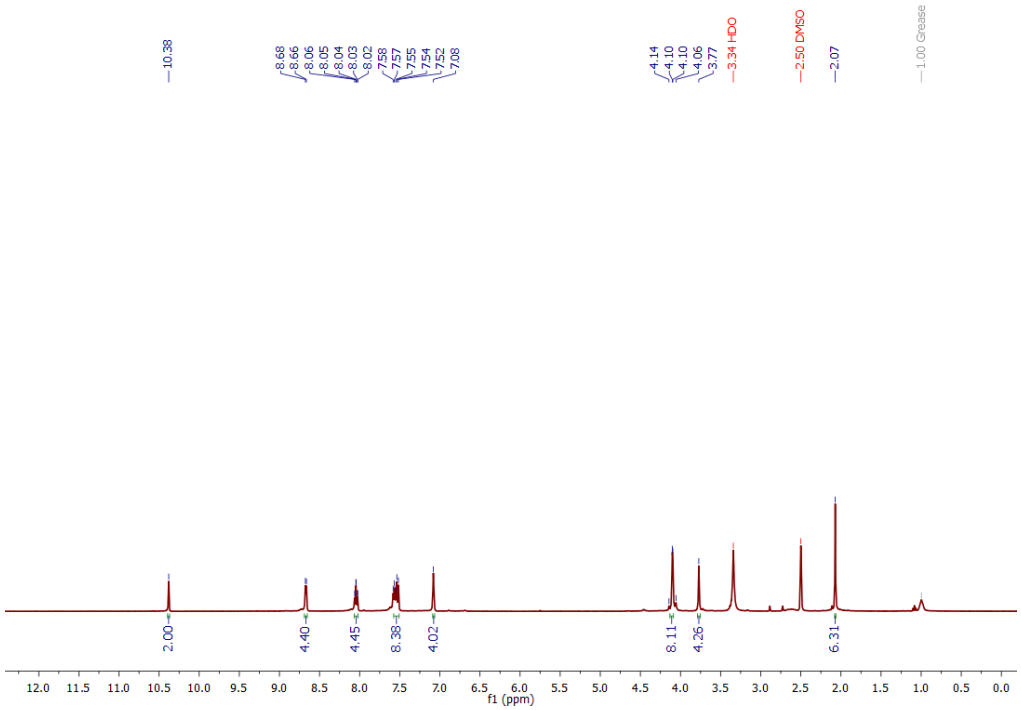

Figure S104. ^{1}H NMR (400 MHz, DMSO-d^{6}) spectrum of [(Py2ald)Zn]$_2$(BF$_4$)$_2$ (**5^{Zn}**(BF$_4$)$_2$) obtained from the reaction of [(Py2ald)Zn(SePh)] (**2^{Zn}**) with CH_2Br_2 in DMF.

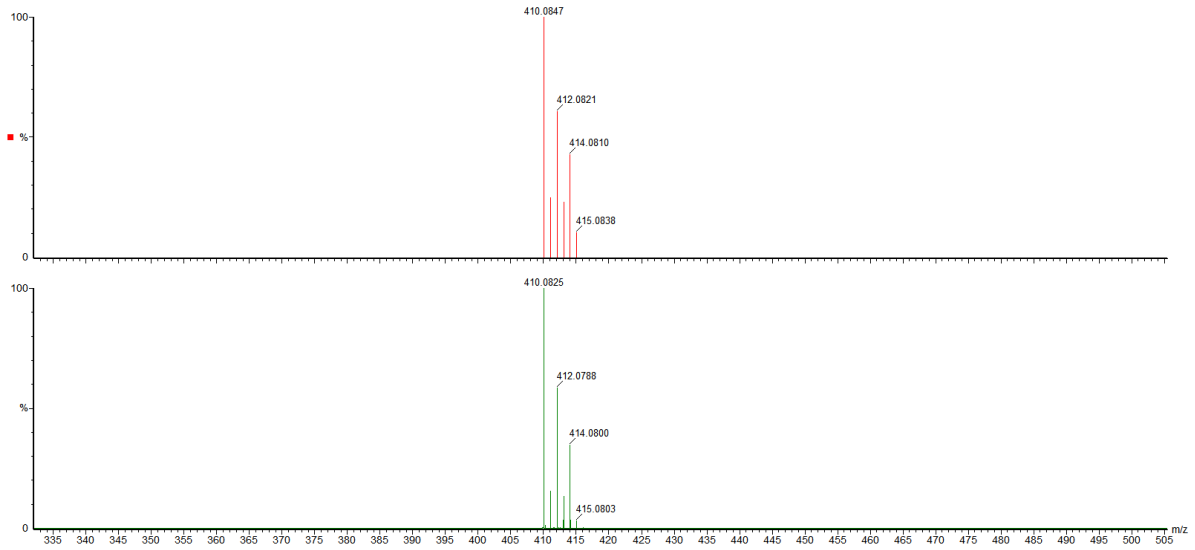

Figure S105. Mass spectrometric data (in MeCN) for $[(Py2ald)Zn]_2(BF_4)_2$ ($\mathbf{5^{Zn}}(BF_4)_2$) obtained from the reaction of [(Py2ald)Zn(SPh)] ($\mathbf{1a^{Zn}}$) with MeI shows the presence of $[(Py2ald)Zn]^+$ (m/z: 410.0847, simulated data, orange line; 410.0825, observed data, green line).

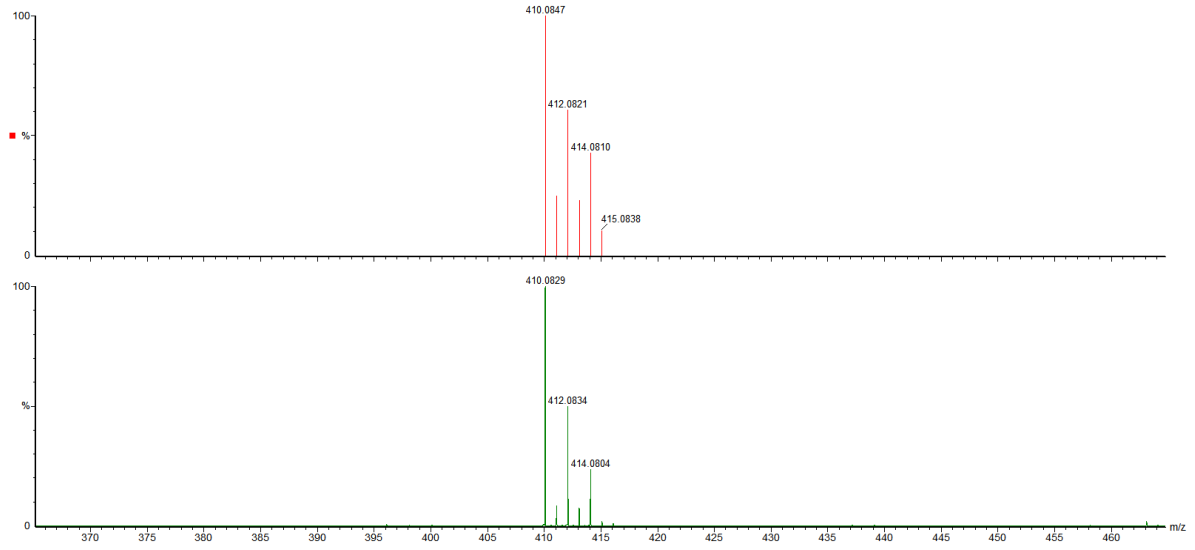

Figure S106. Mass spectrometric data (in MeCN) for $[(Py2ald)Zn]_2(BF_4)_2$ ($\mathbf{5^{Zn}}(BF_4)_2$) obtained from the reaction of [(Py2ald)Zn(SPh)] ($\mathbf{1a^{Zn}}$) with $PhCH_2Br$ shows the presence of $[(Py2ald)Zn]^+$ (m/z: 410.0847, simulated data, orange line; 410.0829, observed data, green line).

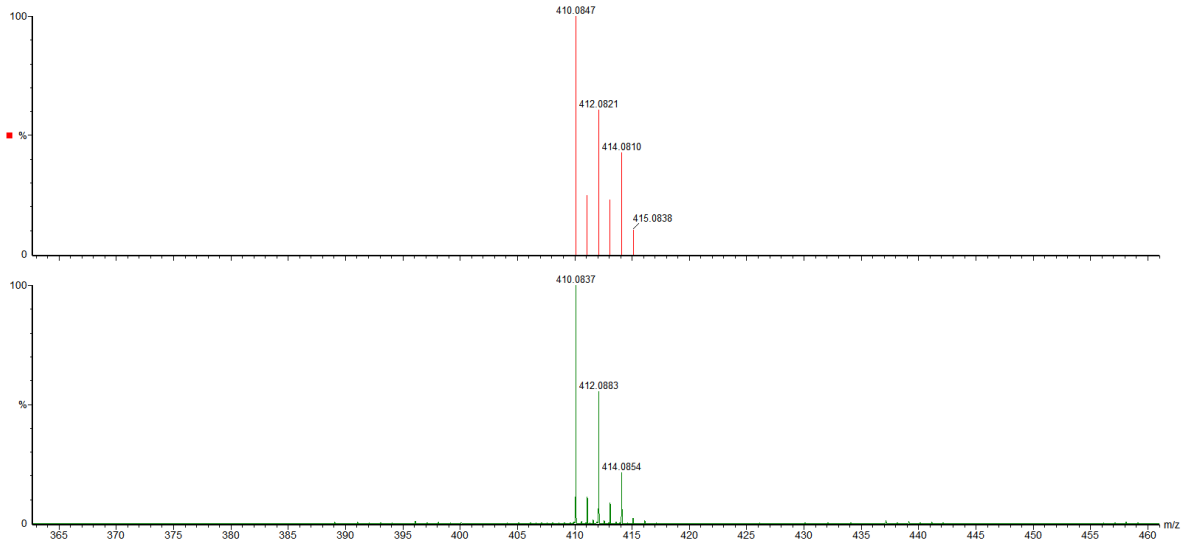

Figure S107. Mass spectrometric data (in MeCN) for $[(Py2ald)Zn]_2(BF_4)_2$ ($\mathbf{5^{Zn}}(BF_4)_2$) obtained from the reaction of [(Py2ald)Zn(SPh)] ($\mathbf{1a^{Zn}}$) with MeC(O)Cl, which shows the presence of $[(Py2ald)Zn]^+$ (m/z: 410.0847, simulated data, orange line; 410.0837, observed data, green line).

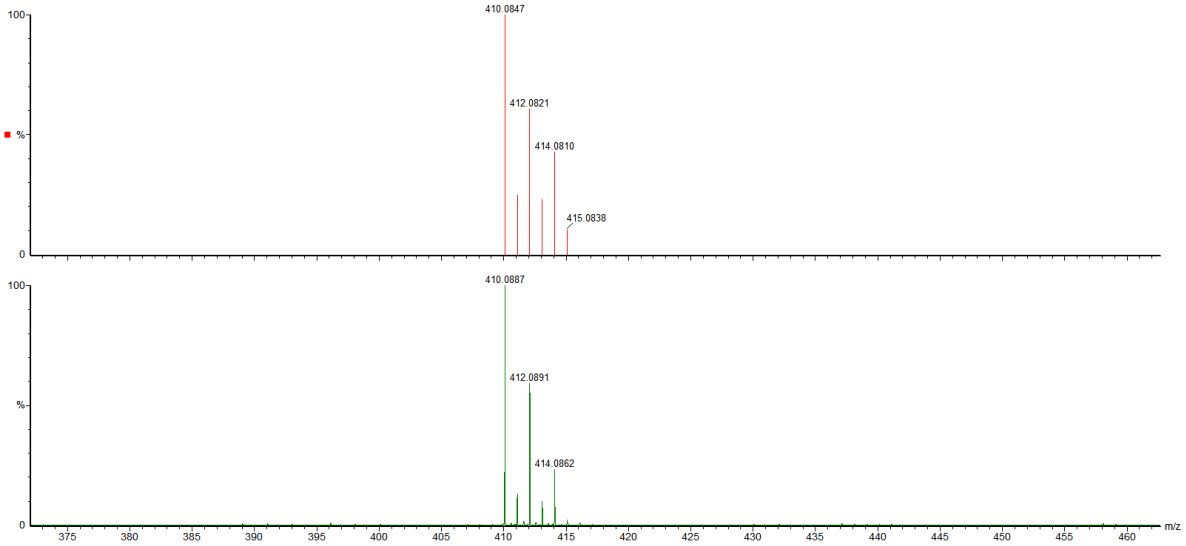

Figure S108. Mass spectrometric data (in MeCN) for $[(Py2ald)Zn]_2(BF_4)_2$ ($\mathbf{5^{Zn}}(BF_4)_2$) obtained from the reaction of [(Py2ald)Zn(SPh)] ($\mathbf{1a^{Zn}}$) with PhC(O)Cl, shows the presence of $[(Py2ald)Zn]^+$ (m/z: 410.0847, simulated data, orange line; 410.0887, observed data, green line).

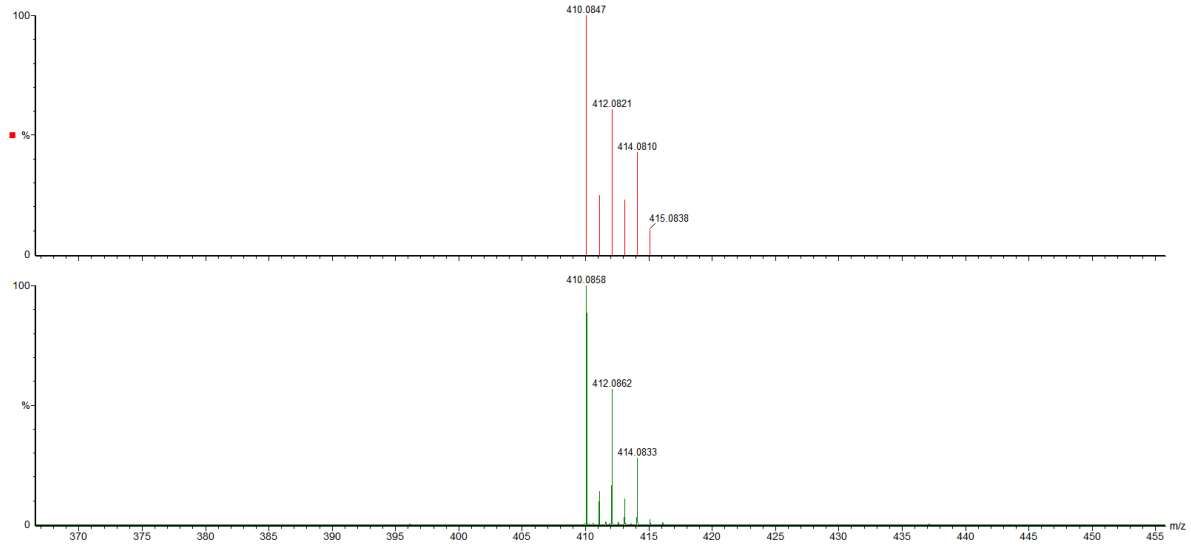

Figure S109. Mass spectrometric data (in MeCN) for $[(Py2ald)Zn]_2(BF_4)_2$ ($\mathbf{5^{Zn}}(BF_4)_2$) obtained from the reaction of [(Py2ald)Zn(SPh)] ($\mathbf{1a^{Zn}}$) with CH_2Br_2 shows the presence of $[(Py2ald)Zn]^+$ (m/z: 410.0847, simulated data, orange line; 410.0858, observed data, green line).

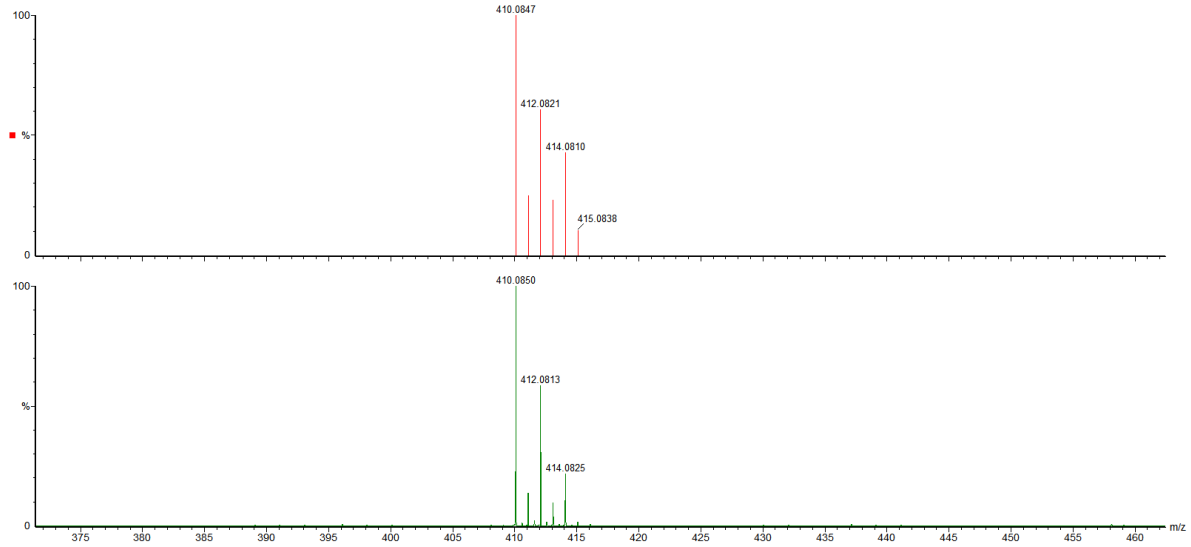

Figure S110. Mass spectrometric data (in MeCN) for $[(Py2ald)Zn]_2(BF_4)_2$ ($\mathbf{5^{Zn}}(BF_4)_2$) obtained from the reaction of [(Py2ald)Zn(SePh)] ($\mathbf{2^{Zn}}$) with MeI shows the presence of $[(Py2ald)Zn]^+$ (m/z: 410.0847, simulated data, orange line; 410.0850, observed data, green line).

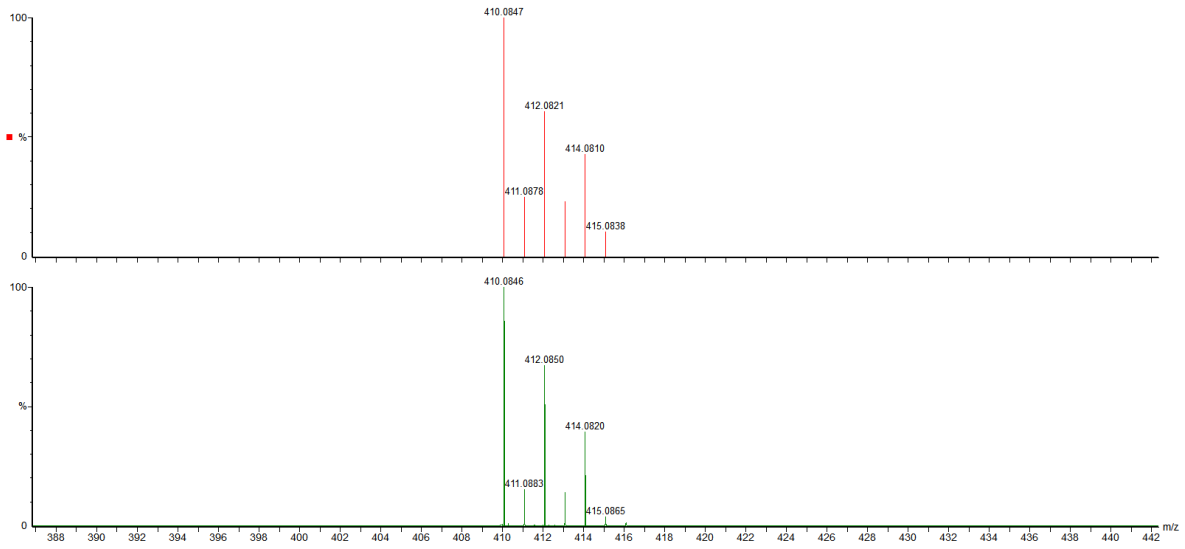

Figure S111. Mass spectrometric data (in MeCN) for $[(Py2ald)Zn]_2(BF_4)_2$ ($\mathbf{5^{Zn}}(BF_4)_2$) obtained from the reaction of [(Py2ald)Zn(SePh)] ($\mathbf{2^{Zn}}$) with $PhCH_2Br$, which shows the presence of $[(Py2ald)Zn]^+$ (m/z: 410.0847, simulated data, orange line; 410.0846, observed data, green line).

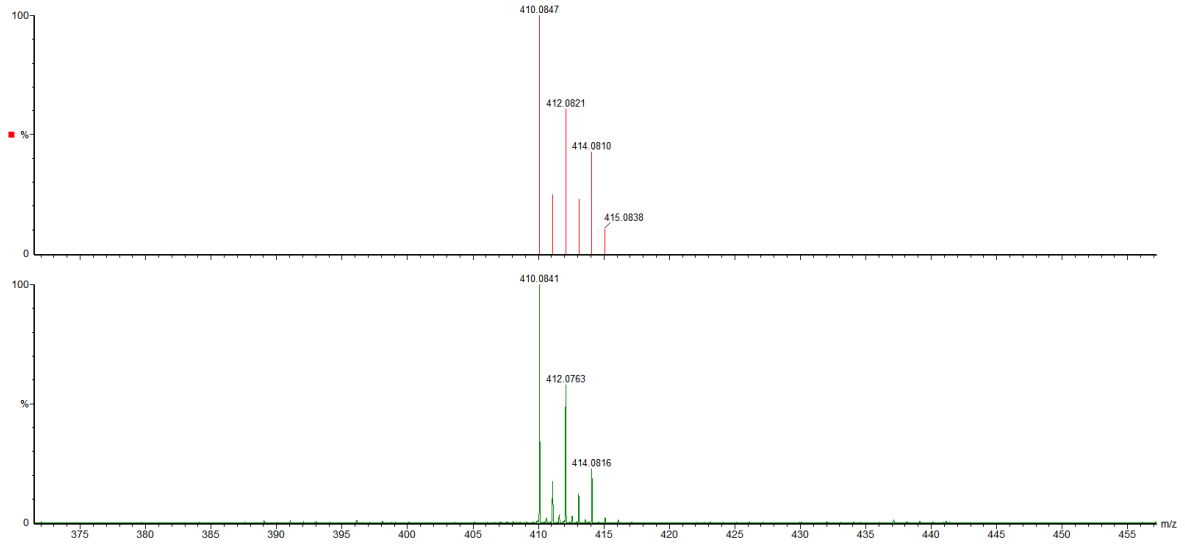

Figure S112. Mass spectrometric data (in MeCN) for $[(Py2ald)Zn]_2(BF_4)_2$ ($\mathbf{5^{Zn}}(BF_4)_2$) obtained from the reaction of [(Py2ald)Zn(SePh)] ($\mathbf{2^{Zn}}$) with MeC(O)Cl shows the presence of $[(Py2ald)Zn]^+$ (m/z: 410.0847, simulated data, orange line; 410.0841, observed data, green line).

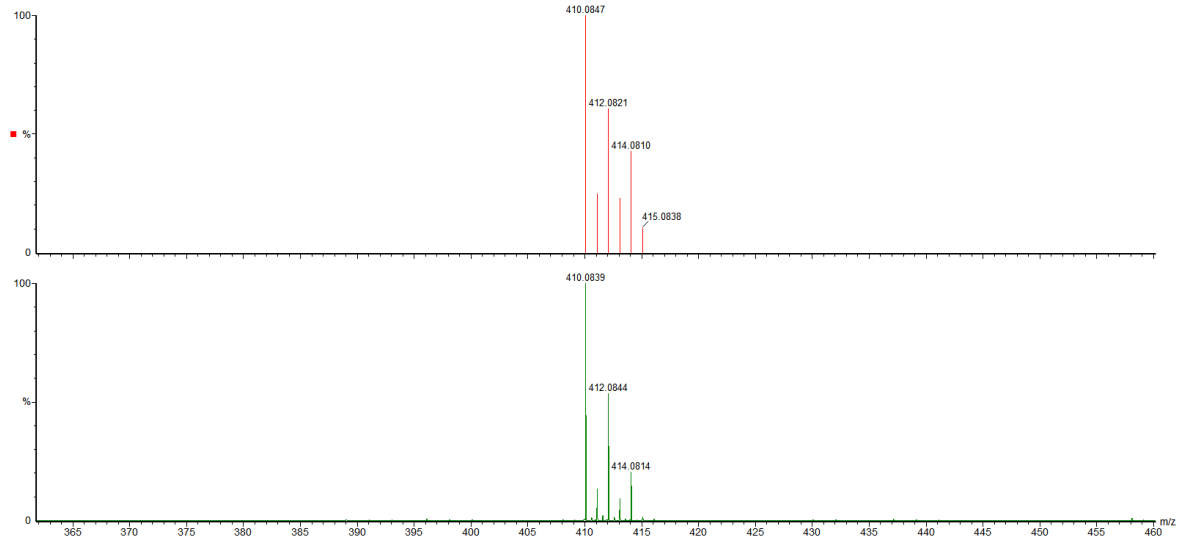

Figure S113. Mass spectrometric data (in MeCN) for $[(Py2ald)Zn]_2(BF_4)_2$ ($\mathbf{5^{Zn}}(BF_4)_2$) obtained from the reaction of [(Py2ald)Zn(SePh)] ($\mathbf{2^{Zn}}$) with PhC(O)Cl, which shows the presence of $[(Py2ald)Zn]^+$ (m/z: 410.0847, simulated data, orange line; 410.0839, observed data, green line).

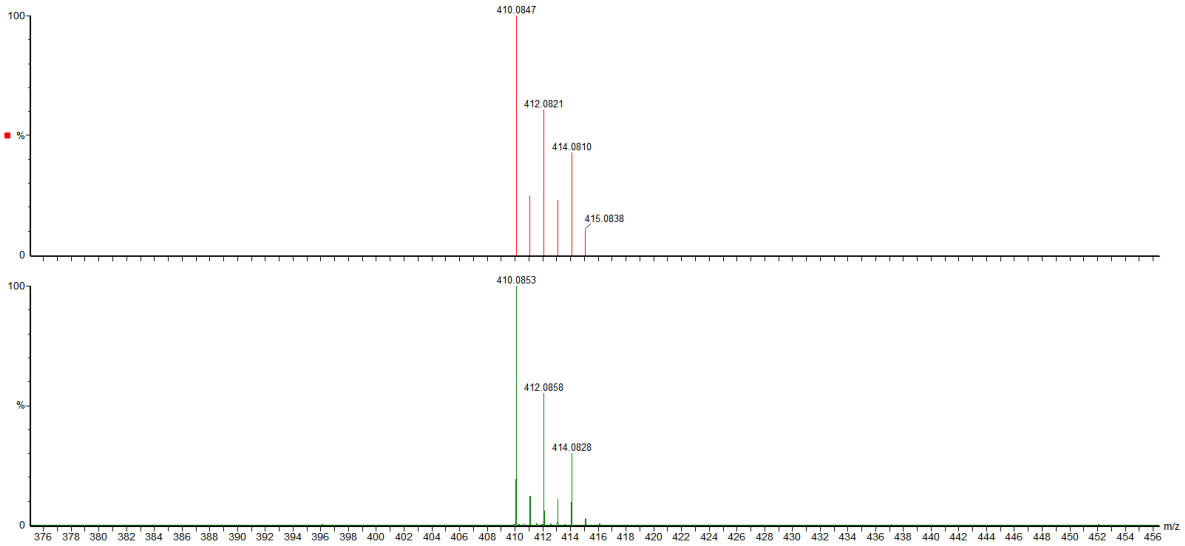

Figure S114. Mass spectrometric data (in MeCN) for $[(Py2ald)Zn]_2(BF_4)_2$ ($\mathbf{5^{Zn}}(BF_4)_2$) obtained from the reaction of [(Py2ald)Zn(SePh)] ($\mathbf{2^{Zn}}$) with CH_2Br_2 shows the presence of $[(Py2ald)Zn]^+$ (m/z: 410.0847, simulated data, orange line; 410.0853, observed data, green line).

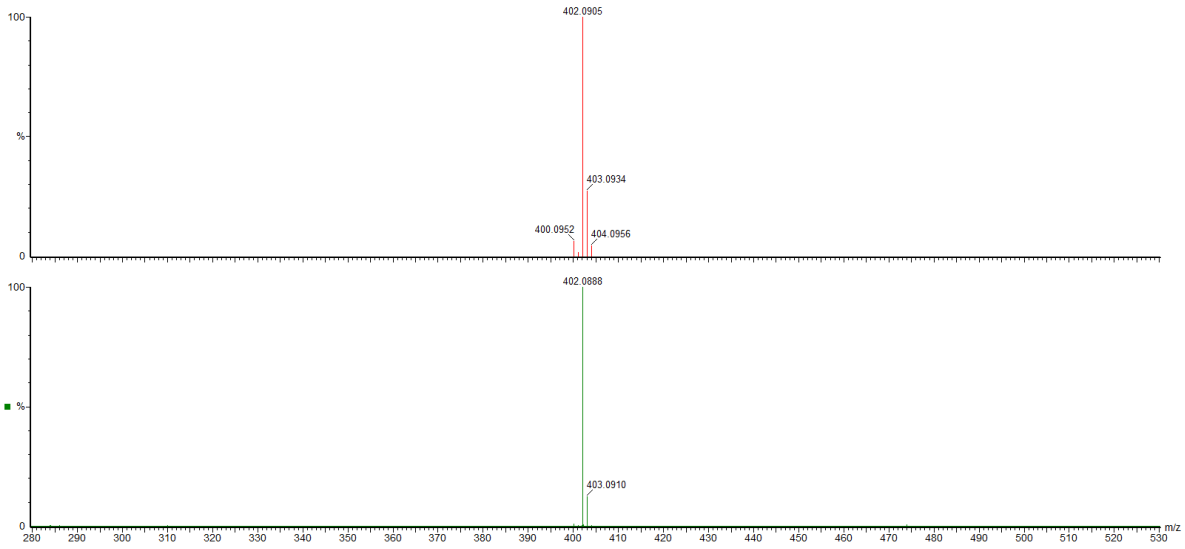

Figure S115. Mass spectrometric data (in MeCN) for $[(Py2ald)Fe]_2(BPh_4)_2$ ($\mathbf{5^{Fe}}(BPh_4)_2$) obtained from the reaction of [(Py2ald)Fe(SPh)] ($\mathbf{1a^{Fe}}$) with MeI ((in the presence of 2 equiv of $NaBPh_4$) shows the presence of $[(Py2ald)Fe]^+$ (m/z: 402.0905, simulated data, orange line; 402.0888, observed data, green line).

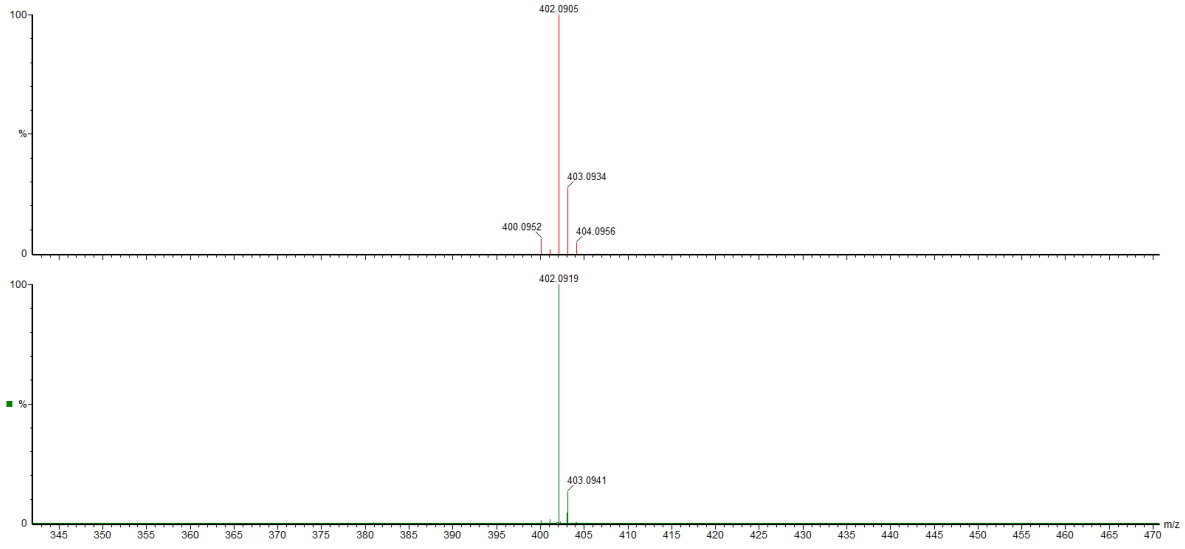

Figure S116. Mass spectrometric data (in MeCN) for $[(Py2ald)Fe]_2(BPh_4)_2$ ($\mathbf{5^{Fe}}(BPh_4)_2$) obtained from the reaction of [(Py2ald)Fe(SPh)] ($\mathbf{1a^{Fe}}$) with $PhCH_2Br$ (in the presence of 2 equiv of $NaBPh_4$) shows the presence of $[(Py2ald)Fe]^+$ (m/z: 402.0905, simulated data, green line; 402.0919,observed data, orange line).

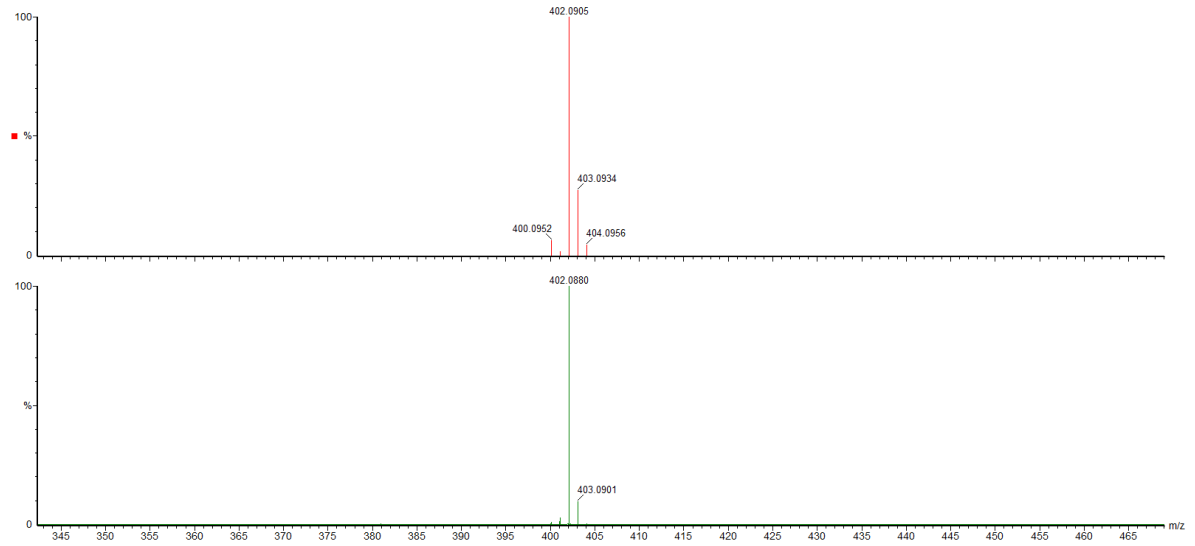

Figure S117. Mass spectrometric data (in MeCN) for $[(Py2ald)Fe]_2(BPh_4)_2$ ($\mathbf{5}^{\mathbf{Fe}}(BPh_4)_2$) obtained from the reaction of [(Py2ald)Fe(SPh)] ($\mathbf{1a}^{\mathbf{Fe}}$) with MeC(O)Cl (in the presence of 2 equiv of $NaBPh_4$) shows the presence of $[(Py2ald)Fe]^+$ (m/z: 402.0905, simulated data, orange line; 402.0880, observed data, green line).

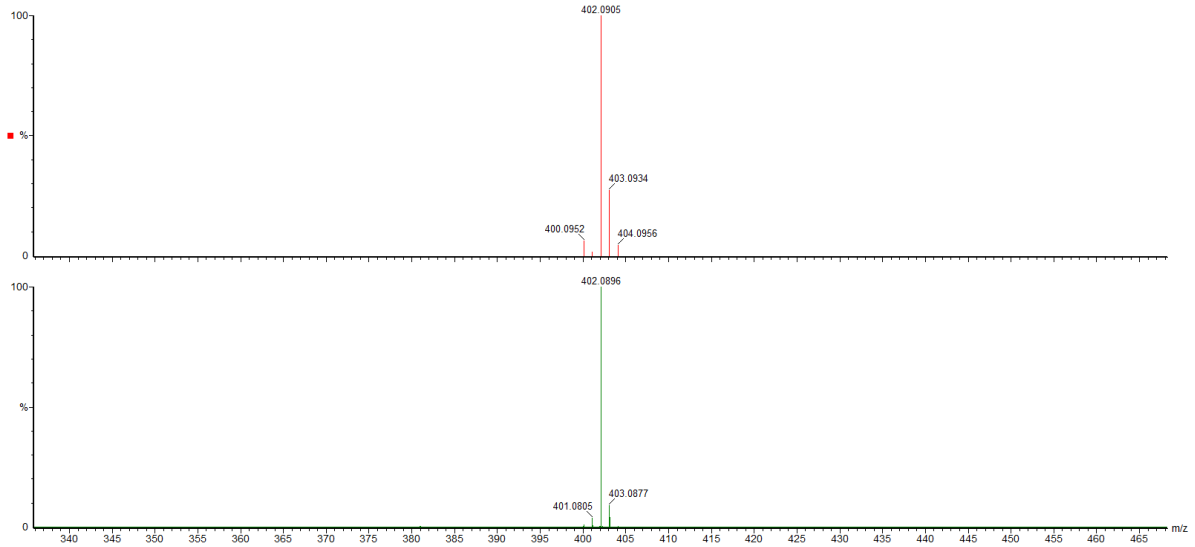

Figure S118. Mass spectrometric data (in MeCN) for $[(Py2ald)Fe]_2(BPh_4)_2$ ($\mathbf{5}^{\mathbf{Fe}}(BPh_4)_2$) obtained from the reaction of [(Py2ald)Fe(SPh)] ($\mathbf{1a}^{\mathbf{Fe}}$) with PhC(O)Cl (in the presence of 2 equiv of $NaBPh_4$) shows the presence of $[(Py2ald)Fe]^+$ (m/z: 402.0905, simulated data, orange line; 402.0896, observed data, green line).

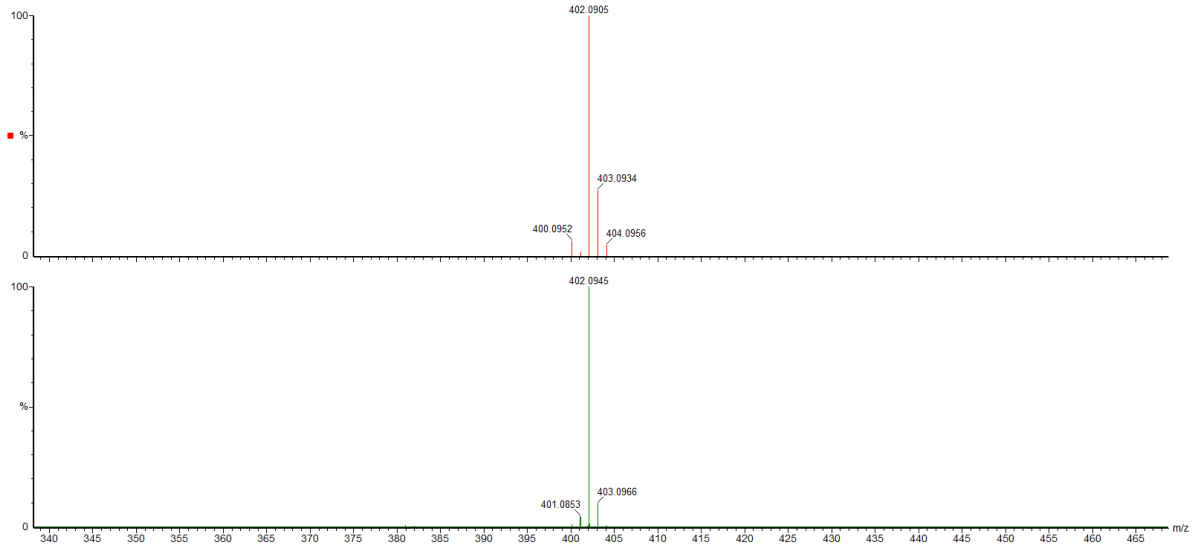

Figure S119. Mass spectrometric data (in MeCN) for $[(Py2ald)Fe]_2(BPh_4)_2$ ($\mathbf{5^{Fe}}(BPh_4)_2$) obtained from the reaction of [(Py2ald)Fe(SPh)] ($\mathbf{1a^{Fe}}$) with CH_2Br_2 (in the presence of 2 equiv of $NaBPh_4$) shows the presence of $[(Py2ald)Fe]^+$ (m/z: 402.0905, simulated data, orange line; 402.0945, observed data, green line).

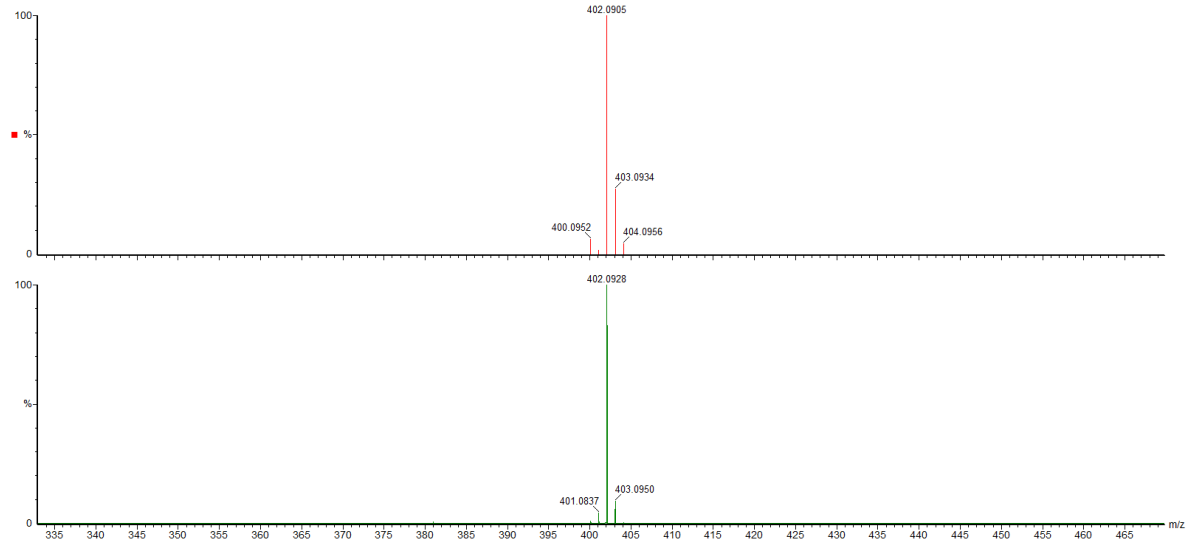

Figure S120. Mass spectrometric data (in MeCN) for $[(Py2ald)Fe]_2(BPh_4)_2$ ($\mathbf{5^{Fe}}(BPh_4)_2$) obtained from the reaction of [(Py2ald)Fe(SePh)] ($\mathbf{2^{Fe}}$) with MeI (in the presence of 2 equiv of $NaBPh_4$) shows the presence of $[(Py2ald)Fe]^+$ (m/z: 402.0905, simulated data, orange line; 402.0928,observed data, purple line).

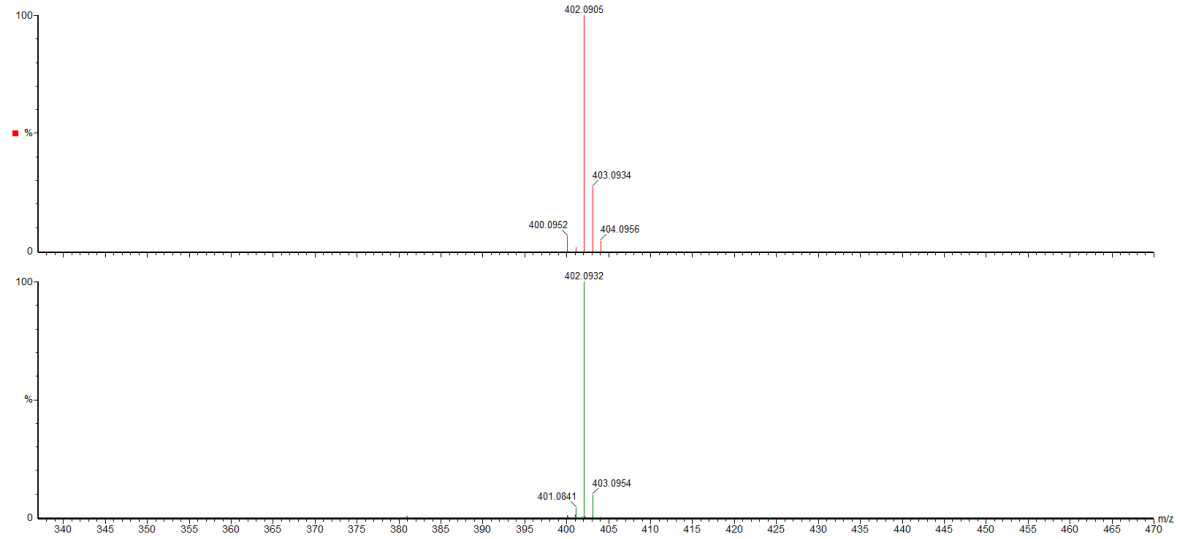

Figure S121. Mass spectrometric data (in MeCN) for $[(Py2ald)Fe]_2(BPh_4)_2$ ($\mathbf{5^{Fe}}(BPh_4)_2$) obtained from the reaction of [(Py2ald)Fe(SePh)] ($\mathbf{2^{Fe}}$) with $PhCH_2Br$ (in the presence of 2 equiv of $NaBPh_4$) shows the presence of $[(Py2ald)Fe]^+$ (m/z: 402.0905, simulated data, orange line; 402.0932, observed data, green line).

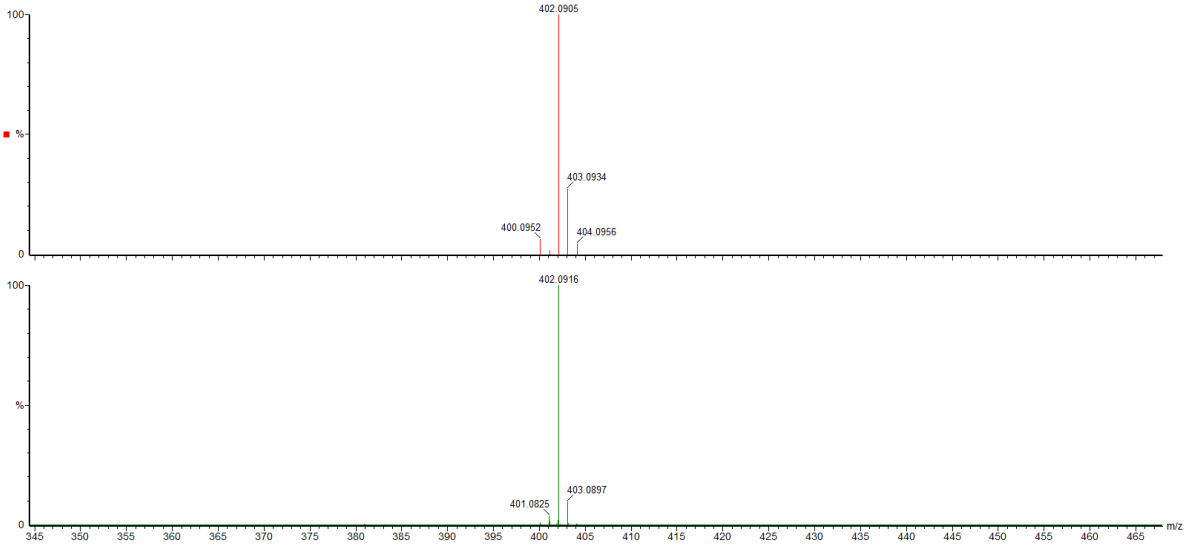

Figure S122. Mass spectrometric data (in MeCN) for $[(Py2ald)Fe]_2(BPh_4)_2$ ($\mathbf{5^{Fe}}(BPh_4)_2$) obtained from the reaction of [(Py2ald)Fe(SePh)] ($\mathbf{2^{Fe}}$) with MeC(O)Cl (in the presence of 2 equiv of $NaBPh_4$) shows the presence of $[(Py2ald)Fe]^+$ (m/z: 402.0916, simulated data, orange line; 402.0901, observed data, green line).

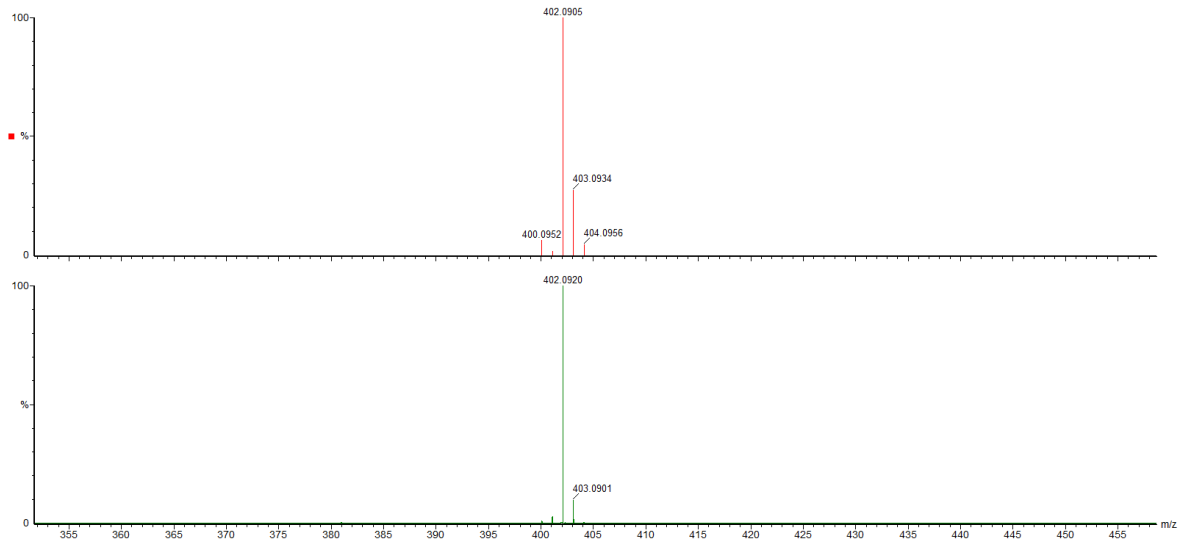

Figure S123. Mass spectrometric data (in MeCN) for $[(Py2ald)Fe]_2(BPh_4)_2$ ($\mathbf{5^{Fe}}(BPh_4)_2$) obtained from the reaction of [(Py2ald)Fe(SePh)] ($\mathbf{2^{Fe}}$) with PhC(O)Cl (in the presence of 2 equiv of $NaBPh_4$) shows the presence of $[(Py2ald)Fe]^+$ (m/z: 402.0905, simulated data, orange line; 402.0920, observed data, green line).

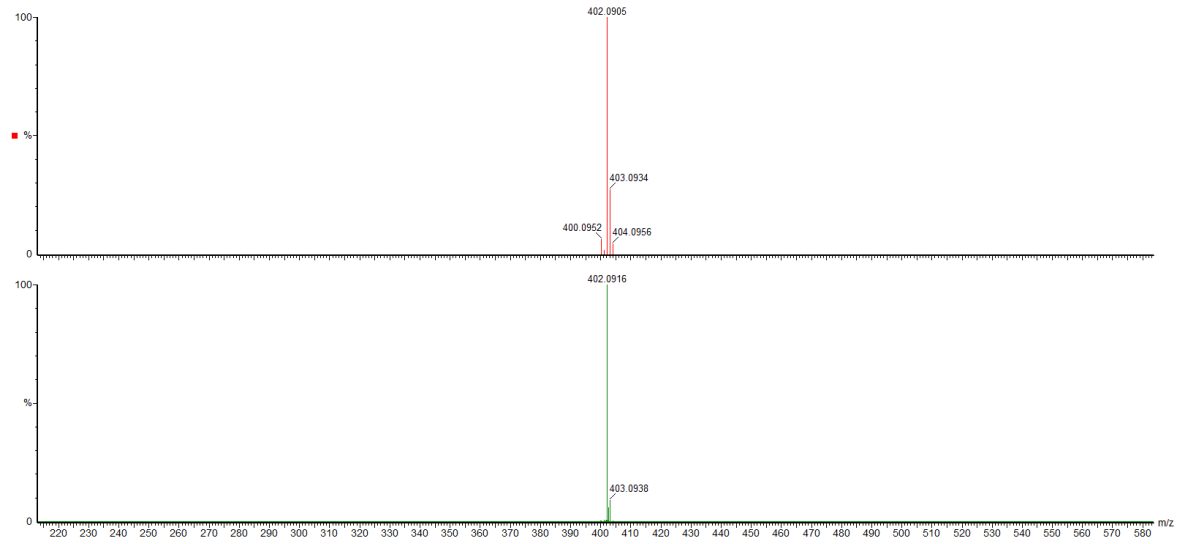

Figure S124. Mass spectrometric data (in MeCN) for $[(Py2ald)Fe]_2(BPh_4)_2$ ($\mathbf{5^{Fe}}(BPh_4)_2$) obtained from the reaction of [(Py2ald)Fe(SePh)] ($\mathbf{2^{Fe}}$) with CH_2Br_2 (in the presence of 2 equiv of $NaBPh_4$) shows the presence of $[(Py2ald)Fe]^+$ (m/z: 402.0905, simulated data, orange line; 402.0916, observed data, green line).

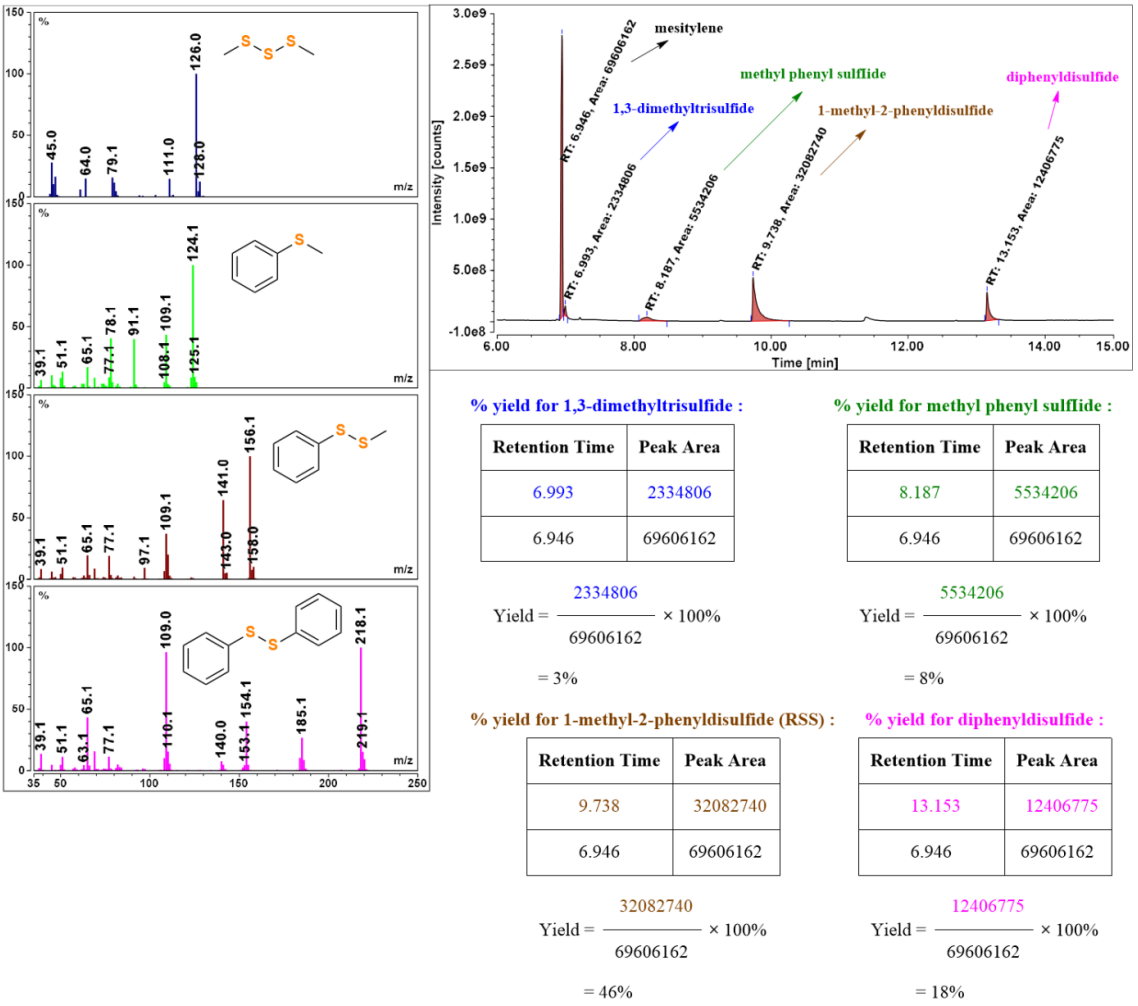

% yield for 1,3-dimethyltrisulfide :

Retention Time	Peak Area
6.993	2334806
6.946	69606162

$$\text{Yield} = \frac{2334806}{69606162} \times 100\% = 3\%$$

% yield for methyl phenyl sulfide :

Retention Time	Peak Area
8.187	5534206
6.946	69606162

$$\text{Yield} = \frac{5534206}{69606162} \times 100\% = 8\%$$

% yield for 1-methyl-2-phenyldisulfide (RSS) :

Retention Time	Peak Area
9.738	32082740
6.946	69606162

$$\text{Yield} = \frac{32082740}{69606162} \times 100\% = 46\%$$

% yield for diphenyldisulfide :

Retention Time	Peak Area
13.153	12406775
6.946	69606162

$$\text{Yield} = \frac{12406775}{69606162} \times 100\% = 18\%$$

Figure S125. GC-MS data for the identification and yield calculation of 1-methyl-2-phenyldisulfide (Me-S-S-Ph, yield = 46%) produced in the reaction of [(Py2ald)Zn(SPh)] (**1a^{Zn}**) with S_8 and MeI.

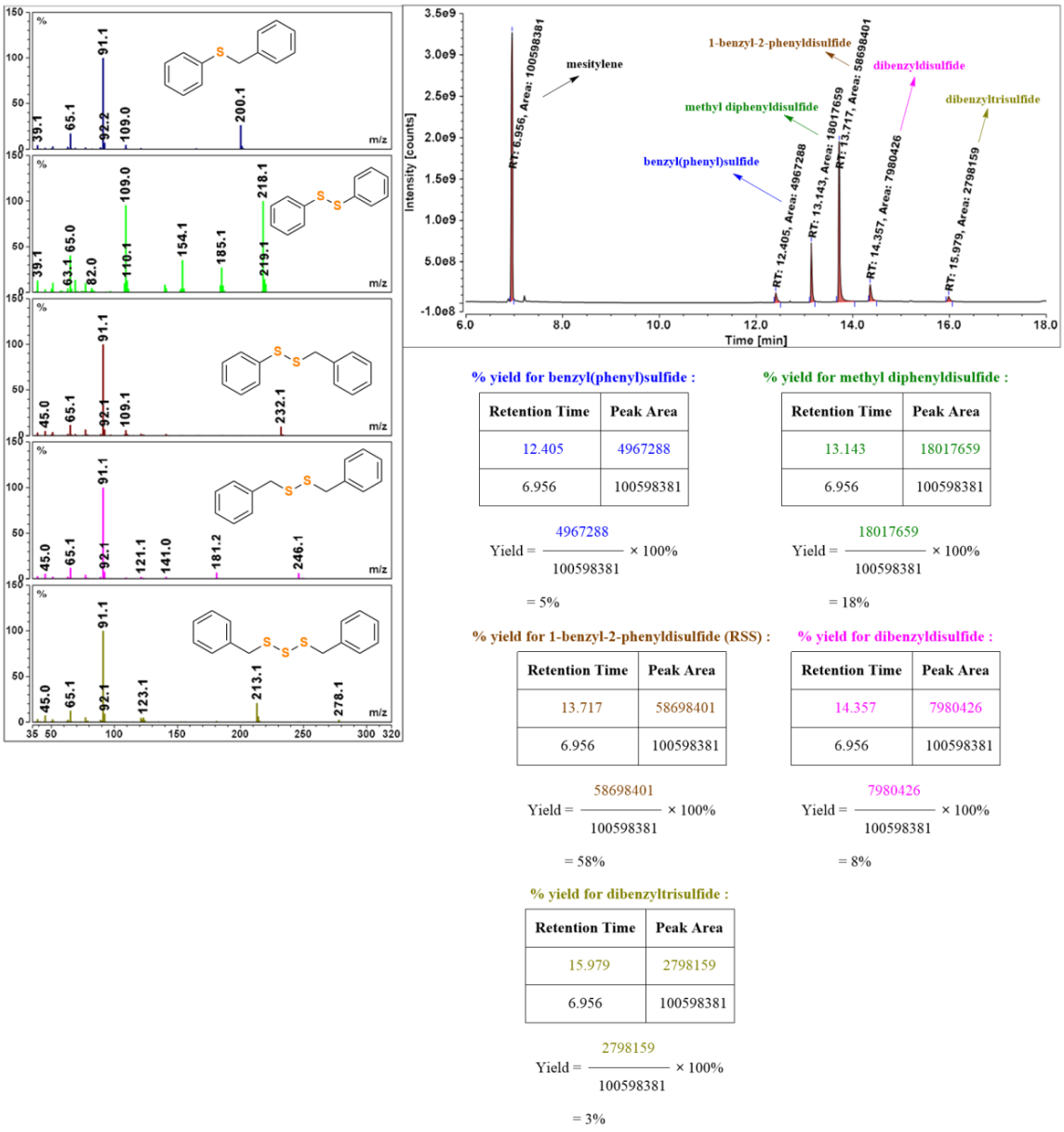

% yield for benzyl(phenyl)sulfide :

Retention Time	Peak Area
12.405	4967288
6.956	100598381

$$\text{Yield} = \frac{4967288}{100598381} \times 100\%$$

= 5%

% yield for methyl diphenyldisulfide :

Retention Time	Peak Area
13.143	18017659
6.956	100598381

$$\text{Yield} = \frac{18017659}{100598381} \times 100\%$$

= 18%

% yield for 1-benzyl-2-phenyldisulfide (RSS) :

Retention Time	Peak Area
13.717	58698401
6.956	100598381

$$\text{Yield} = \frac{58698401}{100598381} \times 100\%$$

= 58%

% yield for dibenzyldisulfide :

Retention Time	Peak Area
14.357	7980426
6.956	100598381

$$\text{Yield} = \frac{7980426}{100598381} \times 100\%$$

= 8%

% yield for dibenzyltrisulfide :

Retention Time	Peak Area
15.979	2798159
6.956	100598381

$$\text{Yield} = \frac{2798159}{100598381} \times 100\%$$

= 3%

Figure S126. Gas chromatographic data for the identification and yield calculation of 1-benzyl-2-phenyldisulfide ($PhCH_2$-S-S-Ph, yield = 58%) produced in the reaction of [(Py2ald)Zn(SPh)] (**1a**^{Zn}) with S_8 and $PhCH_2Br$ in 1:1 ratio.

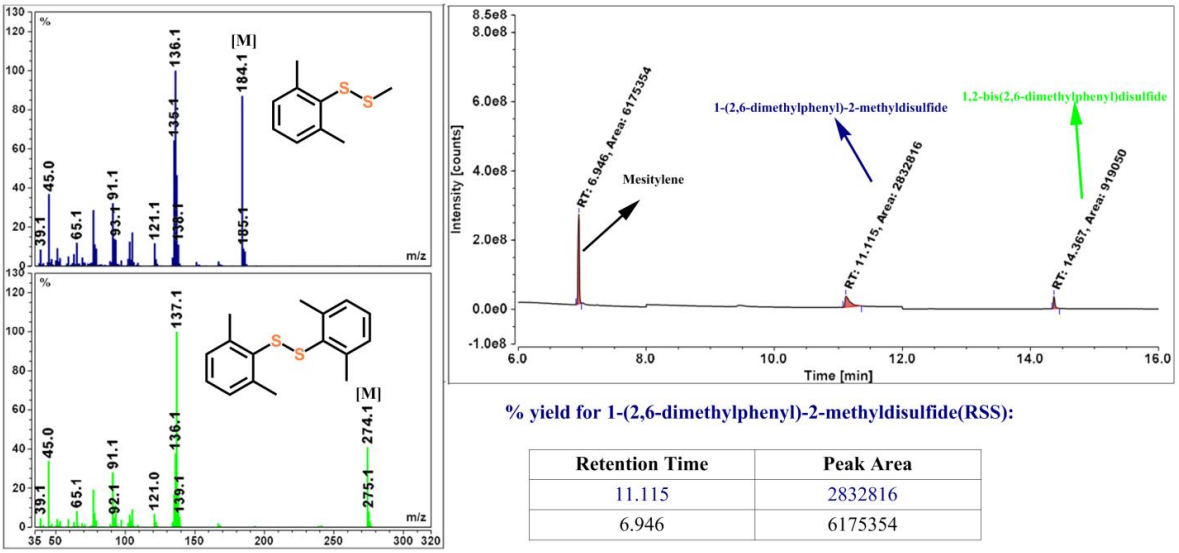

% yield for 1-(2,6-dimethylphenyl)-2-methyldisulfide(RSS):

Retention Time	Peak Area
11.115	2832816
6.946	6175354

$$\text{Yield} = \frac{2832816}{6175354} \times 100\%$$

$$= 46\%$$

% yield for 1,2-bis(2,6-dimethylphenyl)disulfide:

Retention Time	Peak Area
14.367	919050
6.946	6175354

$$\text{Yield} = \frac{919050}{6175354} \times 100\%$$

$$= 15\%$$

Figure S127. GC-MS data for the identification and yield calculation of 1-(2,6-dimethylphenyl)-2-methyldisulfide (Me-S-S-2,6-Me_2-C_6H_4, yield = 46%) produced in the reaction of [(Py2ald)Zn(SC_6H_4-2,6-Me_2)] (**1b^{Zn}**) with S_8 and MeI.

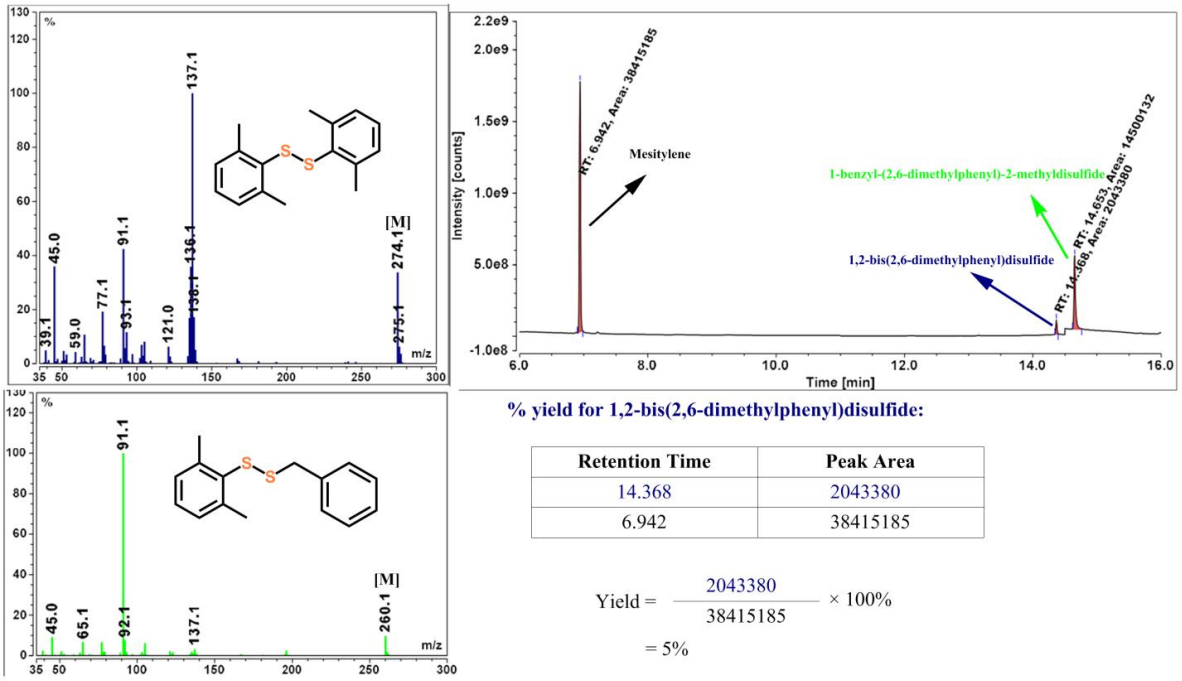

% yield for 1,2-bis(2,6-dimethylphenyl)disulfide:

Retention Time	Peak Area
14.368	2043380
6.942	38415185

$$\text{Yield} = \frac{2043380}{38415185} \times 100\%$$

$$= 5\%$$

% yield for 1-benzyl-(2,6-dimethylphenyl)-2-methyldisulfide(RSS):

Retention Time	Peak Area
14.653	14500132
6.942	38415185

$$\text{Yield} = \frac{14500132}{38415185} \times 100\%$$

$$= 38\%$$

Figure S128. GC-MS data for the identification and yield calculation of 1-benzyl-(2,6-dimethylphenyl)-2-methyldisulfide ($PhCH_2$-S-S-2,6-Me_2-C_6H_4, yield = 38%) produced in the reaction of [(Py2ald)Zn(SC_6H_4-2,6-Me_2)] (**1b^{Zn}**) with S_8 and $PhCH_2Br$.

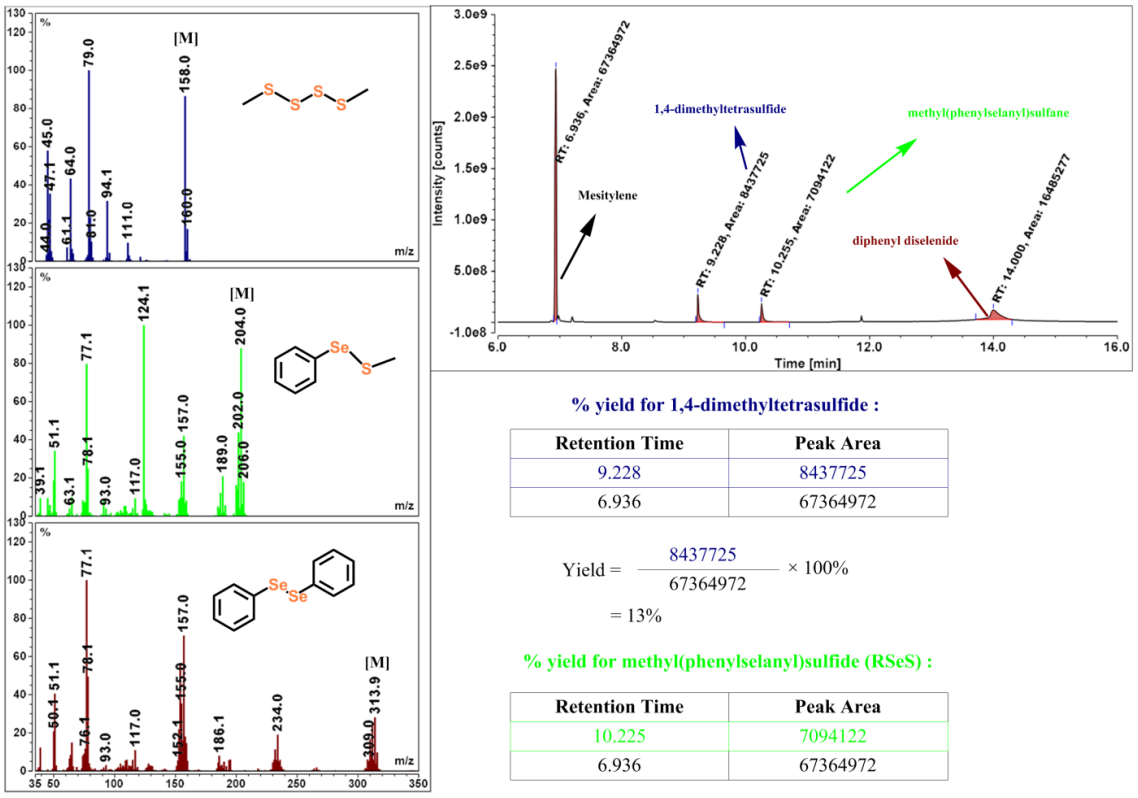

% yield for 1,4-dimethyltetrasulfide :

Retention Time	Peak Area
9.228	8437725
6.936	67364972

$$\text{Yield} = \frac{8437725}{67364972} \times 100\%$$

$$= 13\%$$

% yield for methyl(phenylselanyl)sulfide (RSeS) :

Retention Time	Peak Area
10.225	7094122
6.936	67364972

$$\text{Yield} = \frac{7094122}{67364972} \times 100\%$$

$$= 11\%$$

% yield for diphenyl diselenide :

Retention Time	Peak Area
14.000	16485277
6.936	67364972

$$\text{Yield} = \frac{16485277}{67364972} \times 100\%$$

$$= 24\%$$

Figure S129. GC-MS data for the identification and yield calculation of methyl(phenylselanyl)sulfide (Me-S-Se-Ph, yield = 11%) produced in the reaction of [(Py2ald)Zn(SePh)] (**2**$^{\mathbf{Zn}}$) with S_8 and MeI.

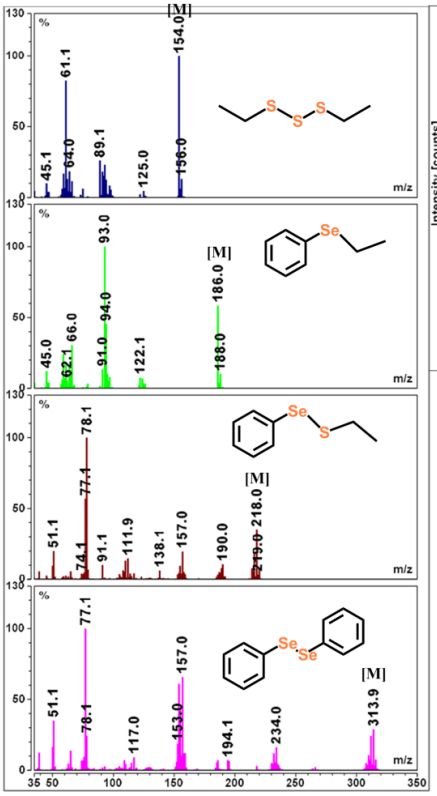

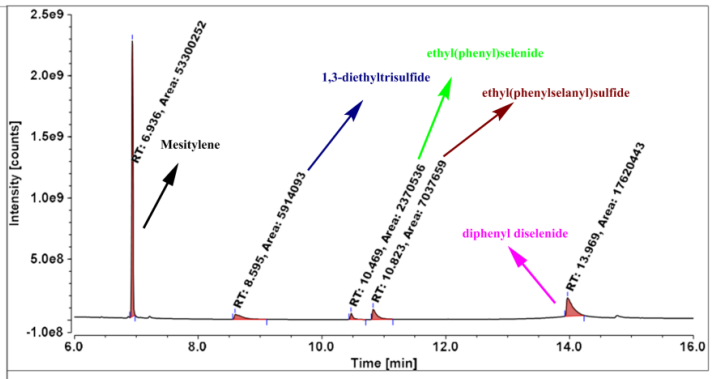

% yield for 1,3-diethyltrisulfide :

Retention Time	Peak Area
8.595	5914093
6.936	53300352

$$\text{Yield} = \frac{5914093}{53300352} \times 100\%$$

$$= 11\%$$

% yield for ethyl(phenyl)selenide:

Retention Time	Peak Area
10.469	2370536
6.936	53300352

$$\text{Yield} = \frac{2370536}{53300352} \times 100\%$$

$$= 4\%$$

% yield for ethyl(phenylselanyl)sulfide (RSeS) :

Retention Time	Peak Area
10.823	7037659
6.936	53300352

$$\text{Yield} = \frac{7037659}{53300352} \times 100\%$$

$$= 13\%$$

% yield for diphenyl diselenide :

Retention Time	Peak Area
13.969	17620443
6.936	53300352

$$\text{Yield} = \frac{17620443}{53300352} \times 100\%$$

$$= 33\%$$

Figure S130. GC-MS data for the identification and yield calculation of ethyl(phenylselanyl)sulfide (Et-S-Se-Ph, yield = 13%) produced in the reaction of [(Py2ald)Zn(SePh)] (**2**^{Zn}) with S_8 and EtBr.

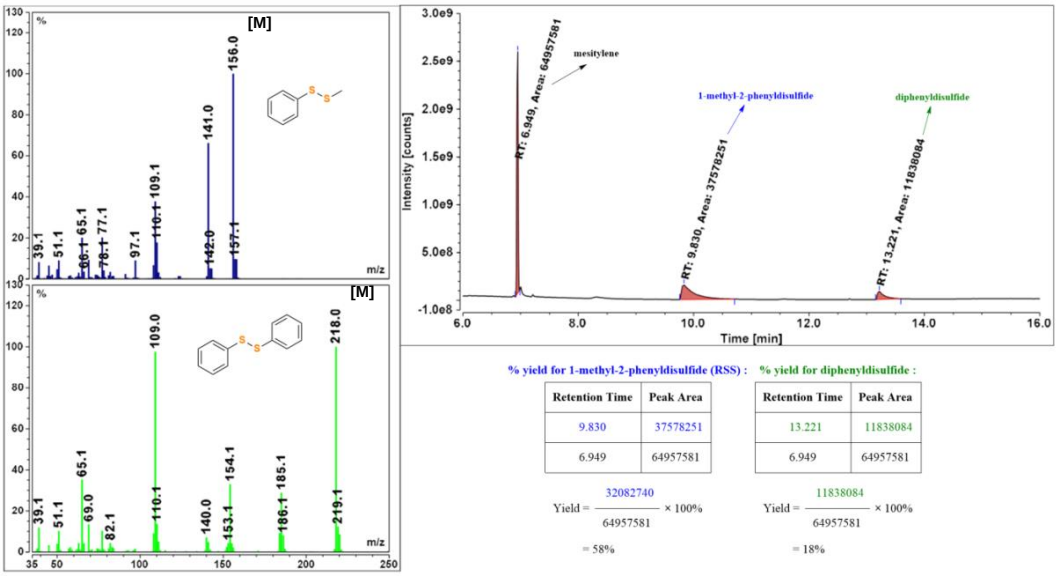

Figure S131. GC-MS data for the identification and yield calculation of 1-methyl-2-phenyldisulfide (Me-S-S-Ph, yield = 58%) produced in the reaction of [(Py2ald)Fe(SPh)] (**1a**^{Fe}) with S_8 and MeI.

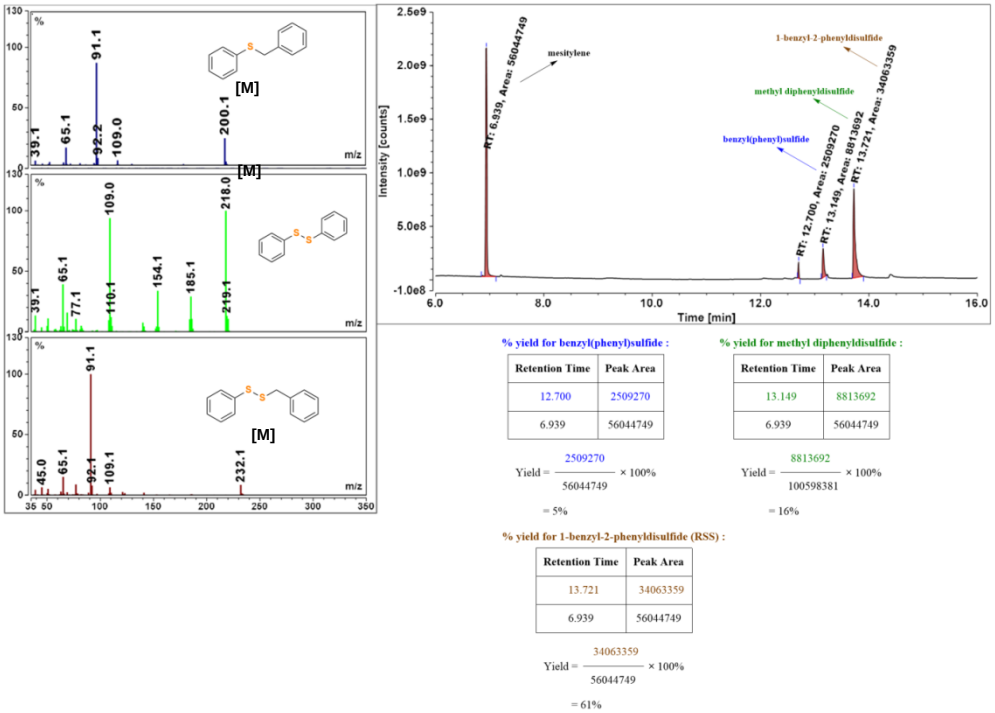

Figure S132. GC-MS data for the identification and yield calculation of 1-benzyl-2-phenyldisulfide ($PhCH_2$-S-S-Ph, yield = 61%) produced in the reaction of [(Py2ald)Fe(SPh)] (**1a**^{Fe}) with S_8 and $PhCH_2Br$.

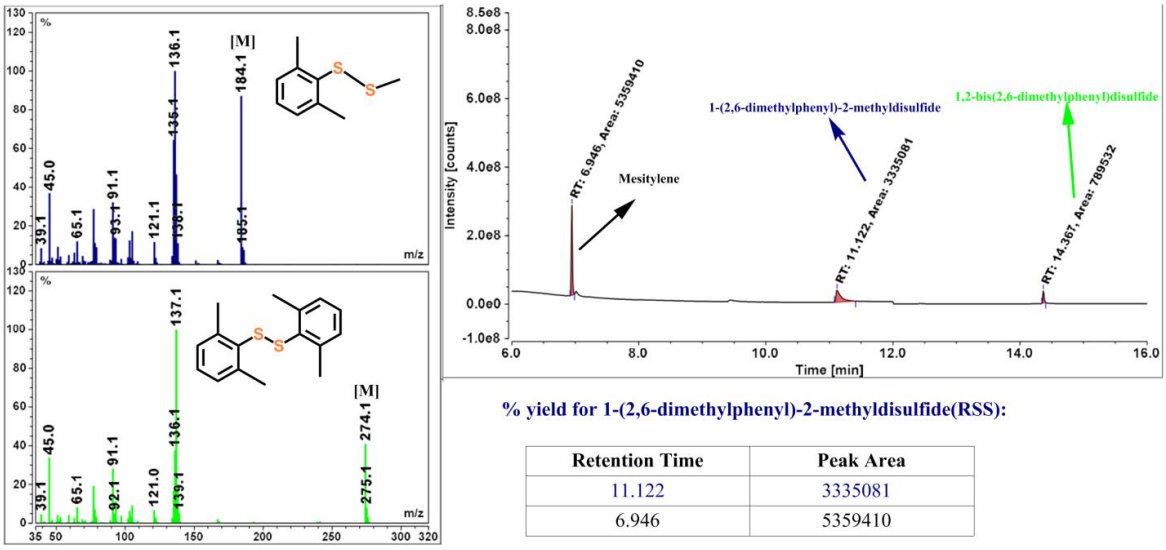

% yield for 1-(2,6-dimethylphenyl)-2-methyldisulfide(RSS):

Retention Time	Peak Area
11.122	3335081
6.946	5359410

$$\text{Yield} = \frac{3335081}{5359410} \times 100\%$$

$$= 62\%$$

% yield for 1,2-bis(2,6-dimethylphenyl)disulfide:

Retention Time	Peak Area
14.367	789532
6.946	5359410

$$\text{Yield} = \frac{789532}{5359410} \times 100\%$$

$$= 15\%$$

Figure S133. GC-MS data for the identification and yield calculation of 1-(2,6-dimethylphenyl)-2-methyldisulfide (Me-S-S-2,6-Me_2-C_6H_4, yield = 62%) produced in the reaction of [(Py2ald)Fe(SC_6H_4-2,6-Me_2)] (**1b^{Fe}**) with S_8 and MeI.

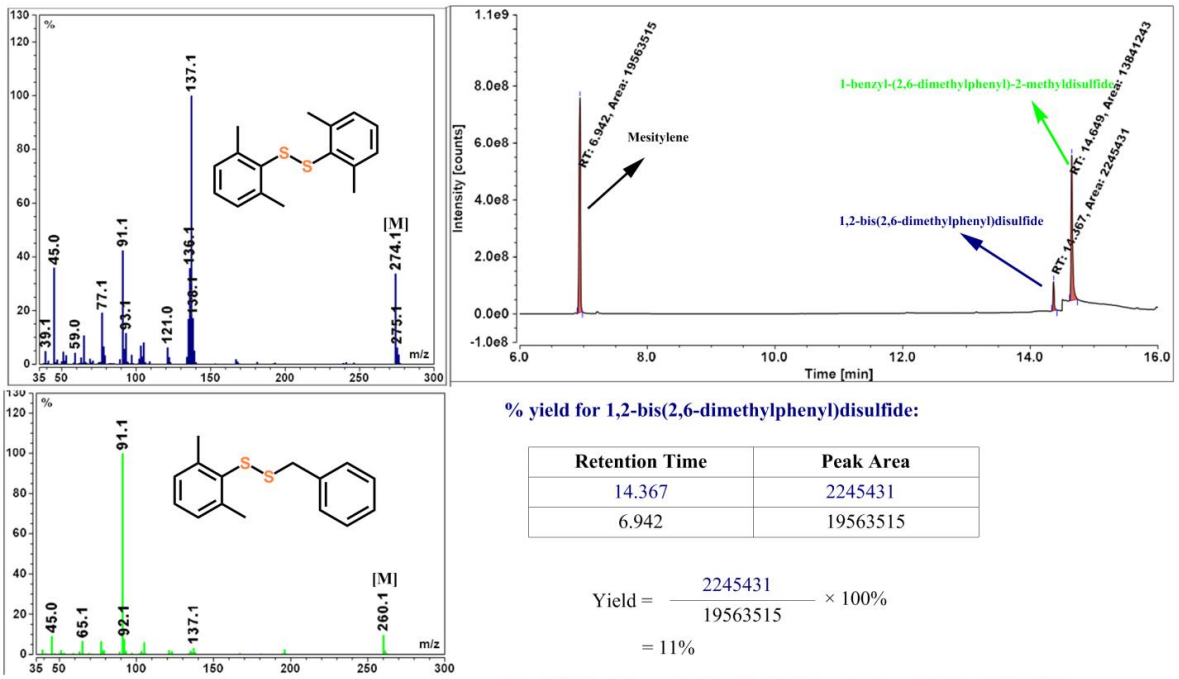

% yield for 1,2-bis(2,6-dimethylphenyl)disulfide:

Retention Time	Peak Area
14.367	2245431
6.942	19563515

$$\text{Yield} = \frac{2245431}{19563515} \times 100\%$$

$$= 11\%$$

% yield for 1-benzyl-(2,6-dimethylphenyl)-2-methyldisulfide(RSS):

Retention Time	Peak Area
14.649	13841243
6.942	19563515

$$\text{Yield} = \frac{13841243}{19563515} \times 100\%$$

$$= 71\%$$

Figure S134. GC-MS data for the identification and yield calculation of 1-benzyl-(2,6-dimethylphenyl)-2-methyldisulfide ($PhCH_2$-S-S-2,6-Me_2-C_6H_4, yield = 71%) produced in the reaction of [(Py2ald)Fe(SC_6H_4-2,6-Me_2)] (**1b^{Fe}**) with S_8 and $PhCH_2Br$.

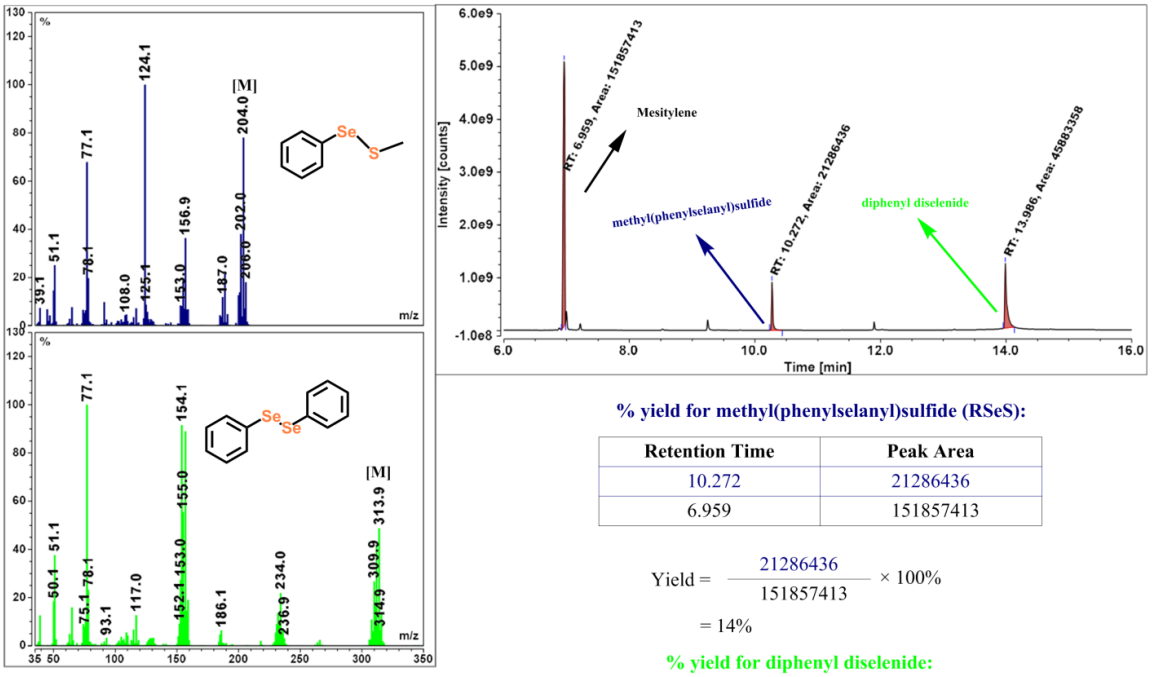

% yield for methyl(phenylselanyl)sulfide (RSeS):

Retention Time	Peak Area
10.272	21286436
6.959	151857413

$$\text{Yield} = \frac{21286436}{151857413} \times 100\%$$

$$= 14\%$$

% yield for diphenyl diselenide:

Retention Time	Peak Area
13.986	45883358
6.959	151857413

$$\text{Yield} = \frac{45883358}{151857413} \times 100\%$$

$$= 30\%$$

Figure S135. GC-MS data for the identification and yield calculation of methyl(phenylselanyl)sulfide (Me-S-Se-Ph, yield = 14%) produced in the reaction of [(Py2ald)Fe(SePh)] (**2**^{Fe}) with S_8 and MeI.

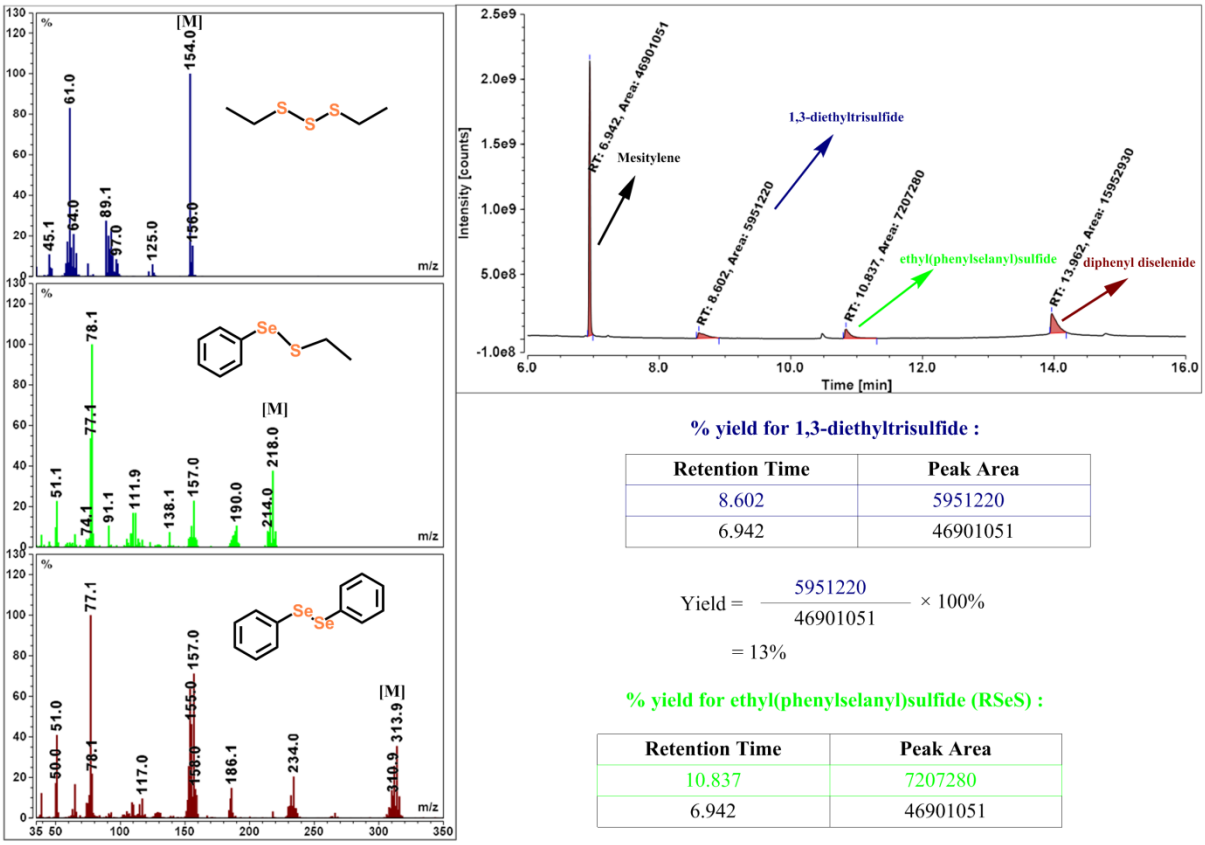

% yield for 1,3-diethyltrisulfide :

Retention Time	Peak Area
8.602	5951220
6.942	46901051

$$\text{Yield} = \frac{5951220}{46901051} \times 100\%$$

$$= 13\%$$

% yield for ethyl(phenylselanyl)sulfide (RSeS) :

Retention Time	Peak Area
10.837	7207280
6.942	46901051

$$\text{Yield} = \frac{7207280}{46901051} \times 100\%$$

$$= 15\%$$

% yield for diphenyl diselenide :

Retention Time	Peak Area
13.962	15952930
6.942	46901051

$$\text{Yield} = \frac{15952930}{46901051} \times 100\%$$

$$= 34\%$$

Figure S136. Gas chromatographic data for the identification and yield calculation of ethyl(phenylselanyl)sulfide (Et-S-Se-Ph, yield = 15%) produced in the reaction of [(Py2ald)Fe(SePh)] (**2**^{Fe}) with S_8 and EtBr.

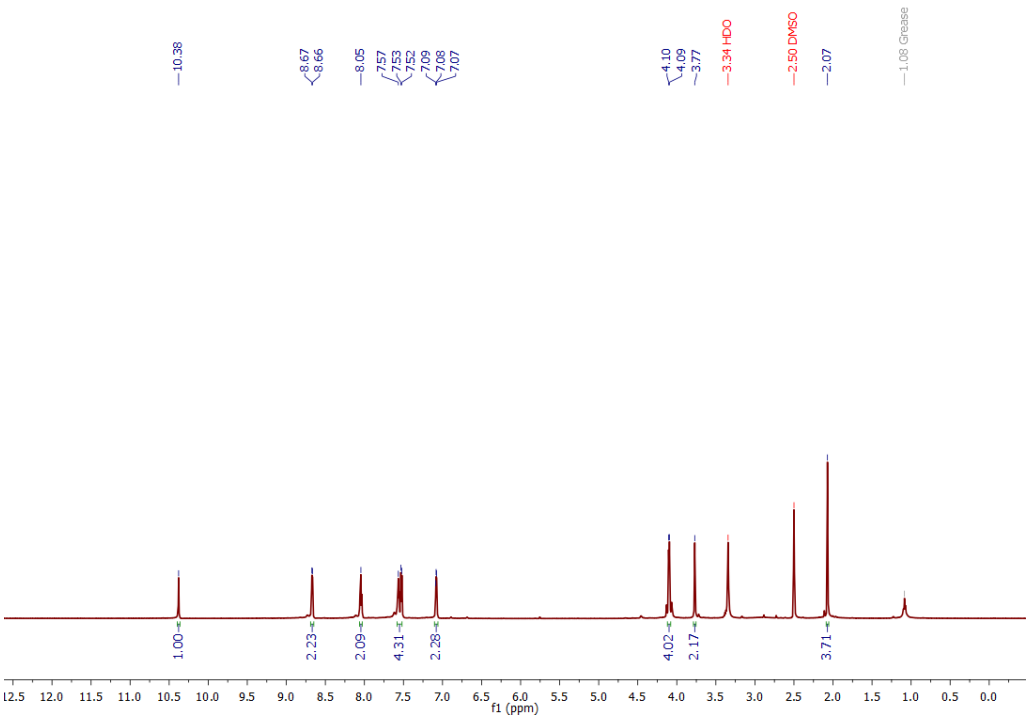

Figure S137. ^{1}H NMR (600 MHz, DMSO-d^{6}) spectrum of [(Py2ald)Zn]$_2$(BF$_4$)$_2$ (**5**$^{\mathbf{Zn}}$(BF$_4$)$_2$) obtained from the reaction of [(Py2ald)Zn(SPh)] (**1a**$^{\mathbf{Zn}}$) with S$_8$ and MeI.

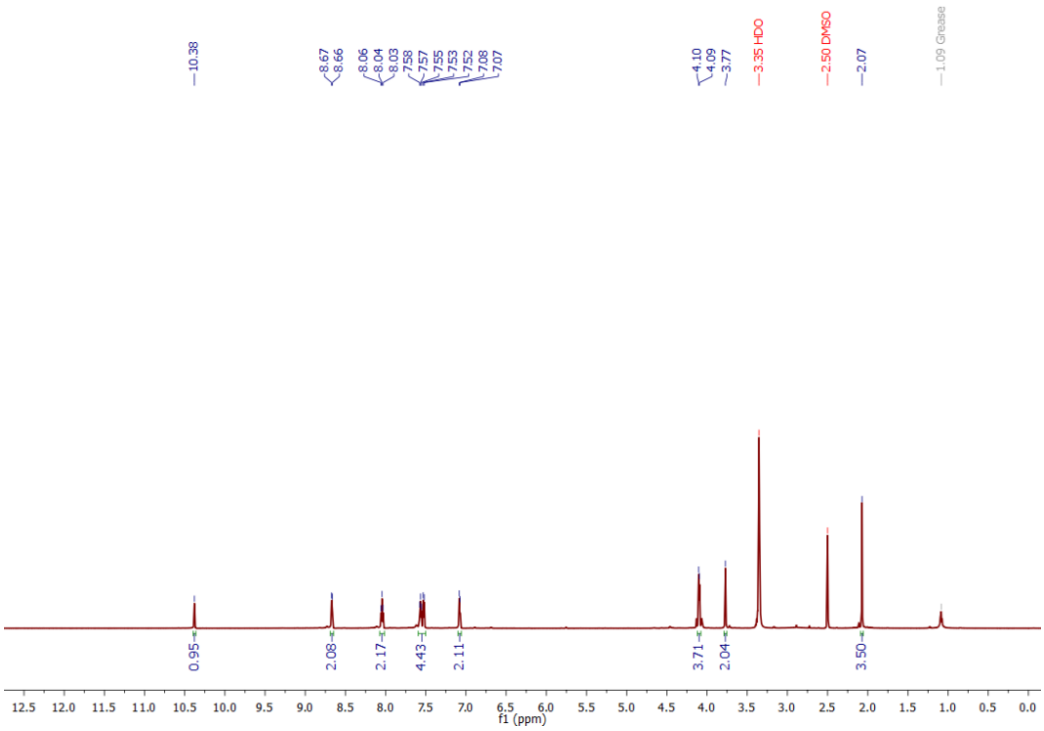

Figure S138. ^{1}H NMR (600 MHz, DMSO-d^{6}) spectrum of [(Py2ald)Zn]$_2$(BF$_4$)$_2$ (**5**$^{\mathbf{Zn}}$(BF$_4$)$_2$) obtained from the reaction of [(Py2ald)Zn(SPh)] (**1a**$^{\mathbf{Zn}}$) with S$_8$ and PhCH$_2$Br.

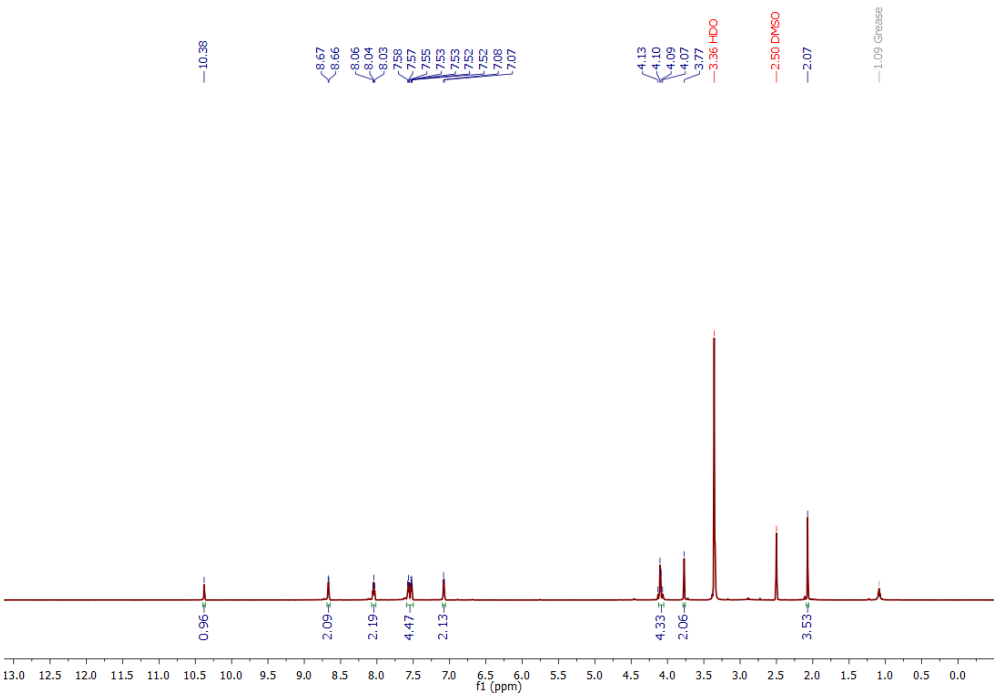

Figure S139. ^{1}H NMR (600 MHz, DMSO-d^{6}) spectrum of [(Py2ald)Zn]$_2$(BF$_4$)$_2$ (**5**$^{\mathbf{Zn}}$(BF$_4$)$_2$) obtained from the reaction of [(Py2ald)Zn(SC$_6$H$_4$-2,6-Me$_2$)] (**1b**$^{\mathbf{Zn}}$) with S$_8$ and MeI.

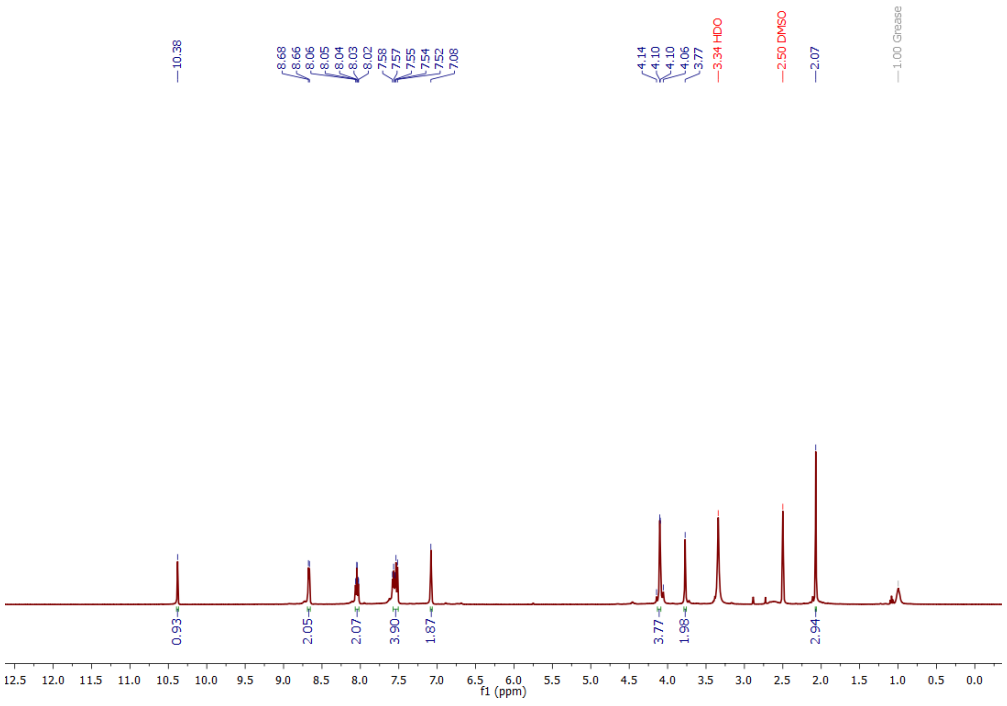

Figure S140. ^{1}H NMR (400 MHz, DMSO-d^{6}) spectrum of [(Py2ald)Zn]$_2$(BF$_4$)$_2$ (**5**$^{\mathbf{Zn}}$(BF$_4$)$_2$) obtained from the reaction of [(Py2ald)Zn(SC$_6$H$_4$-2,6-Me$_2$)] (**1b**$^{\mathbf{Zn}}$) with S$_8$ and PhCH$_2$Br.

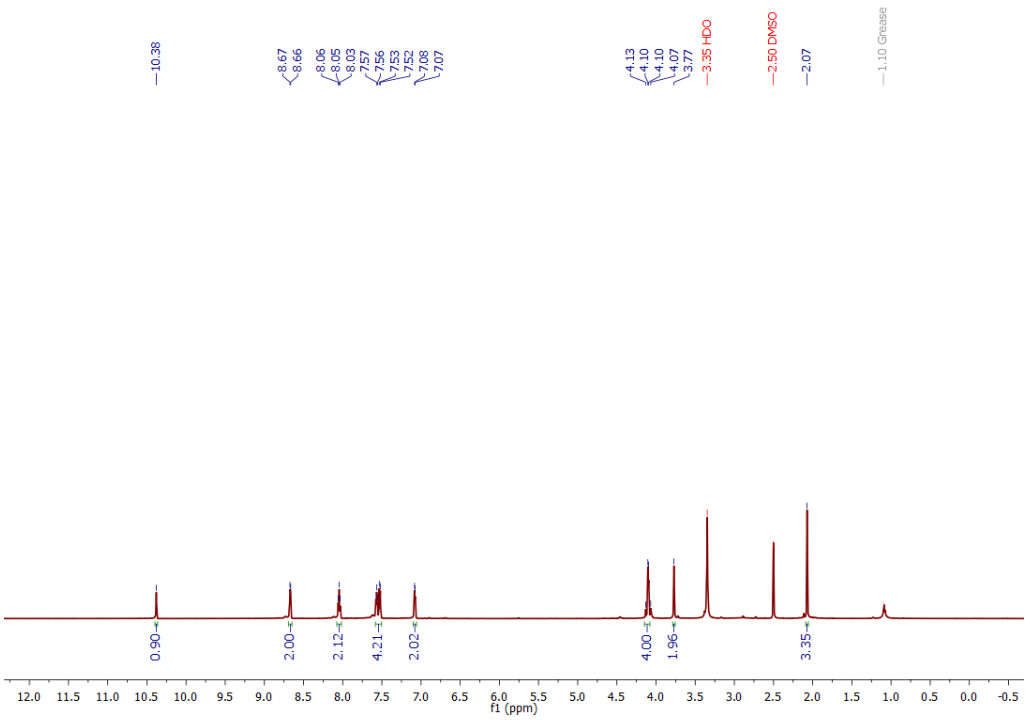

Figure S141. ^{1}H NMR (600 MHz, DMSO-d^{6}) spectrum of [(Py2ald)Zn]$_2$(BF$_4$)$_2$ (**5^{Zn}**(BF$_4$)$_2$) obtained from the reaction of [(Py2ald)Zn(SePh)] (**2^{Zn}**) with S$_8$ and MeI.

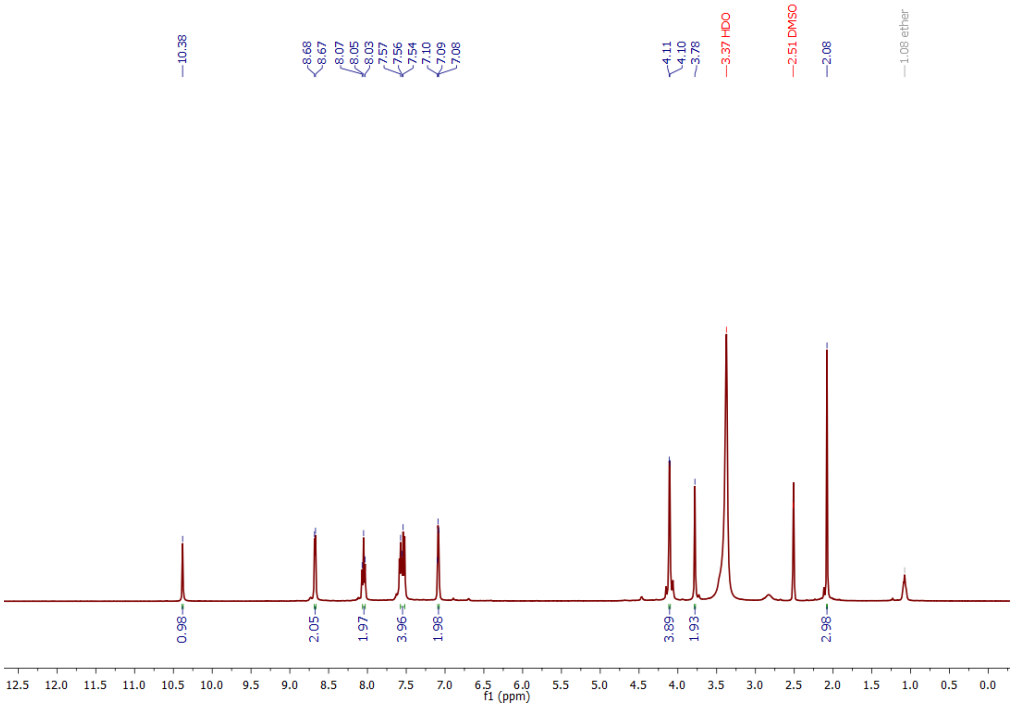

Figure S142. ^{1}H NMR (400 MHz, DMSO-d^{6}) spectrum of [(Py2ald)Zn]$_2$(BF$_4$)$_2$ (**5^{Zn}**(BF$_4$)$_2$) obtained from the reaction of [(Py2ald)Zn(SePh)] (**2^{Zn}**) with S$_8$ and EtBr.

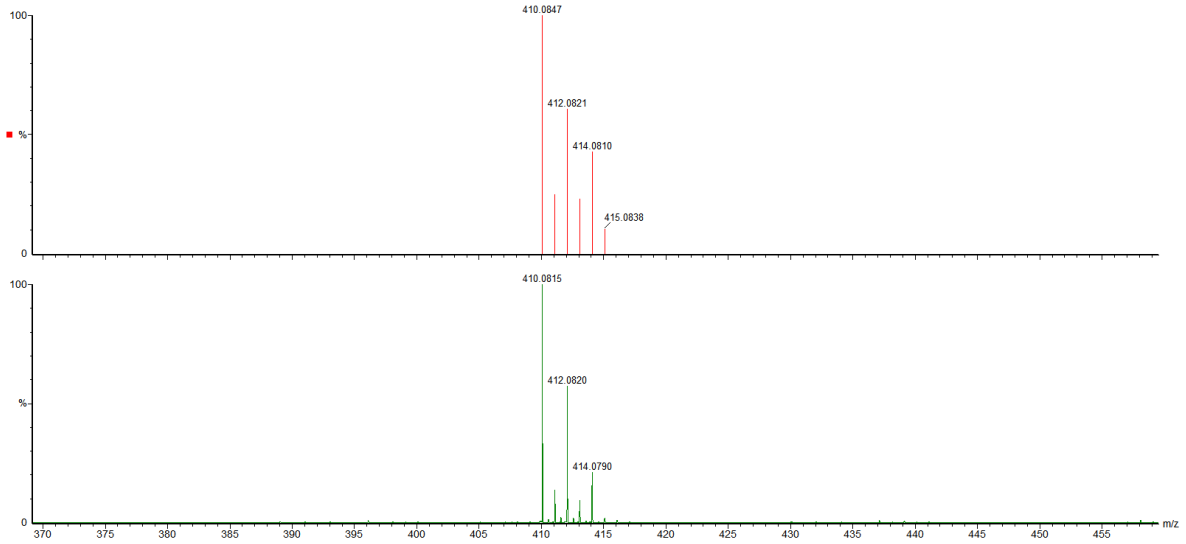

Figure S143. Mass spectrometric data (in MeCN) for $[(Py2ald)Zn]_2(BF_4)_2$ ($\mathbf{5^{Zn}}(BF_4)_2$) obtained from the reaction of [(Py2ald)Zn(SPh)] (**1a^{Zn}**) with S_8 and MeI shows the presence of $[(Py2ald)Zn]^+$ (m/z: 410.0847, simulated data, orange line; 410.0815, observed data, green line).

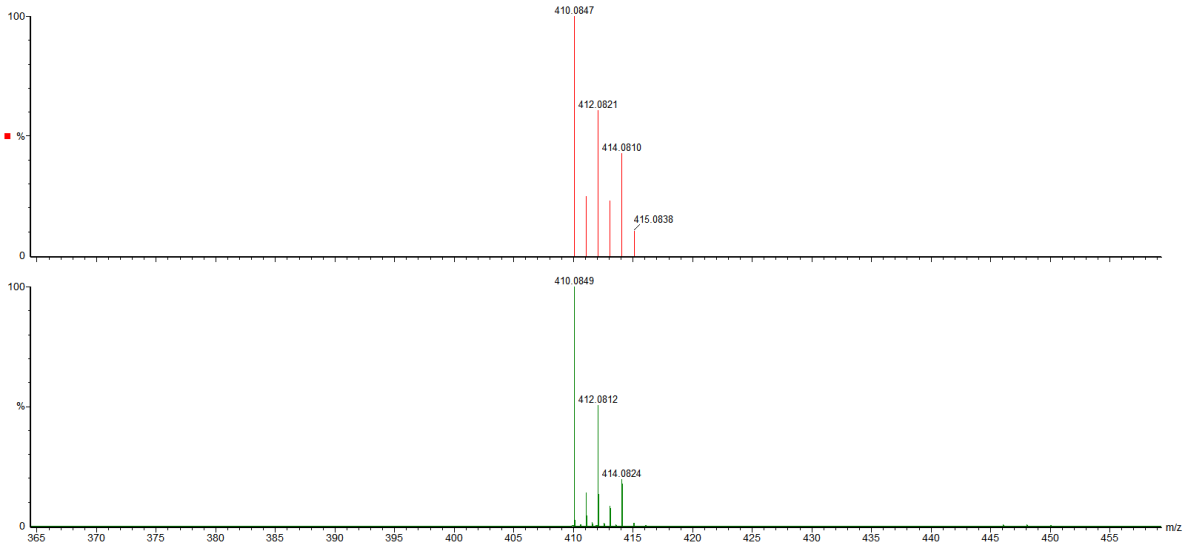

Figure S144. Mass spectrometric data (in MeCN) for $[(Py2ald)Zn]_2(BF_4)_2$ ($\mathbf{5^{Zn}}(BF_4)_2$) obtained from the reaction of [(Py2ald)Zn(SPh)] (**1a^{Zn}**) S_8 and $PhCH_2Br$, which shows the presence of $[(Py2ald)Zn]^+$ (m/z: 410.0847, simulated data, orange line; 410.0849, observed data, green line).

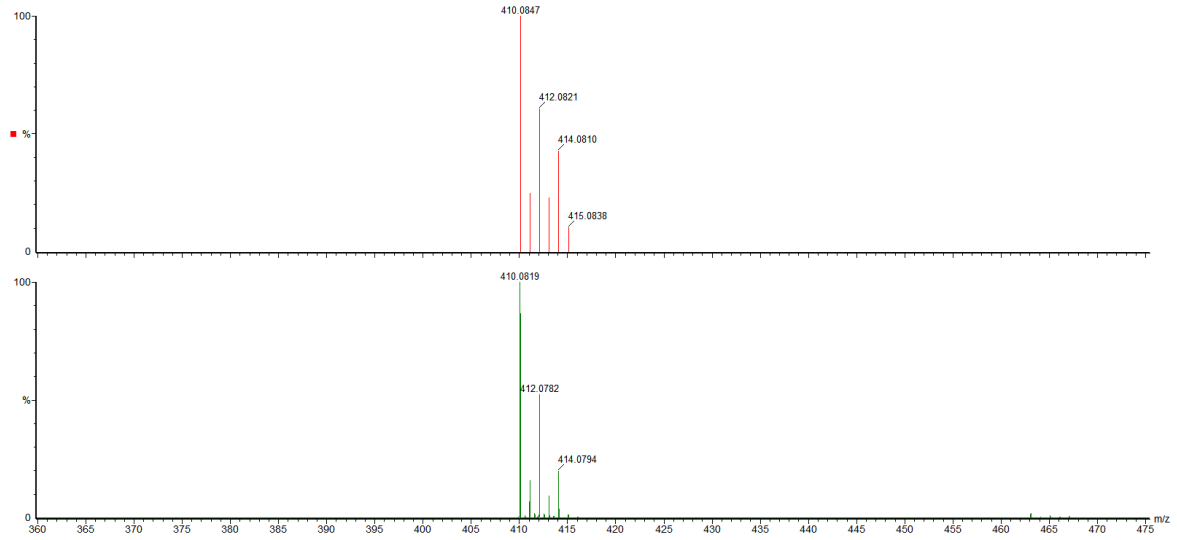

Figure S145. Mass spectrometric data (in MeCN) for $[(Py2ald)Zn]_2(BF_4)_2$ ($\mathbf{5^{Zn}}(BF_4)_2$) obtained from the reaction of $[(Py2ald)Zn(SC_6H_4\text{-}2,6\text{-}Me_2)]$ ($\mathbf{1b^{Zn}}$) with S_8 and MeI, which shows the presence of $[(Py2ald)Zn]^+$ (m/z: 410.0847, simulated data, orange line; 410.0819, observed data, green line).

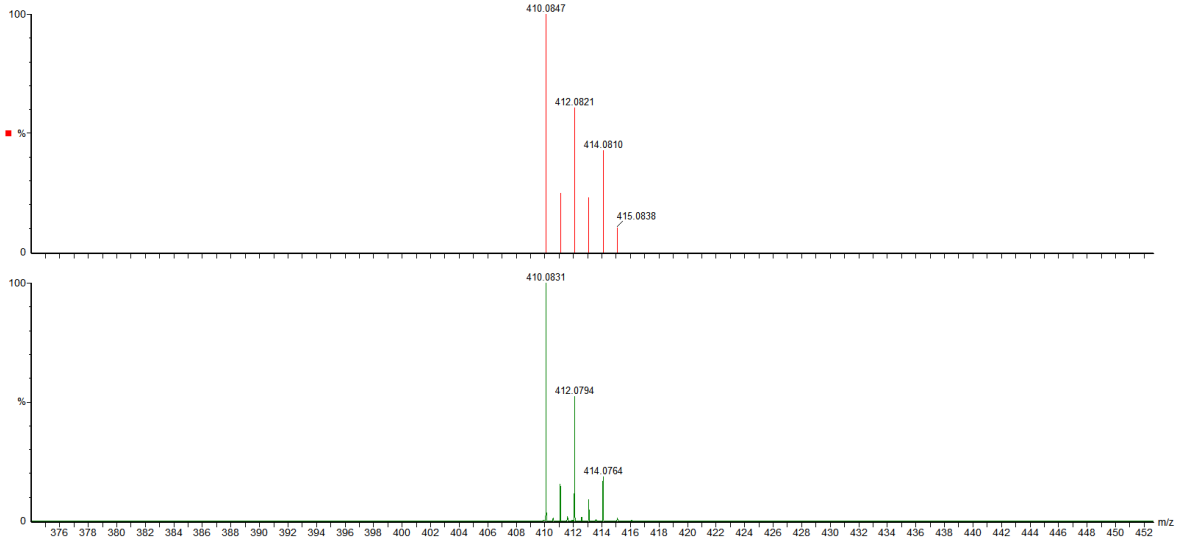

Figure S146. Mass spectrometric data (in MeCN) for $[(Py2ald)Zn]_2(BF_4)_2$ ($\mathbf{5^{Zn}}(BF_4)_2$) obtained from the reaction of $[(Py2ald)Zn(SC_6H_4\text{-}2,6\text{-}Me_2)]$ ($\mathbf{1b^{Zn}}$) with S_8 and $PhCH_2Br$ shows the presence of $[(Py2ald)Zn]^+$ (m/z: 410.0847, simulated data, orange line; 410.0831, observed data, green line).

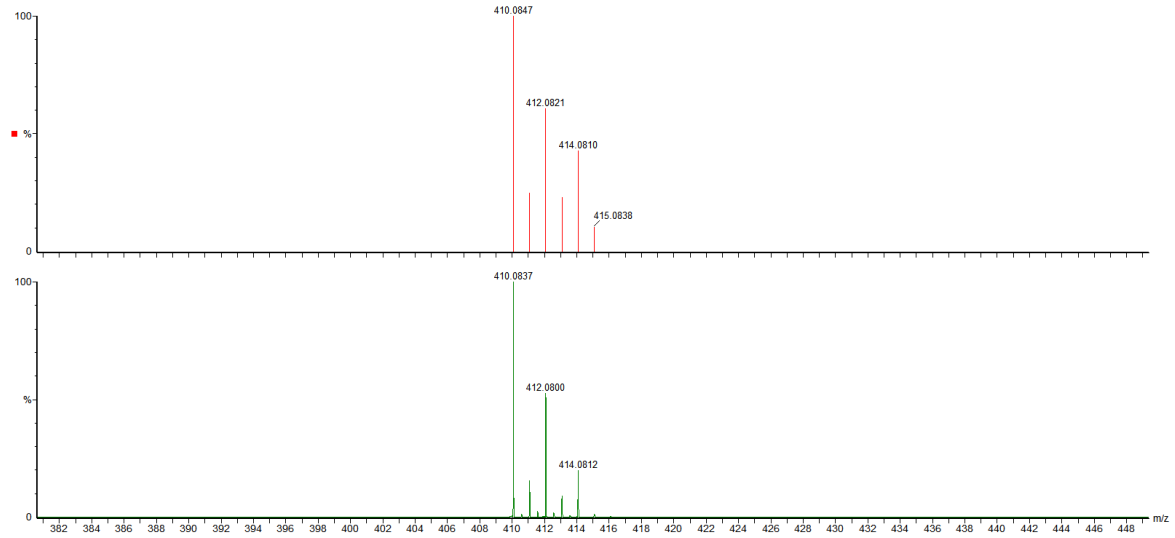

Figure S147. Mass spectrometric data (in MeCN) for $[(Py2ald)Zn]_2(BF_4)_2$ ($\mathbf{5^{Zn}}(BF_4)_2$) obtained from the reaction of [(Py2ald)Zn(SePh)] ($\mathbf{2^{Zn}}$) with S_8 and MeI shows the presence of $[(Py2ald)Zn]^+$ (m/z: 410.0847, simulated data, orange line; 410.0837, observed data, green line).

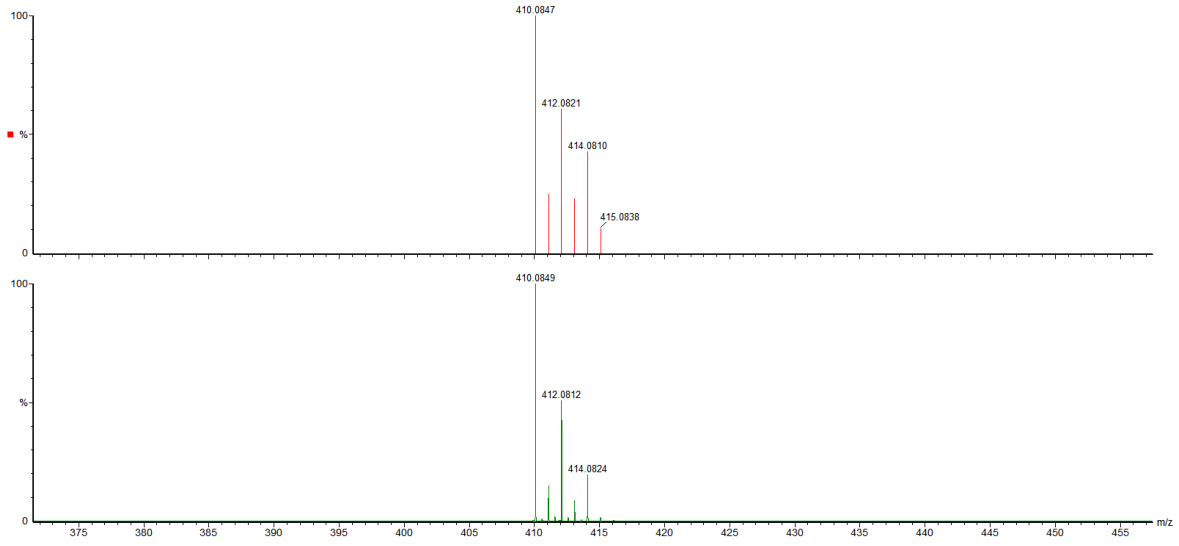

Figure S148. Mass spectrometric data (in MeCN) for $[(Py2ald)Zn]_2(BF_4)_2$ ($\mathbf{5^{Zn}}(BF_4)_2$) obtained from the reaction of [(Py2ald)Zn(SePh)] ($\mathbf{2^{Zn}}$) with S_8 and EtBr shows the presence of $[(Py2ald)Zn]^+$ (m/z: 410.0847, simulated data, orange line; 410.0849, observed data, green line).

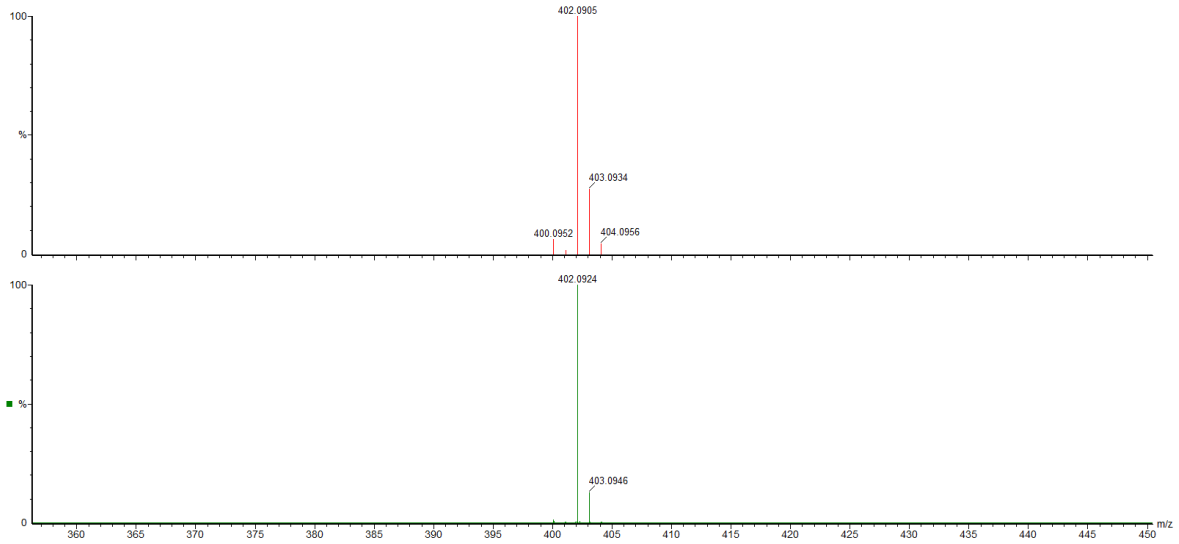

Figure S149. Mass spectrometric data (in MeCN) for $[(Py2ald)Fe]_2(BPh_4)_2$ ($\mathbf{5^{Fe}}(BPh_4)_2$) obtained from the reaction of [(Py2ald)Fe(SPh)] ($\mathbf{1a^{Fe}}$) with S_8 and MeI, which shows the presence of $[(Py2ald)Fe]^+$ (m/z: 402.0905, simulated data, orange line; 402.0924, observed data, green line).

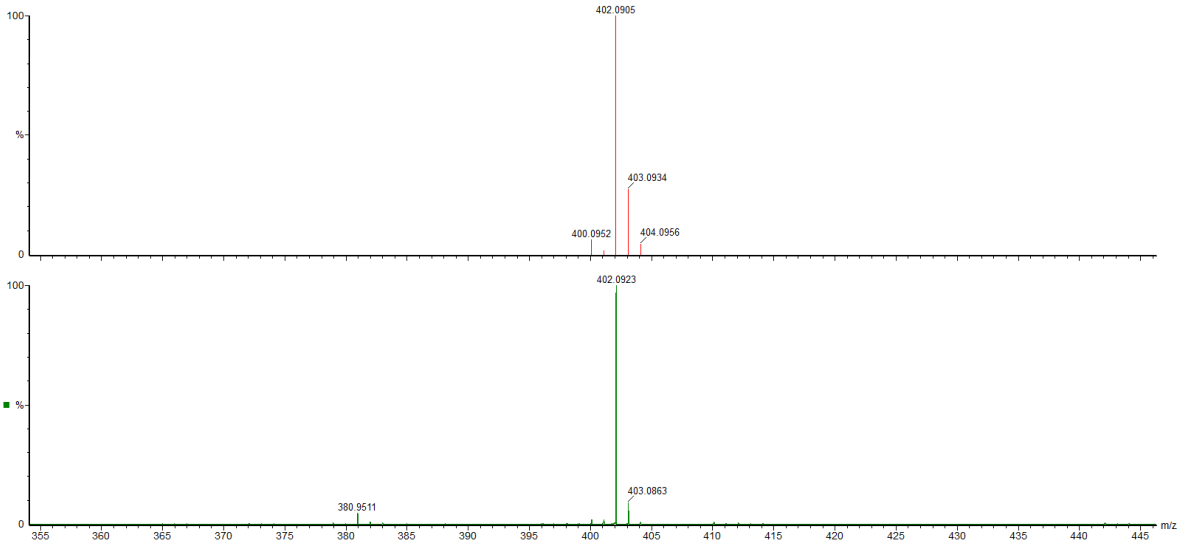

Figure S150. Mass spectrometric data (in MeCN) for $[(Py2ald)Fe]_2(BPh_4)_2$ ($\mathbf{5^{Fe}}(BPh_4)_2$) obtained from the reaction of [(Py2ald)Fe(SPh)] ($\mathbf{1a^{Fe}}$) with S_8 and $PhCH_2Br$, which shows the presence of $[(Py2ald)Fe]^+$ (m/z: 402.0905, simulated data, orange line; 402.0923, observed data, green line).

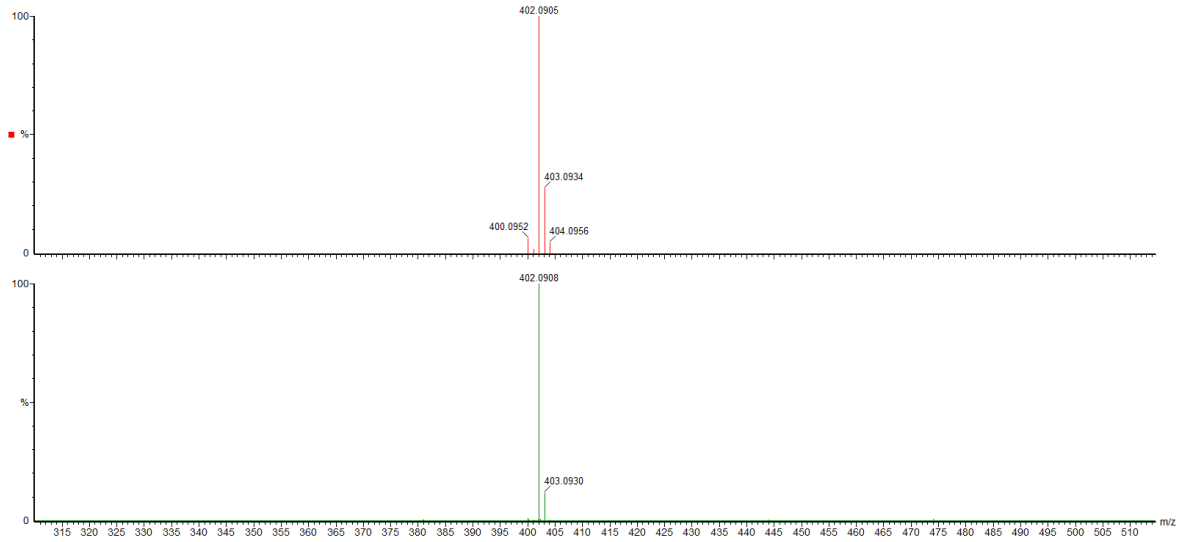

Figure S151. Mass spectrometric data (in MeCN) for $[(Py2ald)Fe]_2(BPh_4)_2$ ($\mathbf{5^{Fe}}(BPh_4)_2$) obtained from the reaction of $[(Py2ald)Fe(SC_6H_4\text{-}2,6\text{-}Me_2)]$ ($\mathbf{1b^{Fe}}$) with S_8 and MeI, which shows the presence of $[(Py2ald)Fe]^+$ (m/z:402.0905, simulated data,orange line; 402.0908,observed data, green line).

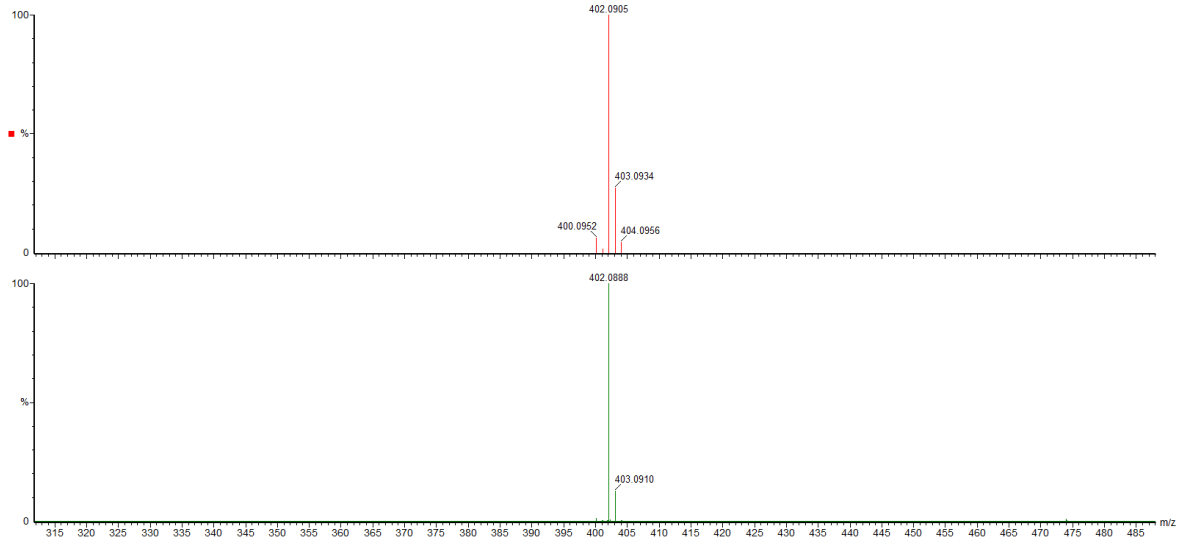

Figure S152. Mass spectrometric data (in MeCN) for $[(Py2ald)Fe]_2(BPh_4)_2$ ($\mathbf{5^{Fe}}(BPh_4)_2$) obtained from the reaction of $[(Py2ald)Fe(SC_6H_4\text{-}2,6\text{-}Me_2)]$ ($\mathbf{1b^{Fe}}$) with S_8 and $PhCH_2Br$ shows the presence of $[(Py2ald)Fe]^+$ (m/z: 402.0905, simulated data, orange line; 402.0888, observed data, green line).

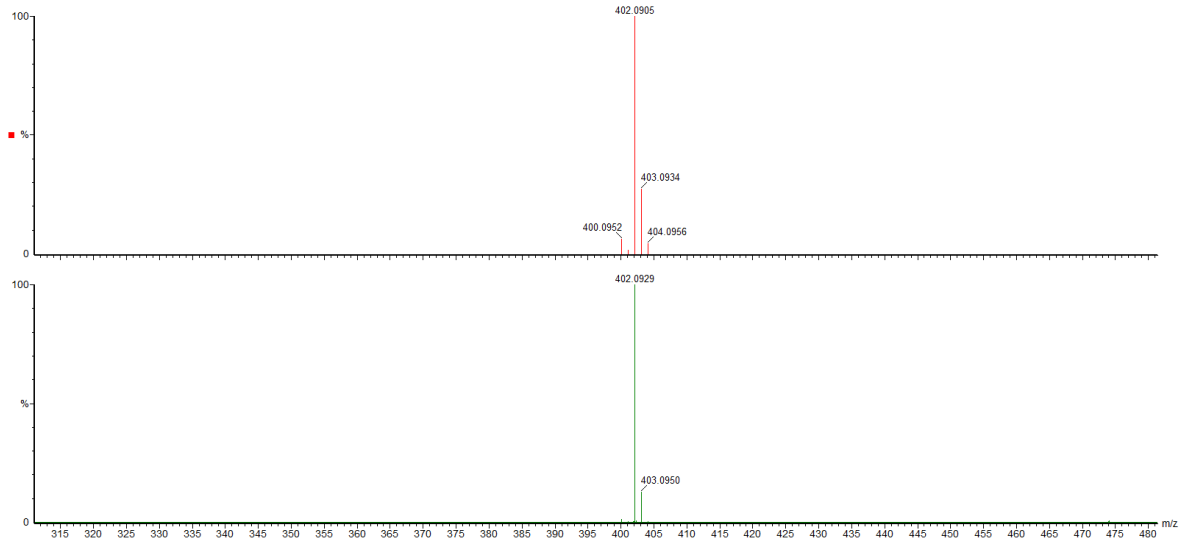

Figure S153. Mass spectrometric data (in MeCN) for $[(Py2ald)Fe]_2(BPh_4)_2$ ($\mathbf{5^{Fe}}(BPh_4)_2$) obtained from the reaction of [(Py2ald)Fe(SePh)] ($\mathbf{2^{Fe}}$) with S_8 and MeI, which shows the presence of $[(Py2ald)Fe]^+$ (m/z: 402.0905, simulated data, orange line; 402.0929, observed data, green line).

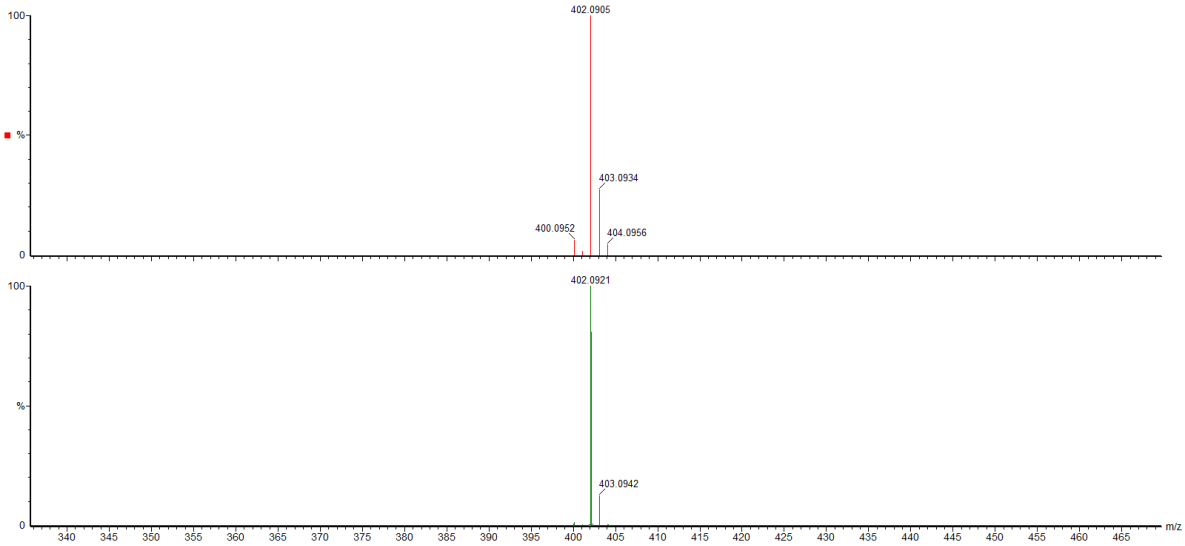

Figure S154. Mass spectrometric data (in MeCN) for $[(Py2ald)Fe]_2(BPh_4)_2$ ($\mathbf{5^{Fe}}(BPh_4)_2$) obtained from the reaction of [(Py2ald)Fe(SePh)] ($\mathbf{2^{Fe}}$) with S_8 and EtBr, which shows the presence of $[(Py2ald)Fe]^+$ (m/z: 402.0905, simulated data, orange line; 402.0921, observed data, green line).